NUTRIOMICS IN LIVESTOCK RESEARCH

EDITED BY: Rajib Deb and Rita Payan Carreira
PUBLISHED IN: Frontiers in Veterinary Science

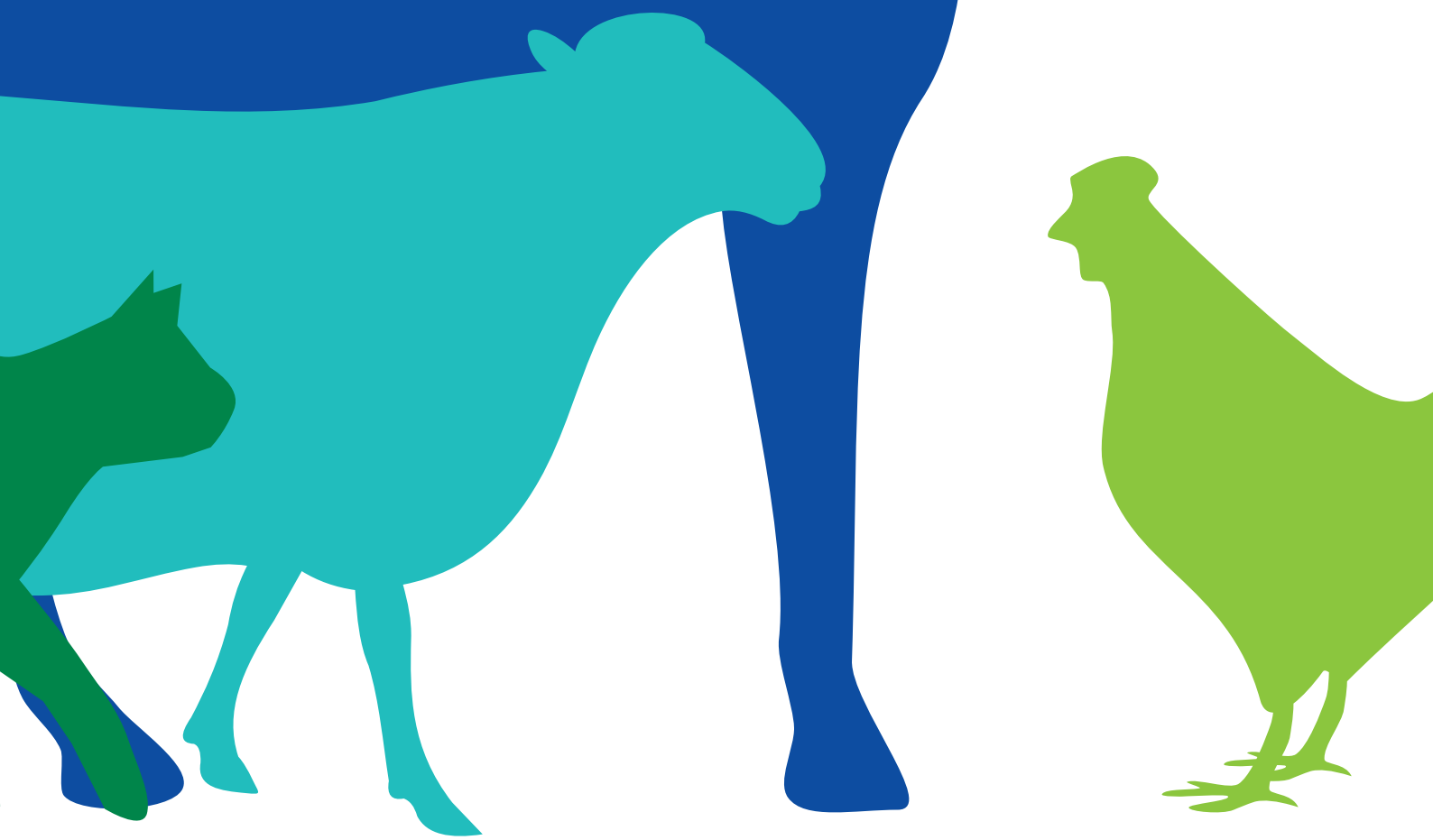

frontiers Research Topics

ISSN 1664-8714
ISBN 978-2-83250-889-3
DOI 10.3389/978-2-83250-889-3

About Frontiers

Frontiers is more than just an open-access publisher of scholarly articles: it is a pioneering approach to the world of academia, radically improving the way scholarly research is managed. The grand vision of Frontiers is a world where all people have an equal opportunity to seek, share and generate knowledge. Frontiers provides immediate and permanent online open access to all its publications, but this alone is not enough to realize our grand goals.

Frontiers Journal Series

The Frontiers Journal Series is a multi-tier and interdisciplinary set of open-access, online journals, promising a paradigm shift from the current review, selection and dissemination processes in academic publishing. All Frontiers journals are driven by researchers for researchers; therefore, they constitute a service to the scholarly community. At the same time, the Frontiers Journal Series operates on a revolutionary invention, the tiered publishing system, initially addressing specific communities of scholars, and gradually climbing up to broader public understanding, thus serving the interests of the lay society, too.

Dedication to Quality

Each Frontiers article is a landmark of the highest quality, thanks to genuinely collaborative interactions between authors and review editors, who include some of the world's best academicians. Research must be certified by peers before entering a stream of knowledge that may eventually reach the public - and shape society; therefore, Frontiers only applies the most rigorous and unbiased reviews.
Frontiers revolutionizes research publishing by freely delivering the most outstanding research, evaluated with no bias from both the academic and social point of view. By applying the most advanced information technologies, Frontiers is catapulting scholarly publishing into a new generation.

What are Frontiers Research Topics?

Frontiers Research Topics are very popular trademarks of the Frontiers Journals Series: they are collections of at least ten articles, all centered on a particular subject. With their unique mix of varied contributions from Original Research to Review Articles, Frontiers Research Topics unify the most influential researchers, the latest key findings and historical advances in a hot research area! Find out more on how to host your own Frontiers Research Topic or contribute to one as an author by contacting the Frontiers Editorial Office: frontiersin.org/about/contact

NUTRIOMICS IN LIVESTOCK RESEARCH

Topic Editors:
Rajib Deb, National Research Centre on Pig (ICAR), India
Rita Payan Carreira, University of Evora, Portugal

Citation: Deb, R., Carreira, R. P., eds. (2022). Nutriomics in Livestock Research. Lausanne: Frontiers Media SA. doi: 10.3389/978-2-83250-889-3

Table of Contents

frontiers | Frontiers in Veterinary Science

TYPE Editorial
PUBLISHED 15 November 2022
DOI 10.3389/fvets.2022.1071290

OPEN ACCESS

EDITED AND REVIEWED BY
Duy Ngoc Do,
Dalhousie University, Canada

*CORRESPONDENCE
Rajib Deb
drrajibdeb@gmail.com

SPECIALTY SECTION
This article was submitted to Livestock Genomics, a section of the journal Frontiers in Veterinary Science

RECEIVED 16 October 2022
ACCEPTED 07 November 2022
PUBLISHED 15 November 2022

CITATION
Deb R and Payan-Carreira R (2022) Editorial: Nutriomics in livestock research. *Front. Vet. Sci.* 9:1071290. doi: 10.3389/fvets.2022.1071290

Editorial: Nutriomics in livestock research

Rajib Deb[1]* and Rita Payan-Carreira[2]

[1]Animal Health Division, Indian Council of Agricultural Research (ICAR)-National Research Center on Pig, Guwahati, India, [2]Comprehensive Health Research Centre and Department of Veterinary Medicine, University of Evora, Évora, Portugal

KEYWORDS

nutriomics, livestock, feeding, productivity, vaccine

Editorial on the Research Topic
Nutriomics in livestock research

The development of high-throughput technology offers robust platforms to measure the components of the gut microbiota as well as proteins, metabolites, and coding and non-coding RNAs. Transcriptomics, proteomics, metabolomics, and metagenomics are just a few of the technologies that can be used to gather information about the genome and other biological molecules, and they are all effectively applied in the field of nutrigenomics, also known as nutritionomics, to shed light on the interactions between nutrition and the livestock genome. Integrating genomics and nutrition facilitates understanding the differences or similarities in how different candidate genes express themselves in response to food. Since nutriomics is still in its infancy, it presents an exciting potential in animal nutrition to ensure the quality of nutrition and its impact on general improvement of animal production. This Research Topic aims to assemble papers examining the effects of various diets (and/or nutrients) while feeding livestock, using nutriomics to increase productivity, enhance reproductive parameters, and prevent or modify livestock disease prevention. The nine publications that integrate this unique e-collection discuss various nutriomics topics in livestock.

From a nutrigenomic perspective, dairy cows' metabolic difficulties between conception and lactation is of great interest. A state of energetic insufficiency is driven by a decline in feed intake and a sudden rise in energy demands caused by the quickly shifting of the cow metabolic landscape. The mobilization of non-esterified fatty acids (NEFA), which are used as energy, balances this situation. The Peroxisome Proliferator-Stimulated Receptor (PPAR), a transcriptional regulator with established nutrigenomic characteristics, is interestingly activated by peripartum NEFA. Precision-cut liver slices (PCLS) from liver biopsies were studied by Busato et al. as a model for PPAR activation in periparturient dairy cows. A subset of 91 genes among the differentially expressed genes in the bovine liver was been identified as potential novel PPAR targets.

Understanding the biological mechanisms governing feed efficiency using a readily available and non-invasive sample, like as blood, is crucial for the future of livestock production systems regarding profitability and animal welfare concerns. Critical pathways related to beef cattle's residual feed intake (RFI) were identified using the

gene set enrichment technique to analyze whole blood transcriptome data. Such finding revealed that depending on whether beef steers were divergently selected for low or high RFI, the expression of genes involved in protein metabolism and stress response varied (Taiwo et al.).

In the USA, intramuscular fat deposition or marbling is a key factor in determining the quality and worth of the carcass. The transient rise in intramuscular fat deposition suggests the involvement of an epigenetic adaptation. Bta-miR-122 was identified by small RNA sequencing as a possible miRNA of interest that may be related to intramuscular fat accumulation with rising time-on-concentrates (TOC). Using real-time ultrasound measurements of intramuscular fat, the authors suggest that preadipocyte differentiation may first be stimulated, triggering then a global up-regulation of lipogenic genes involved in *de novo* fatty acid synthesis, which provides fatty acids for subsequent hypertrophy. This hypothesis is supported by differential gene expression and increased intramuscular fat content (Duckett and Greene).

Wang X. et al. coupled multi-omics analyses with microbiome and metabolomics research to assess the impact of dietary protein levels on Tibetan sheep ruminal microbial communities and metabolites. According to this study, the optimal dietary protein intake for Tibetan sheep during the winter season is between 12.1 and 14.1% protein. This research improved our knowledge of ruminal microbial and metabolic processes and may influence the amount of protein needed in Tibetan sheep diets and of the nutritional control.

Allium mongolicum (AMO) Regel essential oil's effects on sheep growth performance, nutritional digestibility, rumen fermentation, and bacterial populations were studied by Yaxing et al. This study found higher cellulase, beta-amylase, and proteinase activity levels existed in the AMO group compared to the control group ($P < 0.05$). Dry matter (DM) and crude protein (CP) appeared to be more digestible in the AMO group than in the control group ($P < 0.05$). In conclusion, using AMO supplements may enhance growth efficiency. AMO supplementation also improved the rumen fermentation, bacterial populations, and nutrient digestibility in sheep.

By comparing the effects of food supplementation with and without *Bacillus subtilis* (*B. subtilis*), Tang X. et al. looked at how broiler chicken carcass characteristics, meat quality, amino acids, and fatty acids were affected. The findings indicated that adding *B. subtilis* to the feed could enhance broilers' meat quality and carcass characteristics. This would be advantageous for customers given the improved fatty acid profile and amino acid composition.

A significant commercial crop, soybean is the primary plant protein source for food, feed, and other industries. One of the eight allergenic foods, soybeans have the potential to negatively impact animal growth and health as well as the respiratory and digestive systems. The primary antigenic element of soybean protein is 11S glycinin. Wang L. et al., demonstrated that 11S Glycinin up-Regulated NLRP-3-Induced Pyroptosis by Triggering Reactive Oxygen Species (ROS) in Porcine Intestinal Epithelial Cells.

Lactobacillus plantarum (*L. plantarum*) CGMCC 1258 and Lactobacillus reuteri (*L. reuteri*) LR1 are two significant probiotic strains. According to research done by Tang Q. et al., dietary *L. reuteri* LR1 resulted in better growth performance, a lower incidence of diarrhea, better intestinal morphology, and a higher degree of immune activation in weaned pigs, while dietary *L. plantarum* CGMCC 1258 improved intestinal morphology, intestinal permeability, intestinal immunity, and antioxidant function in weaned pigs.

Shao et al. investigated how dietary selenium homolanthionine (SeHLan) affected the immune system and antioxidant status in puppies receiving canine parvovirus (CPV) vaccinations. Their research discovered that dietary SeHLan supplementation promoted immunological function, elevated CPV antibody titers, and improved antioxidant activity in puppies after weaning. A dose of SeHLan of 12 mg/kg DM in puppies may benefit their nutrition.

The articles on this Research Topic offer superb illustrations of nutriomics investigations and their significance for the wellbeing and output of livestock.

Author contributions

All authors listed have made a substantial, direct, and intellectual contribution to the work and approved it for publication.

Conflict of interest

The authors declare that the research was conducted in the absence of any commercial or financial relationships that could be construed as a potential conflict of interest.

Publisher's note

frontiers in Veterinary Science

ORIGINAL RESEARCH
published: 30 September 2021
doi: 10.3389/fvets.2021.728358

Supplemental Dietary Selenohomolanthionine Improve Antioxidant Activity and Immune Function in Weaned Beagle Puppies

Chunyan Shao[1†], Moufeng Zheng[1†], Ziwei Yu[1†], Sheng Jiang[1], Bin Zhou[1], Quanjiang Song[1], Tianning Ma[1], Yingshan Zhou[1], Wanyu Dong[1], Ding Li[2], Yao Gu[2], Xiaodu Wang[1*] and Houhui Song[1*]*

[1] Key Laboratory of Applied Technology on Green-Eco-Healthy Animal Husbandry of Zhejiang Province, Zhejiang Provincial Engineering Laboratory for Animal Health Inspection and Internet Technology, College of Animal Science and Technology, College of Veterinary Medicine, Zhejiang A&F University, Hangzhou, China, [2] ABNA Trading (Shanghai) Co., Ltd., Shanghai, China

OPEN ACCESS

Edited by:
Rita Payan Carreira,
University of Evora, Portugal

Reviewed by:
Maria Anjos Pires,
University of Trás-os-Montes and Alto Douro, Portugal
Dario Loureiro Santos,
Universidade de Trás-os-Montes e Alto Douro, Portugal

***Correspondence:**
Xiaodu Wang
xdwang@zafu.edu.cn
Houhui Song
songhh@zafu.edu.cn
Chunyan Shao
shaocy@zafu.edu.cn

[†] These authors have contributed equally to this work

Specialty section:
This article was submitted to Animal Nutrition and Metabolism, a section of the journal Frontiers in Veterinary Science

Received: 21 June 2021
Accepted: 23 August 2021
Published: 30 September 2021

Citation:
Shao C, Zheng M, Yu Z, Jiang S, Zhou B, Song Q, Ma T, Zhou Y, Dong W, Li D, Gu Y, Wang X and Song H (2021) Supplemental Dietary Selenohomolanthionine Improve Antioxidant Activity and Immune Function in Weaned Beagle Puppies. Front. Vet. Sci. 8:728358. doi: 10.3389/fvets.2021.728358

The purpose of this study was to investigate the effects of dietary Selenohomolanthionine (SeHLan) on antioxidant status and immune response in canine parvovirus (CPV) vaccinated puppies. In this study, 30 weaned puppies were randomly divided into six groups: control group (–Se/–Vacc), immunization group (–Se/+Vacc), supplementation of sodium selenite group (SS/+Vacc, 0.35 mg/kg DM), low-dose SeHLan group (SeHLan-L/+Vacc, 0.35 mg/kg DM), mid-dose SeHLan group (SeHLan-M/+Vacc, 1.0 mg/kg DM), and high-dose SeHLan group (SeHLan-H/+Vacc, 2.0 mg/kg DM). The puppies were fed for 42 days and vaccinated with Vanguard Plus 5 on day 0 and day 21. Blood samples were collected on 7, 14, 21, 28, 35, 42 days post-immunization (PI) for determination of antioxidant indicators, lymphocyte proliferation index, serum cytokine concentration (IL-2, IL-4), canine polymorphonuclear neutrophils (PMN) phagocytic function, and the level of CPV antibody titers. The results showed that SeHLan supplementation raised the serum Se concentration and glutathione peroxidase (GSH-Px) activity in a dose-dependent manner ($P < 0.05$). It also increased the activity of serum superoxide dismutase (SOD) and decreased serum malondialdehyde (MDA) content, especially in SeHLan-M/+Vacc group (1.0 mg/kg DM) ($P < 0.01$). SeHLan supplementation significantly increased lymphocyte proliferation, IL-2, and IL-4 levels in canine serum, and enhanced phagocytosis of PMN in vaccinated puppies ($P < 0.05$). Moreover, SeHLan supplementation shortened the CPV antibody production time and increased the CPV antibody titers ($P < 0.05$). Of note, the beneficial effects of SeHLan were superior to those of SS. In conclusion, dietary SeHLan supplementation improved antioxidant activity, increased CPV antibody titers, and enhanced immune function in puppies after weaning. An appropriate dosage of SeHLan (1∼2 mg/kg DM) may confer nutritional benefits in puppies.

Keywords: selenium, selenohomolanthionine, antioxidant activity, immune function, weaned puppies

INTRODUCTION

Selenium (Se) is a trace element that is necessary for human and animal life activities and has also been used as a natural antioxidant (1–3). Besides, it is a cofactor of antioxidant enzymes such as glutathione peroxidase (GSH-Px), which is involved in the elimination of peroxides and hydroxyl free radicals produced during metabolism (4–7). Furthermore, studies have shown that Se plays an important role in regulating innate and adaptive immune activity (8, 9), such as improving pro-inflammatory gene expression in macrophages (10), enhancing neutrophils functions (11) and promoting Chlamydia antibody production in sheep (12). The immune-enhancing activity of Se is largely attributed to the scavenging of free radicals and neutralizing of reactive oxygen species (ROS), thus, reducing oxidative stress (13). Dietary Se supplements are mainly in two forms: inorganic Se and organic Se. At present, inorganic Se remains the main source of Se in poultry (14) and livestock (15) nutrition. However, the application of inorganic Se is reduced in humans and companion animals due to its high toxicity and low biological utilization rate (16).

Weaning is a challenging stage for neonatal mammals, as they are more susceptible to various stresses (i.e., oxidative stress) due to reduced maternal antibodies, changes in living conditions, and food transition from liquid to solid (17). The immune status of weaned puppies gradually weakens and become more susceptible to viral infections, such as canine distemper virus (CDV) and canine parvovirus (CPV). In dogs vaccinated against *Taenia hydatigena*, the combination of vitamin E and Se supplementation group dogs showed the best immune response (18). An optimal immune response to rabies primovaccination was observed in cattle supplemental Se with a dose of 3.6 mg/d, whereas, the 5.4 and 6.4 mg/d doses were only just above control levels, suggesting that over-supplementation could cause immunosuppression (19). Therefore, the effect of Se is closely related to the dosage and form of supplemental Se. Selenohomolanthionine [4,4′-selenobis (2-aminobutanoic acid), SeHLan] is a kind of organic Se that is biosynthesized in *Candida utilis*, whose metabolic pathway is simple and can synthesize selenoprotein more effectively than selenomethionine (SeMet) (20, 21). However, as a new Se source, researches of SeHLan on companion animals are rarely reported. In this study, the effects of supplementing different levels of SeHLan on antioxidant activity and immune efficacy in beagle puppies were investigated to provide a basis for the application of SeHLan.

MATERIALS AND METHODS

Materials

Thirty 7-week-old male beagles with a weight of 3.05 ± 0.13 kg was purchased from Changzhou Bayle Experimental Animal Breeding Co., LTD [Ethics approval number SCXK (SU) 2018-0007]. Before the start of the experiment, all puppies underwent a normal basic physical examination and deworming, and the CPV antigen detection result was negative. Vanguard Plus 5 (Zoetis Inc., Lincoln, USA) was used for the vaccination of experimental puppies. Sodium selenite (SS) was purchased from Sigma and SeHLan was obtained from ABNA Trading Co., LTD. CPV strain was a generous gift from Dr. Wenbo Liu (Yangzhou University) and used for CPV antibody titers determination.

Experimental Design and Animal Trial

In a completely randomized experimental design, 30 beagles were randomly divided into six groups of 5 each: the control group (–Se/–Vacc), immunization group (–Se/+Vacc), SS group (SS/+Vacc) and three SeHLan supplemented group (SeHLan-L/+Vacc, SeHLan-M/+Vacc, SeHLan-H/+Vacc). The control and immunization group feeds were not supplemented with Se, while the SS group received SS in 0.35 mg/kg of food dry matter (DM). The SeHLan groups were fed on diets supplemented with different doses of SeHLan (0.35, 1.0, 2.0 mg/kg of food DM). Puppies except the control group were vaccinated with Vanguard Plus 5, the control group puppies were inoculated with equal amount of saline. The first day of vaccination was recorded as day 0, a second vaccination was performed on day 21 post-immunization (PI) as a booster dose. SS and SeHLan diet were given to puppies on the first day of vaccination and lasted for 42 days.

According to the Guidelines for The Nutrition of Pet Food for Cats and Dogs issued by the European Pet Food Industry Federation (FEDIAF), the standard of nutrition for the healthy growth of dogs requires that each beagle's daily energy intake is not <397.5 kJ/kg BW (22, 23). The basic diet formula and nutrient composition (**Table 1**) were analyzed by Zhejiang Guozheng Inspection Technology Co., LTD. The SeHLan used in this experiment was a commercial Se product with a Se concentration of 4 g/kg, thus, the supplemented dose in each SeHLan group was calculated as Se. The right dose of SS and SeHLan powder for each puppy were thoroughly mixed with their own diet. All puppies were allowed *ad libitum* access to fresh water. The beagles were placed in unit cages in the isolation area of the experimental base of Zhejiang A&F University. The indoor temperature was maintained at 20- 25°C, and all experimental protocols were approved by the Animal Care and Use Committee of Zhejiang A&F University.

Sample Collection and Preparation

Blood samples were collected from the canine cephalic vein on 0, 7, 14, 21, 28, 35, and 42 d PI. Part of the whole

TABLE 1 | Basic diet composition and nutrient level (Dry matter basis).

Ingredients	%	Nutrition level	Contents
Corn	28	Metabolic energy (MJ/kg)	16.45
Broken rice	12	Dry matter (g/100 g)	91.7
Wheat wheat	12	Crude fat crude fat (%)	15.2
Fishmeal	5	Calcium (%)	0.96
Chicken powder	25	Crude fiber crude fiber (%)	1.4
Egg powder	6	Crude protein (%)	27.1
Grease	4	Methionine (g/100 g)	0.45
Puree	6	Lysine lysine (g/100 g)	1.39
Dried carrots	2	Selenium (mg/kg)	0.06
Total	100	Total phosphorus total (%)	0.69

blood anticoagulated with heparin was separated and used for peripheral blood mononuclear cells (PBMCs) proliferation test and polymorphonuclear neutrophils (PMN) phagocytosis test. Besides, canine serum was collected and stored at −20°C for later use in the determination of serum Se concentration, glutathione peroxidase (GSH-Px), superoxide dismutase (SOD), malondialdehyde (MDA), cytokines (IL-2, IL-4), and CPV hemagglutination inhibition (HI) test.

Determination of Serum Se Concentration

The serum Se concentration was determined according to the method described by Donadio et al. (24) using a hydride generation-atomic absorption spectrophotometry. The serum is rapidly digested with a mixture of nitric and perchloric acids at a temperature of 180 ± 10°C, and hydrochloric acid is used to reduce Se (VI) to Se (IV).

Determination of the Activity of Serum Antioxidant Parameters

GSH-Px, SOD, and MDA levels were determined using assay kits obtained from Jiancheng Biochemical Co., LTD. (Nanjing, Jiangsu, China), according to the manufacturer's instructions. Briefly, GSH-Px activity was determined by the colorimetric method; SOD activity was determined by the hydroxylamine method (WST-1); MDA was assayed by the thiobarbituric acid (TBA) method. All experiments were performed in triplicate.

ConA-Induced PBMCs Proliferation Assay

The isolation of PBMCs and PMNs from whole blood was performed by the gradient density method using Histopaque-1077 and 1119 (Sigma, USA) simultaneously. In brief, 2.5 ml of whole blood was mixed with equivalent volume D-Hank's and layered onto 2.5 ml Histopaque-1077 and 2.5 ml Histopaque-1119 in 15 ml tubes. After centrifugation at 2,000 r/min for 20 min, the mixed solution was divided into six layers: plasma layer, mononuclear cells layer, cell separation solution layer (1077), granulocyte layer, cell separation solution layer (1119) and red blood cell layer. PBMCs were washed twice in D-Hank's and re-suspended in 1 ml $RPMI^+$ (RPMI-1640 with 100 Units/ml of Penicillin and 100 μg/ml of Streptomycin, 2 mM L-glutamine, and 10% heat-inactivated fetal calf serum), and stained with trypan blue to assess cell viability and ensure that the number of viable cells was above 90%. The cell suspension concentration was adjusted to 1×10^6/ml, dispensed at 100 μl/well in a 96-well plate, and ConA (Sigma, USA) was added at a final concentration at 2.5 μg/ml in the sample groups. In the control group: 100 μl PBMCs suspension and 100 μl $RPMI^+$, and in the Zero Group: 200 μl $RPMI^+$ were added. All the plates were incubated for 48 h at 37°C and 5% CO_2, and MTT (5 mg/mL) was added and incubated for 4 h. DMSO was used for lysis and dissolution of the crystals and the absorbance of each well was measured at OD_{570}. The stimulation index (SI) was used to determine the PBMCs proliferation function, SI = (sample group OD_{570} Value – zero group OD_{570} Value)/(control group OD $_{570}$ Value – zero group OD_{570} Value).

Enzyme-Linked Immunosorbent Assay for Detection of IL-2 and IL-4

The serum levels of IL-2 and IL-4 were determined using sandwich ELISA kits obtained from Wuhan Huamei Biotech Co., LTD (Wuhan, Hubei, China) according to the manufacturer's instructions individually. Optical density (OD) was measured at 450 nm for IL-2 and IL-4 using an automated microplate reader (BioTek SynergyTM H1, USA). All samples were tested in triplicate reactions.

Determination of PMN Phagocytosis of FITC-Labeled Bacteria

The isolated PMN from whole blood were washed twice in D-Hank's and re-suspended in 1 ml $RPMI^+$ at a concentration of 0.5×10^6/ml. *Staphylococcus aureus* (*S. aureus*) was cultured overnight and inactivated at 80°C for 1 h. Bacterial were washed and re-suspended in 1 ml PBS and labeled with 5 mg/ml fluorescein isothiocyanate (FITC, Sigma, USA) in 100 μl by incubating at room temperature (RT) for 1.5 h. The FITC bacteria were washed and re-suspended to 1×10^9/ml in PBS and stored at 4°C in the dark for subsequently use. 500 μl PMN suspension and 25 μl FITC-labeled *S. aureus* were thoroughly mixed and incubated at 28°C for 10 min. The mixed samples were centrifuged at 300 r/min for 5 min at 4°C, and the sediments were washed twice with D-Hank's solution and fixed with 1% paraformaldehyde. The percentage phagocytic activity of PMN was analyzed by flow cytometry (BD Accuri C6, USA). Generally, 10,000 cells were measured for each sample.

CPV HI Test

CPV antibodies were assayed as described by Carmichael et al. (25). Briefly, porcine whole blood was diluted 1:10 (v/v) with Alsever's solution and stored at 4°C. Before use, the solution was centrifuged at 1,500 r/min for 5 min and the supernatant was discarded. The sediments were washed three times with phosphate buffered solution (PBS, pH 7.2), then 1% porcine erythrocytes suspension was prepared in PBS. The CPV strain titer was determined by hemagglutination (HA) assay. A two-fold serial dilution of the virus was added in a V-96-well plate, mixed with equal volume 1% erythrocytes, and then incubated at 4°C for 1 h. The hemagglutination unit (HAU) was defined as the highest dilution that completely agglutinated reciprocal, and four HAU was used for HI experiments. The serum samples with double gradient dilution and 4 HAU of CPV were mixed and incubated at RT for 30 min, and then 1% erythrocytes were added and incubated at 4°C for 1 h. The CPV HI titers of the serum were determined based on the highest dilution of the four HAU that were completely inhibited and presented as log base 2 in the figure Y-axis. The protective antibody titer (PAT) of CPV was ≥1:80 (26), and log base 2 of 80 was $2^{6.3}$. Each serum sample was tested in triplicate.

Statistical Analysis

All statistical analyses were performed with SPSS Statistics 21.0 (IBM, USA). One-way ANOVA was used to compare the differences between groups. All values in each treatment group

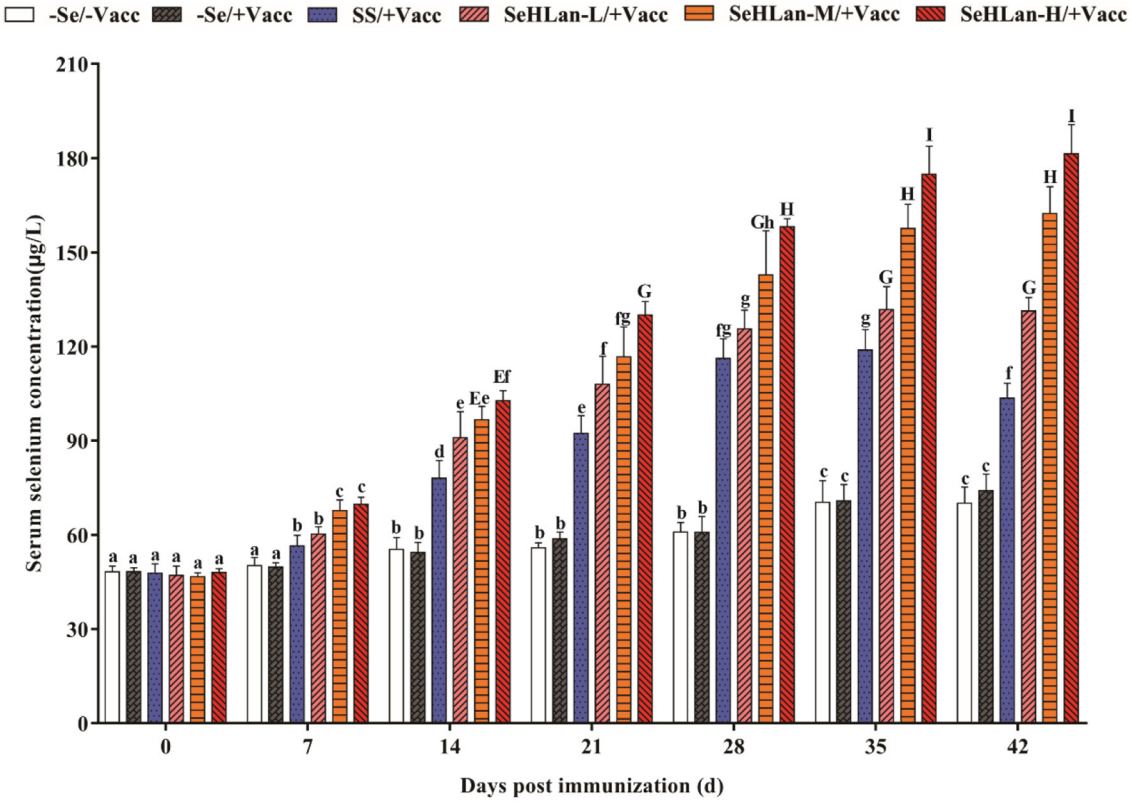

FIGURE 1 | Effects of Se supplementation on serum Se concentration of puppies at different days post-immunization. All values in each treatment group are presented as means ± SD ($n = 5$). Within a panel, bars labeled with the same letters but different capitalization indicate significant differences ($P < 0.05$), and the absence of the same letters indicate extremely significant differences ($P < 0.01$). –Se/–Vacc: puppies were fed with basal diet and unvaccinated; –Se/+Vacc: puppies were fed with basal diet and vaccinated with Vanguard Plus 5; SS/+Vacc: puppies were fed with SS (0.35 mg/kg DM) and vaccinated; SeHLan-L(M/H)/+Vacc: puppies were fed with SeHLan (0.35, 1, 2 mg/kg DM, respectively) and vaccinated.

are presented as mean ± standard deviation. $P < 0.05$ was considered significant.

RESULTS

SeHLan Significantly Increased Serum Se Concentration in Weaned Puppies

As shown in **Figure 1**, there was no significant difference in serum Se concentration between the –Se/–Vacc and –Se /+Vacc groups during the entire experiment. The serum Se concentration in the two Se unsupplementation groups showed a significantly increase on 14 d PI, and a 1.45-fold increase in serum Se concentration was observed in the control group on 42 d PI compared with that on 0 d PI. While the serum Se concentration in the SS and SeHLan groups showed an extremely high increase on 7 d PI ($P < 0.01$). The serum Se concentration of puppies in the SeHLan-L/+Vacc group was significantly higher compared with that in the SS group during 14∼42 days PI ($P < 0.05$). Besides, the serum Se concentration gradually increased in the SeHLan groups with an increase in supplementation. The most significant increase of serum Se concentration of puppies was observed in the SeHLan-H/+Vacc group with a 3.78-fold increase on 42 d PI compared with that on 0 d PI.

SeHLan Significantly Improved Serum Antioxidant Activity in Weaned Puppies

An upward trend of serum GSH-Px activity in puppies were observed in the control and immunization groups throughout the study (**Figure 2A**). The serum GSH-Px activity in the SS and SeHLan supplementation groups significantly increased on 7 d PI. SS showed lower GSH-Px activity compared with the SeHLan supplementation group with a same Se dosage (0.35 mg/kg DM). The serum GSH-Px activity significantly increased with an increase in the dosage of SeHLan ($P < 0.01$), which was similar to the changes in serum Se concentration.

The activity of serum SOD in all groups with or without Se supplementation increased and peaked around 28 d PI, then decreased gradually (**Figure 2B**). The increased range of serum SOD activity was significantly higher in SS and the three SeHLan supplementation groups compared with the control group. There was no significant difference in serum SOD activity between the SS/+Vacc and SeHLan-L/+Vacc groups. Notably, the serum SOD activity in the SeHLan-M/+Vacc group was highest and showed a significant difference on 28 d PI.

The serum MDA content remained stable for 21 days in the control group at the beginning of the experiment and later began to decline (**Figure 2C**). Serum MDA levels were significantly

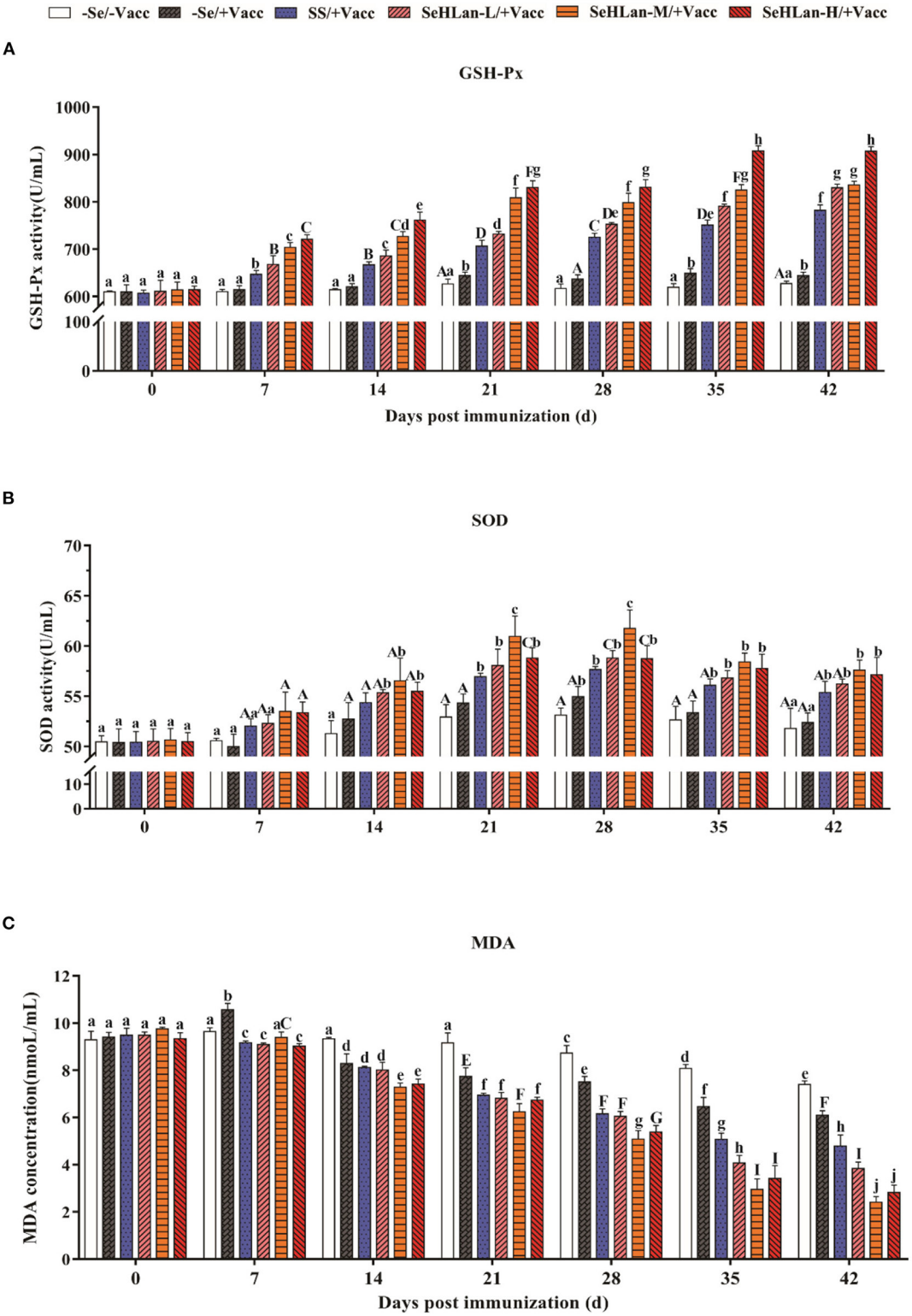

FIGURE 2 | The influence of Se Supplementation on serum GSH-Px **(A)**, SOD **(B)** activities and MDA **(C)** content of puppies at different days post-immunization. All values in each treatment group are presented as means ± SD ($n = 5$). Within a panel, bars labeled with the same letters but different capitalization indicate significant differences ($P < 0.05$), and the absence of the same letters indicate extremely significant differences ($P < 0.01$). –Se/–Vacc: puppies were fed with basal diet and unvaccinated; –Se/+Vacc: puppies were fed with basal diet and vaccinated with Vanguard Plus 5; SS/+Vacc: puppies were fed with SS (0.35 mg/kg DM) and vaccinated; SeHLan-L(M/H)/+Vacc: puppies were fed with SeHLan (0.35, 1, 2 mg/kg DM, respectively) and vaccinated.

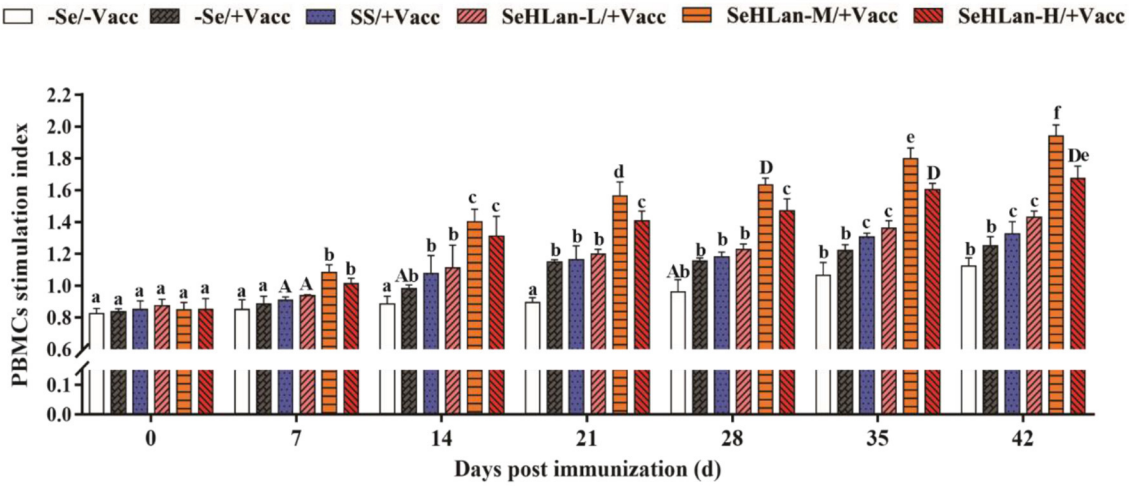

FIGURE 3 | The influence of Se supplementation on PBMCs stimulation index of puppies at different days post-immunization. All values in each treatment group are presented as means ± SD ($n = 5$). Within a panel, bars labeled with the same letters but different capitalization indicate significant differences ($P < 0.05$), and the absence of the same letters indicate extremely significant differences ($P < 0.01$). –Se/–Vacc: puppies were fed with basal diet and unvaccinated; –Se/+Vacc: puppies were fed with basal diet and vaccinated with Vanguard Plus 5; SS/+Vacc: puppies were fed with SS (0.35 mg/kg DM) and vaccinated; SeHLan-L(M/H)/+Vacc: puppies were fed with SeHLan (0.35, 1, 2, respectively) and vaccinated.

decreased in the SS group and the three SeHLan supplementation groups on 7 d PI ($P < 0.01$). Furthermore, the decrease was significantly higher in all Se supplementation groups than in the control group and the immunization group throughout the study ($P < 0.01$). Among all the groups, the serum MDA content decreased the most in the moderate SeHLan supplementation group (1.0 mg/kg DM).

SeHLan Significantly Improved the Proliferation of PBMCs in Weaned Puppies

The proliferation of PBMCs showed no significant changes in the first 21 d in the experiment but later gently increased in the control group (**Figure 3**). Vaccination stimulated the proliferation of PBMCs which was significantly higher in the immunization group compared with the control group between 14∼28 days PI ($P < 0.05$). A significant increase in PBMCs proliferation was observed in SS and SeHLan supplementation groups. Besides, the increase in PBMCs proliferation was most significant in the SeHLan-M/+Vacc group compared with the control group on 42 d PI ($P < 0.01$).

SeHLan Significantly Increased Serum IL-2 and IL-4 Concentration in Weaned Puppies

No significant changes were reported both in serum of IL-2 and IL-4 concentration in the first 14 d in the experiment but later gently increased in the control group (**Figure 4**). However, a two-fold increase both in IL-2 and IL-4 production was observed in the immunization group compared with the control group on 7 d PI. Se supplementation contributed to IL-2 and IL-4 production. The improved effect of serum IL-2 and IL-4 concentration at low dosage SeHLan supplementation (0.35 mg/kg DM) was higher than that in the SS supplementation group ($P < 0.05$). Among the three SeHLan supplementation groups, the SeHLan-M/+Vacc group showed the greatest improvement in serum concentration of IL-2 on 35 d PI and IL-4 on 21 d PI, respectively. The serum IL-2 concentration peaked two times on 14 d and 35 d PI, respectively. However, serum IL-4 concentration peaked on 21 d PI in the SeHLan-M/+Vacc group, then decreased gradually, and showed significant difference compared with the immunization group.

SeHLan Significantly Improved PMN Phagocytosis in Weaned Puppies

As shown in **Figures 5A,B**, there was no significant difference in PMN phagocytosis in the control group until on 21 d PI. However, the immunization group showed a sharp increase in PMN phagocytosis following vaccination. Se supplementation increased the phagocytic ability of PMN. There was no significant difference in PMN phagocytosis between the –Se/+Vacc and SS/+Vacc groups in the first 14 d ($P > 0.05$), however, during the trial period, PMN phagocytosis in the SS/+Vacc group was significantly higher compared with that in the –Se/+Vacc group ($P < 0.01$). Among all the Se supplementation groups, the improved effect of PMN phagocytosis in the SeHLan group was higher than that in the SS group. The SeHLan-M/+Vacc and SeHLan-H/+Vacc groups showed the similar and higher phagocytic ability of PMN, with the phagocytic rate maintained above 90% between 14 ∼ 42 d PI, and was significantly higher than that in the SeHLan-L/+Vacc group ($P < 0.05$).

SeHLan Significantly Improved CPV HI Titers in Weaned Puppies

The CPV antibody titers were similar and below the PAT of $2^{6.3}$ at the start of the experiment in all puppies. However, during the experiment period, the CPV HI titers increased and then decreased, with a small range variation and still under PAT

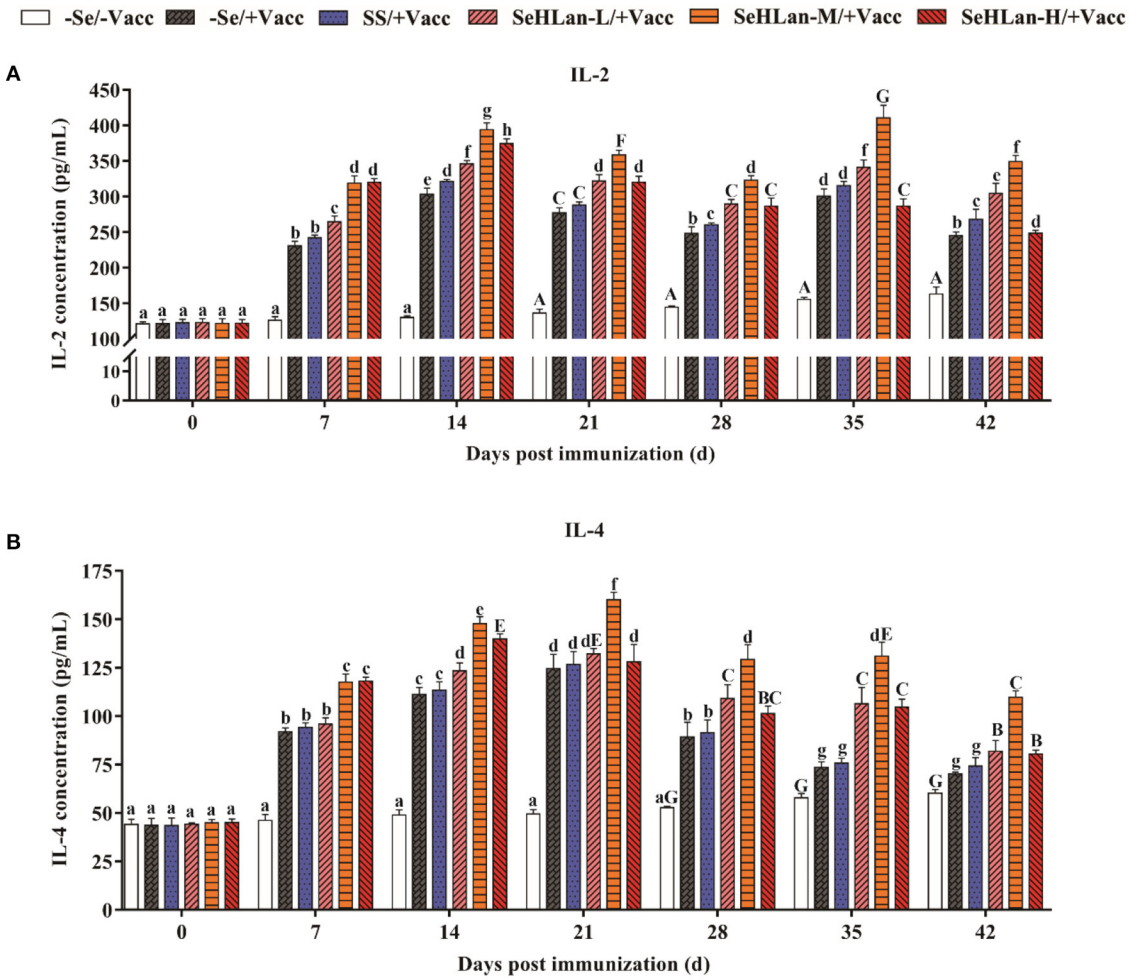

FIGURE 4 | The influence of Se supplementation on serum IL-2 **(A)** and IL-4 **(B)** concentration of puppies at different days post immunization. All values in each treatment group are presented as means ± SD ($n = 5$). Within a panel, bars labeled with the same letters but different capitalization indicate significant differences ($P < 0.05$), and the absence of the same letters indicate extremely significant differences ($P < 0.01$). –Se/–Vacc: puppies were fed with basal diet and unvaccinated; –Se/+Vacc: puppies were fed with basal diet and vaccinated with Vanguard Plus 5; SS/+Vacc: puppies were fed with SS (0.35 mg/kg DM) and vaccinated; SeHLan-L(M/H)/+Vacc: puppies were fed with SeHLan (0.35, 1, 2 mg/kg DM, respectively) and vaccinated.

levels. As shown in **Figure 6**, CPV HI titers increased in all the vaccinated puppies but remained below the PAT level on 7 d PI, except in the SeHLan-H/+Vacc group. A rapid increase in CPV HI titers was observed on 14 d PI in all vaccinated puppies, and all the titers were higher than the PAT level. The results showed that Se supplementation improved CPV antibody production. With a same Se dosage, the promoting effects of CPV antibody showed a significant difference between the SeHLan-L/+Vacc (0.35 mg/kg DM) group and the SS group ($P < 0.05$). Among the three SeHLan supplementation groups, the SeHLan-H/+Vacc group showed the highest promoting effect for CPV antibody titers.

DISCUSSION

In this study, we investigated the antioxidative and immunomodulatory effects of SeHLan in weaned puppies during a vaccination period. Serum Se concentration is sensitive to changes in diet supplemented with extra Se source and can be used as a biomarker of Se concentration in dogs (22, 23). In this study, the daily intake of the basal diet was increased based on the age and weight of puppies in the control and immunization groups. The Se concentration of the basal diet was 0.06 mg/kg, hence, the serum Se concentration in the two groups was moderately increased. According to AAFCO, the minimum and maximum amount of Se used in dog food are 0.35 and 2.0 mg/kg DM, meaning that the dosage of SS and SeHLan adopted in this study was safe. The results showed that there was a dose-dependent relationship between serum Se concentration and the amount of SeHLan in all the three SeHLan supplementation groups. Moreover, the serum Se concentration in the SeHLan supplementation groups was significantly higher than in the SS group supplied with equivalent doses. Similar results were observed in lambs treated with different sources of Se (27).

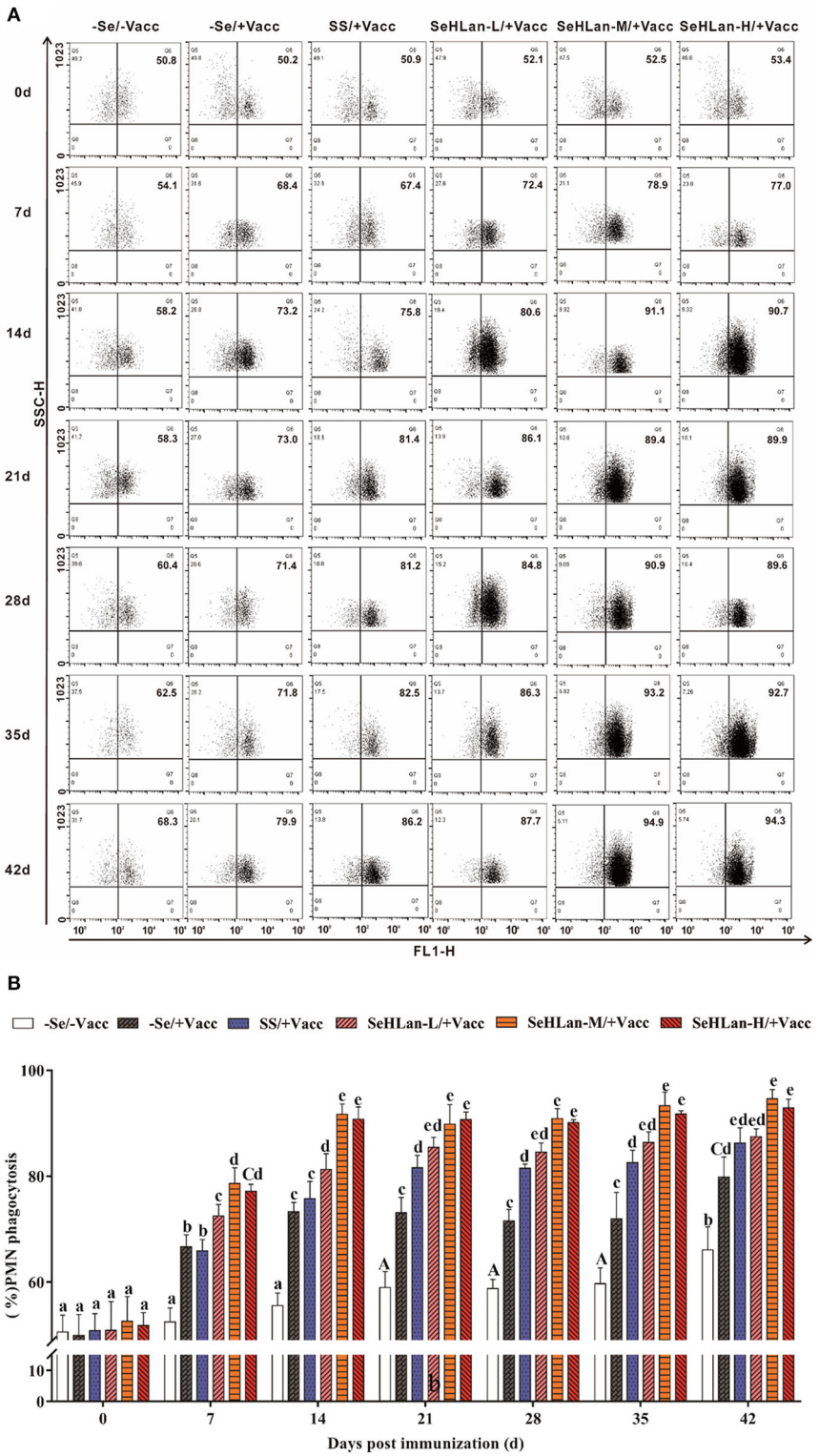

FIGURE 5 | The influence of Se supplementation on PMN phagocytosis of puppies at different days post-immunization. **(A)** Flow cytometric analysis of the phagocytosis of the *S. aureus* treated PMN. **(B)** Quantitative analysis of PMN undergoing phagocytosis. All values in each treatment group are presented as means ± SD ($n = 5$). Within a panel, bars labeled with the same letters but different capitalization indicate significant differences ($P < 0.05$), and the absence of the same letters indicate extremely significant differences ($P < 0.01$). –Se/–Vacc: puppies were fed with basal diet and unvaccinated; –Se/+Vacc: puppies were fed with basal diet and vaccinated with Vanguard Plus 5; SS/+Vacc: puppies were fed with SS (0.35 mg/kg DM) and vaccinated; SeHLan-L(M/H)/+Vacc: puppies were fed with SeHLan (0.35, 1, 2 mg/kg DM, respectively) and vaccinated.

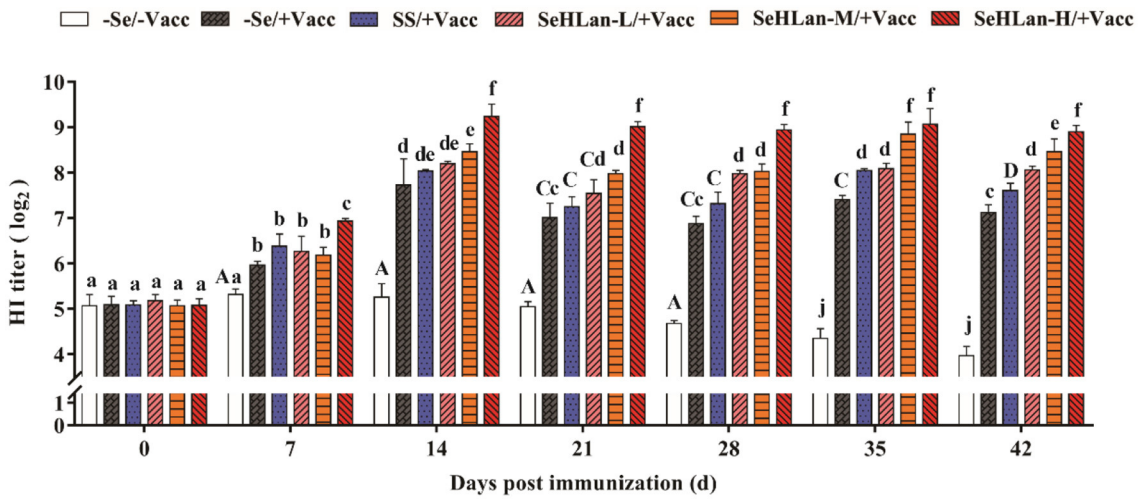

FIGURE 6 | Effect of Se supplementation on serum CPV HI titers of puppies at different days post-immunization. All values in each treatment group are presented as means ± SD ($n = 5$). Within a panel, bars labeled with the same letters but different capitalization indicate significant differences ($P < 0.05$), and the absence of the same letters indicate extremely significant differences ($P < 0.01$). –Se/–Vacc: puppies were fed with basal diet and unvaccinated; –Se/+Vacc: puppies were fed with basal diet and vaccinated with Vanguard Plus 5; SS/+Vacc: puppies were fed with SS (0.35 mg/kg DM) and vaccinated; SeHLan-L(M/H)/+Vacc: puppies were fed with SeHLan (0.35, 1, 2 mg/kg DM, respectively) and vaccinated.

The level of immunity in puppies at weaning is relatively low and they are susceptible to a variety of diseases. Similarly, the frequency of infections in puppies with diarrhea around weaning is high. A recent study reported that selenium-enriched yeast elevated the GSH-Px levels and decreased the MDA content in laying ducks (28). As expected, the antioxidative capacity was significantly increased by Se in this study, and the promoting effects of SeHLan supplementation were better than that in SS supplied with equivalent doses. As a Se containing peroxidase, GSH-Px is a major group of enzymes that eliminate hydrogen peroxide which is extremely harmful to the cell. In the present study, SeHLan promoted the GSH-Px activity in a time and dose-dependent manner. The moderate doses of SeHLan supplementation (1 mg/kg DM) exhibited the highest increase in SOD activity and the highest decrease in MDA content in serum. However, significant changes in the antioxidative capacity were observed in the control and immunization groups, which was largely attributed to the increase in age. Similarly, SeMet supplementation in the diet significantly improved the antioxidant capacity and plasma Se concentration in weaning piglets (29). Moreover, oxidative stress-induced intestinal mucosa disruption were attenuated by adding selenium-enriched yeast in weaned pigs in a HO-1/Nrf2 pathway, which is a critical transcription signal in antioxidant enzymes production (17).

PMN constitute the first line of defense in the protection of the host from invading microorganisms. During phagocytosis, ROS are produced and the consequent production of free radicals which are eliminated through the antioxidant defense system (30). Administration of Se to goats fed on Se-deficient diet resulted in increased PMN function which was associated with physiologic changes in the GSH-Px level (31). As expected, the phagocytic ability of PMN increased in the SS and three SeHLan supplementation groups in this study. Numerous researches have confirmed that Se enhances the function of various kinds of immunocompetent cells. PBMCs proliferation is routinely used to evaluate lymphocyte response stimulated by non-specific mitogens. In the present study, vaccination with Vanguard Plus 5 increased PBMCs proliferation and PMN phagocytosis and promoted the production of IL-2 and IL-4. Meanwhile, Se supplementation in basal diet improved the immune response, while the moderate doses of SeHLan supplementation (1 mg/kg DM) showed the greatest-promoting effect. IL-2 is mainly produced by type 1 T helper (Th1) cells and plays a significant role in macrophage activation and in promoting a cell-mediated immune response (32). Previous studies have reported consistent results, that Se promotes glutathione peroxidase (GPx1) and thioredoxin reductase 1 (TR1) expression, and enhances ConA induced T-cell activation and secretion of IL-2 in porcine splenocytes (33). The ability of Se to induce augmented expression of IL-2 appears to occur through the increased expression of the IL-2 receptor (34). As a major product of type 2 T helper (Th2) cells, IL-4 is also a potent inducer of Th2 differentiation (35). Besides, IL-4 can promote B lymphocyte proliferation and immunoglobulin secretion (36). In this study, maternal antibody serum HI titers declined to 2^5 at 7 weeks of age and kept decreasing in the control group, and the levels were below the PAT level. About 14 days were needed after vaccination to achieve a protective titer against CPV. Therefore, the lack of a protective stage was highly important for puppies needing more protection. In a previous study, Se supplemented chicken showed higher IgM and IgY titers after vaccination with low pathogenicity avian influenza virus vaccine (37). Besides, a previous study in humans

showed that the mRNA expression levels of selenoprotein S (SEPS1) significantly increased 7 days after an influenza vaccine challenge with Se supplementation (38). As shown in our study, Se supplementation not only improved the CPV antibody HI titers but also shortened antibody production time. The high doses of SeHLan supplementation (2 mg/kg DM) manifested the greatest CPV HI titers promoting effect.

CONCLUSIONS

The present study suggested that dietary SeHLan supplementation improved the antioxidant activity, increased CPV antibody HI titers, and enhanced the immune function in puppies after weaning. Moreover, the beneficial effects of SeHLan were superior to those in the SS group supplied with equivalent doses of SS. Finally, we conclude that the right amount of SeHLan (1∼2 mg/kg DM) can serve as a potential nutrition additive in puppy feeding.

DATA AVAILABILITY STATEMENT

The original contributions presented in the study are included in the article/supplementary material, further inquiries can be directed to the corresponding author/s.

ETHICS STATEMENT

This study was approved by the Institutional Animal Care and Use Committee of Zhejiang Province (Permit Number: SYXK-2018-0010).

AUTHOR CONTRIBUTIONS

XW and HS conceived and designed the study. CS, MZ, ZY, and TM performed the experiments. SJ, BZ, and QS analyzed the data. CS wrote the manuscript. YZ, WD, DL, and YG revised it critically for important content. All authors have read and approved the final version of the manuscript.

FUNDING

This study was supported by Zhejiang Provincial Natural Science Foundation (Nos. LQ19C180003 and LQ20C180002); the National Natural Science Foundation of China (Nos. 31902249, 31802258, and 31602119); Zhejiang A&F University (Nos. 2015FR042, 2018FR009, 2018FR015, and 2019FR013); Department of Education of Zhejiang Province (No. Y202044917); and Key Research and Development Program of Zhejiang Province (2019C02043).

REFERENCES

1. Schrauzer GN. The nutritional significance, metabolism and toxicology of selenomethionine. *Adv Food Nutr Res.* (2003) 47:73-112. doi: 10.1016/S1043-4526(03)47002-2
2. Rayman MP, Infante HG, Sargent M. Food-chain selenium and human health: spotlight on speciation. *Br J Nutr.* (2008) 100:238-53. doi: 10.1017/S0007114508922522
3. Roman M, Jitaru P, Barbante C. Selenium biochemistry and its role for human health. *Metallomics.* (2014) 6:25-54. doi: 10.1039/C3MT00185G
4. Wang N, Tan HY, Li S, Xu Y, Guo W, Feng Y. Supplementation of micronutrient selenium in metabolic diseases: its role as an antioxidant. *Oxid Med Cell Longev.* (2017) 2017:7478523. doi: 10.1155/2017/7478523
5. Solovyev ND. Importance of selenium and selenoprotein for brain function: from antioxidant protection to neuronal signalling. *J Inorg Biochem.* (2015) 153:1-12. doi: 10.1016/j.jinorgbio.2015.09.003
6. Liu K, Liu H, Zhang T, Mu L, Liu X, Li G. Effects of vitamin E and selenium on growth performance, antioxidant capacity, and metabolic parameters in growing furring blue foxes (Alopex lagopus). *Biol Trace Elem Res.* (2019) 192:183-95. doi: 10.1007/s12011-019-1655-4
7. Surai PF, Fisinin VI, Karadas F. Antioxidant systems in chick embryo development. Part 1. Vitamin E, carotenoids and selenium. *Anim Nutr.* (2016) 2:1-11. doi: 10.1016/j.aninu.2016.01.001
8. Beck MA, Nelson HK, Shi Q, Van Dael P, Schiffrin EJ, Blum S, et al. Selenium deficiency increases the pathology of an influenza virus infection. *FASEB J.* (2001) 15: 1481-3. doi: 10.1096/fj.00-0721fje
9. Beck MA, Levander OA, Handy J. Selenium deficiency and viral infection. *J Nutr.* (2003) 133:1463S-7S. doi: 10.1093/jn/133.5.1463S
10. Vunta H, Belda BJ, Arner RJ, Channa Reddy C, Vanden Heuvel JP, Sandeep Prabhu K. Selenium attenuates pro-inflammatory gene expression in macrophages. *Mol Nutr Food Res.* (2008) 52:1316-23. doi: 10.1002/mnfr.200700346
11. Ibeagha AE, Ibeagha-Awemu EM, Mehrzad J, Baurhoo B, Kgwatalala P, Zhao X. The effect of selenium sources and supplementation on neutrophil functions in dairy cows. *Animal.* (2009) 3:1037-43. doi: 10.1017/S1751731109004303
12. Giadinis N, Koptopoulos G, Roubles N, Siarkou V, Papasteriades A. Selenium and vitamin E effect on antibody production of sheep vaccinated against enzootic abortion (Chlamydia psittaci). *Comp Immunol Microbiol Infect Dis.* (2000) 23:129-37. doi: 10.1016/S0147-9571(99)00066-1
13. Hoffmann PR, Berry MJ. The influence of selenium on immune responses. *Mol Nutr Food Res.* (2008) 52:1273-80. doi: 10.1002/mnfr.200700330
14. Surai PF, Kochish, II, Fisinin VI, Velichko OA. Selenium in poultry nutrition: from sodium selenite to organic selenium sources. *J Poul Sci.* (2018) 55:79-93. doi: 10.2141/jpsa.0170132
15. Grilli E, Gallo A, Fustini M, Fantinati P, Piva A. Microencapsulated sodium selenite supplementation in dairy cows: effects on selenium status. *Animal.* (2013) 7:1944-9. doi: 10.1017/S1751731113001547
16. Brodin O, Eksborg S, Wallenberg M, Asker-Hagelberg C, Larsen EH, Mohlkert D, et al. Pharmacokinetics and toxicity of sodium selenite in the treatment of patients with carcinoma in a phase i clinical trial: the SECAR study. *Nutrients.* (2015) 7:4978-94. doi: 10.3390/nu7064978
17. Liu L, Wu C, Chen D, Yu B, Huang Z, Luo Y, et al. Selenium-enriched yeast alleviates oxidative stress-induced intestinal mucosa disruption in weaned pigs. *Oxid Med Cell Longev.* (2020) 2020:5490743. doi: 10.1155/2020/5490743
18. Kandil OM, Abou-Zeina HA. Effect of parenteral vitamin E and selenium supplementation on immune status of dogs vaccinated with subunit and somatic antigens against Taenia hydatigena. *J Egypt Soc Parasitol.* (2005) 35:537-50.
19. Reis LS, Chiacchio SB, Oba E, Pardo PE, Frazatti-Gallina NM. Selenium supplementation and rabies antibody titres in cattle. *Veter Rec.* (2008) 163:343-4. doi: 10.1136/vr.163.11.343-b
20. Tsuji Y, Mikami T, Anan Y, Ogra Y. Comparison of selenohomolanthionine and selenomethionine in terms of selenium distribution and toxicity in rats by bolus administration. *Metallomics.* (2010) 2:412-8. doi: 10.1039/c004026f
21. Liu K, Ding T, Fang L, Cui L, Li J, Meng X, et al. Organic Selenium Ameliorates *Staphylococcus aureus*-induced mastitis in rats by inhibiting the activation of NF-kappaB and MAPK signaling pathways. *Front Veter Sci.* (2020) 7:443. doi: 10.3389/fvets.2020.00443
22. van Zelst M, Hesta M, Gray K, Staunton R, Du Laing G, Janssens GP. Biomarkers of selenium status in dogs. *BMC Veter Res.* (2016) 12:15. doi: 10.1186/s12917-016-0639-2

23. Pedrinelli V, Gomes MOS, Carciofi AC. Analysis of recipes of home-prepared diets for dogs and cats published in Portuguese. *J Nutr Sci.* (2017) 6:e33. doi: 10.1017/jns.2017.31
24. Donadio JL, Guerra-Shinohara EM, Rogero MM, Cozzolino SM. Influence of gender and SNPs in GPX1 gene on biomarkers of selenium status in healthy Brazilians. *Nutrients.* (2016) 8:81. doi: 10.3390/nu8050081
25. Carmichael LE, Joubert JC, Pollock RV. Hemagglutination by canine parvovirus: serologic studies and diagnostic applications. *Am J Veter Res.* (1980) 41:784-91.
26. Lechner ES, Crawford PC, Levy JK, Edinboro CH, Dubovi EJ, Caligiuri R. Prevalence of protective antibody titers for canine distemper virus and canine parvovirus in dogs entering a Florida animal shelter. *J Am Vet Med Assoc.* (2010) 236:1317-21. doi: 10.2460/javma.236.12.1317
27. Tiwary AK, Stegelmeier BL, Panter KE, James LF, Hall JO. Comparative toxicosis of sodium selenite and selenomethionine in lambs. *J Veter Diagn Invest.* (2006) 18:61-70. doi: 10.1177/104063870601800108
28. Zhang X, Tian L, Zhai S, Lin Z, Yang H, Chen J, et al. Effects of selenium-enriched yeast on performance, egg quality, antioxidant balance, and egg selenium content in laying ducks. *Front Veter Sci.* (2020) 7:591. doi: 10.3389/fvets.2020.00591
29. Cao J, Guo F, Zhang L, Dong B, Gong L. Effects of dietary Selenomethionine supplementation on growth performance, antioxidant status, plasma selenium concentration, and immune function in weaning pigs. *J Anim Sci Biotechnol.* (2014) 5:46. doi: 10.1186/2049-1891-5-46
30. Kono M, Saigo K, Matsuhiroya S, Takahashi T, Hashimoto M, Obuchi A, et al. Detection of activated neutrophils by reactive oxygen species production using a hematology analyzer. *J Immunol Methods.* (2018) 463:122-6. doi: 10.1016/j.jim.2018.10.004
31. Aziz ES, Klesius PH, Frandsen JC. Effects of selenium on polymorphonuclear leukocyte function in goats. *Am J Veter Res.* (1984) 45:1715-8.
32. Hwang ES, Hong JH, Glimcher LH. IL-2 production in developing Th1 cells is regulated by heterodimerization of RelA and T-bet and requires T-bet serine residue 508. *J Exp Med.* (2005) 202:1289-300. doi: 10.1084/jem.20051044
33. Ren F, Chen X, Hesketh J, Gan F, Huang K. Selenium promotes T-cell response to TCR-stimulation and ConA, but not PHA in primary porcine splenocytes. *PLoS ONE.* (2012) 7:e35375. doi: 10.1371/journal.pone.0035375
34. Baum MK, Miguez-Burbano MJ, Campa A, Shor-Posner G. Selenium and interleukins in persons infected with human immunodeficiency virus type 1. *J Infect Dis.* (2000) 182(Suppl 1): S69-73. doi: 10.1086/315911
35. Vijayanand P, Seumois G, Simpson LJ, Abdul-Wajid S, Baumjohann D, Panduro M, et al. Interleukin-4 production by follicular helper T cells requires the conserved Il4 enhancer hypersensitivity site V. *Immunity.* (2012) 36:175-87. doi: 10.1016/j.immuni.2011.12.014
36. Wang X, Zuo Z, Deng J, Zhang Z, Chen C, Fan Y, et al. Protective role of selenium in immune-relevant cytokine and immunoglobulin production by piglet splenic lymphocytes exposed to deoxynivalenol. *Biol Trace Elem Res.* (2018) 184:83-91. doi: 10.1007/s12011-017-1160-6
37. Shojadoost B, Taha-Abdelaziz K, Alkie TN, Bekele-Yitbarek A, Barjesteh N, Laursen A, et al. Supplemental dietary selenium enhances immune responses conferred by a vaccine against low pathogenicity avian influenza virus. *Veter Immunol Immunopathol.* (2020) 227:110089. doi: 10.1016/j.vetimm.2020.110089
38. Goldson AJ, Fairweather-Tait SJ, Armah CN, Bao Y, Broadley MR, Dainty JR, et al. Effects of selenium supplementation on selenoprotein gene expression and response to influenza vaccine challenge: a randomised controlled trial. *PLoS ONE.* (2011) 6:e14771. doi: 10.1371/journal.pone.0014771

Conflict of Interest: DL and YG were employed by ABNA Trading (Shanghai) Co., Ltd.

The remaining authors declare that the research was conducted in the absence of any commercial or financial relationships that could be construed as a potential conflict of interest.

Publisher's Note: All claims expressed in this article are solely those of the authors and do not necessarily represent those of their affiliated organizations, or those of the publisher, the editors and the reviewers. Any product that may be evaluated in this article, or claim that may be made by its manufacturer, is not guaranteed or endorsed by the publisher.

frontiers in Veterinary Science

ORIGINAL RESEARCH
published: 11 November 2021
doi: 10.3389/fvets.2021.728849

Comparative Effects of *L. plantarum* CGMCC 1258 and *L. reuteri* LR1 on Growth Performance, Antioxidant Function, and Intestinal Immunity in Weaned Pigs

Qingsong Tang[1,2†], Hongbo Yi[1†], Weibin Hong[1], Qiwen Wu[1], Xuefen Yang[1], Shenglan Hu[1], Yunxia Xiong[1], Li Wang[1] and Zongyong Jiang[1*]*

[1] State Key Laboratory of Livestock and Poultry Breeding, Ministry of Agriculture Key Laboratory of Animal Nutrition and Feed Science in South China, Guangdong Key Laboratory of Animal Breeding and Nutrition, Maoming Branch, Guangdong Laboratory for Lingnan Modern Agriculture, Institute of Animal Science, Guangdong Academy of Agricultural Sciences, Guangzhou, China, [2] College of Animal Science, Institute of Animal Nutrition and Feed Science, Guizhou University, Guiyang, China

OPEN ACCESS

Edited by:
Rita Payan Carreira,
University of Evora, Portugal

Reviewed by:
Richard Faris,
Cargill, United States
Susana María Martín-Orúe,
Universitat Autònoma de Barcelona, Spain

***Correspondence:**
Li Wang
wangli1@gdaas.cn
Zongyong Jiang
jiangzy@gdaas.cn

[†]These authors have contributed equally to this work

Specialty section:
This article was submitted to Animal Nutrition and Metabolism, a section of the journal Frontiers in Veterinary Science

Received: 22 June 2021
Accepted: 12 October 2021
Published: 11 November 2021

Citation:
Tang Q, Yi H, Hong W, Wu Q, Yang X, Hu S, Xiong Y, Wang L and Jiang Z (2021) Comparative Effects of L. plantarum CGMCC 1258 and L. reuteri LR1 on Growth Performance, Antioxidant Function, and Intestinal Immunity in Weaned Pigs. Front. Vet. Sci. 8:728849. doi: 10.3389/fvets.2021.728849

Lactobacillus plantarum CGMCC 1258 and *Lactobacillus reuteri* LR1 are two important strains of probiotics. However, their different advantages in the probiotic effect of weaned pigs are still poorly understood. Therefore, the study was to investigate the comparative effects of dietary supplementation of *L. plantarum* CGMCC 1258 and *L. reuteri* LR1 on growth performance, antioxidant function, and intestinal immunity in weaned pigs. Ninety barrows [initial body weight (BW) = 6.10 ± 0.1 kg] 21 days old were randomly divided into 3 treatments with 5 replicates, each replicate containing 6 pigs. Pigs in control (CON) were fed a basal diet, and the basal diets supplemented with 5×10^{10} CFU/kg *L. plantarum* CGMCC 1258 (LP) or *L. reuteri* LR1 (LR) for 42 days, respectively. The results showed that LP increased ($p < 0.05$) serum superoxide dismutase (SOD), and decreased ($p < 0.05$) serum malondialdehyde (MDA) and the expression and secretion of interleukin-1β (IL-1β), tumor necrosis factor-α (TNF-α), and interferon-γ (IFN-γ) in intestinal mucosa, but has no significant effect on growth performance and diarrheal incidence. However, LR increased ($p < 0.05$) final BW and average daily gain (ADG), reduced ($p < 0.05$) 29–42-day diarrheal incidence, decreased ($p < 0.05$) the expression and secretion of IL-1β, IL-6, TNF-α, and IFN-γ, and increased ($p < 0.05$) the expression of transforming growth factor-β (TGF-β) in intestinal mucosa. In addition, the serum glutathione peroxidase (GSH-PX), mRNA relative expression of Na+-K+-2Cl– co-transporter 1 (NKCC1) and cystic fibrosis transmembrane conductance regulator (CFTR) and the content of toll-like relative (TLR2) and TLR4 in the jejunum, and secretory immunoglobulin (sIgA) content of ileal mucosa were higher ($p < 0.05$) than LP. Collectively, dietary *L. plantarum* CGMCC 1258 improved intestinal morphology, intestinal permeability, intestinal immunity, and antioxidant function in weaned pigs. Dietary *L. reuteri* LR1 showed better growth performance, a lower incidence of diarrhea, better intestinal morphology, and a higher extent of immune activation in weaned pigs.

Keywords: *Lactobacillus plantarum*, *Lactobacillus reuteri*, antioxidant function, intestinal immunity, weaned pigs

INTRODUCTION

Early weaning is often associated with a range of disorders in pigs including digestive upset, low feed intake, poor immunocompetence, diarrhea, and reduced growth performance (1, 2). After the widespread restriction of the use of growth-promoting antibiotics, probiotic additives have played an important role in improving immune response, intestinal microbial balance, and the pH of the gastrointestinal tract of weaned pigs (3). *Lactobacillus* is a widely used probiotic agent. *Lactobacillus plantarum* and *Lactobacillus reuteri* have been used in vertebrates such as pigs, chickens, and humans (4). *L. plantarum* and *L. reuteri* improve intestinal health by producing exopolysaccharides to increase intestinal adhesion and colonization of probiotics. Currently, *L. plantarum* and *L. reuteri* may promote host immunity and intestinal physiological functions by coregulating pro-inflammatory and anti-inflammatory cytokines that has been proven in many ways (5, 6). In addition, previous studies have shown that *L. plantarum* CJLP243 (1×10^{10} CFU/kg) or *L. plantarum* CGMCC 1258 (5×10^{10} CFU/kg) can improve growth performance and enhance the defense of intestinal epithelial barrier in weaned pigs challenged by *Escherichia coli* (7, 8). *L. plantarum* ZJ316 also improved the growth performance of weaned pigs under normal feeding conditions (9). For *L. reuteri*, *L. reuteri* D8 promotes the development of intestine mucosal system and maintains intestinal mucosal barrier (10). Previous studies in this laboratory have showed that a strain of *L. reuteri* LR1 isolated from the feces of healthy piglets showed bile resistance and notable acid (11). Dietary *L. reuteri* LR1 supplemented at 5×10^{10} CFU/kg improved growth performance, epithelial barrier function, and enhanced amino acid metabolism in weaned pigs (12, 13). However, under the premise that the two strains of *L. plantarum* CGMCC 1258 and *L. reuteri* LR1 are known to have good probiotic effects on weaned pigs, their different advantages in the probiotic effect on weaned pigs are still lacking. Hence, the present study was conducted to investigate the differential effects of *L. plantarum* CGMCC 1258 and *L. reuteri* LR1 on the growth performance, antioxidant function, and intestinal immunity in weaned pigs.

MATERIALS AND METHODS

These experiments were conducted in accordance with Chinese guidelines for animal welfare and experimental protocols, and all animal procedures were approved by the Animal Care and Use Committee of Guangdong Academy of Agricultural Sciences (Permit Number: GAASIAS-2015-012). The *L. plantarum* CGMCC 1258 strain was provided by Dr. Hang Xiaomin (Institute of Science Life of Onlly, Shanghai Jiao Tong University, Shanghai, China), and the strain was originally isolated from the feces of healthy infants (14). The *L. reuteri* LR1 strain was originally isolated from the feces of healthy 35-day-old weaned pigs in our laboratory (11).

Animals and Diets

A total of 90 barrows [Duroc × (Landrace × Yorkshire), 21 d of age, body weight (BW) = 6.10 ± 0.1 kg] were randomly allocated to three groups (five replicates per group and six pigs per replicate). Control group (CON) were fed a corn–soybean meal basal diet, *L. plantarum* CGMCC 1258 group (LP) were fed the basal diet supplemented with 5×10^{10} CFU/kg *L. plantarum* CGMCC 1258, and *L. reuteri* LR1 group (LR) were fed the basal diet supplemented with 5×10^{10} CFU/kg *L. reuteri* LR1 for 42 days. Experimental diets were formulated to meet the nutrient requirements for pigs proposed by the National Research Council (15), and the ingredient compositions and nutrient levels of the basal diets are listed in **Table 1**. The measurements of crude protein (CP), Ca, and P refer to GB/T 6432-2018 (China), GB/T 6436-2018 (China), and GB/T 6437-2018 (China), respectively. The diets used in the experiment were all mash feed. The pigs were provided feed and water *ad libitum* throughout the experiment.

TABLE 1 | The formulations and chemical composition of the basal diet (as-fed basis).

Ingredient	%
Corn	57.55
Soybean meal	27.59
Whey powder	5.00
Soybean oil	1.89
Fish meal	3.00
L-Lys·HCl	0.73
L-Thr	0.29
DL-Met	0.24
L-Trp	0.03
$CaHPO_4$	1.40
Limestone	0.85
Wheat middlings	0.30
NaCl	0.14
Premix[a]	1.00
Total	100.00
Energy and nutrient composition	
NE, MJ/kg	10.51
CP, %	20.01
Standardized ileal digestible Lys, %	1.57
Standardized ileal digestible Met + Cys, %	0.82
Standardized ileal digestible Thr, %	0.94
Standardized ileal digestible Trp, %	0.25
Ca, %	0.85
Total P, %	0.70
Available phosphorus P, %	0.48

[a] *The premix provided following per kg of the diet: vitamin A, 5,500 IU; vitamin D, 500 IU; vitamin E, 66.1 IU; vitamin B_{12} 28.2 μg; vitamin B_2, 5.1 mg; pantothenic acid, 12.6 mg; niacin, 29.8 mg; choline chloride, 540 mg; Mn ($MnSO_4 \cdot H_2O$), 100 mg; Zn ($ZnSO_4 \cdot H_2O$), 100 mg; Fe ($FeSO_4 \cdot H_2O$), 100 mg; Cu ($CuSO_4 \cdot 5H_2O$), 150 mg; Co ($CoSO_4 \cdot 7H_2O$) 1 mg; and Se (Na_2SeO_3), 0.48 mg.*

Except for the calculated values of net energy, available phosphorus, and standardized ileal digestible AA, dietary nutrients were all measured values.

Sample Collection

For each pen, two pigs were randomly selected for blood collection and slaughter sampling. Blood samples and tissue sampling from all weaned pigs were completed on day 43. Blood samples were collected intravenously into 10-ml vacuum tubes without anticoagulant, centrifuged at 3,000 × g at 4°C for 15 min to obtain serum, and stored at −80°C until further assay. After blood collection, one pig per pen was anesthetized by intravenous injection of pentobarbital sodium (30 mg/kg BW) and killed by bloodletting. Approximately 1-cm lengths of middle duodenum, middle jejunum, and distal ileum specimens were collected without rinsing and fixed in 4% paraformaldehyde. Approximately 10-cm lengths of jejunum and ileum were cut open to expose the intestinal lumen, rinsed with phosphate buffered saline, and the mucosa were scraped by sterile glass microscope slide, and then the samples were quickly frozen in liquid nitrogen and stored at −80°C until analyses.

Performance and Diarrhea Measurements

Feed intake was measured every day during the entire experiment, and pigs were weighed on days 0 and 42 to calculate average daily gain (ADG), average daily feed intake (ADFI), and gain:feed ratio (G/F). In addition, the diarrhea was observed and recorded in each pen at 9:00 and 16:00 every day. Diarrhea is evaluated according to the shape of the stool; strips or pellets are normal stools, while flat or liquid stools are diarrhea stools. Diarrhea incidence was calculated at the end of the experiment for each enclosure from 1 to 14 days, 15 to 28 days, 28 to 42 days, and 1 to 42 days. Diarrhea incidence was calculated according to the formula: diarrheal incidence (%) = [total number of pigs with diarrhea in each pen × diarrhea days/(6 pigs × the number of days)] × 100.

Analysis of Intestinal Morphology

The collected fixed samples ileum, jejunum, and duodenum were dehydrated and embedded in paraffin. Sections of 5 μm thickness were stained coated with H&E. Nine well-oriented and intact villi and adjacent crypts were measured each section using Image-Pro software (Media Cybernetics, Rockville, MD), and the villus height to crypt depth ratio (V/C) was calculated. The images were obtained by an Axio Scope A1 microscope (Zeiss, Germany).

Analysis of Antioxidant Function and Intestinal Cytokines

Lactate dehydrogenase (LDH, A020-2-2), the activities of superoxide dismutase (SOD, A001-3-2), malondialdehyde (MDA, A003-1-2), glutathione peroxidase (GSH-PX, A005-1-2), urea nitrogen (SUN, C013-2-1), and glucose (GLU, F006-1-1) in serum were estimated using a commercial kit (Nanjing Jiancheng Bioengineering Institute, Nanjing, China). The contents of immunoglobulin G (IgG, FU-Z076), lipopolysaccharide (LPS, YS04547B), insulin-like growth factor 1 (IGF-1, FU-Z135), and diamine oxidase (DAO, FU-Z050) in serum were estimated using ELISA kits (Beijing FangCheng Bioengineering Institute, Beijing, China). To obtain a 10% intestinal mucosa supernatant, 0.4 g of intestinal mucosa was added to 3.6 ml of 0.86% normal saline, homogenized in ice water with a tissue homogenizer, and centrifuged at 3,000 × g at 4°C for 10 min. The content of total protein in the supernatant was determined by BCA protein analysis kit (Thermo Fisher Scientific, Waltham, MA, 23227). The levels of interleukin-1β (IL-1β, H002), IL-6, tumor necrosis factor-α (TNF-α, FU-Z149), transforming growth factor-β (TGF-β, FU- FU-Z014), interferon-γ (IFN-γ, FU-Z054), secretory immunoglobulin (sIgA, H108-2) (Beijing FangCheng Bioengineering Institute), and TLR2 (ml027585) and TLR4 (ml027583) in intestinal mucosa were estimated using ELISA kits (Mlbio Bioengineering, Shanghai, China).

Real-Time PCR for Relative Measurement of Intestinal Diarrhea-Related Ion Channel Genes and Cytokines

Total RNA of the mucosa of jejunum and ileum was extracted following the Trizol Reagent Instructions (Invitrogen, Carlsbad, CA). The total RNA was quantified using a NanoDrop 1000 spectrophotometer (Thermo Fisher Scientific, Waltham, MA). RNA purity was assessed by determining the ratio of absorbance at 260 nm to that at 280 nm, and RNA (2 μg) was used to generate cDNA in a volume of 20 μl using a PrimeScript II 1st Strand cDNA Synthesis Kit (Takara, Tokyo, Japan). PCR amplification was performed in a total volume of 20 μl containing 10 μl of master mix (SYBR PCR Master Mix; Applied Biosystems), 1.0 μl of gene-specific primers (**Table 2**), 6.0 μl of RNAse-free water, and 2 μl 10-fold diluted cDNA. The thermocycler protocol consisted of 1 min at 95°C followed by 39 cycles of 10 s at 95°C, 30 s at 60°C, and 30 s at 72°C. β-Actin was used as a housekeeping gene. The fold changes were calculated for each sample using the $2^{-\Delta\Delta Ct}$ method, and data for each target transcript were normalized to control pigs; $\Delta\Delta C_T = (C_{T,Target} - C_{T,\beta-actin})_{Treatment} - (C_{T,Target} - C_{T,\beta-actin})_{Control}$.

Statistical Analyses

The pen was the experimental unit. Statistical significance analysis was determined by one-way ANOVA with Tukey's test using SPSS 19.0 software (SPSS Inc., Chicago, IL). All data were expressed as the means ± SEM. The differences were significant at $p < 0.05$.

RESULTS

Effects of *L. plantarum* CGMCC 1258 and *L. reuteri* LR1 on Growth Performance and Diarrhea in Weaned Pigs

LR but not LP increased final BW ($p = 0.013$) and ADG ($p = 0.013$), and reduced ($p = 0.025$) 29–42-day diarrheal incidence compared with CON (**Table 3**). However, no significant differences were observed on ADFI and neither on 1–42-day diarrheal incidence between treatments ($p = 0.154$).

Effects of *L. plantarum* CGMCC 1258 and *L. reuteri* LR1 on Antioxidant Function in Weaned Pigs

LR increased serum GLU ($p = 0.007$) compared with CON and LP (**Table 4**). In addition, the LP increased ($p = 0.043$)

TABLE 2 | Primers for the real-time PCR analysis.

Gene	Accession number	Sequence (5′-3′)	Size (bp)
NKCC1	CU855646.2	Forward: CAAGAAAAGGTGCTGTGTC	109
		Reverse: GTAAGGACGCTCTGATGATT	
CFTR	AY585334.1	Forward: TTCCTCGTAGTCCTCGCC	204
		Reverse: GGTCAGTTTCAGTTCCGTTTG	
IL-1β	NM214055.1	Forward: CTCCAGCCAGTCTTCATTGTTC	132
		Reverse: TGCCTGATGCTCTTGTTCCA	
IL-6	M80258.1	Forward: TACATCCTCGGCAAAATC	168
		Reverse: TCTCATCAAGCAGGTCTCC	
IFN-γ	JF906510	Forward: TGTTTTTCTGGCTCTTACTGC	99
		Reverse: CCTTTGAATGGCCTGGTT	
TGF-β	NM_214379.1	Forward: GAAGCGCATCGAGGCCATTC	162
		Reverse: GGCTCCGGTTCGACACTTTC	
TNF-α	NM_214022.1	Forward: CCAATGGCAGAGTGGGTATG	116
		Reverse: TGAAGAGGACCTGGGAGTAG	
TLR2	NM_213761	Forward: ACGGACTGTGGTGCATGAAG	101
		Reverse: GGACACGAAAGCGTCATAGC	
TLR4	NM_001113039	Forward: CATACAGAGCCGATGGTG	136
		Reverse: CCTGCTGAGAAGGCGATA	
β-Actin	DQ845171	Forward: CGGGACATCAAGGAGAAGC	273
		Reverse: ACAGCACCGTGTTGGCGTAGAG	

NKCC1, Na+-K+-2Cl– co-transporter 1; CFTR, cystic fibrosis transmembrane conductance regulator; IL, interleukin; IFN-γ, interferon-γ; TGF-β, transforming growth factor-β; TLR, toll-like receptor.

serum SOD compared with CON. LR increased serum GSH-Px compared with both CON ($p = 0.002$) and LP ($p = 0.001$).

Effects of *L. plantarum* CGMCC 1258 and *L. reuteri* LR1 on Intestinal Morphology in Weaned Pigs

LP increased duodenal villus height compared with CON ($p = 0.0003$) and LR ($p = 0.018$), and the jejunal villus height of LR was higher ($p = 0.041$) than that of CON (**Table 5**). In addition, LP increased ($p = 0.001$) the V/C of duodenum compared with CON. LR increased the V/C of jejunum ($p = 0.011$) and ileum ($p = 0.018$) compared with CON.

Effects of *L. plantarum* CGMCC 1258 and *L. reuteri* LR1 on Intestinal Permeability in Weaned Pigs

The expression of Na+-K+-2Cl– co-transporter 1 (NKCC1) in jejunal mucosa was decreased by LR compared with CON ($p = 0.025$) and LP ($p = 0.029$) (**Figure 1**). Meanwhile, LR decreased the expression of and cystic fibrosis transmembrane conductance regulator (CFTR) in jejunal mucosa compared with CON ($p = 0.036$) and LP ($p = 0.038$). In addition, both LP ($p = 0.001$) and LR ($p = 0.002$) decreased serum DAO above CON, similar to the effect of LP ($p = 0.0002$) and LR ($p = 0.0004$) on serum LPS compared with CON.

TABLE 3 | Effects of *L. plantarum* CGMCC 1258 and *L. reuteri* LR1 on growth performance and diarrhea of weaned pigs.

Item	Treatments			SEM	*P*-value
	CON	LP	LR		
Initial BW, kg	6.10	6.10	6.11	0.065	0.893
Final BW, kg	14.9^{b}	16.4^{a,b}	17.5^{a}	0.43	0.017
ADFI, g/day	321	358	384	13.4	0.154
ADG, g/day	207^{b}	244^{a,b}	274^{a}	10.3	0.017
G/F	0.664	0.681	0.714	0.0219	0.686
Diarrhea incidence, %					
1–14 days	23.9	22.0	18.5	1.86	0.509
15–28 days	22.1	21.2	18.8	2.11	0.829
29–42 days	21.5^{a}	16.5^{a,b}	13.2^{b}	1.72	0.046
1–42 days	21.4	19.0	16.0	1.42	0.309

n = 5.
CON, a basal diet; LP, a basal diet supplemented with 5 × 10^{10} CFU/kg L. plantarum CGMCC 1258; LR, a basal diet supplemented with 5 ×10^{10} CFU/kg L. reuteri LR1.
^{a,b}Values within a row with different superscripts differ significantly at $p < 0.05$.

TABLE 4 | Effects of *L. plantarum* CGMCC 1258 and *L. reuteri* LR1 on serum indices of pigs.

Item	Treatments			SEM	*P*-value
	CON	LP	LR		
GLU (mmol/L)	7.79^{b}	7.87^{b}	8.88^{a}	0.146	0.001
SUN (mmol/L)	20.6	18.2	18.1	0.74	0.093
IGF-1 (μg/L)	80.3	79.0	80.4	4.61	0.991
IgG (μg/ml/L)	156	156	175	6.0	0.355
SOD (U/ml)	93.0^{b}	102^{a}	98.0^{a,b}	1.41	0.052
GSH-Px (U/ml)	417^{b}	406^{b}	505^{a}	12.2	<0.001
LDH (U/ml)	2,494	2,420	2,403	43.4	0.673
MDA (nmol/ml)	2.31	1.63	2.01	0.144	0.153

n = 5.
CON, a basal diet; LP, a basal diet supplemented with 5 × 10^{10} CFU/kg L. plantarum CGMCC 1258; LR, a basal diet supplemented with 5 × 10^{10} CFU/kg L. reuteri LR1.
^{a,b}Values within a row with different superscripts differ significantly at $p < 0.05$.

Effects of *L. plantarum* CGMCC 1258 and *L. reuteri* LR1 on Intestinal Cytokines in Weaned Pigs

Figure 2, **Table 6** show that both LP ($p = 0.029$) and LR ($p = 0.025$) decreased IL-1β transcripts in jejunal mucosa and LP decreased ($p = 0.004$) ileal mucosa content of IL-1β compared with CON. LR decreased jejunal mucosa ($p = 0.041$) and ileal mucosa ($p = 0.004$) content of IL-6 compared with CON. The relative mRNA expression of TNF-α in jejunal mucosa was decreased by LR compared with CON ($p = 0.046$) and LP ($p = 0.049$). Both LP ($p = 0.017$) and LR ($p = 0.011$) decreased the TNF-α content of jejunal mucosa compared with CON. LR decreased ($p = 0.039$) the mRNA expression of IFN-γ in ileum mucosa compared with CON. LR increased ($p < 0.05$) the mRNA expression of TGF-β in jejunal mucosa compared with CON, and

TABLE 5 | Effects of *L. plantarum* CGMCC 1258 and *L. reuteri* LR1 on intestinal morphology in weaned pigs.

Item	Treatments			SEM	*P*-value
	CON	LP	LR		
Duodenum					
Villus height, μm	351[b]	505[a]	415[b]	19.3	<0.001
Crypt depth, μm	435	307	347	37.8	0.106
Villus height/crypt depth	0.850[b]	1.72[a]	1.27[a,b]	0.1163	0.001
Jejunum					
Villus height, μm	387[b]	415[a,b]	480[a]	22.7	0.045
Crypt depth, μm	314	273	221	27.6	0.113
Villus height/crypt depth	1.28[b]	1.60[a,b]	2.24[a]	0.180	0.013
Ileum					
Villus height, μm	359	408	425	31.2	0.331
Crypt depth, μm	261	247	173	30.5	0.137
Villus height/crypt depth	1.41[b]	1.96[a,b]	2.42[a]	0.223	0.023

n = 5.

CON, a basal diet; LP, a basal diet supplemented with 5 × 10^{10} CFU/kg L. plantarum CGMCC 1258; LR, a basal diet supplemented with 5 × 10^{10} CFU/kg L. reuteri LR1.

[a,b]Values within a row with different superscripts differ significantly at p < 0.05.

the TGF-β content in jejunal mucosa was increased in pigs fed LR compared with CON ($p = 0.001$) and LP ($p = 0.043$). In addition, LP ($p = 0.0002$) and LR ($p = 0.0003$) increased the sIgA content of the jejunal mucosa compared with CON, and concentrations of sIgA in ileal mucosa in LR was higher than in CON ($p = 0.018$) and LP ($p = 0.009$).

Effects of *L. plantarum* CGMCC 1258 and *L. reuteri* LR1 on TLRs in the Intestinal Mucosa in Weaned Pigs

LR increased ($p = 0.003$) content of TLR2 in the ileal mucosa compared with CON, and the content of TLR2 in the jejunal mucosa of LR is higher ($p = 0.015$) than that of LP (**Figure 3**). Both LP ($p = 0.001$) and LR ($p = 0.003$) increased content of TLR4 in ileal mucosa compared with CON, and LR increased content of TLR4 in jejunal mucosa compared with CON ($p = 0.012$) and LP ($p = 0.003$).

DISCUSSION

In the present study, we compared the effects of *L. plantarum* CGMCC 1258 and *L. reuteri* LR1 on the growth performance,

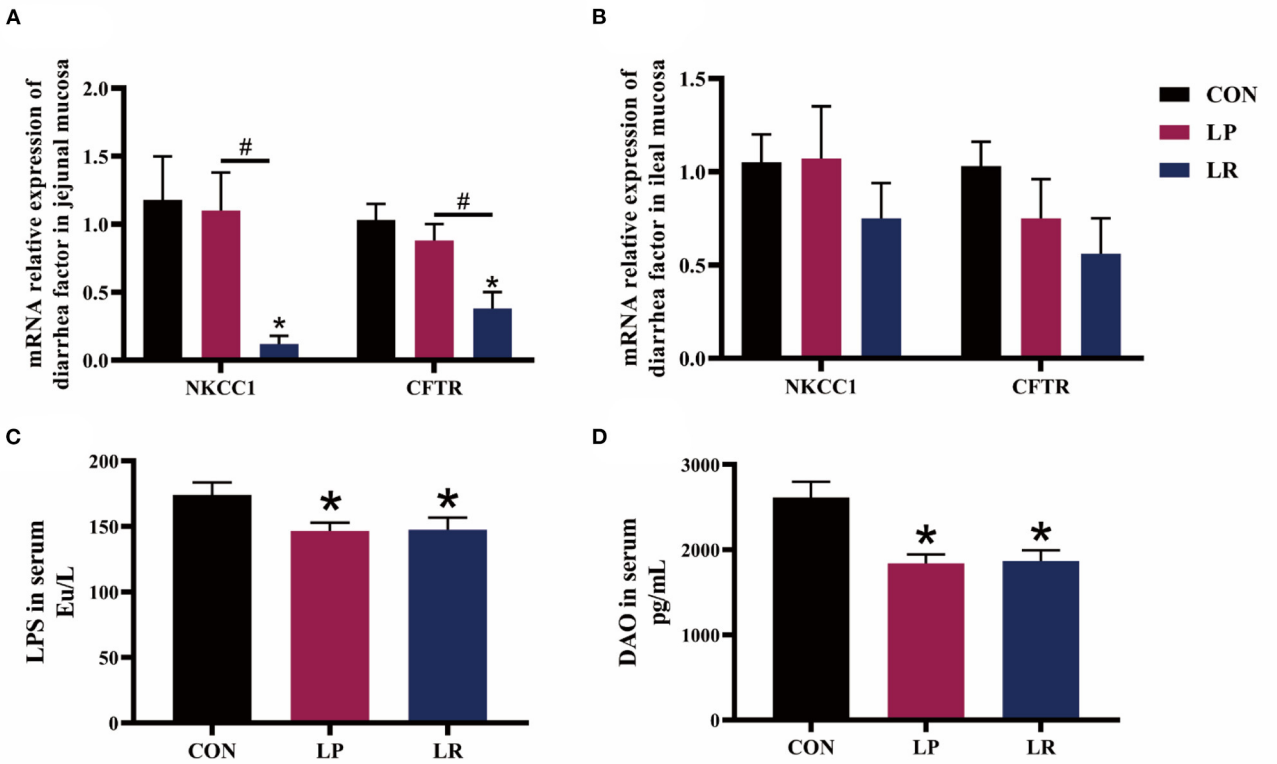

FIGURE 1 | Effects of *L. plantarum* CGMCC 1258 and *L. reuteri* LR1 on diarrhea-related ion channel genes and intestinal permeability in weaned pigs. The relative mRNA expression levels of NKCC1 and CFTR in jejunal mucosa **(A)** and ileal mucosa **(B)** were determined via real-time PCR. Levels of LPS **(C)** and DAO **(D)** in serum determined by ELISA. NKCC1, Na+-K+-2Cl– co-transporter 1; CFTR, cystic fibrosis transmembrane conductance regulator; LPS, lipopolysaccharide; DAO, diamine oxidase. All data are expressed as the mean ± SEM ($n = 5$). Differences were determined by one-way ANOVA followed by Tukey test. *$p < 0.05$ compared with CON, #$p < 0.05$ compared with LP.

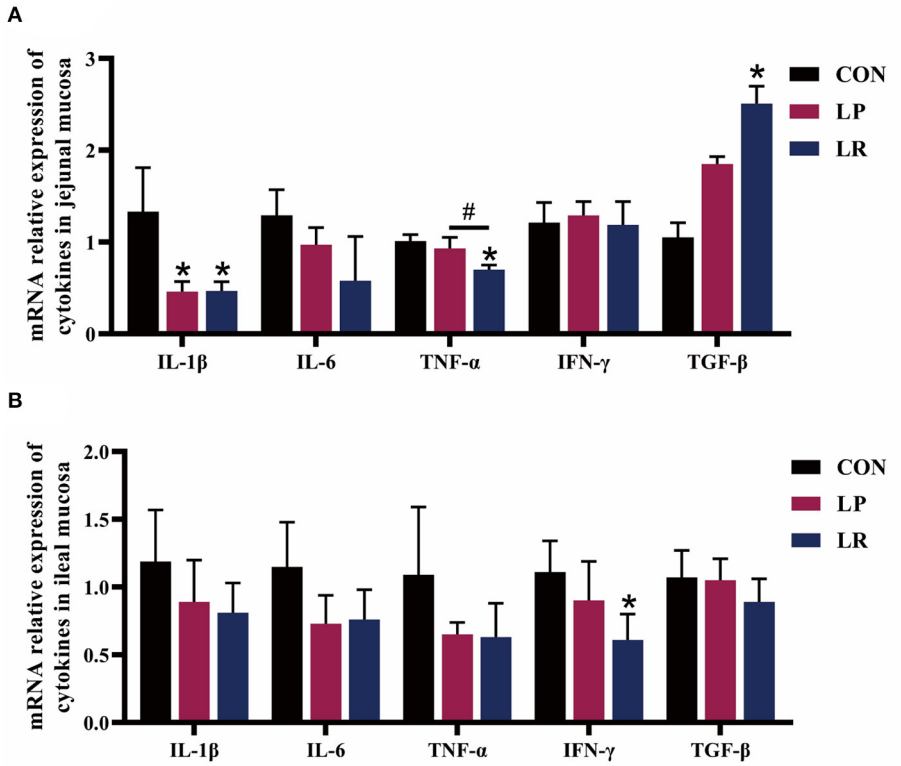

FIGURE 2 | Effect of *L. plantarum* CGMCC 1258 and *L. reuteri* LR1 on the expression of cytokines in intestinal in weaned pigs. The relative mRNA expression levels of IL-1β, IL-6, TNF-α, IFN-γ, and TGF-β in the jejunal mucosa **(A)** and ileal mucosa **(B)** were determined via real-time PCR. All data are expressed as the mean ± SEM ($n = 5$). Differences were determined by one-way ANOVA followed by Tukey test. $^{*}p < 0.05$ compared with CON, $^{\#}p < 0.05$ compared with LP.

TABLE 6 | Effects of *L. plantarum* CGMCC 1258 and *L. reuteri* LR1 on intestinal mucosal cytokines and sIgA concentrations of weaned pigs.

Item	Treatments			SEM	*P*-value
	CON	LP	LR		
Jejunal mucosa					
IL-1β, pg/ml	148	141	130	6.5	0.571
IL-6, pg/ml	20.5^{a}	18.1^{a,b}	16.5^{b}	0.68	0.049
TNF-α, pg/ml	109^{a}	88.8^{b}	90.3^{b}	3.44	0.007
IFN-γ, pg/ml	314	240	246	14.9	0.066
TGF-β, pg/ml	22.5^{b}	27.9^{b}	33.8^{a}	1.48	0.001
sIgA, μg/ml	65.9^{b}	75.1^{a}	77.6^{a}	1.50	<0.001
Ileal mucosa					
IL-1β, pg/ml	103^{a}	64.9^{b}	101^{a}	5.83	0.003
IL-6, pg/ml	19.3^{a}	16.4^{a,b}	14.8^{b}	0.66	0.005
TNF-α, pg/ml	63.6	48.4	57.6	3.74	0.260
IFN-γ, pg/ml	207	193	200	9.1	0.841
TGF-β, pg/ml	26.2	26.4	27.6	1.27	0.901
sIgA, μg/ml	24.9^{b}	23.5^{b}	35.7^{a}	2.85	0.006

n = 5.

CON, a basal diet; LP, a basal diet supplemented with 5 × 10^{10} CFU/kg L. plantarum CGMCC 1258; LR, a basal diet supplemented with 5 × 10^{10} CFU/kg L. reuteri LR1.

^{a,b}Values within a row with different superscripts differ significantly at $p < 0.05$.

antioxidant function, and intestinal immune function of weaned pigs. The results showed that both dietary *L. plantarum* CGMCC 1258 and *L. reuteri* LR1 supplementation at 5 × 10^{10} CFU/kg improved the antioxidant function, intestinal morphology, and intestinal immunity of weaned pigs, and they are consistent in improving intestinal permeability. However, *L. plantarum* CGMCC 1258 has a better effect on SOD and *L. reuteri* LR1 has better effects on ADG, diarrheal incidence, GLU, GSH-Px, intestinal morphology, and intestinal immunity.

Generally, the level of GLU is positively correlated with the digestion and absorption of carbohydrates in the intestine of pigs. In this study, *L. reuteri* LR1 but not *L. plantarum* CGMCC 1258 significantly increased the GLU content in the serum. The results suggest that *L. reuteri* LR1 improves serum GLU of weaned pigs, which was more advantageous than *L. plantarum* CGMCC 1258.

Weaning often induces a large number of reactive oxygen radicals in the piglets, causing oxidative stress and resulting in reduced piglet production performance and immune function (16). SOD and GSH-Px can scavenge reactive oxygen radicals in the body and are the main antioxidant enzymes in the body. MDA is a small molecule product produced at the termination stage of lipid peroxidation reaction, and its content can reflect the degree of lipid oxidation caused by reactive oxygen species in the organism (17). The strain of *L. plantarum* 423,

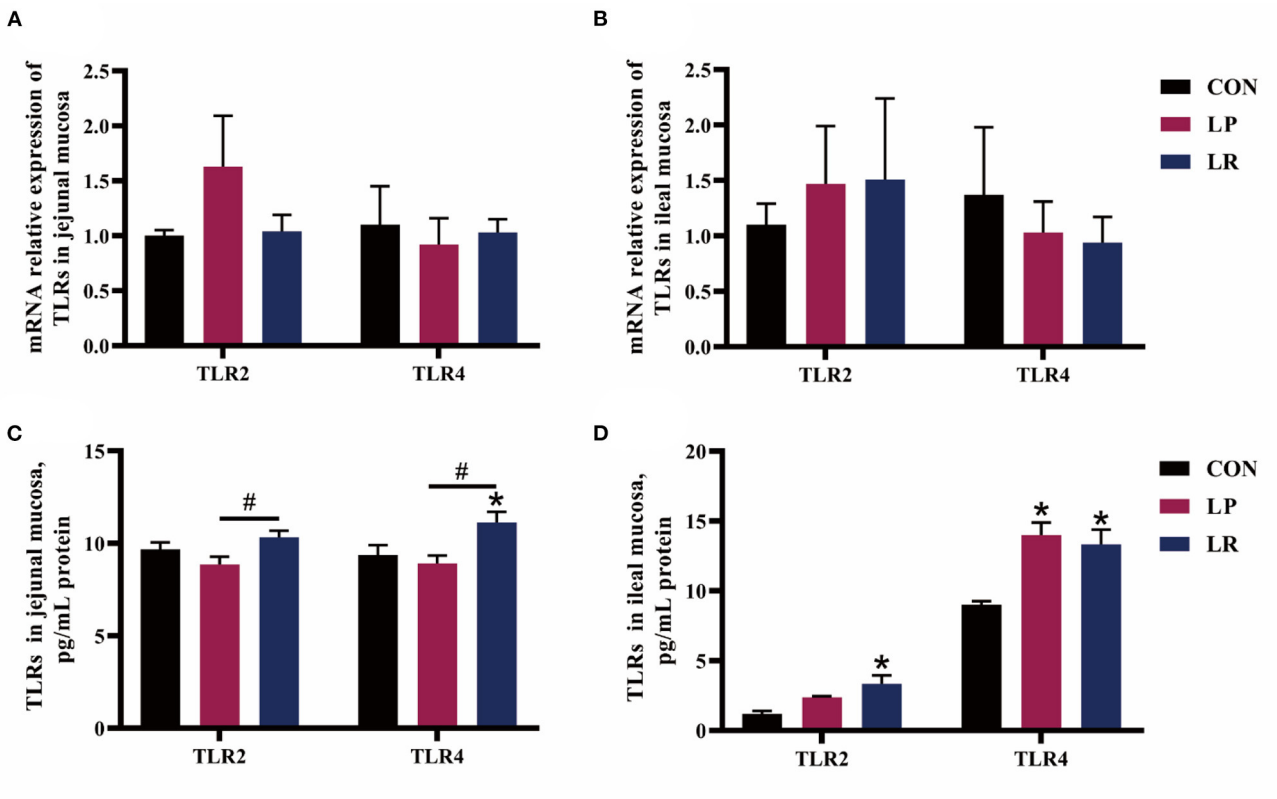

FIGURE 3 | Effects of *L. plantarum* CGMCC 1258 and *L. reuteri* LR1 on TLRs in intestinal mucosa in weaned pigs. The relative mRNA expression levels of TLRs in the jejunal mucosa **(A)** and ileal mucosa **(B)** were determined via real-time PCR. Levels of TLRs in the jejunal mucosa **(C)** and ileal mucosa **(D)** determined by ELISA. All data are expressed as the mean ± SEM ($n = 5$). Differences were determined by one-way ANOVA followed by Tukey test. $^{*}p < 0.05$ compared with CON, $^{\#}p < 0.05$ compared with LP.

L. plantarum 200655, and *L. plantarum* RG14 showed strong free radical–scavenging activity, and exert strong antioxidant capacity of human umbilical vein endothelial cells, human colon adenocarcinoma cell line, and post-weaning lambs, respectively (18–20). According to the mechanisms related to probiotic effects, *L. plantarum* and *L. reuteri* have been reported to limit excessive amounts of reactive radicals against oxidative stress *in vivo* (21, 22). Another study showed that dietary supplementation of *L. plantarum* ZLP001 increased the activity of serum SOD and GSH-Px in weaned pigs and reduced MDA content (23). The feeding with *L. reuteri* KT260178 increased the plasma total antioxidant capacity (T-AOC), SOD, and GSH-Px, which did not increase MDA in suckling piglets (24). However, the antioxidant function of *L. plantarum* CGMCC 1258 and *L. reuteri* LR1 has not been reported. In this study, *L. plantarum* CGMCC1258 increased serum SOD enzyme activity of weaned pigs, while *L. reuteri* LR1 increased the enzyme activity of GSH-Px. Taken together, *L. reuteri* LR1 improved the antioxidant function mainly by regulating GSH-Px, while *L. plantarum* CGMCC 1258 mainly affects SOD.

Probiotics are often used to improve the performance and intestinal health of pigs. Our data showed that the *L. reuteri* LR1 increased the ADG, but *L. plantarum* CGMCC 1258 has no significant effects on the growth performance of weaned pigs. The results of *L. plantarum* CGMCC 1258 in this experiment was different from a previous study, but the results of *L. reuteri* LR1 are consistent. Other strains of *L. plantarum* (such as CJLP243) and the our previous researched on *L. plantarum* CGMCC 1258 strain can improve the growth performance of weaned pigs by *Escherichia coli* challenge (7, 8), and *L. plantarum* ZJ316 and *L. reuteri* LR1 also improved the growth performance of weaned pigs under normal feeding conditions (9, 12, 25). We have also previously study that the *L. reuteri* LR1 strain improved the growth performance of weaned pigs under normal feeding conditions (12). Under normal feeding conditions of this experiment, there was no significant effect of *L. plantarum* CGMCC 1258 on growth performance of weaned pigs, which is quite different from the past, which may be related to the isolation of *L. plantarum* CGMCC 1258 strain from infant feces and the different experimental conditions. However, its influence mechanism needs more in-depth study.

In the present study, *L. reuteri* LR1 but not *L. plantarum* CGMCC1258 reduced the incidence of diarrhea in weaned pigs during the period of 29–42 days. Lee et al. (7), Yang et al. (8), and Suo et al. (9) showed that *L. plantarum* ZJ316 was effective in reducing diarrhea incidence in weaned pigs, but the reductions

in diarrhea incidence with *L. plantarum* CGMCC1258 were all in the *Escherichia coli* challenge feeding mode (7–9). Probiotics play a detoxification role by inhibiting the reproduction of pathogenic bacteria, removing intestinal metabolites and bacteriocins (26). In the absence of *E. coli* challenge and under conditions of good intestinal health, *L. plantarum* CGMCC1258 was unable to exert significant antimicrobial and detoxification abilities in the intestine of weaned pigs. This may be the reason why *L. plantarum* CGMCC1258 is different from previous studies. In addition, stimulants such as enterotoxin and inflammatory mediators stimulate intestinal mucosal cells, and activate CFTR at the top of intestinal mucosal cells through G protein-coupled signaling pathways and phosphorylation, leading to a large amount of intracellular Cl– and water secretion, causing watery diarrhea (27). The activities of basolateral transport proteins NKCC1 are the rate-limiting steps of ion and fluid secretions in Cl-secreting epithelia (28, 29). For diarrhea-related ion channel genes, we found that *L. reuteri* LR1 reduced the expression of NKCC1 and CFTR in the intestine of piglets, which may be one of the reasons for its reduction of diarrhea. Taken together, *L. reuteri* LR1 showed better effects on reduced diarrhea of weaned pigs than *L. plantarum* CGMCC 1258.

The intestinal barrier plays an important role in resisting the invasion of intestinal bacteria and pathogenic allergens into the mucosa (30). When the intestinal mucosa is damaged, the increase in intestinal permeability leads to more DAO and LPS from the tissues into the peripheral blood circulation (31, 32). Pan et al. (33) have found that the addition of probiotics (mainly *Bacillus licheniformis* and *Saccharomyces cerevisiae*) could reduce the intestinal damage caused by the enterotoxigenic *Escherichia coli* K88 challenge through reducing the serum DAO content of weaned pigs (33). In this study, both *L. plantarum* CGMCC1258 and *L. reuteri* LR1 reduced the content of DAO and LPS in the serum in weaned pigs. The formation of villi and crypt in the intestine enlarged the surface area of the intestinal mucosa, and not only promoted the efficient absorption of nutrients but also generated a protected stem cell niche (10). We found that *L. plantarum* CGMCC1258 improved the intestinal morphology of the duodenum, while *L. reuteri* LR1 improved the intestinal morphology of the jejunum and ileum. This result showed that *L. plantarum* CGMCC1258 and *L. reuteri* LR1 enhanced the intestinal barrier function, and *L. reuteri* LR1 can better improve the intestinal morphology of weaned pigs.

The increased expression and secretion of pro-inflammatory factors IL-1β, IL-6, TNF-α, and IFN-γ are stimulated by weaning stress or pathogenic invasion (34, 35). The strain of *L. plantarum* CGMCC1258 and *L. plantarum* ACTT 8014 could effectively increase the protein levels of the natural cytotoxic receptor family of natural killer cells, and alleviates the pathological changes of intestinal tissues of animal intestinal inflammation models (36, 37). The *L. plantarum* 299v facilitates the gut health of suckling piglets by improved the intestinal morphology and intestinal barrier function and microflora (38). In this study, *L. plantarum* CGMCC1258 reduced the gene expression of IL-1β and the content of IL-1β and TNF-α in the intestinal mucosa, while *L. reuteri* LR1 reduced the gene expression of IL-1β, TNF-α, and IFN-γ and the content of IL-6 and TNF-α, and increased the TGF-β expression. Yi et al. (12) found that *L. reuteri* LR1 increased the content of TGF-β in the ileum and improve the intestinal immunity of weaned pigs (12). Collectively, these two strains of *Lactobacillus* have great differences in regulating the expression of IL-1β, IL-6, TNF-α, and TGF-β in the intestinal mucosa, and *L. reuteri* LR1 showed better anti-inflammatory ability than *L. plantarum* CGMCC 1258. The different effects of *L. reuteri* LR1 and *L. plantarum* CGMCC 1258 on intestinal immunity in weaned pigs may be related to the different hosts from which the strains originate, with *L. reuteri* LR1 from piglet feces readily attaching to the gastrointestinal tract and acting, while *L. plantarum* CGMCC 1258 from infants has lower effects because the piglet probably has not evolved to specifically recognize this strain.

The sIgA has been proven as the first line of defense in intestinal mucosa, effectively preventing the adhesion and penetration of pathogen in intestinal epithelial cells (39). The TLRs play an important role in recognizing bacterial signals and initiating intestinal immune responses. The TLR2 detects lipoprotein and peptidoglycans of gram-positive bacteria and gram-negative bacteria, and TLR4 can recognize LPS of gram-negative bacteria (40). The activation of TLR2 enhances the expression of antimicrobial peptides and tight junction proteins (41, 42). The *L. plantarum* 299v or *L. plantarum* CGMCC 1258 increased the expression of tight junction proteins, which was related to the expression of TLR2 in the pig intestine (8, 38). Another study showed that *L. reuteri* LR1 increased the expression of intestinal antimicrobial peptides, tight junction protein, and sIgA secretion, which was related to the increase of TLR2 and TLR4 expression (12). In the present study, *L. plantarum* CGMCC 1258 increased TLR4 levels only in ileum, and *L. reuteri* LR1 increased TLR2 and TLR4 levels in jejunum and ileum. The probiotic preparations containing *L. plantarum* CGMCC 1258 can significantly increase the sIgA content of the ileal mucosa of pigs 21 days after weaning, and also increased the sIgA content of jejunal mucosa (43). We found that dietary supplement *L. plantarum* CGMCC 1258 and *L. reuteri* LR1 increased the sIgA content in the jejunal mucosa of pigs, and *L. reuteri* LR1 can increase the sIgA content in the ileal mucosa. Collectively, these data suggest that *L. plantarum* CGMCC 1258 and *L. reuteri* LR1 may mediate TLRs-related pathways to regulate the secretion of sIgA and improved the intestinal immune response, but LR has a stronger influence.

CONCLUSIONS

In conclusion, dietary *L. plantarum* CGMCC 1258 supplementation at 5×10^{10} CFU/kg improved intestinal morphology, intestinal permeability, intestinal immunity, and antioxidant function in weaned pigs. However, dietary *L. reuteri* LR1 supplementation at 5×10^{10} CFU/kg showed higher improvements in growth performance, incidence of diarrhea,

intestinal morphology, and a higher extent of immune activation in weaned pigs.

DATA AVAILABILITY STATEMENT

The raw data supporting the conclusions of this article will be made available by the authors, without undue reservation.

ETHICS STATEMENT

These experiments were conducted in accordance with Chinese guidelines for animal welfare and experimental protocols, and all animal procedures were approved by the Animal Care and Use Committee of Guangdong Academy of Agricultural Sciences (Permit Number: GAASIAS-2015-012).

AUTHOR CONTRIBUTIONS

QT, HY, and LW: conceptualization and investigation. QW and XY: methodology. SH, WH, and YX: data curation, formal analysis, and software. HY, QW, and YX: validation and visualization. QT and HY: writing—original draft preparation. LW and ZJ: writing—review and editing, funding acquisition, project administration, and resources. All authors have read and agreed to the published version of the article.

FUNDING

This study was funded by the National Key Research and Development Program of China (2018YFD0501101), China Agriculture Research System of MOF and MARA, the Science and Technology Program of Guangdong Academy of Agricultural Sciences (R2020PY-JG009), and Special fund for scientific innovation strategy-construction of high-level Academy of Agriculture Science (R2016YJ-YB2003, R2019PY-QF005, R2018QD-068).

ACKNOWLEDGMENTS

We thank the staff and postgraduate students of Institute of Animal Science of Guangdong Academy of Agricultural Sciences for providing technical assistance.

REFERENCES

1. Che L, Zhan L, Fang Z, Lin Y, Yan T, Wu D. Effects of dietary protein sources on growth performance and immune response of weanling pigs. *Livest Sci.* (2012) 148:1–9. doi: 10.1016/j.livsci.2012.04.019
2. Pu J, Chen D, Tian G, He J, Zheng P, Mao X, et al. Effects of benzoic acid, bacillus coagulans and oregano oil combined supplementation on growth performance, immune status and intestinal barrier integrity of weaned piglets. *Anim Nutr.* (2020) 6:152–9. doi: 10.1016/j.aninu.2020.02.004
3. Hu S, Wang L, Jiang Z. Dietary additive probiotics modulation of the intestinal microbiota. *Protein Peptide Lett.* (2017) 24:382–7. doi: 10.2174/0929866524666170223143615
4. Shin D, Chang SY, Bogere P, Won K, Choi J, Choi Y, et al. Beneficial roles of probiotics on the modulation of gut microbiota and immune response in pigs. *PLoS ONE.* (2019) 14:e220843. doi: 10.1371/journal.pone.0220843
5. Hou C, Zeng X, Yang F, Liu H, Qiao S. Study and use of the probiotic *Lactobacillus reuteri* in pigs: a review. *J Anim Sci Biotechnol.* (2015) 6:14. doi: 10.1186/s40104-015-0014-3
6. Zhao W, Peng C, Sakandar HA, Kwok L, Zhang W. Meta-analysis: randomized trials of *Lactobacillus plantarum* on immune regulation over the last decades. *Front Immunol.* (2021) 12:643420. doi: 10.3389/fimmu.2021.643420
7. Lee JS, Awji EG, Lee SJ, Tassew DD, Park YB, Park KS, et al. Effect of *Lactobacillus plantarum* CJLP243 on the growth performance and cytokine response of weaning pigs challenged with enterotoxigenic *Escherichia coli*. *J Anim. Sci.* (2012) 90:3709–17. doi: 10.2527/jas.2011-4434
8. Yang KM, Jiang ZY, Zheng CT, Wang L, Yang XF. Effect of *Lactobacillus plantarum* on diarrhea and intestinal barrier function of young piglets challenged with enterotoxigenic *Escherichia coli* K88. *J Anim Sci.* (2014) 92:1496–503. doi: 10.2527/jas.2013-6619
9. Suo C, Yin Y, Wang X, Lou X, Song D, Wang X, et al. Effects of *Lactobacillus plantarum* ZJ316 on pig growth and pork quality. *BMC Vet Res.* (2012) 8:89. doi: 10.1186/1746-6148-8-89
10. Wang M, Wu H, Lu L, Jiang L, Yu Q. *Lactobacillus reuteri* promotes intestinal development and regulates mucosal immune function in newborn piglets. *Front Vet Sci.* (2020) 7:42. doi: 10.3389/fvets.2020.00042
11. Wang Z, Wang L, Chen Z, Ma X, Yang X, Zhang J, et al. *In vitro* evaluation of swine-derived *Lactobacillus reuteri*: probiotic properties and effects on intestinal porcine epithelial cells challenged with enterotoxigenic *Escherichia coli* K88. *J Microbiol Biotechn.* (2016) 26:1018–25. doi: 10.4014/jmb.1510.10089
12. Yi H, Wang L, Xiong Y, Wen X, Wang Z, Yang X, et al. Effects of *Lactobacillus reuteri* LR1 on the growth performance, intestinal morphology, and intestinal barrier function in weaned pigs. *J Anim Sci.* (2018) 96:2342–51. doi: 10.1093/jas/sky129
13. Yi H, Yang G, Xiong Y, Wu Q, Xiao H, Wen X, et al. Integrated metabolomic and proteomics profiling reveals the promotion of *Lactobacillus reuteri* LR1 on amino acid metabolism in the gut-liver axis of weaned pigs. *Food Funct.* (2019) 1:7387–96. doi: 10.1039/C9FO01781J
14. Xia Y, Chen H, Zhang M, Jiang Y, Hang X, Qin H. Effect of *Lactobacillus plantarum* LP-Onlly on gut flora and colitis in interleukin-10 knockout mice. *J Gastroen Hepatol.* (2011) 26:405–11. doi: 10.1111/j.1440-1746.2010.06498.x
15. NRC. *Nutrient Requirements of Swine.* 11th revised ed. Washington, DC: The National Academies Press (2012).
16. Atkins HL, Geier MS, Prisciandaro LD, Pattanaik AK, Forder REA, Turner MS, et al. Effects of a *Lactobacillus reuteri* BR11 mutant deficient in the cystine-transport system in a rat model of inflammatory bowel disease. *Digest Dis Sci.* (2012) 57:713–9. doi: 10.1007/s10620-011-1943-0
17. Tsikas D. Assessment of lipid peroxidation by measuring malondialdehyde (MDA) and relatives in biological samples: analytical and biological challenges. *Anal Biochem.* (2017) 524:13–30. doi: 10.1016/j.ab.2016.10.021
18. Wang M, Lei M, Samina N, Chen L, Liu C, Yin T, et al. Impact of *Lactobacillus plantarum* 423 fermentation on the antioxidant activity and flavor properties of rice bran and wheat bran. *Food Chem.* (2020) 330:127156. doi: 10.1016/j.foodchem.2020.127156
19. Yang S, Lee J, Lim S, Kim Y, Lee N, Paik H. Antioxidant and immune-enhancing effects of probiotic *Lactobacillus plantarum* 200655 isolated from kimchi. *Food Sci Biotechnol.* (2019) 28:491–9. doi: 10.1007/s10068-018-0473-3
20. Izuddin WI, Humam AM, Loh TC, Foo HL, Samsudin AA. Dietary postbiotic *Lactobacillus plantarum* improves serum and ruminal antioxidant activity and upregulates hepatic antioxidant enzymes and ruminal barrier function in post-weaning lambs. *Antioxidants.* (2020) 9:250. doi: 10.3390/antiox9030250
21. DÜz M, DoGan YN, DoGan I. Antioxidant activity of *Lactobacillus plantarum*, *Lactobacillus sake* and *Lactobacillus curvatus* strains isolated from fermented Turkish Sucuk. *An Acad Bras Cienc.* (2020) 92:e20200105. doi: 10.1590/0001-3765202020200105

22. Amaretti A, di Nunzio M, Pompei A, Raimondi S, Rossi M, Bordoni A. Antioxidant properties of potentially probiotic bacteria: *in vitro* and *in vivo* activities. *Appl Microbiol Biot.* (2013) 97:809–17. doi: 10.1007/s00253-012-4241-7
23. Wang J, Ji HF, Wang SX, Zhang DY, Liu H, Shan DC, et al. *Lactobacillus plantarum* ZLP001: *in vitro* assessment of antioxidant capacity and effect on growth performance and antioxidant status in weaning piglets. *Asian Austral J Anim.* (2012) 25:1153–8. doi: 10.5713/ajas.2012.12079
24. Yang J, Wang C, Liu L, Zhang M. *Lactobacillus reuteri* KT260178 supplementation reduced morbidity of piglets through its targeted colonization, improvement of cecal microbiota profile, and immune functions. *Probiotics Antimicrob Proteins.* (2020) 12:194–203. doi: 10.1007/s12602-019-9514-3
25. Tian Z, Cui Y, Lu H, Ma X. Effects of long-term feeding diets supplemented with *Lactobacillus reuteri* LR1 on growth performance, digestive and absorptive function of the small intestine in pigs. *J Funct Foods.* (2020) 71:104010. doi: 10.1016/j.jff.2020.104010
26. Suez J, Zmora N, Segal E, Elinav E. The pros, cons, and many unknowns of probiotics. *Nat Med.* (2019) 25:716–29. doi: 10.1038/s41591-019-0439-x
27. Viswanathan VK, Hodges K, Hecht G. Enteric infection meets intestinal function: how bacterial pathogens cause diarrhoea. *Nat Rev Microbiol.* (2009) 7:110–9. doi: 10.1038/nrmicro2053
28. Hoque KM, Chakraborty S, Sheikh IA, Woodward OM. New advances in the pathophysiology of intestinal ion transport and barrier function in diarrhea and the impact on therapy. *Expert Rev Anti-Infe.* (2012) 10:687–99. doi: 10.1586/eri.12.47
29. Reynolds A, Parris A, Evans LA, Lindqvist S, Sharp P, Lewis M, et al. Dynamic and differential regulation of NKCC1 by calcium and cAMP in the native human colonic epithelium. *J Physiol.* (2007) 582:507–24. doi: 10.1113/jphysiol.2007.129718
30. Camilleri M, Madsen K, Spiller R, Van Meerveld BG, Verne GN. Intestinal barrier function in health and gastrointestinal disease. *Neurogastroenterol Motil.* (2012) 24:503–12. doi: 10.1111/j.1365-2982.2012.01921.x
31. Fukudome I, Kobayashi M, Dabanaka K, Maeda H, Okamoto K, Okabayashi T, et al. Diamine oxidase as a marker of intestinal mucosal injury and the effect of soluble dietary fiber on gastrointestinal tract toxicity after intravenous 5-fluorouracil treatment in rats. *Med Mol Morphol.* (2014) 47:100–7. doi: 10.1007/s00795-013-0055-7
32. Nielsen C, Lindholt JS, Erlandsen EJ, Mortensen FV. D-lactate as a marker of venous-induced intestinal ischemia: an experimental study in pigs. *Int J Surg.* (2011) 9:428–32. doi: 10.1016/j.ijsu.2011.04.004
33. Pan L, Zhao PF, Ma XK, Shang QH, Xu YT, Long SF, et al. Probiotic supplementation protects weaned pigs against enterotoxigenic *Escherichia coli* K88 challenge and improves performance similar to antibiotics. *J Anim Sci.* (2017) 95:2627–39. doi: 10.2527/jas.2016.1243
34. Yang F, Wang A, Zeng X, Hou C, Liu H, Qiao S. *Lactobacillus reuteri* I5007 modulates tight junction protein expression in IPEC-J2 cells with LPS stimulation and in newborn piglets under normal conditions. *BMC Microbiol.* (2015) 15:32. doi: 10.1186/s12866-015-0372-1
35. Zanello G, Berri M, Dupont J, Sizaret P, D'Inca R, Salmon H, et al. Saccharomyces cerevisiae modulates immune gene expressions and inhibits ETEC-mediated ERK1/2 and p38 signaling pathways in intestinal epithelial cells. *PLoS ONE.* (2011) 6:e18573. doi: 10.1371/journal.pone.0018573
36. Qiu Y, Jiang Z, Hu S, Wang L, Ma X, Yang X. *Lactobacillus plantarum* enhanced il-22 production in natural killer (nk) cells that protect the integrity of intestinal epithelial cell barrier damaged by enterotoxigenic *Escherichia coli*. *Int J Mol Sci.* (2017) 18:2409. doi: 10.3390/ijms18112409
37. Ciobanu L, Tefas C, Oancea DM, Berce C, Vodnar D, Mester A, et al. Effect of *Lactobacillus plantarum* ACTT 8014 on 5-fluorouracil induced intestinal mucositis in Wistar rats. *Exp Ther Med.* (2020) 20:209. doi: 10.3892/etm.2020.9339
38. Wang Q, Sun Q, Qi R, Wang J, Qiu X, Liu Z, et al. Effects of *Lactobacillus plantarum* on the intestinal morphology, intestinal barrier function and microbiota composition of suckling piglets. *J Anim Physiol An N.* (2019) 103:1908–18. doi: 10.1111/jpn.13198
39. Russell MW, Kilian M. Biological activities of IgA. *Mucosal Immunol.* (2005) 14:267–89. doi: 10.1016/B978-012491543-5/50018-8
40. Kawai T, Akira S. Toll-like receptors and their crosstalk with other innate receptors in infection and immunity. *Immunity.* (2011) 34:637–50. doi: 10.1016/j.immuni.2011.05.006
41. Cario E, Gerken G, Podolsky DK. Toll-like receptor 2 enhances ZO-1-associated intestinal epithelial barrier integrity via protein kinase C. *Gastroenterology.* (2004) 127:224–38. doi: 10.1053/j.gastro.2004.04.015
42. Lai Y, Cogen AL, Radek KA, Park HJ, Macleod DT, Leichtle A, et al. Activation of TLR2 by a small molecule produced by Staphylococcus epidermidis increases antimicrobial defense against bacterial skin infections. *J Invest Dermatol.* (2010) 130:2211–21. doi: 10.1038/jid.2010.123
43. Liu H, ZHANG. Effects of probiotic preparation on growth performance and immune indices of early weaner piglets. *Chinese J Anim Nutr.* (2012) 24:1124–31. doi: 10.3969/j.issn.1006-267x.2012.06.019

Conflict of Interest: The authors declare that the research was conducted in the absence of any commercial or financial relationships that could be construed as a potential conflict of interest.

Publisher's Note: All claims expressed in this article are solely those of the authors and do not necessarily represent those of their affiliated organizations, or those of the publisher, the editors and the reviewers. Any product that may be evaluated in this article, or claim that may be made by its manufacturer, is not guaranteed or endorsed by the publisher.

frontiers in Veterinary Science

ORIGINAL RESEARCH
published: 22 November 2021
doi: 10.3389/fvets.2021.767802

Effects of Dietary Probiotic (*Bacillus subtilis*) Supplementation on Carcass Traits, Meat Quality, Amino Acid, and Fatty Acid Profile of Broiler Chickens

Xiaopeng Tang[1]*, *Xuguang Liu*[1] and *Hu Liu*[2]*

[1] State Engineering Technology Institute for Karst Desertfication Control, School of Karet Science, Guizhou Normal University, Guiyang, China, [2] State Key Laboratory of Grassland Agro-Ecosystems, School of Life Sciences, Lanzhou University, Lanzhou, China

The aim of the present study was to evaluate the effects of dietary supplementation with or without *Bacillus subtilis* (*B. subtilis*) on carcass traits, meat quality, amino acids, and fatty acids of broiler chickens. In total, 160 1-day-old *Arbor Acres* male broiler chicks were divided into two groups with eight replicates of 10 chicks each. Chickens received basal diets without (CN group) or with 500 mg/kg *B. subtilis* (BS group) for 42 days. Eight chickens from each group were slaughtered at the end of the trial, and carcass traits, meat quality, chemical composition, amino acid, and fatty acid profile of meat were measured. The results showed that the breast muscle (%) was higher in BS than in CN ($p < 0.05$), while abdominal fat decreased ($p < 0.05$). The pH_{24h} of thigh muscle was increased ($p < 0.05$) when supplemented with BS; however, drip loss, cooking loss of breast muscle, and shear force of thigh muscle decreased ($p < 0.05$). Lysine (Lys), methionine (Met), glutamic acid (Glu), and total essential amino acid (EAA) in breast muscle and Glu in thigh muscle were greater in BS than in CN ($p < 0.05$). C16:1, C18:1n9c, and MUFA in breast muscle and thigh muscle were greater in BS than in CN ($p < 0.05$). In conclusion, dietary supplementation with *B. subtilis* could improve the carcass traits and meat quality of broilers, which is beneficial for the consumers due to the improved fatty acid profile and amino acid composition.

Keywords: *Bacillus subtilis*, broiler, carcass trait, meat quality, amino acid, fatty acid

OPEN ACCESS

Edited by:
Rita Payan Carreira, University of Evora, Portugal

Reviewed by:
Ayman Abdel-Aziz Swelum, Zagazig University, Egypt
Samiru Sudharaka Wickramasuriya, Agricultural Research Service (USDA), United States

***Correspondence:**
Xiaopeng Tang
tangxiaopeng110@126.com
orcid.org/0000-0002-4789-5687
Hu Liu
liuh2018@lzu.edu.cn
orcid.org/0000-0002-7506-774X

Specialty section:
This article was submitted to Animal Nutrition and Metabolism, a section of the journal Frontiers in Veterinary Science

Received: *31 August 2021*
Accepted: *22 October 2021*
Published: *22 November 2021*

Citation:
Tang X, Liu X and Liu H (2021) Effects of Dietary Probiotic (Bacillus subtilis) Supplementation on Carcass Traits, Meat Quality, Amino Acid, and Fatty Acid Profile of Broiler Chickens. Front. Vet. Sci. 8:767802. doi: 10.3389/fvets.2021.767802

INTRODUCTION

The widespread use of antibiotics has led to the emergence of resistant bacteria and drug residues in animal products, which directly or indirectly endangers human's health and environmental safety (1, 2). Nowadays, with the development of molecular biology, genetic improvements in broiler production have improved body size and growth rate of broilers, resulting in a higher yield of meat in broilers (3). However, the meat quality was decreased drastically with the rapid growth of broilers. Thus, in order to satisfy people's growing demand for high-quality meat, the improvement of meat quality becomes a current hot topic in the field of animal nutrition. Previous studies have demonstrated that probiotics can play a role in improving the microbial balance and intestinal environment (4–7) and are believed to promote the growth performance (8) and meat quality of broilers by multiple ways (9, 10). It is important to note that in all of these studies, *Bacillus* species,

including *Bacillus subtilis* (*B. subtilis*), *Bacillus cereus* (*B. cereus*), *Bacillus clausii* (*B. clausii*), and *Bacillus coagulans* (*B. coagulans*), have been identified as effective probiotics to promote animal growth, maintain intestinal barrier function, and promote meat quality of broilers (9, 11–16).

The adverse environment such as low pH value, high temperature, and relatively greater bile salt within gastrointestinal tract is a severe challenge for probiotics survival (17). *B. subtilis* is a spore gram-positive aerobic bacterium that has a better heat stability and higher acid tolerance, making it a potential feed additive in animal production (18, 19). Previous studies have demonstrated that the properties of probiotic bacteria vary from strain to strain (20). With respect to *B. subtilis*, multiple strains, including *B. subtilis* DSM 17299 (19), *B. subtilis* fmbJ (12), *B. subtilis* RX7 and B2A (13), *B. subtilis* C-3102 (21), *B. subtilis* 29784 (22), *B. subtilis* BYS2 and BG5 (23), *B. subtilis* 1781 and 747 (24), and *B. subtilis* DSM 32315 (25–28), have been gaining interest as they have been indicated to improve the growth performance, feed efficiency, antioxidant capability, immune function, and intestinal microflora balance of broilers. *B. subtilis* DSM 32315, a unique naturally occurring strain, has shown to improve growth performance and intestinal microflora balance of broilers (25–29). For example, Ma et al. (25) showed that dietary supplementation with *B. subtilis* DSM 32315 improved growth performance, intestinal structure, and the manipulation of cecal microbial composition of broilers. Sokale et al. (26) indicated that dietary supplementation with *B. subtilis* DSM 32315 can maintain the intestinal structural integrity and ameliorate the pathology and performance detriments associated with necrotic enteritis challenge. However, previous studies about the application of *B. subtilis* DSM 32315 in poultry mainly concentrated in growth performance and intestinal health; the effect of dietary supplementation with *B. subtilis* DSM 32315 on carcass traits and meat quality of broiler chickens has not been investigated in detail. Thus, the present study aims to investigate the effects of *B. subtilis* DSM 32315 supplementation on carcass traits, meat quality, amino acid (AA), and fatty acid profile of broiler chickens to provide more references for the application of *B. subtilis* in poultry production.

MATERIALS AND METHODS

Birds, Experimental Design, Diets, and Management

The experimental procedures involving animals were reviewed and approved by the animal welfare committee of the Guizhou Normal University (Guiyang, China). A total of 160 1-day-old Arbor Acres (AA) male broiler chicks with similar initial body weights were randomly divided into two groups with eight replicates of 10 chicks each. Chickens received basal diets without (CN group) or with 500 mg/kg *B. subtilis* (BS group, *B. subtilis* DSM 32315, 2.0×10^9 spores/g, Evonik Nutrition & Care GmbH, Germany) throughout the trial period (25). The basal diets (**Table 1**) were formulated according to the nutrient requirements of the Chinese Feeding Standard of Chicken (NY/T 33-2004, China's Ministry of Agriculture). The experiment lasted for 42 days, which was divided into two phases (phase 1: days 1–21 and phase 2: days 22–42). All birds were raised in wire cages in an environmentally controlled room with continuous incandescent white light throughout the experiment and had *ad libitum* access to water and feed. The room temperature was maintained at 33°C for the first 3 days and at 32°C to 30°C for days 4–7, and then reduced by 23°C per week until it reached 22–24°C.

TABLE 1 | Composition and nutrient level of basal diet (as feed basis).

Ingredients	1–21 days	22–42 days
Corn	58.52	61.80
Soybean meal	34.45	30.77
Soybean oil	3.15	3.97
$CaHPO_4$	1.63	1.30
Limestone	0.90	0.91
NaCl	0.35	0.35
DL-Met	0.18	0.10
L-Lys·HCl	0.02	0.00
Vitamin premix[a]	0.10	0.10
Mineral premix[b]	0.25	0.25
Choline chloride	0.20	0.20
Zeolite powder	0.25	0.25
Total	100	100
Nutrient levels[c]		
ME (MJ/kg)	12.51	12.87
CP (%)	21.48	19.99
Ca (%)	1.00	0.90
Available phosphorus (%)	0.45	0.40
Total phosphorus (%)	0.68	
Lysine (%)	1.15	1.00
Methionine (%)	0.50	0.40
Methionine + cystine (%)	0.92	0.78
Threonine (%)	0.81	0.75

[a] *Vitamin premix provided the following per kilogram of diets: VA 12,000 IU, VD_3 2,500 IU, VE 30 IU, VK_3 2.65 mg, VB_1 2 mg, VB_2 6 mg, VB_3 10 mg, VB_{12} 0.025 mg, biotin 0.12 mg, folic acid 1.25 mg, pantothenic acid 12 mg, nicotinic acid 50 mg.*

[b] *Mineral premix provided the following per kilogram of diets: Cu (as copper sulfate) 8 mg, Zn (as zinc sulfate) 75 mg, Fe (as ferrous sulfate) 80 mg, Mn (as manganese sulfate) 100 mg, Se (as sodium selenite) 0.15 mg, and I (as potassium iodide) 0.35 mg.*

[c] *Nutrition levels were calculated values.*

Carcass Traits

At the end of the feeding trial, the diet was removed 12 h before slaughter. Eight middle-weighted birds (one bird/replicate) in each treatment were selected for sample collection. All selected animals were weighed individually, and then slaughtered by severing the jugular vein after electroshock. Then, the carcasses were cut according to a standardized procedure (NY/T 823-2004) to determine the dressing percentage, semi-eviscerated percentage (%), eviscerated percentage (%), breast muscle (%), and abdominal fat (%). After defeathering, head removal, hock cut, and evisceration, the carcass weight, semi-eviscerated weight, and eviscerated weight were recorded. The dressing percentage (%) was calculated by dividing final body weight

with carcass weight [(carcass weight/body weight) × 100], the semi-eviscerated percentage (%) was calculated by dividing final body weight with semi-eviscerated weight [(semi-eviscerated weight/body weight) × 100], and the eviscerated percentage (%) was calculated by dividing final body weight with eviscerated weight [(eviscerated weight/body weight) × 100]. The breast muscle, leg muscle, and abdominal fat were removed and weighed. The breast muscle (%) was calculated by dividing eviscerated weight with breast muscle weight [(breast muscle weight/eviscerated weight) × 100], the leg muscle (%) was calculated by dividing eviscerated weight with leg muscle weight [(leg muscle weight/eviscerated weight) × 100], and the abdominal fat (%) was calculated by dividing eviscerated weight plus abdominal fat weight with abdominal fat weight [abdominal fat weight/(eviscerated weight + abdominal fat weight) × 100]. Approximately 5.0 g of muscles from the medial pectoralis major and thigh were sampled for chemical composition measurement. The remaining muscles from each bird were kept at 4°C for the analysis of meat quality.

Meat Quality Assessment

Meat quality was assessed by determining pH, meat color, drip loss, shear force (N), and cooking loss of the breast and thigh muscle. The pH of breast and thigh muscle was measured at 24 h (pH_{24h}) postmortem by insertion of a handheld pH meter (Russell CD700, Russell pH Limited, Germany). Meat color, including lightness (L*), redness (a*), and yellowness (b*), was measured using Chroma Meter (Opto-Star Lab, Matthaus, Germany) according to the manufacturer's instructions. The measurements of drip loss from 0 to 24 h were conducted as described by Zhou et al. (16). Briefly, ∼30 g of muscle sample was weighed and put into zip-lock plastic bags and stored in a chilling room at 4°C for 24 h and then reweighed after wiping out the surface moisture, and the drip loss was calculated as: drip loss (%) = [(initial weight – final weight)/final weight] × 100. The measurements of shear force and cooking loss were conducted as described by Cai et al. (3) with appropriate modification. Approximately 20 g of a sample of muscle sample was weighted and heated in a water bath to a final internal temperature of 75°C. After cooling to room temperature, the muscle sample was reweighed after wiping out the surface moisture and the cooking loss was calculated as: cooking loss (%) = [(initial weight – final weight)/final weight] × 100. The sample used for the measurement of cooking loss was then used for the measurement of shear force. The sample was cut into 2 cm (length) × 1 cm (width) × 0.5 cm (height) along the direction of the muscle fibers, and the shear force was measured using a digital texture analyzer (Model 2000D, G-R, US).

Chemical Composition Analysis

Muscle samples were cut into slices, dried in a vacuum-freeze dryer, and then ground into powder. The moisture, crude ash, crude protein (CP), and extracted fat (EE) were measured according to the methods described by AOAC [2000; (30)].

To measure the AA content in breast and thigh muscle, the samples were pretreated according to AOAC [2000; (30)]. Briefly, ∼200 mg of fresh muscle sample was accurately weighed into the hydrolysis tube (about 15 ml), 10 ml of hydrochloric acid (6 mol/L) was added, and the mixed sample was filled with nitrogen, sealed, and put in a constant temperature drying box at 110°C for hydrolysis for 24 h; after cooling and mixing well, 100 μl of mixed sample was taken out and dried at 55°C and then 1,000 μl of AA sample diluent was added and mixed well; 1 ml of mixed sample was filtered used a needle filter (diameter 0.2 μm) and then analyzed using an automatic AA analyzer (L-8800; Hitachi, Tokyo, Japan) according to the manufacturer's instructions, and the contents of AA were expressed as mg/g wet tissue.

To measure the fatty-acid profiles in breast and thigh muscle, the samples were pretreated according to AOAC [2000; (30)]. Briefly, ∼50–200 mg of freeze-dried powder samples was accurately weighed into a 10-ml glass tube, and 3 ml of chloroform–methanol–water (volume ratio: 8:4:3) mixture was added. The mixture was shaken in a whirlpool for 1 min, followed by ultrasound for 5 min in an ice bath, repeated three to five times, left for 2 h, and centrifuged at 1,500 rpm for 15 min. The chloroform layer was transferred to another 10-ml glass centrifuge tube and dried in a vacuum drying oven to obtain the mixture of fatty acid and glyceryl ester; 2 ml of KOH-CH_3OH (0.5 mol/L) was added and placed in a slightly boiling water bath for 10 min; after cooling for 3 min, 2 ml of BF_3-CH_3OH solution (10%) was added and then placed in a water bath at 80°C to heat reflux for 2 min, cooled to room temperature, added 1 ml n-hexane and 3 ml of saturated NaCl solution, fully mixed, and centrifuged at room temperature at 2,000 rpm for 5 min, and then the upper n-hexane layer was absorbed into the gas phase vial for the fatty-acid profiles analyzed using an automatic fatty acid analyzer (Shimadzu GC-2010 plus, Japan) according to the manufacturer's instructions.

Statistical Analysis

All the data were subjected to the paired *t*-test using SPSS 21.0 programs (SPSS, Inc., Chicago, IL, USA). Results are expressed as the mean ± standard deviation (SD). Probability values < 0.05 were taken to indicate statistical significance.

RESULTS

Carcass Traits

The effects of *B. subtilis* supplementation on carcass traits of broiler chickens are presented in **Table 2**. Compared to the control group, diet supplementation with *B. subtilis* improved the breast muscle percentage (27.14 vs. 25.04%; $p < 0.05$), but decreased the abdominal fat percentage (1.52 vs. 1.74%; $p < 0.05$). No influences were observed in carcass weight, dressing percentage, semi-eviscerated percentage, eviscerated percentage, and leg muscle percentage ($P > 0.10$) among the treatments.

Meat Quality

The effects of *B. subtilis* supplementation on meat quality of broiler chickens are presented in **Table 3**. Supplementation with *B. subtilis* improved the pH_{24h} value (5.97 vs. 5.73; $p < 0.05$), but decreased the shear force (15.19 vs. 18.04; $p < 0.05$) in the thigh muscle compared to the control group. For the breast muscle, dietary supplementation with *B. subtilis* significantly increased

TABLE 2 | Effects of *Bacillus subtilis* supplementation on carcass traits of broiler chickens.

Item	CN	BS	*p*-value
Final body weight (g)	2,531.90 ± 130.28	2,568.92 ± 141.50	0.595
Carcass weight (g)	2,265.75 ± 69.53	2,320.53 ± 121.27	0.286
Dressing percentage (%)	89.58 ± 2.23	90.36 ± 2.05	0.477
Semi-eviscerated percentage (%)	81.80 ± 4.10	82.13 ± 4.49	0.877
Eviscerated percentage (%)	70.17 ± 2.14	71.40 ± 0.64	0.342
Breast muscle (%)	25.04 ± 1.60	27.14 ± 1.82	0.028
Leg muscle (%)	19.76 ± 1.46	20.01 ± 2.01	0.779
Abdominal fat (%)	1.74 ± 0.15	1.52 ± 0.18	0.017

Values are expressed as means ± SD, n = 8; CN, Control group, chickens received a basal diet; BS, Bacillus subtilis group, chickens received a basal diet supplemented with Bacillus subtilis; p < 0.05 were taken to indicate statistical significance.

TABLE 3 | Effects of *Bacillus subtilis* supplementation on meat quality of broiler chickens.

Item	Muscle	CN	BS	*p*-value[#]	*p*-value[‡]
pH_{24h}	Breast	5.71 ± 0.26	5.87 ± 0.22	0.204	0.479
	Thigh	5.73 ± 0.10	5.97 ± 0.24	0.023	
Lightness (L*)	Breast	46.19 ± 4.48	48.10 ± 3.94	0.381	<0.001
	Thigh	37.92 ± 3.26	40.96 ± 5.13	0.178	
Redness (a*)	Breast	5.22 ± 1.46	6.20 ± 1.69	0.231	<0.001
	Thigh	10.08 ± 4.61	12.73 ± 2.57	0.178	
Yellowness (b*)	Breast	7.61 ± 0.86	7.89 ± 1.31	0.036	<0.001
	Thigh	5.74 ± 1.56	6.38 ± 1.17	0.370	
Drip loss (%)	Breast	4.08 ± 0.74	3.24 ± 0.68	0.017	0.001
	Thigh	2.91 ± 0.61	2.53 ± 0.66	0.251	
Cooking loss (%)	Breast	18.27 ± 0.73	16.66 ± 1.35	0.010	<0.001
	Thigh	13.61 ± 2.44	12.74 ± 2.43	0.484	
Shear force (N)	Breast	24.67 ± 6.61	19.81 ± 2.49	0.072	0.001
	Thigh	18.04 ± 2.84	15.19 ± 1.66	0.028	

Values are expressed as means ± SD, n = 8; CN, Control group, chickens received a basal diet; BS, Bacillus subtilis group, chickens received a basal diet supplemented with Bacillus subtilis; [#]difference between CN group and BS group; [‡]difference between breast muscle and thigh muscle; p < 0.05 were taken to indicate statistical significance.

Yellowness (b*) (7.89 vs. 7.61; $p < 0.05$) compared to the control group, but decreased the drip loss (3.24 vs. 4.08; $p < 0.05$) and the cooking loss (16.66 vs. 18.27; $p < 0.05$) compared to the control group. In addition, dietary supplementation with *B. subtilis* had a tendency to decrease shear force (19.81 vs. 24.67; $p = 0.072$) in the breast muscle compared to the control group. It seems that the thigh muscle had a lower Lightness (L*), Yellowness (b*), drip loss, cooking loss, and shear force ($p < 0.05$), but had a higher Redness (a*) ($P < 0.05$) than breast muscle.

Meat Chemical Composition

The effects of *B. subtilis* supplementation on meat chemical composition (moisture, crude protein, ether extract, and crude ash) of broiler chickens are presented in **Table 4**. Dietary supplementation with *B. subtilis* had no effect on chemical composition of both breast and thigh muscles of broilers, and only had a tendency ($p = 0.093$) to increase ether extract content in the thigh muscle. In addition, the content of crude protein in breast muscle was higher, and ether extract was much lower than thigh muscle ($P < 0.05$).

TABLE 4 | Effects of *Bacillus subtilis* supplementation on conventional chemical composition of broiler chickens.

Item	Muscle	CN	BS	*p*-value[#]	*p*-value[‡]
Moisture (%)	Breast	73.14 ± 3.55	72.22 ± 3.85	0.628	0.249
	Thigh	71.09 ± 2.51	70.73 ± 6.58	0.888	
Crude protein (%)	Breast	22.31 ± 2.41	24.37 ± 2.72	0.132	<0.001
	Thigh	19.23 ± 2.22	20.35 ± 2.40	0.351	
Ether extract (%)	Breast	1.50 ± 0.27	1.71 ± 0.22	0.120	<0.001
	Thigh	5.39 ± 0.70	6.01 ± 0.67	0.093	
Crude ash (%)	Breast	1.28 ± 0.59	1.27 ± 0.28	0.975	0.197
	Thigh	1.13 ± 0.38	1.08 ± 0.15	0.739	

Values are expressed as means ± SD, n = 8; CN, Control group, chickens received a basal diet; BS, Bacillus subtilis group, chickens received a basal diet supplemented with Bacillus subtilis; [#]difference between CN group and BS group; [‡]difference between breast muscle and thigh muscle; p < 0.05 were taken to indicate statistical significance tendency.

Meat Amino Acid Composition

The AA contents in breast muscle and thigh muscle are presented in **Table 5**. In the breast muscle, the content of lysine (Lys, 20.26 vs. 18.53 mg/g; $p < 0.05$), methionine (Met, 4.28 vs. 3.74 mg/100 g; $p < 0.05$), glutamic acid (Glu, 18.03 vs. 16.88 mg/100 g; $p < 0.05$), and the total essential amino acid (EAA, 81.19 vs. 77.20 mg/100 g; $p < 0.05$) was greater when supplemented with *B. subtilis* than the control group. In addition, dietary supplementation with *B. subtilis* had a tendency to increase the total AA (164.32 vs. 155.44 mg/100 g; $p = 0.073$) content in the breast muscle compared to the control group. In the thigh muscle, dietary *B. subtilis* supplementation increased the Glu (16.83 vs. 15.78 mg/100 g; $p < 0.05$) content and had a tendency to increase the Lys content (17.98 vs. 16.70 mg/100 g; $p = 0.078$) compared to the control group. It seems that most AAs [except phenylalanine (Phe), cysteine (Cys), glycine (Gly), and proline (Pro)] in the breast muscle were much higher than in the thigh muscle ($p < 0.05$).

Meat Fatty Acid Composition

The fatty acid contents in breast muscle and thigh muscle are presented in **Table 6**. The palmitoleic acid (C16:1, 3.228 vs. 1.938%; $p < 0.05$), oleic acid (C18:1n9c, 36.671 vs. 33.904%; $p < 0.05$), *Cis*-8,11,14-eicosatrienoate (C20:3n6, 1.387 vs. 1.109%; $p < 0.05$), and total monounsaturated fatty acid (MUFA, 41.190 vs. 37.074%; $p < 0.05$) were higher when supplemented with *B. subtilis*, but the palmitic acid (C16:0, 26.762 vs. 29.049%; $p < 0.05$) and arachidic acid (C20:0, 0.256 vs. 0.437%; $p < 0.05$) decreased in the breast muscle. In addition, dietary supplementation with *B. subtilis* had a tendency to increase eicosadienoic acid (C20:2, 0.468 vs. 0.569%) and the total unsaturated fatty acids (UFA, 59.160 vs. 55.514%, $p = 0.083$), and

TABLE 5 | Effects of *Bacillus subtilis* supplementation on amino acid content in breast muscle and thigh muscle of broiler chickens (mg/100 g DM).

Amino acids	Breast muscle			Thigh muscle			*p*-value‡
	CN	BS	*p*-value#	CN	BS	*p*-value†	
Essential amino acid (EAA)							
Threonine (Thr)	7.45 ± 0.54	7.88 ± 0.48	0.112	6.70 ± 0.42	6.86 ± 0.66	0.578	<0.001
Valine (Val)	6.78 ± 0.45	6.95 ± 0.33	0.402	5.87 ± 0.50	6.12 ± 0.60	0.385	<0.001
Methionine (Met)	3.74 ± 0.35	4.28 ± 0.50	0.025	3.45 ± 0.52	3.60 ± 0.44	0.528	0.009
Isoleucine (Ile)	7.29 ±0.69	7.42 ± 0.54	0.685	6.34 ± 0.59	6.56 ± 0.65	0.494	<0.001
Leucine (Leu)	9.80 ± 0.70	10.37 ± 0.63	0.107	8.80 ± 0.63	9.05 ± 0.88	0.517	<0.001
Histidine (His)	8.72 ± 0.98	8.85 ± 1.18	0.816	10.62 ± 1.29	11.46 ± 3.44	0.529	0.003
Phenylalanine (Phe)	4.33 ± 0.56	4.07 ± 0.29	0.263	3.84 ± 0.95	3.96 ±0.95	0.807	0.253
Arginine (Arg)	10.56 ± 0.77	11.09 ± 1.00	0.253	9.40 ± 0.60	9.70 ± 0.66	0.368	<0.001
Lysine (Lys)	18.53 ± 1.29	20.26 ± 1.05	0.011	16.70 ± 1.18	17.98 ± 1.49	0.078	<0.001
Non-essential amino acid (NEAA)							
Alanine (Ala)	12.56 ± 1.85	12.65 ± 2.65	0.736	10.71 ± 1.08	11.22 ± 1.22	0.393	0.007
Cysteine (Cys)	7.63 ± 0.48	8.46 ± 1.34	0.121	7.34 ± 0.73	7.84 ± 0.79	0.215	0.178
Aspartic acid (Asp)	14.26 ± 1.02	14.58 ± 0.61	0.472	12.39 ± 0.89	12.79 ± 1.22	0.469	<0.001
Serine (Ser)	5.10 ± 0.30	5.21 ± 0.33	0.518	4.70 ± 0.28	4.80 ± 0.37	0.550	0.001
Glutamic acid (Glu)	16.88 ± 1.21	18.03 ± 0.86	0.046	15.78 ± 0.87	16.83 ± 1.05	0.047	0.007
Glycine (Gly)	9.47 ± 0.72	10.80 ± 2.47	0.166	9.34 ± 1.55	10.13 ± 1.65	0.343	0.523
Tyrosine (Tyr)	4.93 ± 0.44	4.52 ± 0.49	0.105	4.25 ± 0.0.51	4.42 ± 0.57	0.546	0.039
Proline (Pro)	7.39 ± 0.47	8.58 ± 3.12	0.306	7.09 ± 0.85	7.45 ± 0.76	0.389	0.239
Total EAA	77.20 ± 2.46	81.19 ±3.74	0.025	72.20 ± 5.88	74.84 ± 9.07	0.501	0.009
Total NEAA	78.24 ± 4.08	83.13 ± 8.45	0.162	71.94 ±6.20	75.11 ± 6.31	0.328	0.007
Total AA	155.44 ± 5.78	164.32 ± 11.62	0.073	144.14 ± 4.05	149.95 ± 5.17	0.391	0.004
FAA	63.74 ± 3.89	67.46 ± 5.32	0.133	57.97 ± 4.77	60.31 ± 4.96	0.353	0.001

Values are expressed as means ± SD, n = 8; CN, Control group, chickens received a basal diet; BS, Bacillus subtilis group, chickens received a basal diet supplemented with Bacillus subtilis; AA, amino acids; FAA (flavor amino acid), the sum of Glu, Asp, Gly, Arg, and Ala; # difference between CN group and BS group in breast muscle; † difference between CN group and BS group in thigh muscle; ‡ difference between breast muscle and thigh muscle; p < 0.05 were taken to indicate statistical significance.

had a tendency to decrease the total saturated fatty acid (SFA, 40.842 vs. 44.486%, $p = 0.059$) in the breast muscle compared to the control group. For the thigh muscle, dietary supplementation with *B. subtilis* increased the C16:1 (4.972 vs. 3.874%; $p < 0.05$), C18:1n9c (36.116 vs. 33.261%; $p < 0.05$), and MUFA (43.062 vs. 38.880%; $p < 0.05$), and decreased the C16:0 (23.747 vs. 24.924%; $p < 0.05$) and the total SFA (37.061 vs. 40.247%; $p < 0.05$) compared to the control group. There is a tendency to increase the myristoleic acid (C14:1, 0.060 vs. 0.054%, $p = 0.057$), nervonic acid (C24:1n9, 0.052 vs. 0.032%, $p = 0.076$), and the total UFA (62.939 vs. 59.752%, $p = 0.066$) in the thigh muscle when supplemented with *B. subtilis*. The results from the present study showed that the fatty acid content in breast muscle and thigh muscle is greatly different.

DISCUSSION

In the present study, we mainly investigated the effects of dietary supplementation with *B. subtilis* DSM 32315 on carcass traits, meat quality, AA, and fatty acid profile of broiler chickens. The results of the present study showed that dietary supplementation with *B. subtilis* DSM 32315 has a remarkable effect on carcass traits and could improve the meat quality and meat flavor of broiler chickens through improving the AA and fatty acid profiles. Carcass traits provide important indices in broiler production. In the present study, dietary supplementation with *B. subtilis* significantly increased the breast muscle and significantly decreased the abdominal fat of broiler chickens. However, *B. subtilis* supplementation had no effect on the carcass weight, dressing percentage, semi-eviscerated percentage, eviscerated percentage, and leg muscle, which is consistent with the results from Yadav et al. (31) who reported that dietary supplementation with *B. subtilis* (DM 03, TAM 4 and IQB 350) significantly increased the breast muscle weight of broilers. In contrast, Cramer et al. (11) reported that dietary supplementation with *B. subtilis* did not affect the breast muscle weight of broilers exposed to chronic heat stress, and Park and Kim (13) reported that dietary supplementation with *B. subtilis* RX7 or B2A did not affect the abdominal fat of broilers challenged with *Salmonella typhimurium*. This is probably because the beneficial effects of *B. subtilis* in broilers were markedly strain-dependent (7, 32). Abdominal fat is an important index used to measure lipid deposition in broilers (33, 34). Excessive fat deposition is undesirable, because it degrades meat quality, decreases feed efficiency, and increases production and health costs (35, 36). The lower abdominal fat in broiler chickens supplemented with *B. subtilis* in the present study indicated that *B. subtilis* can lead

TABLE 6 | Effects of *Bacillus subtilis* supplementation on fatty acids content in breast muscle and thigh muscle of broiler chickens (%).

Fatty acids	Breast muscle			thigh muscle			*p*-value‡
	CN	BS	*p*-value#	CN	BS	*p*-value†	
Saturated fatty acid (SFA)							
C12:0	0.048 ± 0.017	0.040 ± 0.017	0.387	0.054 ± 0.011	0.047 ± 0.022	0.489	0.262
C14:0	0.432 ± 0.065	0.472 ± 0.080	0.290	0.602 ± 0.156	0.535 ± 0.053	0.267	0.002
C15:0	0.114 ± 0.014	0.104 ± 0.013	0.290	0.107 ± 0.018	0.087 ± 0.015	0.290	0.068
C16:0	29.049 ± 1.449	26.762 ± 2.031	0.021	24.924 ± 1.317	23.747 ± 0.798	0.049	<0.001
C17:0	0.340 ± 0.090	0.285 ± 0.063	0.179	0.326 ± 0.075	0.254 ± 0.104	0.132	0.476
C18:0	9.350 ± 0.610	8.855 ± 1.511	0.405	10.231 ± 2.630	8.939 ± 2.064	0.293	0.470
C20:0	0.437 ± 0.179	0.256 ± 0.155	0.048	0.204 ± 0.225	0.174 ± 0.124	0.746	0.020
C21:0	0.364 ± 0.171	0.385 ± 0.317	0.870	0.241 ± 0.142	0.325 ± 0.155	0.278	0.215
C22:0	0.170 ± 0.020	0.207 ± 0.110	0.360	0.107 ± 0.028	0.122 ± 0.052	0.483	0.002
C23:0	4.132 ± 0.692	3.433 ± 1.373	0.220	3.400 ± 1.042	2.794 ± 0.508	0.161	0.059
C24:0	0.017 ± 0.009	0.017 ± 0.007	0.988	0.017 ± 0.010	0.012 ± 0.005	0.233	0.381
Unsaturated fatty acids (UFA)							
C14:1	0.050 ± 0.029	0.085 ± 0.053	0.123	0.112 ± 0.054	0.171 ± 0.060	0.057	0.001
C16:1	1.938 ± 0.396	3.228 ± 1.391	0.024	3.874 ± 0.634	4.972 ± 0.851	0.011	<0.001
C17:1	0.039 ± 0.003	0.046 ± 0.013	0.138	0.064 ± 0.024	0.076 ± 0.031	0.378	0.001
C18:1n9t	0.769 ± 0.218	0.759 ± 0.178	0.921	1.051 ± 0.305	1.174 ± 0.531	0.581	0.005
C18:1n9c	33.904 ± 1.550	36.671 ± 2.556	0.020	33.261 ± 2.324	36.116 ± 2.402	0.030	0.521
C18:2n6t	0.075 ± 0.029	0.076 ± 0.019	0.921	0.037 ± 0.038	0.040 ± 0.051	0.914	0.006
C18:2n6c	11.797 ± 1.056	10.977 ± 2.223	0.362	14.835 ± 2.330	13.750 ± 1.227	0.263	<0.001
C18:3n3	0.881 ± 0.113	0.965 ± 0.263	0.422	1.542 ± 0.439	1.603 ± 0.431	0.782	<0.001
C18:3n6	0.219 ± 0.023	0.242 ± 0.051	0.253	0.301 ± 0.061	0.287 ± 0.122	0.781	0.018
C20:1n9	0.3160.037 ±	0.350 ± 0.066	0.323	0.439 ± 0.092	0.444 ± 0.117	0.926	0.001
C20:2	0.569 ± 0.060	0.468 ± 0.130	0.065	0.426 ± 0.070	0.370 ± 0.138	0.322	0.004
C20:3n6	1.109 ± 0.158	1.387 ± 0.247	0.018	0.562 ± 0.095	0.568 ± 0.228	0.955	<0.001
C20:3n3	0.065 ± 0.016	0.052 ± 0.020	0.196	0.051 ± 0.037	0.053 ± 0.044	0.952	0.534
C20:5N3	0.392 ± 0.082	0.386 ± 0.184	0.931	0.129 ± 0.035	0.152 ± 0.102	0.544	<0.001
C22:1n9	0.055 ± 0.013	0.046 ± 0.015	0.235	0.046 ± 0.027	0.056 ± 0.031	0.502	0.938
C22:2	0.015 ± 0.008	0.020 ± 0.008	0.207	0.022 ± 0.013	0.029 ± 0.011	0.318	0.031
C22:6n3	3.317 ± 0.553	3.395 ± 1.040	0.855	2.965 ± 1.086	3.024 ± 0.631	0.897	0.228
C24:1n9	0.004 ± 0.005	0.005 ± 0.005	0.642	0.032 ± 0.022	0.052 ± 0.020	0.076	<0.001
SFA	44.486 ± 2.141	40.842 ± 4.535	0.059	40.247 ± 3.395	37.061 ± 2.171	0.042	0.003
MUFA	37.074 ± 1.842	41.190 ± 3.955	0.018	38.880 ± 2.595	43.062 ± 3.099	0.011	0.157
PUFA	18.440 ± 1.242	17.970 ± 2.277	0.616	20.872 ± 2.988	19.876 ± 2.288	0.466	0.010
UFA	55.514 ± 1.666	59.160 ± 5.274	0.083	59.752 ± 4.178	62.939 ± 1.727	0.066	0.007

Values are expressed as means ± SD, n = 8; CN, Control group, chickens received a basal diet; BS, Bacillus subtilis group, chickens received a basal diet supplemented with Bacillus subtilis; C12:0, Lauric acid; C14:0, Myristic acid; C15:0, Pentadecanoic acid; C16:0, Palmitic acid; C17:0, Heptadecanoic acid; C18:0, Stearic acid; C20:0, Arachidic acid; C21:0, Heneicosanoic acid; C22:0, Docosanoic acid; C23:0, Tricosanic acid; C24:0, Lignoceric acid; C14:1, Myristoleic acid; C16:1, Palmitoleic acid; C17:1, Heptadecenoic acid; C18:1n9t, Elaidic acid; C18:1n9c, Oleic acid; C18:2n6t, Linolelaidic acid; C18:2n6c, Linoleic acid; C18:3n3, Linolenic acid; C18:3n6, γ-Linolenic acid; C20:1n9, Eicosenoic acid; C20:2, Eicosadienoic acid; C20:3n6, Cis-8,11,14-Eicosatrienoate; C20:3n3, Cis-11,14,17-Eicosatrienoate; C20:5N3, Timnodonic acid; C22:1n9, Erucic acid; C22:2, Docosadienoic acid; C22:6n3, Docosahexaenoic acid; C24:1n9, Nervonic acid; MUFA, monounsaturated fatty acid; PUFA, polyunsaturated fatty acid; #difference between CN group and BS group in breast muscle; †difference between CN group and BS group in thigh muscle; ‡difference between breast muscle and thigh muscle; p < 0.05 were taken to indicate statistical significance.

to a higher economic efficiency since the public tends to favor low-fat-content chicken.

The pH value, meat color (lightness, redness, and yellowness), drip loss, cooking loss, and shear force are commonly used indices for evaluating meat quality (37). Previous studies have reported that dietary supplementation with *B. subtilis* could improve the carcass traits and meat quality of broilers by improving the pH, tenderness, and color (11–13). pH is related to shelf life, color, and water-holding capacity of the meat, which are determined mostly by postmortem conversion of muscle glycogen to lactic acid, and often used as an important indicator to evaluate meat quality (38, 39). The higher pH_{24h} in the muscle of broilers fed with *B. subtilis* indicated a better shelf life, color, and water-holding capacity of meat. Similarly, Cramer et al. (11) also showed that dietary supplementation with *B. subtilis* increased the pH_{24h} of breast muscle. In contrast, Park and Kim

(13) and Bai et al. (12) reported that dietary supplementation with *B. subtilis* had no effect on the pH value of meat. *B. subtilis* supplementation did not affect the meat color (a*, b*, and L*) in the present study, which is consistent with Jeong and Kim (21) and Cramer et al. (11), who also reported that *B. subtilis* had no effect on the meat color. However, in contrast, Bai et al. (12) reported that *B. subtilis* could decrease L* and b*, and increase a*. Drip loss and cooking loss could reflect the water-holding capacity and are related to nutrition, flavor, and juiciness, because some nutrients are easily lost during exudation by water loss (40, 41). In the present study, dietary supplementation with *B. subtilis* decreased the drop loss and cooking loss of the breast muscle after storage for 1 day, which suggested the increase of water-holding capacity of meat. The results of our study support the previous research, which concluded that dietary supplementation with *B. subtilis* RX7 or B2A in broiler diets increased the drip loss of breast meat (13). However, the detailed reasons for *B. subtilis* decreased the drip loss and cooking loss was unclear. Tenderness is considered as the most important trait for consumers, which can be represented by shear force (42). It was clear from our study that the administration of *B. subtilis* had a beneficial effect on meat tenderness with a decreased shear force. Inconsistent results between studies have been reported for the impact of *B. subtilis* supplementation on meat tenderness. Similarly to the present study, Bai et al. (43) reported that the administration of *B. subtilis* in the diets could decrease the shear force and thus improve muscle tenderness, whereas Cramer et al. (11) and Abdulla et al. (44) had found that dietary supplementation with *B. subtilis* had no difference in shear force. Therefore, the present study indicated that dietary supplementation with *B. subtilis* could improve the meat quality of broilers by improving the pH and tenderness and by decreasing the drop loss and cooking loss.

In the current study, *B. subtilis* treatment did not affect the routine nutrients (moisture, crude protein, ether extract, and crude ash) in both breast and thigh muscles compared to the control group, but it showed that dietary supplementation with *B. subtilis* had a tendency to improve the ether extract content in the thigh muscle. Similarly, Zhou et al. (16) indicated that dietary probiotic *Bacillus coagulans* supplementation did not affect moisture, crude protein, ether extract, and crude ash content in the muscles of Guangxi Yellow chicken. In contrast, Abdulla et al. (44) showed that dietary supplementation with *B. subtilis* significantly decreased the fat content in breast and thigh muscles of broilers. Intramuscular fat content is an important sensory characteristic of meats and is related to tenderness, succulence, and flavor of meats (45). The higher fat content of thigh muscle from *B. subtilis* treatment in the present study suggested better tenderness, succulence, and flavor of meats.

The AA content in meat is important to evaluate the quality and flavor of meat. EAA determines the muscle protein quality, and flavor amino acid (FAA), such as alanine (Ala), glycine (Gly), Glu, aspartic acid (Asp), and serine (Ser), especially Glu, can greatly contribute to the taste of meat (38, 46). In the breast muscle, Met, Lys, Glu, total EAA, and total AA were increased by *B. subtilis* treatment in the present study. In the thigh muscle, only Glu content was increased by *B. subtilis* treatment. The reasons for this phenomenon might be due to the higher content of total AA in the breast muscle that made it more sensitive to FAAs. The results from Guo et al. (37) and Chen et al. (47) also support this opinion, who reported that breast muscle contained higher levels of total AAs than those of thigh muscle in broiler chickens. Lys and Met are two kinds of important EAA in meat of broilers. The higher Lys and Met in the meat of broilers fed with *B. subtilis* meant that *B. subtilis* had a beneficial effect on improving the protein quality and nutrition value of muscle. Glu is one of the most important FAA, which is the primary flavor molecule and functions in meat freshness and buffering salty and sour tastes (48). The Glu content in breast muscle and thigh muscle both increased due to *B. subtilis* treatment, indicating that *B. subtilis* has a role in promoting the meat flavor. In a word, *B. subtilis* could improve the meat protein quality as well as meat flavor of broilers.

It is well-known that fatty acids, including MUFA, polyunsaturated fatty acids (PUFA), and SFA, are an important indicator to evaluate the quality and nutritional value of meat and they also are the basis for the characteristic flavor of meat (49). The major fatty acids in chicken meat are C16:0, stearic acid (C18:0), C18:1n9c, and linoleic acid (C18:2n6c) (50). It is generally accepted that higher dietary intakes of SFA, especially C16:0 and myristic acid (C14:0), are positively correlated with increased risk of coronary heart disease, due to their ability to raise the total cholesterol and low-density lipoprotein (51, 52). In the present study, *B. subtilis* treatment significantly decreased C14:0, C16:0, and C20:0 in the breast muscle, and significantly decreased C16:0 and total SFA in the thigh muscle, which indicated that the muscles from broilers treated with *B. subtilis* might be more beneficial to human health. The UFA not only is the precursor substance to meat flavor, but also plays a wide range of roles in promoting growth, scavenging free radicals, and regulating lipid metabolism (49). In the present study, *B. subtilis* treatment significantly increased C16:1, C18:1n9c, C20:3n6, and total MUFA in the breast muscle, and significantly increased C16:1, C18:1n9c, and total MUFA in the thigh muscle. C18:1n9c is the most abundant UFA, which is suggested to be positively associated with the softness of fat and the sensory quality of meat; thus, rich oleic acid content can make meat tasty (51, 52). The higher C18:1n9c content in muscles from broilers treated with *B. subtilis* meant a better meat quality. C18:2n6c was reported to cause a negative flavor in meat (53). *B. subtilis* treatment had no effect on C18:2n6c content in both breast and thigh muscles, which meant that there was no adverse effect on meat flavor when broilers are supplemented with *B. subtilis*. In summary, *B. subtilis* could improve the composition of muscle fatty acids by decreasing the SFA content and increasing the UFA content, thus improving the meat quality as well as meat flavor.

CONCLUSIONS

In conclusion, dietary supplementation with *B. subtilis* could improve the carcass traits and meat quality of broilers by

improving the pH and tenderness, decreasing the drip loss and cooking loss, and adjusting the composition of AAs and fatty acids.

DATA AVAILABILITY STATEMENT

The original contributions presented in the study are included in the article/**Supplementary Material**, further inquiries can be directed to the corresponding author/s.

ETHICS STATEMENT

The experimental procedures involving animals were reviewed and approved by the Animal Welfare Committee of the Guizhou Normal University (Guiyang, China).

AUTHOR CONTRIBUTIONS

XT and HL: conceptualization, investigation, resources, and methodology. XT and XL: formal analysis and data curation. XT: writing—original draft preparation, writing—review and editing, project administration, funding acquisition, and supervision. All authors have read and agreed to the published version of the manuscript.

FUNDING

This research was supported by the China Overseas Expertise Introduction Program for Discipline Innovation (No. D17016),the Key Project of Science and Technology Program of Guizhou Province (No. 5411 2017 Qiankehe Pingtai Rencai), the World Top Discipline Program of Guizhou Province (No. 125 2019 Qianjiao Keyan Fa), the Natural Science Research Project of Education Department of Guizhou Province[Qianjiaohe KY Zi (2021) 294], and the Doctoral Launched Scientific Research Program of Guizhou Normal University [GZNUD (2018) 26].

ACKNOWLEDGMENTS

We thank Prof. Kangning Xiong for kindly revising the paper and financial support.

SUPPLEMENTARY MATERIAL

The Supplementary Material for this article can be found online at: https://www.frontiersin.org/articles/10.3389/fvets.2021.767802/full#supplementary-material

REFERENCES

1. Chiesa LM, Nobile M, Panseri, S, Arioli, F. Antibiotic use in heavy pigs: comparison between urine and muscle samples from food chain animals analysed by HPLC-MS/MS. *Food Chem.* (2017) 235:111–8. doi: 10.1016/j.foodchem.2017.04.184
2. Li X, Wang L, Zhen Y, Li S, Xu Y. Chicken egg yolk antibodies (IgY) as non-antibiotic production enhancers for use in swine production: a review. *J Anim Sci Biotechn.* (2015) 6:40. doi: 10.1186/s40104-015-0038-8
3. Cai K, Shao W, Chen X, Campbell YL, Nair MN, Suman SP, et al. Meat quality traits and proteome profile of woody broiler breast (pectoralis major) meat. *Poult Sci.* (2018) 97:337–46. doi: 10.3382/ps/pex284
4. Zhang L, Zhang L, Zhan X, Zeng X, Zhou L, Cao G, et al. Effects of dietary supplementation of probiotic, *clostridium butyricum*, on growth performance, immune response, intestinal barrier function, and digestive enzyme activity in broiler chickens challenged with *escherichia* coli k88. *J Anim Sci Biotechnol.* (2016) 7:3. doi: 10.1186/s40104-016-0061-4
5. Hagihara M, Kuroki Y, Ariyoshi T, Higashi S, Fukuda K, Yamashita R, et al. Clostridium butyricum modulates the microbiome to protect intestinal barrier function in mice with antibiotic-induced dysbiosis. *iScience.* (2020) 23:100772. doi: 10.1016/j.isci.2019.100772
6. Alagawany M, Abd El-Hack ME, Farag MR, Sachan S, Karthik K, Dhama K. The use of probiotics as eco-friendly alternatives for antibiotics in poultry nutrition. *Environ Sci Pollut Res Int.* (2018) 25:10611–8. doi: 10.1007/s11356-018-1687-x
7. Gadde UD, Oh S, Lee Y, Davis E, Zimmerman N, Rehberger T, et al. Dietary bacillus subtilis-based direct-fed microbials alleviate LPS-induced intestinal immunological stress and improve intestinal barrier gene expression in commercial broiler chickens. *Res Vet Sci.* (2017) 114:236–43. doi: 10.1016/j.rvsc.2017.05.004
8. Dela Cruz PJD, Dagaas CT, Mangubat KMM, Angeles AA, Abanto OD. Dietary effects of commercial probiotics on growth performance, digestibility, and intestinal morphometry of broiler chickens. *Trop Anim Health Prod.* (2019) 51:1105–15. doi: 10.1007/s11250-018-01791-0
9. Upadhaya SD, Rudeaux F, Kim IH. Effects of inclusion of bacillus subtilis (Gallipro) to energy- and protein-reduced diet on growth performance, nutrient digestibility, and meat quality and gas emission in broilers. *Poult Sci.* (2019) 98:2169–78. doi: 10.3382/ps/pey573
10. Yu L, Peng Z, Dong L, Wang H, Shi, S. Enterococcus faecium NCIMB 10415 supplementation improves the meat quality and antioxidant capacity of muscle of broilers. *J Anim Physiol Anim Nutr.* (2019) 103:1099–106. doi: 10.1111/jpn.13097
11. Cramer TA, Kim HW, Chao Y, Wang W, Cheng HW, Kim YHB. Effects of probiotic (Bacillus subtilis) supplementation on meat quality characteristics of breast muscle from broilers exposed to chronic heat stress. *Poult Sci.* (2018) 97:3358–68. doi: 10.3382/ps/pey176
12. Bai K, Huang Q, Zhang J, He J, Zhang L, Wang T. Supplemental effects of probiotic bacillus subtilis fmbJ on growth performance, antioxidant capacity, and meat quality of broiler chickens. *Poult Sci.* (2017) 96:74–82. doi: 10.3382/ps/pew246
13. Park JH, Kim IH. The effects of the supplementation of bacillus subtilis RX7 and B2A strains on the performance, blood profiles, intestinal salmonella concentration, noxious gas emission, organ weight and breast meat quality of broiler challenged with salmonella typhimurium. *J Anim Physiol Anim Nutr.* (2015) 99:326–34. doi: 10.1111/jpn.12248
14. Barbosa TM, Serra CR, La Ragione RM, Woodward MJ, Henriques AO. Screening for bacillus isolates in the broiler gastrointestinal tract. *Appl Environ Microbiol.* (2005) 71:968–78. doi: 10.1128/AEM.71.2.968-978.2005
15. Li J, Li W, Li J, Wang Z, Xiao D, Wang Y, et al. Screening of differentially expressed immune-related genes from spleen of broilers fed with probiotic bacillus cereus PAS38 based on suppression subtractive hybridization. *PLoS ONE.* (2019) 14:e0226829. doi: 10.1371/journal.pone.0226829
16. Zhou X, Wang Y, Gu Q, Li W. Effect of dietary probiotic, bacillus coagulans, on growth performance, chemical composition, and meat quality of Guangxi Yellow chicken. *Poult Sci.* (2010) 89:588–93. doi: 10.3382/ps.2009-00319

17. Sarao LK, Arora M. Probiotics, prebiotics, and microencapsulation: a review. *Crit Rev Food Sci Nutr.* (2017) 57:344–71. doi: 10.1080/10408398.2014.887055
18. Hong HA, Hong DL, Cutting SM. The use of bacterial spore formers as probiotics. *FEMS Microbiol Rev.* (2005) 29:813–35. doi: 10.1016/j.femsre.2004.12.001
19. Reis MP, Fassani EJ, Garcia Junior, AAP, Rodrigues PB, Bertechini AG, et al. Effect of bacillus subtilis (DSM 17299) on performance, digestibility, intestine morphology, and pH in broiler chickens. *J Appl Poult Res.* (2017) 26:573–83. doi: 10.3382/japr/pfx032
20. Dowarah R, Verma AK, Agarwal N, Singh P, Singh BR. Selection and characterization of probiotic lactic acid bacteria and its impact on growth, nutrient digestibility, health and antioxidant status in weaned piglets. *PLoS ONE.* (2018) 13:e0192978. doi: 10.1371/journal.pone.0192978
21. Jeong JS, Kim IH. Effect of bacillus subtilis C-3102 spores as a probiotic feed supplement on growth performance, noxious gas emission, and intestinal microflora in broilers. *Poult Sci.* (2014) 93:3097–103. doi: 10.3382/ps.2014-04086
22. Jacquier V, Nelson A, Jlali M, Rhayat L, Brinch KS, Devillard E. Bacillus subtilis 29784 induces a shift in broiler gut microbiome toward butyrate-producing bacteria and improves intestinal histomorphology and animal performance. *Poult Sci.* (2019) 98:2548–54. doi: 10.3382/ps/pey602
23. Guo M, Li M, Zhang C, Zhang X, Wu, Y. Dietary administration of the bacillus subtilisenhances immune responses and disease resistance in chickens. *Front Microbiol.* (2020) 11:1768. doi: 10.3389/fmicb.2020.01768
24. Park I, Zimmerman NP, Smith AH, Rehberger TG, Lillehoj EP, Lillehoj HS. Dietary supplementation with bacillus subtilis direct-fed microbials alters chicken intestinal metabolite levels. *Front Vet Sci.* (2020) 7:123. doi: 10.3389/fvets.2020.00123
25. Ma Y, Wang W, Zhang H, Wang J, Zhang W, Gao J, et al. Supplemental bacillus subtilis DSM 32315 manipulates intestinal structure and microbial composition in broiler chickens. *Sci Rep.* (2018) 8:15358. doi: 10.1038/s41598-018-33762-8
26. Sokale AO, Menconi A, Mathis GF, Lumpkins B, Sims MD, Whelan RA, et al. Effect of bacillus subtilis DSM 32315 on the intestinal structural integrity and growth performance of broiler chickens under necrotic enteritis challenge. *Poult Sci.* (2019) 98:5392–400. doi: 10.3382/ps/pez368
27. Whelan RA, Doranalli K, Rinttilä T, Vienola K, Jurgens G, Apajalahti J. The impact of bacillus subtilis DSM 32315 on the pathology, performance, and intestinal microbiome of broiler chickens in a necrotic enteritis challenge. *Poult Sci.* (2019) 98:3450–63. doi: 10.3382/ps/pey500
28. Bortoluzzi C, Serpa Vieira B, de Paula Dorigam JC, Menconi A, Sokale A, Doranalli K, et al. Bacillus subtilis DSM 32315 supplementation attenuates the effects of clostridium perfringenschallenge on the growth performance and intestinal microbiota of broiler chickens. *Microorganisms.* (2019) 7:71. doi: 10.3390/microorganisms7030071
29. Li CL, Wang J., Zhang HJ, Wu SG, Hui QR, Yang CB, et al. Intestinal morphologic and microbiota responses to dietary bacillus spp. in a broiler chicken model. *Front Physiol.* (2019) 9:1968. doi: 10.3389/fphys.2018.01968
30. AOAC. *Official Methods of Analysis.* 17th ed. Gaithersburg, MD: Assoc. Off. Analysis Chemistry (2000).
31. Yadav M, Dubey M, Yadav M, Shankar KS. Effect of supplementation of probiotic (bacillus subtilis) on growth performance and carcass traits of broiler chickens. *Int J Curr Microbiol App Sci.* (2018) 7:4840–9. doi: 10.20546/ijcmas.2018.708.510
32. Rhayat L, Jacquier V, Brinch KS, Nielsen P, Nelson A, Geraert PA, et al. Bacillus subtilis strain specificity affects performance improvement in broilers. *Poult Sci.* (2017) 96:2274–80. doi: 10.3382/ps/pex018
33. Wan X, Yang Z, Ji H, Li N, Yang Z, Xu L, et al. Effects of lycopene on abdominal fat deposition, serum lipids levels and hepatic lipid metabolism-related enzymes in broiler chickens. *Anim Biosci.* (2021) 34:385–92. doi: 10.5713/ajas.20.0432
34. Chao X, Guo L, Wang Q, Huang W, Liu M, Luan K, et al. miR-429-3p/LPIN1 axis promotes chicken abdominal fat deposition via PPARγ pathway. *Front Cell Dev Biol.* (2020) 8:595637. doi: 10.3389/fcell.2020.595637
35. Na W, Wu YY, Gong PF, Wu CY, Cheng BH, Wang YX, et al. Embryonic transcriptome and proteome analyses on hepatic lipid metabolism in chickens divergently selected for abdominal fat content. *BMC Genomics.* (2018) 19:384. doi: 10.1186/s12864-018-4776-9
36. Zhang M, Liu L, Chen D, Zhang X, Zhou C, Gan Q, et al. Functional microRNA screening for dietary vitamin E regulation of abdominal fat deposition in broilers. *Br Poult Sci.* (2020) 61:344–349. doi: 10.1080/00071668.2020.1736265
37. Guo S, Zhang Y, Cheng Q, Xv J, Hou Y, Wu X, et al. Partial substitution of fermented soybean meal for soybean meal influences the carcass traits and meat quality of broiler chickens. *Animals.* (2020) 10:225. doi: 10.3390/ani10020225
38. Xu X, Li L, Li B, Guo W, Ding X, Xu F. Effect of fermented biogas residue on growth performance, serum biochemical parameters, and meat quality in pigs. *Asian Australas J Anim Sci.* (2017) 30:1464–70. doi: 10.5713/ajas.16.0777
39. Drazbo A, Kozłowski K, Ognik K, Zaworska A, Jankowski J. The effect of raw and fermented rapeseed cake on growth performance, carcass traits, and breast meat quality in turkey. *Poult Sci.* (2019) 98:6161–9. doi: 10.3382/ps/pez322
40. Chen H, Dong X, Yao Z, Xu B, Zhen S, Li C, et al. Effects of prechilling parameters on water-holding capacity of chilled pork and optimization af prechilling parameters using response surface methodology. *J Anim Sci.* (2012) 90:2836–41. doi: 10.2527/jas.2011-4239
41. Shen MM, Zhang LL, Chen YN, Zhang YY, Han HL, Niu Y, et al. Effects of bamboo leaf extract on growth performance, meat quality, and meat oxidative stability in broiler chickens. *Poult Sci.* (2019) 98:6787–96. doi: 10.3382/ps/pez404
42. Zhuang H, Savage EM, Smith DP, Berrang ME. Effect of dry-air chilling on warner-bratzler shear force and water- holding capacity of broiler breast meat deboned four hours postmortem. *Int J Poult Sci.* (2008) 7:743–8. doi: 10.3923/ijps.2008.743.748
43. Bai W K, Zhang FJ, He TJ, Su PW, Ying XZ, Zhang LL, et al. Dietary probiotic bacillus subtilis strain fmbj increases antioxidant capacity and oxidative stability of chicken breast meat during storage. *PLoS ONE.* (2016) 11:e0167339. doi: 10.1371/journal.pone.0167339
44. Abdulla NR, Zamri ANM, Sabow AB, Kareem KY, Nurhazirah S, Ling FH, et al. Physico-chemical properties of breast muscle in broiler chickens fed probiotics, antibiotics or antibiotic–probiotic mix. *J Appl Anim Res.* (2017) 45:64–70. doi: 10.1080/09712119.2015.1124330
45. Chartrin P, Méteau K, Juin H, Bernadet MD, Guy G, Larzul C, et al. Effects of intramuscular fat levels on sensory characteristics of duck breast meat. *Poult Sci.* (2006) 85:914–22. doi: 10.1093/ps/85.5.914
46. Lorenzo JM, Franco D. Fat effect on physico-chemical, microbial and textural changes through the manufactured of dry-cured foal sausage Lipolysis, proteolysis and sensory properties. *Meat Sci.* (2012) 92:704–14. doi: 10.1016/j.meatsci.2012.06.026
47. Chen Y, Qiao Y, Xiao Y, Chen H, Zhao L, Huang M, et al. Differences in physicochemical and nutritional properties of breast and thigh meat from crossbred chickens, commercial broilers, and spent hens. *Asian Australas J Anim Sci.* (2016) 29:855–64. doi: 10.5713/ajas.15.0840
48. Heyer A, Lebret B. Compensatory growth response in pigs: effects on growth performance, composition of weight gain at carcass and muscle levels, and meat quality. *J Anim Sci.* (2002) 85:769–78. doi: 10.2527/jas.2006-164
49. Wood JD, Richardson RI, Nute GR, Fisher AV, Campo MM, Kasapidou E, et al. Effects of fatty acids on meat quality: a review. *Meat Sci.* (2003) 66:21–32. doi: 10.1016/S0309-1740(03)00022-6
50. Amorim A, Rodrigues S, Pereira E, Teixeira A. Physicochemical composition and sensory quality evaluation of capon and rooster meat. *Poult Sci.* (2016), 95:1211-1219. doi: 10.3382/ps/pev448
51. Liu T, Wu J, Lei Z, Zhang M, Gong X, Cheng S, et al. Fatty acid profile of muscles from crossbred angus-simmental, wagyu-simmental, and chinese simmental cattles. *Food Sci Anim Resour.* (2020) 40:563–77. doi: 10.5851/kosfa.2020.e33
52. Zong G, Li Y, Wanders AJ, Alssema M, Zock PL, Willett WC, et al. Intake of individual saturated fatty acids and risk of coronary heart disease in US men and women: two prospective longitudinal cohort studies. *BMJ.* (2016) 355:i5796. doi: 10.1136/bmj.i5796
53. Lee SH, Kim CN, Ko KB, Park SP, Kim HK, Kim JM, et al. Comparisons of beef fatty acid and amino acid characteristics between jeju black

cattle, hanwoo, and wagyu breeds. *Food Sci Anim Resour*. (2019) 39:402–9. doi: 10.5851/kosfa.2019.e33

Conflict of Interest: The authors declare that the research was conducted in the absence of any commercial or financial relationships that could be construed as a potential conflict of interest.

Publisher's Note: All claims expressed in this article are solely those of the authors and do not necessarily represent those of their affiliated organizations, or those of the publisher, the editors and the reviewers. Any product that may be evaluated in this article, or claim that may be made by its manufacturer, is not guaranteed or endorsed by the publisher.

frontiers | Frontiers in Veterinary Science

ORIGINAL RESEARCH
published: 15 April 2022
doi: 10.3389/fvets.2022.883295

Identification of microRNA Transcriptome Involved in Bovine Intramuscular Fat Deposition

Susan K. Duckett and Maslyn A. Greene*

Department of Animal and Veterinary Sciences, Clemson University, Clemson, SC, United States

Background: Intramuscular fat deposition in beef is a major determinant of carcass quality and value in the USA. The objective of this study was to examine changes in microRNA (miRNA) transcriptome that are involved with intramuscular fat deposition with time-on-concentrates (TOC). Yearling steers were individually fed a high concentrate diet and changes in intramuscular fat deposition were monitored by real-time ultrasound at 28 to 33 d intervals. Longissimus muscle biopsies collected on d 0, 92 and 124 TOC to examine changes in miRNA transcriptome that are involved in intramuscular fat deposition.

Results: Steer body weight increased ($P < 0.0001$) at each weigh day during TOC. Fat thickness increased ($P < 0.005$) from d 28 to 124. Ribeye area was larger ($P < 0.001$) on d 124 than d 61, which was larger than d 0 and 28. Ultrasound intramuscular fat content was greater ($P < 0.001$) on d 92 and 124 compared to d 0, 28 or 61. Sequencing of the muscle biopsy samples identified one miRNA, bta-miR-122, that was up-regulated ($P < 0.005$) at d 92 and 124 compared to d 0. At d 92 TOC, mRNA expression levels of fatty acid binding protein 4 (FABP4) and elongase 6 (ELOVL6) were up-regulated ($P < 0.01$) compared to d 0; whereas at d 124, lipogenic genes involved in *de novo* fatty acid synthesis, fatty acid transport, elongation and desaturation were highly up-regulated compared to d0.

Conclusions: Small RNA sequencing identified bta-miR-122 as a potential miRNA of interest that may be involved in intramuscular fat deposition with increasing TOC. Increased intramuscular fat content, as measured by real-time ultrasound, combined with differential gene expression suggests that preadipocyte differentiation may be stimulated first, which is followed by a global up-regulation of lipogenic genes involved in *de novo* fatty acid synthesis that provide fatty acids for subsequent hypertrophy.

Keywords: beef, marbling, microRNA, mRNA, intramuscular fat content

OPEN ACCESS

Edited by:
Rita Payan Carreira, University of Evora, Portugal

Reviewed by:
Endre Károly Kristóf, University of Debrecen, Hungary
Steffen Maak, Leibniz Institute for Farm Animal Biology (FBN), Germany

****Correspondence:***
Susan K. Duckett
sducket@clemson.edu

Specialty section:
This article was submitted to Livestock Genomics, a section of the journal Frontiers in Veterinary Science

Received: *24 February 2022*
Accepted: *23 March 2022*
Published: *15 April 2022*

Citation:
Duckett SK and Greene MA (2022) Identification of microRNA Transcriptome Involved in Bovine Intramuscular Fat Deposition. Front. Vet. Sci. 9:883295. doi: 10.3389/fvets.2022.883295

INTRODUCTION

Marbling or intramuscular fat deposition in beef is a major determinant of carcass quality and value in the USA. Consumer demand for US Prime and branded Choice beef products is at an all-time high but only about 4% of carcasses reach the Prime quality grade (1). Beef producers are working to select genetics with higher genetic ability to marble and evaluating management systems that help produce a greater percentage of carcasses into the premium quality grades. Current premiums

for carcasses grading Prime with a yield grade of 1 to 3 are $0.52/kg carcass weight or an additional $208 premium for a 400 kg carcass (2). Serial slaughter studies indicate that marbling deposition increases after 80 d on a high concentrate diet (3–6). Feeding high concentrates to steers upregulates key lipogenic genes and marbling deposition in early weaned calves (7, 8), normal weaned calves (9, 10) and yearling calves (11). Duckett et al. (3) found that intramuscular fat deposition doubled in the longissimus muscle between 86 and 112 d on concentrates with no change after that when fed for a total of 196 d on concentrates.

The transient increases in intramuscular fat deposition suggest that epigenetic adaptation may be playing a role in this process. microRNA (miRNA) are small, non-coding RNAs that play a role in post-transcriptional gene regulation. Research shows that miRNA expression differs between depot (12, 13) and finishing systems in beef cattle (12) and sheep (14). Others have identified specific miRNAs that can inhibit differentiation of ovine stromal vascular cells = (15). In a review article, Romao and co-workers (16) concluded that miRNA are involved in the adipogenic process in farm animals and that more research was needed to identify specific miRNA that regulate fat deposition. We hypothesize that key miRNAs are involved with increased intramuscular fat deposition with TOC. The objective of this study was to identify key miRNAs and changes in mRNA expression that coincide with enhanced intramuscular fat deposition during TOC.

MATERIALS AND METHODS

Experimental procedures were reviewed and approved by Clemson University Animal Care and Use Committee, AUP2020-001.

Animals

Angus-cross, yearling steers ($n = 7$; 428 ± 22 kg BW; 12.3 mo of age) were selected from Clemson University Piedmont Research and Education Center. All steers were sired by the same Angus bull (Connealy Mentor 7374, +0.73 marbling EPD, 0.67 accuracy). Steers were weighed on consecutive days at the beginning and end of the experiment. Steers were individually fed using Calan gates and adjusted to high concentrate ration using step-up rations (**Table 1**). Steers were weighed and ultrasounded at about 28–33 d intervals during the study. A biopsy of longissimus muscle (LM) was obtained on d 0, 92 and 124 on concentrates. Steers were finished for 124 d (16.6 mo of age) and transported to a commercial packing plant for slaughter. Due to the Covid-19 pandemic, we were unable to enter the packing plant and obtain actual carcass data for this study.

Real-Time Ultrasound

Real-time ultrasound measures of fat thickness, ribeye area and intramuscular fat percentage were collected between the 12th- and 13th-ribs using an Aloka 500-V ultrasound (Corometrics Medical Systems, Wellingford, CT) equipped with a 17-cm, 3.5-MHz linear probe. The images were interpreted using Biosoft Toolbox (Biotronics, Inc., Ames, IA).

TABLE 1 | Composition of the high concentrate diet fed to steers in this study.

Ingredient	Step 1[a]	Step 2[a]	Final[a]
CPC Grower, %	50	33	0
Corn, rolled, %	40	54	80
Soybean meal, %	4.5	6.0	9
Limestone, %	0.25	0.3	0.5
Trace mineral pre-mix with Rumensin[b], %	0.25	0.3	0.5
Oat hay, ground, %	5	6.7	10
Nutrient Composition			
Crude protein, %	13.2	13.3	13.4
NEm, mcal/kg			2.07
NEg, mcal/kg			1.40

[a] *Step1 and Step 2 rations were fed for 7 d each and then they consumed the final ration from d 15 to 124.*

[b] *Trace mineral premix composition: calcium, 0.67%; phosphorus, 0.33%; magnesium 0.15%; potassium, 0.56%; sulphur, 0.17%; copper, 22.78 mg/kg; manganese 72.49 mg/kg; selenium, 0.40 mg/kg; zinc, 98.12 mg/kg; monensin, 38.79 mg/kg.*

Muscle Biopsy

Longissimus muscle needle biopsies were obtained on each steer at 0, 92 and 124 d on concentrate diet. Steers were briefly restrained in a mechanical chute and the LM from the 10th rib to 13th rib region was shaved. A Bergstrom biopsy needle (Millennium Surgical, Bala Cynwyd, PA) was used to obtain about 200 mg from the center of the longissimus muscle. Muscle biopsy samples were trimmed of any external subcutaneous fat or epimysial connective tissue and then immediately frozen in liquid nitrogen. Biopsy samples were transported to Clemson University in liquid N_2 and stored at −80°C until extraction. Skeletal muscle biopsy locations were taken at 11th rib on the left side (d 0), 11th rib on right side (d 92) and 12th rib on left side (d 124) to avoid sampling in a remodeled area.

RNA Extraction

Total RNA was isolated from the muscle biopsy samples using the TriZol procedure (Invitrogen; Thermo-Fisher, Waltham, MA). RNA extracts were DNased (DNA-Free DNA removal kit, ThermoFisher). Total RNA was quantified using a NanoDrop One spectrophotometer (ThermoFisher) and quality assessed using Agilent Bioanalyzer (Agilent, Santa Clara, CA). The RNA integrity number (RIN) for all samples was 7 or greater.

MiRNA Sequencing

RNA samples ($n = 12$; 4 steers x 3 TOC/steer) were shipped on dry ice to PrimBio (Exton, PA) for small RNA sequencing. The four steers selected for the miRNA sequencing were closest to the treatment mean for IMF content at d 92 and d 124. Small RNA was enriched with the Total RNA-seq Kit v2 (ThermoFisher) according to manufacturer. Small RNA samples were run on an Agilent 2100 Bioanalyzer to assess yield and size distribution of the Small RNAs. cDNA libraries were constructed using Ion Total RNA-Seq Kit v2 (4479789; ThermoFisher). Small RNA (30 ng) was hybridized with Ion adapters in a thermocycler for 10 min at 65°C and 5 min at 16°C. Hybridized Small RNA

TABLE 2 | miR-122 sequence alignment for *Bos taurus* (bta), *Ovis aries* (oar), and *Homo sapiens* (hsa).

miR-122 Mature Sequence (miRbase)	
bta-miR-122 (MIMAT0003849)	UGGAGUGUGACAAUGGUGUUUG
oar-miR-122 (17)	UGGAGUGUGACAAUGGUGUUUG
hsa-miR-122-5p (MIMAT0000421)	UGGAGUGUGACAAUGGUGUUUG
TaqMan assay hsa-miR-122-5p[1]	UGGAGUGUGACAAUGGUGUUUG

TaqMan Small RNA Assay kit, catalog no = 4427975, assay no = 002245 (ThermoFisher).

was then incubated overnight at 16°C with ligation enzyme mix to ligate the Ion adapters. Hybridized samples were then mixed with a reverse transcriptase master mix and incubated at 70°C for 10 min, snap cooled, and incubated 42°C for 30 min to generate cDNA libraries. cDNA libraries were purified using nucleic acid binding beads and buffers according to the manufacturer protocol (Magnetic Bead Cleanup Module, 4479789, ThermoFisher). The purified cDNA libraries were amplified by PCR using Platinum PCR Super-Mix High Fidelity and indexed bar codes added with Ion Xpress RNA Barcode reverse and forward primers according to manufacturer. The quality of each final library was assessed using the Agilent® dsDNA High Sensitivity Kit.

Approximately 50 pM of pooled barcoded libraries were used for templating using Thermo Fisher Ion 540 CHEF Kit (A30011) according to the manufacturer's protocol. Samples were assessed for polyclonal percentage using a Qubit 4 (Invitrogen, ThermoFisher). Samples were then loaded onto a 540 chip, placed into an Ion S5 sequencer, and run using an Ion Torrent Small RNAseq run plan. After completion of the proton run, the raw sequence files (fastq) were aligned to the bovine genome (bosTau4) reference sequences by the StrandNGS software using the default parameters. Aligned SAM files were used for further analysis. Quality control was assessed by the Strand NGS program, which determined the pre- and post-alignment quality of the reads for each sample. The aligned reads were normalized and quantified using the Quantile algorithm by the StrandNGS program. The total raw reads generated by sequencing was 87,994,733 with a minimum of 5,194,893 reads per individual sample and all samples had a Q20 of > 90%. Average read length was 22 nucleotides. Statistical analysis was performed using the ANOVA test to determine significant differentially expressed small RNAs by time-on-concentrate. After significant small RNAs were identified, significant fold change was determined and small RNAs that had a significant fold change of 1.3x or higher were identified.

MiRNA qPCR Validation

TaqMan miRNA reverse transcription kit (catalog no = 4366597, ThermoFisher) was used to convert miRNA to cDNA. TaqMan Small RNA Assay kit was used for has-miR-122-5p (catalog no = 4427975, assay no = 002245; ThermoFisher), which has the same sequence as bta-miR-122 (**Table 2**). Relative gene expression of miR-122 was analyzed using ANOVA by TOC (d0, 92, and 124) using GraphPad Prism 9.3.1 (18).

TABLE 3 | Live weight, average daily gain (ADG), dry matter intake (DMI) and feed efficiency (Gain:Feed) for the steers fed concentrates over time.

	Live weight, kg		
d 0	428.2[e]		
d 28	464.2[d]		
d 61	546.8[c]		
d 92	611.7[b]		
d 124	659.4[a]		
SEM	8.79		
P-Level	0.0001		
	ADG, kg/d	**DMI, kg/d**	**Gain:Feed**
Period 1 (d 0–28)	1.28[c]	5.50[c]	0.228[a]
Period 2 (d 29–61)	2.50[a]	11.44[b]	0.220[a]
Period 3 (d 62–92)	2.09[ab]	14.09[a]	0.149[b]
Period 4 (d 93–124)	1.66[bc]	13.33[a]	0.124[b]
SEM	0.181	0.493	0.0158
P-Level	0.0001	0.0001	0.0001

[abcde] *Means in the same column differ (P < 0.05) for that variable.*

MRNA qPCR

RNA (1 ug) was reverse transcribed using qScript (QuantaBio, VWR) for qPCR (QuantStudio3 Real-Time PCR system, Applied Biosystems) using SYBR green (PerfeCTa SYBR Green SuperMix; QuantaBio) according to the manufacturer. Primers for genes involved in adipogenesis and lipogenesis were developed using PrimerQuest Tool (IDT, Coralville, IA) and sequences are listed in **Supplementary Table 1**. Several housekeeping genes (glyceraldehyde 3-phosphate dehydrogenase [GAPDH], β-actin [ACTB], ubiquitously expressed prefoldin like chaperone [UXT], and eukaryotic translation initiation factor 3 subunit K [EIF3K]) were evaluated using RefFinder, https://www.heartcure.com.au/reffinder/, (19) to identify that most stable housekeeping gene(s). The most stable housekeeping genes were EIF3K (comprehensive stability index, M = 1.86) and UXT (M = 2.28). The geometric mean of EIF3K and UXT was calculated (M = 1.19) and used for data normalization (20). Relative gene expression was calculated using the mean ΔC_T of the d 0 values and subjected to ANOVA to determine statistical differences by TOC using GraphPad Prism 9.3.1 (18).

Statistics

Data were analyzed in a completely randomized design using the Mixed procedure of SAS (SAS Inst. Inc., Cary, NC) with time-on-concentrate in the model. Steer was the experimental unit. Least square means were generated and separated using a protected least significant difference test. Significance was determined at $P < 0.05$.

RESULTS

Performance of the steers across TOC for this study is shown in **Table 3**. Steer body weight (BW) increased ($P < 0.0001$) at each time of measurement (28–33 d periods) during TOC. Steers finished with an average 659 kg body weight (BW). Average

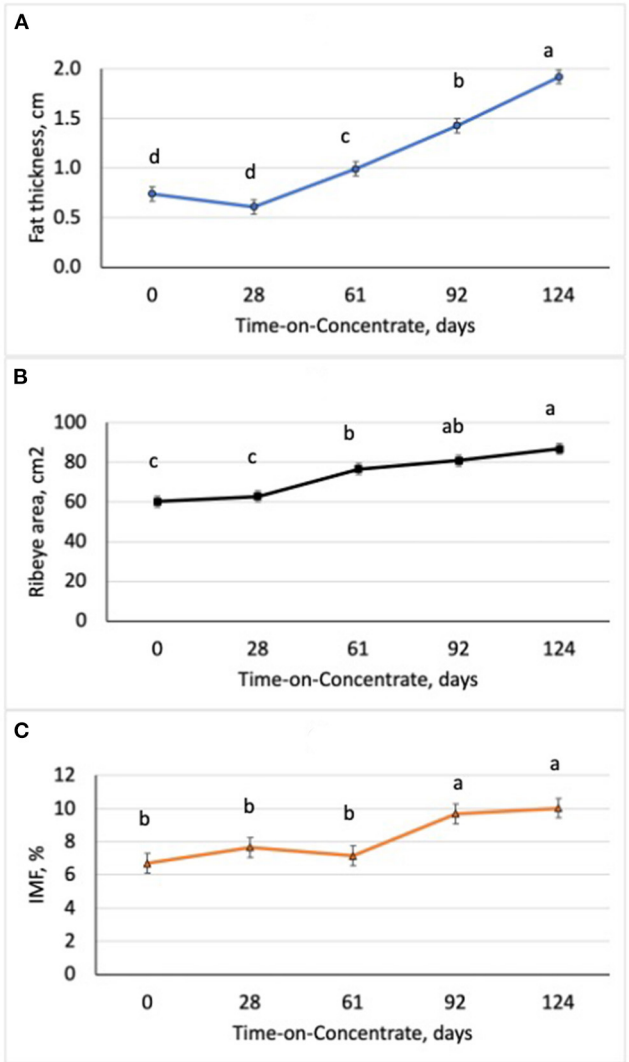

FIGURE 1 | Changes in ultrasound fat thickness **(A)**, ribeye area **(B)**, and intramuscular fat content (IMF; **C**) in steers ($n = 7$/time) with increasing time-on-concentrates. [abc]Means with uncommon superscripts differ ($P < 0.01$) for each graph.

TABLE 4 | Differentially expressed miRNA in skeletal muscle biopsies at d92 on concentrates compared to d0.

Gene ID	*P*-Level	Regulation	Log FC[1]	miRBase
bta-miR-122	0.0048	up	6.719	MI0005063
bta-miR-323	0.0008	down	−1.018	MI0009797
bta-miR-449a	0.0022	down	−1.406	MI0009834
bta-miR-1197	0.0312	down	−1.451	MI0010470
bta-miR-485	0.0002	down	−1.501	MI0009842
bta-miR-2411	0.0176	down	−1.647	MI0011456

Log FC = log fold change From d 0.

TABLE 5 | Differentially expressed miRNA in skeletal muscle biopsies at d 124 on concentrates compared to d0.

Gene ID	*P*-Level	Regulation	Log FC[1]	miRBase
bta-miR-122	0.0268	up	3.832	MI0005063
bta-miR-383	0.0437	up	1.702	MI0009823
bta-miR-2346	0.0265	up	1.505	MI0011374
bta-miR-144	0.0396	up	1.329	MI0009744
bta-miR-505	0.0126	up	1.258	MI0009856
bta-miR-142	0.0203	up	1.169	MI0005011
bta-miR-1248–1	0.0271	up	1.089	MI0010477
bta-miR-1248–2	0.0290	up	1.043	MI0010483
bta-miR-196b	0.0496	down	−1.059	MI0009768
bta-miR-208b	0.0010	down	−1.133	MI0009774
bta-miR-196a-2	0.0243	down	−1.246	MI0009766
bta-miR-362–5p	0.0120	down	−1.292	MI0009811
bta-miR-196a−1	0.0246	down	−1.327	MI0009767
bta-miR-449a	0.0114	down	−1.332	MI0009834
bta-miR-2411	0.0280	down	−1.561	MI0011456

Log FC = log fold change From d 0.

daily gains were greatest ($P < 0.0001$) during period 2 (d 29–61) and lowest ($P < 0.0001$) during period 1 (d 0–28). Dry matter intake was greater ($P < 0.0001$) during period 3 (d 62–92) and 4 (d 93–124) compared to period 1 and 2. Dry matter intake was also greater ($P < 0.0001$) for period 2 than period 1. Feed efficiency was greater ($P < 0.0001$) during periods 1 and 2 than periods 3 and 4 due to higher gains and lower feed intake during the first half of the TOC feeding. Changes in subcutaneous fat deposition, ribeye area, and intramuscular fat deposition were measured during time-on-concentrates using real-time ultrasound to estimate carcass parameters. Fat thickness was similar between d0 and d28 TOC (**Figure 1A**); however, fat thickness increased ($P < 0.001$) at each TOC from d28 to 124 d. Ribeye area was larger ($P < 0.001$) on d 124 than d 61, which were larger than d 0 and 28 (**Figure 1B**). Ultrasound intramuscular fat content did not differ from d 0 to d 61 but was greater ($P < 0.001$) on d 92 and d 124 than d 0, 28 or 61 TOC (**Figure 1C**).

Sequencing of the muscle biopsy samples identified one miRNA, bta-miR-122, that was up-regulated ($P < 0.005$) by 6.72-fold on d 92 compared to d 0 (**Table 4**). Several miRNA were down-regulated ($P < 0.05$) at d 92 by −1 to −2 fold, which included miR-323, −449a, −1197,−485, and−2411. At d 124, 8 miRNAs were up-regulated ($P < 0.05$) and 7 were down-regulated ($P < 0.05$) compared to d 0 (**Table 5**). miR-122 was up-regulated ($P < 0.05$) at d 124 by 3.8-fold compared to d 0. Other miRNAs that were up-regulated included miR-383,−2346,−144,−505,−142,−1248-1 and−1248-2. The down-regulated miRNAs included miR-196b,−208b,−196a-1,−326-5p,−196a-2,−449a, and−2411 from d 124 compared to d 0. The mature sequence of bta-miR-122 is identical to ovine (oar-miR-122) and human (hsa-miR-122-5p) sequences (**Table 2**). Validation of miR-122 expression was conducted by qPCR using

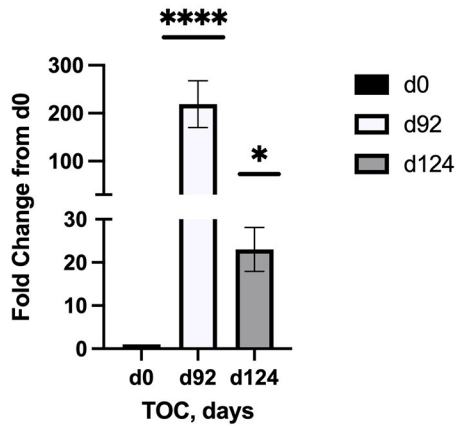

FIGURE 2 | Fold change in miR-122 expression of skeletal muscle biopsies (n = 4/time) at d 92 and d 124 on concentrates compared to d0. Differences are noted (*P < 0.05; **P < 0.01; ***P < 0.001; ****P < 0.0001) in comparison to d 0.

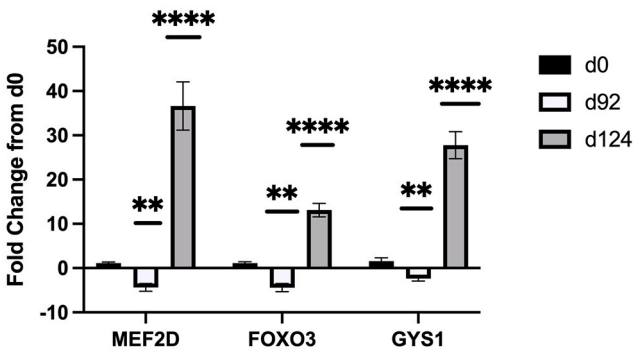

FIGURE 3 | Fold change in mRNA expression of miR-122 targets (MEF2D, FOXO3, GYS1) at d 92, and d 124 compared to d 0 (n = 4/time). Differences are noted (*P < 0.05; **P < 0.01; ***P < 0.001; ****P < 0.0001) in comparison to d 0.

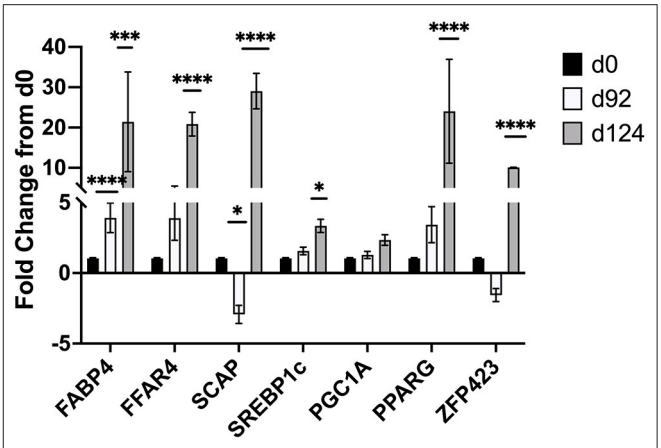

FIGURE 4 | Fold change in mRNA expression of transcription factors (ZFP423, PPARG, SREBP1c), activators (PGC-1A, SCAP), and fatty acid transporters (FABP4, FFAR4) at d 92 and d 124 compared to d 0 (n = 4/time). Differences are noted (*P < 0.05; **P < 0.01; ***P < 0.001; ****P < 0.0001) in comparison to d 0.

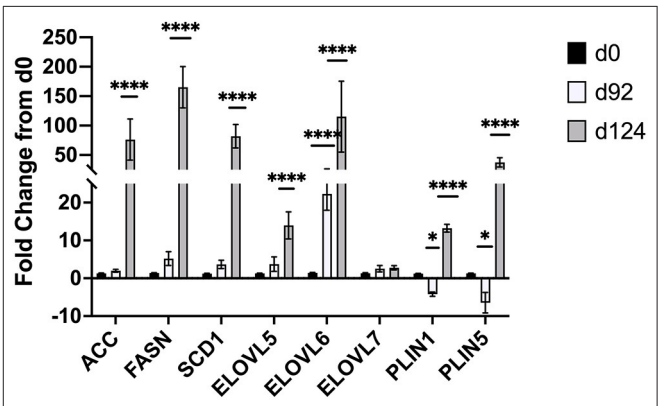

FIGURE 5 | Fold change in mRNA expression of lipogenic (ACC, FASN, SCD1, ELOVL5,6,7) and lipolytic (PLIN1,5) genes at d 92 and d 124 compared to d 0 (n = 4/time). Differences are noted (*P < 0.05; **P < 0.01; ***P < 0.001; ****P < 0.0001) in comparison to d 0.

the hsa-miR-122-5p TaqMan small RNA assay kit. Expression of miR-122 was up-regulated (P < 0.0001) by 217-fold at d 92 and 20.7-fold at d 124 compared to d0 values (**Figure 2**). These results confirm the miRNA sequencing results in that miR-122 was up-regulated at d 92 by a greater fold change than d 124. The magnitude of the fold change as determined by qPCR is higher than small RNA sequencing which may be related to normalization procedures used for sequencing (transcripts per million) vs. for qPCR (C_T values for d0). Predicted targets of miR-122 (glycogen synthase 1 [GYS1], myocyte enhancer factor 2D [MEF2D] and forkhead box O3 [FOXO3]) were down-regulated at d 92 and up-regulated at d 124 (**Figure 3**).

Changes in mRNA expression of adipogenic and lipogenic genes was assessed by qPCR. At d 92 TOC, mRNA expression of fatty acid binding protein 4 (FABP4; **Figure 4**) and fatty acid elongase 6 (ELOVL6; **Figure 5**) was up-regulated (P < 0.0001) compared to d 0. Expression of other adipogenic genes (peroxisome proliferator-activated receptor γ [PPARG], PPAR γ coactivator-1 α [PGC1A], sterol regulator element binding protein 1c [SREBP1c], and zinc finger protein 423 [ZFP423]), fatty acid transporters (fatty acid binding protein 3 [FABP3], free fatty acid receptor 4 [FFAR4]), and lipogenic genes (acetyl-CoA carboxylase [ACC], fatty acid synthase [FASN], stearoyl-CoA desaturase [SCD1], fatty acid elongase [ELOVL5], fatty acid elongase [ELOVL7]) did not differ between d 92 and d 0 biopsy samples. Perilipin (PLIN1 and PLIN5) and sterol regulatory element-binding protein (SREBP1c) cleavage-activating protein (SCAP) mRNA expression was down-regulated (P < 0.05) at d 92 of concentrate feeding compared to d 0. After 124 d on concentrates, lipogenic genes involved in *de novo* fatty acid synthesis (ACC, FASN), fatty acid transport (FABP4, FFAR4), elongation (ELOVL5, ELOVL6) and desaturation (SCD1) were highly up-regulated (P < 0.0001) compared to d0 (**Figure 5**).

Zinc finger protein 423 (ZFP423), PPARG, SREBP1c, and SCAP expression were also up-regulated ($P < 0.05$) at d 124 compared to d 0 (**Figure 4**). Expression of PLIN1 and PLIN5 was up-regulated ($P < 0.0001$) at d 124 compared to d 0.

DISCUSSION

In this study, we examined changes in growth and feed efficiency of steers fed a high concentrate (90% concentrate) diet over TOC. Steer body weight gains did not change during the initial 28 d on feed when they were training to use Calan gates and adjusting to the high concentrate diet. After 28 d, steer BW increased ($P < 0.0001$) at each period (28 to 33 d) across TOC. Steers finished with an average BW of 659 kg after feeding for 124 d. Average daily gain was the greatest during period 2 (d 29–61) when steers were likely exhibiting compensatory growth phase after lower gains in period 1 (d 0–28). Average daily gains were lower during period 4 (d 93–124) compared to period 2 when steers were increasing in external fat deposition and reaching final BW. The steers in this study were very efficient during periods 1 and 2 with gain:feed at 0.22. Ultrasound fat thickness deposition increased from d 28 to 124 at a rate of 1.36 mm per day. Ribeye area increased across TOF with greater ribeye area at d 61 compared to d 0 and 28 and at d 124 compared to d 61. Intramuscular fat content, as measured by real-time ultrasound, increased on average by 37% between d 61 and 92, and remained constant to d 124. Numerous serial slaughter studies have also observed similar changes in intramuscular fat content after feeding concentrates for 80 to 120 d (3–6).

The average level of intramuscular fat content as measured by ultrasound was 10.03%, which would correspond to the moderately abundant marbling score and Prime quality grade (21). Overall, six of the seven steers evaluated for ultrasound IMF at d 92 and d124 would have been above minimum level of 8.0% IMF for the slightly abundant marbling score and Prime quality grade (21); in contrast, only one steer would have reached this minimum level of IMF (8%) at d 62 on concentrates. External fat thickness increased linearly with time-on-concentrates and the steers in this study had excessive levels at the end of the 124 d feeding period. The use of real-time ultrasound to monitor changes in IMF over time allows us to identify key miRNA and mRNA that are associated with enhanced IMF deposition across TOC. Previous research has shown that the real-time ultrasound IMF estimates are highly correlated to actual longissimus muscle lipid content (9, 10).

Small RNA sequencing identified bta-miR-122 as a potential miRNA of interest that may be associated with intramuscular lipid deposition in the bovine. miR-122 was up-regulated on d 92 (6.72-fold change) and d 124 (3.83-fold change) at the same time when ultrasound IMF levels were also above d 0 values. These results were confirmed by qPCR that miR-122 was up-regulated at d 92 and d 124 compared to d 0, and that up-regulation was greater at d 92. In humans, miR-122 is highly abundant and accounts for 70% of all miRNAs present in the liver. Research shows that miR-122 regulates cholesterol and fatty acid metabolism in humans (22) and tilapia (23–25). In pigs, miR-122 was identified as one of three miRNAs that were regulators of fat deposition (26) and appear to be associated with pyruvate kinase in subcutaneous adipose tissues. Not much is known about miR-122 in the bovine but others (27) have also identified miR-122 as an important miRNA along with two others (miR-381 and miR-499) that are involved with intramuscular fat deposition in the Yak (*Bos grunniens*). However, they observed that miR-122 was down-regulated in LM and adipose tissue from 0.5 yr to 2.5 yr of age. In this study, we only examined changes in miRNA transcriptome during a short interval (124 d; 12.3 to 16.6 mo of age) that coincided with increased intramuscular fat deposition due to feeding high concentrate diets.

TargetScan 8.0 (cow; http://www.targetscan.org/vert_80/) and miRDB (human; http://mirdb.org/) programs were used to identify potential targets for miR-122 due to its potential role in intramuscular fat deposition. TargetScan predicted 194 targets and miRDB predicted 490 targets. From these lists, we selected genes that are known to be involved in muscle or lipid metabolism and examined differences in relative gene expression by TOC using qPCR. Glycogen synthase 1 (GYS1) was identified in both programs as a target with high score for miR-122 in human (target score 95, miRDB) and bovine (-0.96 cumulative weighted context++ score; TargetScan8.0). Additional predicted targets for miR-122 included forkhead box O3 (FOXO3) and myocyte enhancer factor 2D (MEF2D). Our results found that miR-122 and mRNA expression of predicted targets (GYS1, FOXO3, and MEF2D) were inversely related. Expression levels of these targets were down-regulated when miR-122 expression was up-regulated by 217-fold at d 92 and up-regulated when miR-122 expression was up-regulated by only 3.8-fold at d124. Song et al. (28) has shown that miR-122 directly targets FOXO3 in cardiomyocytes undergoing hypertrophy. They found that miR-122 negatively regulated FOXO3, which would agree with our results in that miR-122 was highly expressed at d 92 and FOXO3 was down-regulated. MEF2D was confirmed as a miR-122 target in cardiac myxoma cells (29). They reported that PPARG and MEF2D are inversely related and that up-regulation of miR-122 activates PPARG to inhibit MEF2D, which reduces proliferation of cardiac myxoma cells. In order to examine the role of miR-122 in lipid metabolism, Esau and co-workers used an antisense oligonucleotide (ASO) treatment in mice to inhibit miR-122 (30). They found increased expression of GYS1 in the liver tissue of the miR-122 ASO treated mice in a dose-response manner. They also examined changes in lipogenic genes in the liver by microarray and found that miR-122 inhibition down regulated FASN, ACC, and SCD1 expression by about 1.5 to 3-fold change. These authors postulated that miR-122 may alter expression of a transcriptional inhibitor because the seed sequence for miR-122 is not predicted to bind to these lipogenic genes according to the available algorithms (TargetScan, miRDB or others). Miravirsen (SPC3649) can inhibit miR-122 biogenesis and is the first anti-miRNA ASO to enter clinical trials for hepatitis C virus treatment in humans (31). Additional research is needed to determine how miR-122 may be involved in lipogenesis/lipolysis and to determine if miR-122 mimics or enhancers could be used to stimulate intramuscular fat deposition.

There were a few miRNAs (miR-323, −449a,−1197, −485) that were down-regulated at d 92 but they had a low fold change (< −1.7) and no established role in adipose or muscle metabolism. On d 124 TOC, there were other miRNAs that were up or down regulated compared to d 0. Most of these miRNAs (miR-383, 2,346, 505, 1,248, 196, 208, 362, or 449) have no known role in adipose or muscle metabolism. miR-2411 was down-regulated at both d 92 and 124 compared to d 0. Little is known about miR-2411 but it was identified as a novel miRNA in subcutaneous fat of pigs and Meishan had higher expression than Large White pigs but expression levels were low in abundance for both breeds (32). miR-142, −144 and −196 appear to be involved with lipid metabolism and insulin resistance. miR-144 binds to insulin receptor substrate (IRS1) to control its expression and appears to be a potential therapeutic target for type 2 diabetes treatment in humans (33, 34). Muroya and coworkers (35) examined plasma exosomal miRNAs and found that miR-142–5p was down-regulated in cattle after grazing for 3 mo. In subcutaneous fat, miR-142–5p expression was greater in grazing cattle and may be related to fatty acid metabolism (14, 35). miR-196a was identified in swine back fat samples as having a tissue specific expression pattern with mature animals having highest levels of expression in subcutaneous fat and liver (36). *In vitro* experiments that overexpressed miR-196a showed that it stimulated preadipocyte differentiation but did not alter proliferation (36). In our study, miR-142 and miR-144 were up regulated ($P < 0.05$) and miR-196a-1 and miR-196a-2 were down regulated at 124 d on concentrates.

At d 92 of TOC, there was up-regulation of fatty acid binding protein 4 (FABP4, 4-fold change) and fatty acid elongase 6 (ELOVL6; 8-fold change) mRNA expression, and down-regulation of mRNA involved in lipolysis (PLIN1 and PLIN5) and adipogenesis (SCAP) compared to d 0. FABP4 transports intracellular fatty acids to the nucleus where it alters transcription of certain genes (37). FABP4 expression is up-regulated during adipocyte differentiation (38) and serves as a marker of differentiation in bovine adipocytes (37, 39). Michal et al. (40) reported that FABP4 was associated with subcutaneous fat thickness and marbling in Wagyu x Limousin F_2 cattle. Guo and co-workers (41) related gene expression to IMF percentage in cattle and sheep and identified FABP4 as having a significant association with IMF in both species. The up-regulation of FABP4 with greater TOC indicates that concentrate finishing may enhance uptake of fatty acids into the nucleus and promote differentiation of preadipocytes.

Fatty acid elongase 6 (ELOVL6) is involved in the elongation of palmitic (C16:0) acid to stearic (C18:0) acid (42, 43). Knockdown of ELOVL6 in rat insulinoma cell lines (42) and mice (43) demonstrated that ELOVL6 is required for monounsaturated fatty acid synthesis. These results show that ELOVL6 plays a pivotal role in monounsaturated fatty acid synthesis, which is the one of the main fat types in beef muscle and increased concentrations are observed with high concentrate feeding (3, 11). In this study, the up-regulation of ELOVL6 at d 92 precedes the up-regulation of lipogenic genes involved in *de novo* fatty acid synthesis (ACC, FASN) and desaturation (SCD1) observed at d124. Perilipins are associated with intracellular lipid droplets where they stabilize the droplet and limit access by cytosolic lipases thereby regulating triacylglyceride storage under basal conditions (44). Perilipin 1 (PLIN1) is most abundant in white adipose tissues where it is involved with hormone-stimulated lipolysis; whereas perilipin 5 (PLIN5) is expressed in cardiac and skeletal muscle, and brown adipose tissues where it regulates fatty acid supply to the mitochondria (45). In pigs, immunohistochemistry was used to determine where PLIN proteins were located within the longissimus muscle of low or normal birth weight piglets at specific days (5, 12, and 26 d) postnatal (46). PLIN3 and PLIN4 were found at the periphery of muscle fibers and intramuscular adipocytes; in contrast, PLIN5 was localized within an undefined cell type located between the muscle fibers (46). Sterol regulatory element-binding protein (SREBP1c) cleavage-activating protein (SCAP) is required to activate all isoforms of SREBP. In mice, knockdown of SCAP reduces expression of genes involved in cholesterol and fatty acid synthesis by 70-80% in the liver (47). Others have also identified ELOVL6 and PLIN5 as being of high importance in bovine adipose tissues in the Yak (48). Nakajima et al. (49) identified PLIN5 in a genome-wide association study in Japanese Black cattle with high intramuscular fat deposition.

At 124 d of TOC, lipogenic genes involved in *de novo* fatty acid synthesis (ACC, FASN), fatty acid transport (FFAR4, FABP4), elongation (ELOVL5, ELOVL6) and desaturation (SCD1) were highly up-regulated compared to d 0. Other genes involved in lipolysis (PLIN1 and PLIN5) and transcription (ZFP423, PPARG, SREBP1c, SCAP) were up-regulated at d 124 compared to d0. Previous research has also shown up-regulation of FASN and SCD1 in subcutaneous fat from steers fed high concentrate diets compared for forage-finished (11). Others have shown that feeding high concentrates to steers upregulates key lipogenic genes and marbling deposition in early weaned calves (7, 8), normal weaned calves (9, 10) and yearling calves (11). Graugnard and co-workers (8) reported that feeding high starch diets to early-weaned steers up-regulated lipogenic genes (FASN, FABP4, SCD1, PPARG and PGC1A) at d 56 to stimulate differentiation of preadipocytes; whereas feeding low starch diets delayed the up-regulation of lipogenic genes (FABP4, FASN, SCD, DGAT2) until 112 d. Up-regulation of transcription factors (ZFP423, PPARG, SREBP1c, SCAP) at d 124 on concentrates suggests that another wave of proliferation may be occurring. Robelin (50, 51) examined changes in fat deposition from 15 to 65% of mature weight in cattle and reported that fat deposition began with an increase in cell number (hyperplasia) followed by the filling of these cells (hypertrophy), which then stimulated another increase in hyperplasia that occurred at 45 to 55% of mature weight.

CONCLUSIONS

The results of this study identified bta-miR-122 as a potential miRNA of interest that may be involved in intramuscular fat

deposition with increasing time-on-concentrates. More research is needed to further define the role of miR-122 but potential target genes were identified and differentially expressed. Changes in mRNA expression show that FABP4, ELOVL6, PLIN1 and PLIN5 are differentially expressed at d 92 prior to the up-regulation of lipogenic genes involved in *de novo* fatty acid synthesis at d 124. The greater intramuscular fat content as measured by real-time ultrasound at d 92 combined with differential gene expression suggest that preadipocyte differentiation may be promoted at this stage of TOC, which is followed by a global up-regulation of key lipogenic genes, fatty acid transporters, and desaturases that provide fatty acids for adipocyte hypertrophy.

DATA AVAILABILITY STATEMENT

The datasets presented in this study can be found in online repositories. The names of the repository/repositories and accession number(s) can be found below at https://www.ncbi.nlm.nih.gov/geo/query/acc.cgi?acc=GSE197315.

ETHICS STATEMENT

The animal study was reviewed and approved by Experimental procedures were reviewed and approved by Clemson University Animal Care and Use Committee, AUP2020-001.

AUTHOR CONTRIBUTIONS

SD designed the research project, conducted skeletal muscle biopsies, and molecular analyses. MG assisted with miRNA sequencing design and data analyses. SD drafted the manuscript and MG assisted with editing. Both authors contributed to the article and approved the submitted version.

FUNDING

Technical contribution No. 7036 of Clemson University Experiment Station. This material is based upon work supported by NIFA/USDA, under project number SC-1700580.

ACKNOWLEDGMENTS

We appreciate the assistance of A.R. Thomas, S.M. Justice, S.T. Justice, T. West and C. Creamer in animal management and sample collection.

SUPPLEMENTARY MATERIAL

The Supplementary Material for this article can be found online at: https://www.frontiersin.org/articles/10.3389/fvets.2022.883295/full#supplementary-material

REFERENCES

1. Boykin CA, Eastwood LC, Harris MK, Hale DS, Kerth CR, Griffin DB, et al. National beef quality audit−2016: in-plant survey of carcass characteristics related to quality, quantity, and value of fed steers and heifers. *J Anim Sci.* (2017) 95:2993. doi: 10.2527/jas2017.1543
2. *USDA Beef Carcass Price Equivalent Index, NW_LS410.* (2020). Available online at: https://www.ams.usda.gov/mnreports/nw_ls410.txt
3. Duckett SK, Wagner DG, Yates LD, Dolezal HG, May SG. Effects of time on feed on beef nutrient composition. *J Anim Sci.* (1993) 71:2079–88. doi: 10.2527/1993.7182079x
4. Bruns KW, Pritchard RH. Boggs DL. The effect of stage of growth the implant exposure on performance and carcass composition in steers. *J Anim Sci.* (2005) 83:108–16. doi: 10.2527/2005.831108x
5. Bruns KW, Pritchard RH, Boggs DL. The relationship among body weight, body composition, and intramuscular fat content in steers. *J Anim Sci.* (2004) 82:1315–22. doi: 10.2527/2004.8251315x
6. Greene BB, Backus WR, Riemann MJ. Changes in lipid content of ground beef from yearling steers serially slaughtered after varying lengths of grain finishing. *J Anim Sci.* (1989) 67:711–5. doi: 10.2527/jas1989.673711x
7. Moisá SJ, Shike DW, Shoup L, Rodriguez-Zas SL, Loor JJ. Maternal plane of nutrition during late gestation and weaning age alter angus × simmental offspring longissimus muscle transcriptome and intramuscular fat. *PLoS ONE.* (2015) 10:e0131478. doi: 10.1371/journal.pone.0131478
8. Graugnard DE, Berger LL, Faulkner DB, Loor JJ. High-starch diets induce precocious adipogenic gene network up-regulation in longissimus lumborum of early-weaned angus cattle. *British J Nutr.* (2010) 103:953–63. doi: 10.1017/S0007114509992789
9. Koch BM, Pavan E, Andrae JG. Duckett SK. Timing of exposure to high-concentrates versus high-quality forages on growth and marbling deposition in steers. *Meat Muscle Biol.* (2018) 2:321–33. doi: 10.22175/mmb2018.06.0017
10. Koch BM, Pavan E, Long NM, Andrae JG, Duckett SK. Post-weaning exposure to high concentrates versus forages alters marbling deposition and lipid metabolism in steers. *Meat Muscle Biol.* (2019) 3:244–53. doi: 10.22175/mmb2018.12.0040
11. Duckett SK, Pratt SL, Pavan E. Corn oil or corn grain supplementation to steers grazing endophyte-free tall fescue. II. effects on subcutaneous fatty acid content and lipogenic gene expression. *J Anim Sci.* (2009) 87:1120–8. doi: 10.2527/jas.2008-1420
12. Romao JM, Jin W, He M, McAllister T, Guan LL. Altered microRNA expression in bovine subcutaneous and visceral adipose tissues from cattle under different diet. *PLoS ONE.* (2012) 7:e40605. doi: 10.1371/journal.pone.0040605
13. Wang H, Zheng Y, Wang G, Li H. Identification of microRNA and bioinformatics target gene analysis in beef cattle intramuscular fat and subcutaneous fat. *Mol Biosyst.* (2013) 9:2154–62. doi: 10.1039/c3mb70084d
14. Meale SJ. Romao †JM, He ML, Chaves AV, Mcallister TA, Guan LL. Effect of diet on microRNA expression in ovine subcutaneous and visceral adipose tissues 1. *J Anim Sci.* (2014) 92:3328. doi: 10.2527/jas.2014-7710
15. Pan Y, Jing J, Qiao L, Liu J, An L, Li B, et al. MiRNA-seq reveals that miR-124-3p inhibits adipogenic differentiation of the stromal vascular fraction in sheep via targeting C/EBPα. *Domest Anim Endocrinol.* (2018) 65:17–23. doi: 10.1016/j.domaniend.2018.05.002
16. Romao JM, Jin W, Dodson MV, Hausman GJ, Moore SS, Guan LL. MicroRNA regulation in mammalian adipogenesis. *Exp Biol Med.* (2011) 236:997–1004. doi: 10.1258/ebm.2011.011101
17. Sheng X, Song X, Yu Y, Niu L, Li S, Li H, et al. Characterization of microRNAs from sheep (Ovis aries) using computational and experimental analyses. *Mol Biol Rep.* (2010) 38:3161–71. doi: 10.1007/s11033-010-9987-3
18. Livak KJ, Schmittgen TD. Analysis of relative gene expression data using real-time quantitative PCR and the 2(−Δ Δ C(T)) method. *Methods (San Diego, Calif).* (2001) 25:402–8. doi: 10.1006/meth.2001.1262
19. Xie F, Xiao P, Chen D, Xu L, Zhang B. miRDeepFinder: a miRNA analysis tool for deep sequencing of plant small RNAs. *Plant Mol Biol.* (2012) 80:75–84. doi: 10.1007/s11103-012-9885-2

20. Vandesompele J, De Preter K, Pattyn F, Poppe B, Van Roy N, De Paepe A, et al. Accurate normalization of real-time quantitative RT-PCR data by geometric averaging of multiple internal control genes. *Genome Biol.* (2002) 3:research0034.1-0034.11. doi: 10.1186/gb-2002-3-7-research0034
21. Savell JW, Cross HR, Smith GC. Percentage ether extractable fat and moisture content of beef longissimus muscle as related to USDA marbling score. *J Food Sci.* (1986) 51:838–9. doi: 10.1111/j.1365-2621.1986.tb13946.x
22. Moore KJ, Rayner KJ, Suárez Y, Fernández-Hernando C. microRNAs and cholesterol metabolism. *Trends Endocrinol and Meta.* (2010) 21:699–706. doi: 10.1016/j.tem.2010.08.008
23. Qiang J, Tao YF, Bao JW, Chen DJ Li HX, He J, et al. High fat diet-induced miR-122 regulates lipid metabolism and fat deposition in genetically improved farmed tilapia (GIFT, Oreochromis niloticus) liver. *Front Physiol.* (2018) 9:1422. doi: 10.3389/fphys.2018.01422
24. Tao Y, Qiang J, Bao J, Chen D, Yin G, Xu P, et al. Changes in physiological parameters, lipid metabolism, and expression of microRNAs in genetically improved farmed tilapia (Oreochromis niloticus) with fatty liver induced by a high-fat diet. *Front Physiol.* (2018) 10:1521. doi: 10.3389/fphys.2018.01521
25. Qiang J, Tao Y, He J, Xu P, Bao J, Sun Y. miR-122 promotes hepatic antioxidant defense of genetically improved farmed tilapia (GIFT, Oreochromis niloticus) exposed to cadmium by directly targeting a metallothionein gene. *Aquat Toxicol.* (2017) 182:39–48. doi: 10.1016/j.aquatox.2016.11.009
26. Xing K, Zhao X, Liu Y, Zhang F, Tan Z, Qi X, et al. Identification of differentially expressed microRNAs and their potential target genes in adipose tissue from pigs with highly divergent backfat thickness. *Animals (Basel).* (2020)10:624. doi: 10.3390/ani10040624
27. Wang H, Zhong J, Zhang C, Chai Z, Cao H, Wang J, et al. The whole-transcriptome landscape of muscle and adipose tissues reveals the ceRNA regulation network related to intramuscular fat deposition in yak. *BMC Genomics*. (2020) 21:347–631. doi: 10.1186/s12864-020-6757-z
28. Song G, Zhu L, Ruan Z, Wang R, Shen Y. MicroRNA-122 promotes cardiomyocyte hypertrophy via targeting FoxO3. *Biochem Biophys Res Commun*. (2019) 519:682–8. doi: 10.1016/j.bbrc.2019.09.035
29. Qiu Y, Yang J, Bian S, Chen G, Yu J. PPARγ suppresses the proliferation of cardiac myxoma cells through downregulation of MEF2D in a miR-122-dependent manner. *Biochem Biophys Res Commun.* (2016) 474:560–5. doi: 10.1016/j.bbrc.2016.04.112
30. Esau C, Davis S, Murray SF Yu XX, Pandey SK, Pear M, et al. miR-122 regulation of lipid metabolism revealed by in vivo antisense targeting. *Cell Metab.* (2006) 3:87–98. doi: 10.1016/j.cmet.2006.01.005
31. Gebert LFR, Rebhan MAE, Crivelli SEM, Denzler R, Stoffel M, Hall J. Miravirsen (SPC3649) can inhibit the biogenesis of miR-122. *Nucleic Acids Res.* (2014) 42:609–21. doi: 10.1093/nar/gkt852
32. Chen C, Deng B, Qiao M, Zheng R, Chai J, Ding Y, et al. Solexa sequencing identification of conserved and novel microRNAs in backfat of Large White and Chinese Meishan pigs. *PLoS ONE.* (2012) 7:e31426. doi: 10.1371/journal.pone.0031426
33. Setyowati Karolina D, Armugam A, Tavintharan S, T K Wong M, Chi Lim S, Fang Sum C, et al. MicroRNA 144 impairs insulin signaling by inhibiting the expression of insulin receptor substrate 1 in type 2 diabetes mellitus. *Plos ONE.* (2011) 6:e22839. doi: 10.1371/annotation/698b7123-174f-4a09-95c9-fd6f5017d622
34. Kaur P, Kotru S, Singh S, Behera BS, Munshi A. Role of miRNAs in the pathogenesis of T2DM, insulin secretion, insulin resistance, and β cell dysfunction: the story so far. *J Physiol Biochem*. (2020) 76:485–502. doi: 10.1007/s13105-020-00760-2
35. Muroya S, Ogasawara H, Nohara K, Oe M, Ojima K, Hojito M. Coordinated alteration of mRNA-microRNA transcriptomes associated with exosomes and fatty acid metabolism in adipose tissue and skeletal muscle in grazing cattle. *Asian-Australas J Anim Sci.* (2020) 33:1824–36. doi: 10.5713/ajas.19.0682
36. Ning X, Liu S, Qiu Y, Li G, Li Y, Li M, et al. Expression profiles and biological roles of miR-196a in Swine. *Genes*. (2016) 7:5. doi: 10.3390/genes7020005
37. Yonekura S, Hirota S, Miyazaki H, Tokutake Y. Subcellular localization and polymorphism of bovine FABP4 in bovine intramuscular adipocytes. *Anim Biotechnol.* (2016) 27:96. doi: 10.1080/10495398.2015.1102148
38. Bernlohr DA, Bolanowski MA, Kelly TJ, Lane MD. Evidence for an increase in transcription of specific mRNAs during differentiation of 3T3-L1 preadipocytes. *J Biol Chem.* (1985) 260:5563–7. doi: 10.1016/S0021-9258(18)89059-7
39. Taniguchi M, Guan LL, Zhang B, Dodson MV, Okine E, Moore SS. Gene expression patterns of bovine perimuscular preadipocytes during adipogenesis. *Biochem Biophys Res Commun*. (2008) 366:346–51. doi: 10.1016/j.bbrc.2007.11.111
40. Michal JJ, Zhang ZW, Gaskins CT, Jiang Z. The bovine fatty acid binding protein 4 is significantly associated with marbling and subcutaneous fat depth in Wagyu x Limousin F2 crosses. *Anim Genet.* (2006) 37:400–2. doi: 10.1111/j.1365-2052.2006.01464.x
41. Guo B, Kongsuwan K, Greenwood PL, Zhou G, Zhang W, Dalrymple BP, et al. gene expression estimator of intramuscular fat percentage for use in both cattle and sheep. *J Anim Sci Biotechnol.* (2014) 5:379–90. doi: 10.1186/2049-1891-5-35
42. Green CD, Ozguden-Akkoc CG, Wang Y, Jump DB, Olson LK. Role of fatty acid elongases in determination of *de novo* synthesized monounsaturated fatty acid species[S]. *J Lipid Res.* (2010) 51:1871–7. doi: 10.1194/jlr.M004747
43. Moon Y, Ochoa CR, Mitsche MA, Hammer RE, Horton JD. Deletion of ELOVL6 blocks the synthesis of oleic acid but does not prevent the development of fatty liver or insulin resistance[S]. *J Lipid Res.* (2014) 55:2597–605. doi: 10.1194/jlr.M054353
44. Frühbeck G, Méndez-Giménez L, Fernández-Formoso J, Fernández S, Rodríguez A. Regulation of adipocyte lipolysis. *Nutr Res Rev.* (2014) 27:63–93. doi: 10.1017/S095442241400002X
45. Itabe H, Yamaguchi T, Nimura S, Sasabe N. Perilipins: a diversity of intracellular lipid droplet proteins. *Lipids Health Dis*. 2017—04-28;16(1). doi: 10.1186/s12944-017-0473-y
46. Zhao Y, Albrecht E, Li Z, Schregel J, Sciascia QL, Metges CC, et al. Distinct roles of perilipins in the intramuscular deposition of lipids in glutamine-supplemented, low-, and normal-birth-weight piglets. *Front Vet Sci.* (2021) 8:633898. doi: 10.3389/fvets.2021.633898
47. Moon YA. The SCAP/SREBP pathway: a mediator of hepatic steatosis. *Endocrinology metabolism (Seoul).* (2017) 32:6–10. doi: 10.3803/EnM.2017.32.1.6
48. Xiong L, Pei J, Chu M, Wu X, Kalwar Q, Yan P, et al. Fat Deposition in the muscle of female and male yak and the correlation of yak meat quality with fat. *Animals (Basel).* (2021) 11:2142. doi: 10.3390/ani1107 2142
49. Nakajima A, Kawaguchi F, Uemoto Y, Fukushima M, Yoshida E, Iwamoto E, et al. A genome-wide association study for fat-related traits computed by image analysis in Japanese Black cattle. *Animal science J.* (2018) 89:743–51. doi: 10.1111/asj.12987
50. Robelin J. Growth of adipose tissues in cattle: partitioning between depots, chemical composition and cellularity. *Rev Livestock Prod Science.* (1986) 14:349–64. doi: 10.1016/0301-6226(86)90014-X
51. Robelin J. Cellularity of bovine adipose tissues: developmental changes from 15 to 65 percent mature weight. *J Lipid Res.* (1981) 22:452. doi: 10.1016/S0022-2275(20)34959-2

Conflict of Interest: The authors declare that the research was conducted in the absence of any commercial or financial relationships that could be construed as a potential conflict of interest.

Publisher's Note: All claims expressed in this article are solely those of the authors and do not necessarily represent those of their affiliated organizations, or those of the publisher, the editors and the reviewers. Any product that may be evaluated in this article, or claim that may be made by its manufacturer, is not guaranteed or endorsed by the publisher.

frontiers | Frontiers in Veterinary Science

BRIEF RESEARCH REPORT
published: 18 April 2022
doi: 10.3389/fvets.2022.848027

Identification of Key Pathways Associated With Residual Feed Intake of Beef Cattle Based on Whole Blood Transcriptome Data Analyzed Using Gene Set Enrichment Analysis

Godstime A. Taiwo[1], *Modoluwamu Idowu*[1], *James Denvir*[2], *Andres Pech Cervantes*[3] *and Ibukun M. Ogunade*[1]*

[1] Division of Animal and Nutritional Science, West Virginia University, Morgantown, WV, United States, [2] Department of Medicine, Surgery, and Biomedical Sciences, Joan C. Edwards School of Medicine, Marshall University, Huntington, WV, United States, [3] Agricultural Research Station, Fort Valley State University, Fort Valley, GA, United States

OPEN ACCESS

Edited by:
Rajib Deb,
National Research Centre on Pig (ICAR), India

Reviewed by:
Jon Schoonmaker,
Purdue University, United States
Sara Pegolo,
University of Padua, Italy
John B. Hall,
University of Idaho, United States

***Correspondence:**
Ibukun M. Ogunade
ibukun.ogunade@mail.wvu.edu

Specialty section:
This article was submitted to Animal Nutrition and Metabolism, a section of the journal Frontiers in Veterinary Science

Received: 03 January 2022
Accepted: 08 March 2022
Published: 18 April 2022

Citation:
Taiwo GA, Idowu M, Denvir J, Cervantes AP and Ogunade IM (2022) Identification of Key Pathways Associated With Residual Feed Intake of Beef Cattle Based on Whole Blood Transcriptome Data Analyzed Using Gene Set Enrichment Analysis. Front. Vet. Sci. 9:848027. doi: 10.3389/fvets.2022.848027

We applied whole blood transcriptome analysis and gene set enrichment analysis to identify pathways associated with divergent selection for low or high RFI in beef cattle. A group of 56 crossbred beef steers (average BW = 261 ± 18.5 kg) were adapted to a high-forage total mixed ration in a confinement dry lot equipped with GrowSafe intake nodes for period of 49 d to determine their residual feed intake (RFI). After RFI determination, whole blood samples were collected from beef steers with the lowest RFI (most efficient; low-RFI; $n = 8$) and highest RFI (least efficient; high-RFI; $n = 8$). Prior to RNA extraction, whole blood samples collected were composited for each steer. Sequencing was performed on an Illumina NextSeq2000 equipped with a P3 flow. Gene set enrichment analysis (GSEA) was used to analyze differentially expressed gene sets and pathways between the two groups of steers. Results of GSEA revealed pathways associated with metabolism of proteins, cellular responses to external stimuli, stress, and heat stress were differentially inhibited (false discovery rate (FDR) < 0.05) in high-RFI compared to low-RFI beef cattle, while pathways associated with binding and uptake of ligands by scavenger receptors, scavenging of heme from plasma, and erythrocytes release/take up oxygen were differentially enriched (FDR < 0.05) in high-RFI, relative to low-RFI beef cattle. Taken together, our results revealed that beef steers divergently selected for low or high RFI revealed differential expressions of genes related to protein metabolism and stress responsiveness.

Keywords: protein metabolism, cellular response, feed efficiency, oxidative stress, heat stress

INTRODUCTION

Residual feed intake (RFI), a measure of feed efficiency, continues to be of great economic importance due to increasing cost of animal feeds (1). Residual Feed Intake is the difference between an animal's actual feed intake and its predicted feed intake for a given level of maintenance and body weight gain (1). Feed efficient animals consume less than expected and have a low (negative) RFI, while inefficient animals consume more than expected and have a high (positive) RFI. Thus, beef

cattle selected for low RFI have decreased feed costs because they consume less dry matter when compared with high-RFI beef cattle while maintaining similar growth performance.

Due to the great economic importance of RFI, the biological mechanisms underlying variation in this trait have always been of great interest; however, these mechanisms have not been fully understood. Difference in RFI has been suggested to be an indication of differences in metabolism rather than differences in growth performance because the trait is phenotypically independent of growth performance (1). Several studies have applied whole transcriptome analysis of several tissues such as liver and ruminal epithelium to further understand the biological mechanisms regulating feed efficiency traits including RFI in beef cattle (2–4). For instance, Kong et al. (3) analyzed the rumen epithelial transcriptome from low-RFI and high-RFI beef steers and observed increased tissue morphogenesis and greater expression of mitochondrial genes in low-RFI compared to high-RFI steers. Mukiibi et al. (4) analyzed liver tissue transcriptome profile and observed differential expressions of genes involved in nutrient metabolisms and cellular development in beef steers divergent for low and high RFI. However, these studies involve invasive sample collection procedures. Despite the convenience of collection and relatively non-invasive accessibility of blood in ruminants, very few attempts have been made to apply whole-blood transcriptome to understand the biological mechanisms associated with RFI in animals. Genes expressed in peripheral blood cells have been demonstrated to reflect physiological changes in different body tissues and can highlight biological processes related to overall metabolisms. Therefore, the objective of this study was to analyze the whole-blood transcriptome data of beef steers via gene-set enrichment analysis to identify key pathways associated with divergent selection for low or high RFI in beef cattle.

MATERIALS AND METHODS

Animals and Sample Collection

A total of 56 crossbred growing beef steers with average BW of 261.3 ± 18.5 kg were fed a high-forage total mixed ration (TMR; primarily consisting of triticale silage; rye grass silage; and a ration balancing **Supplementary Table 1**) in five confinement dry lot pens (15 by 47 m^2), each served by three GrowSafe 8000 (GrowSafe Systems Ltd., Airdrie, Alberta, Canada) feeding nodes to measure individual feed intake and two In-Pen Weighing Positions (IPW Positions, Vytelle LLC) to measure daily BW for a total of 49 d after 15-d adjustment period to the feeding facilities. The use of IPW Positions has enabled the measurement of individual animal BW multiple times in a day (5). The IPW Positions measure the partial BW by weighing the front end of an animal (6). The IPW positions were positioned at a water trough in each pen such that an animal must place its front feet on the scale in order to drink (7). The partial BW of the animals was measured every second the animals stayed on the scale while drinking. More details on the accuracy, use and applicability of IPW positions have been described in previous studies (5, 6). In this study, approximately 617 ± 92 daily BW data points (after filtering outliers) per animal were generated and were regressed on time to calculate beginning BW, mid-test BW, and average daily gain (ADG) of each animal. Animal ADG and metabolic mid-test BW (mid-test $BW^{0.75}$) were regressed against individual average daily intake, and RFI was calculated as the residual or the difference between the predicted value of the regression and the actual measured value based on the following equation: $Y = \beta_0 + \beta_1 X_1 + \beta_2 X_2 + \varepsilon$, where Y is the observed DMI (kg/d), β_0 is the regression intercept, β_1 and β_2 are the partial regression coefficients, X_1 is the mid-test metabolic BW (kg), X_2 is the ADG (kg/d), and ε indicates the RFI [kg/d; (8)]. After the determination of RFI values for all animals, the most-efficient with the lowest RFI (low-RFI; $n = 8$) and the least-efficient with the highest RFI (high-RFI; $n = 8$) beef steers were selected, kept separate from others, and kept on the same diet for additional 21 d (designated in this study as d 50–70). On d 56, 63, and 70, 10 mL of blood samples were collected before morning feeding into tubes containing sodium heparin. Immediately after collection, subsamples (500 μL each) were transferred into RNA-protect tubes (Cat. No. 76554; Qiagen) containing a reagent that lyses blood cells and stabilizes intracellular RNA and stored at −80°C until later analysis.

RNA Extraction, Library Preparation, and Sequencing

Prior to RNA extraction, whole blood samples collected on d 56, 63, and 70 were composited for each steer. Total RNA was extracted from the composited samples using RNeasy Protect Animal Blood kit (Cat. No. 73224; Qiagen) following the manufacturer's instructions. RNA concentration was measured using a NanoDrop One C spectrophotometer with an A260:A280 ratio from 1.8 to 2.0 (Thermo Fisher Scientific, Waltham, MA, USA). All RNA samples had RNA integrity numbers >8.0. Dual indexed RNA Libraries were prepared from 100 to 250 ng of total RNA per sample using the KAPA RNA HyperPrep Kit with RiboErase (Human, Mouse, Rat) Globin Reduction method in the WVU Genomics Core according to the kit manufacturer's instructions. Library quality was assessed by electrophoretic analysis on the Agilent 4,200 TapeStation system with High Sensitivity D1000 screentape. RNA libraries were sequenced in a dual indexed 2 × 50 paired-end run on an Illumina NextSeq2000 equipped with a P3 flow.

Data and Statistical Analysis

For the RNA-seq data, reads were trimmed using Trimmomatic v 0.39 to remove low-quality base calls and adapter sequences (9), and then aligned to the Bovine reference genome ARS-UCD1.2 (10) using HISAT2 v 2.2.1 (11). Resulting files were sorted and indexed, and PCR and optical duplicate reads were marked using SamTools v1.12 (12). The numbers of reads mapping to each gene for each sample were counted using the R/Bioconductor package GenomicAlignments v 1.26.0 (13). Log_2 fold change values were computed using DESeq2 version 1.30.1 (14). We used gene set enrichment analysis (GSEA), a pathway enrichment method that utilizes predefined gene sets from the reactome pathways (15), to analyze differentially expressed gene sets using the R/Bioconductor package fgsea v 1.16.0. The GSEA was performed to determine the key pathways that were enriched or inhibited

by considering the expression levels of sets of biologically related genes (16). Genes identified by DESeq2 as expressing over a minimal threshold were ranked by Log_2 fold change and analyzed by the GSEA algorithm (17). The altered pathways were filtered based on FDR $\leq$ 0.05 and were arranged in the order of their normalized enrichment scores.

RESULTS

The average RFI values of low- and high-RFI steers were−1.93 and 2.01, respectively. An average of 36 million reads per sample was generated (**Supplementary Table 2**). Results of GSEA revealed gene sets (pathways) associated with metabolism of proteins, cellular responses to external stimuli, stress, heat stress, and regulation of HSF-1-mediated heat shock response were differentially inhibited (FDR = 0.01) in high-RFI compared to low-RFI beef cattle (**Table 1**, **Supplementary Figure 1**). The gene set associated with metabolism of proteins consists of 248 genes, and 85 of which were leading edge genes (significantly enriched genes). Both cellular response to external stimuli and cellular response to stress shared the same nineteen leading edge genes including *HSPA1A, HSPH1, BAG2, DNAJA1, DNAJB1, H3C13, H2BC7, H4C2, ELOC, JUN,* and *HSPA4. Five* of the leading edge genes (*HSPA1A, HSPH1, BAG2, HSPA4,* and *DNAJB1*) associated with cellular response to external stimuli and stress were also leading edge genes in gene sets associated with response to heat stress and regulation of HSF-1-mediated heat shock response (**Table 1**).

Gene sets associated with binding and uptake of ligands by scavenger receptors, scavenging of heme from plasma, erythrocytes take up/release carbon dioxide and release/take up oxygen share the same leading edge genes (*HBB, HBA1,* and *HBA*) and were all differentially enriched (FDR < 0.05) in high-RFI, relative to low-RFI beef cattle (**Table 1**, **Supplementary Figure 2**).

DISCUSSION

Understanding the biological mechanisms regulating feed efficiency using easily accessible and non-invasive sample such as blood is essential to the future of livestock production systems in terms of profitability and animal welfare concern.

In this study, protein metabolism is the most enriched metabolic pathway based on the number of leading edge genes (such as *LOC101907518, RPL39, LOC101902490, UBE2D1, FUCA2*) in the gene set. In addition to the function of amino acids as the building blocks of proteins, amino acids regulate key metabolism essential for growth, performance, reproduction, and immunity (18). Research studies have shown that protein (amino acids) metabolism is essential for optimizing efficiency of nutrient absorption and metabolism to enhance immunity against diseases and stress, growth performance, and milk production of animals (18). Several published articles have identified protein metabolism as one of the most important metabolic processes associated with RFI in animals (19, 20). In our previous study, we identified plasma amino acid metabolites as the most significant metabolic signatures associated with RFI in beef cattle (20). Elolimy et al. (21) reported differences in signaling mechanisms controlling protein turnover in ruminal epithelium of beef cattle divergent for low- or high-RFI. In a similar study, Kong et al. (3) reported increased expression of genes involved in protein and cell turnover in the ruminal epithelium of low-RFI beef cattle, compared with high-RFI beef cattle. 4 performed RNA-seq analysis of liver tissue in beef cattle divergent for low and high RFI and observed downregulation of genes involved in amino acid degradation and urea synthesis in low-RFI beef cattle. In fact, some studies have reported significant association of blood metabolites involved in urea cycle with RFI in beef cattle (22, 23). Our results and those of others that utilized tissues with relatively more invasive collection methods suggest that amino acid metabolism plays a considerable role in regulating RFI of beef cattle and its enrichment in low-RFI beef steers probably explains their similar growth performance with high-RFI beef steers despite lower DMI.

Amino acids play a functional role in regulating stress response, including oxidative stress, in animals (24). Stress response has significant implication on health and production efficiency of animals (25). In fact, difference in stress responsiveness has been suggested to contribute to variation in feed efficiency of beef cattle (19, 26). In this study, we observed downregulation of gene set including *HSPA1A, HSPH1, BAG2,* and *DNAJA1* associated with cellular responses to external stimuli, stress, heat stress, and regulation of HSF-1-mediated heat shock response in high-RFI beef steers, which suggests that these steers are more susceptible to stress. When an animal can no longer cope with a stressor, level of blood cortisol increases via activation of hypothalamic–pituitary–adrenal axis (HPA) axis which causes a fight or flight response that increases energy expenditure. Thus, stress response in animals is often determined by blood cortisol level and activity of the HPA axis (27). In a study that determined the response of beef heifers to an exogenous adrenocorticotropic hormone (ACTH) challenge, there was a positive association of plasma cortisol level with RFI status and low-RFI had a lower cortisol response than high-RFI heifers indicating that low-RFI heifers coped better with the stress challenge (28). Richardson et al. (19) and Gomes et al. (29) reported lower blood levels of cortisol in low-RFI beef cattle when compared to high-RFI beef cattle. A similar result was observed in crossbred rams following ACTH challenge (26). Taken together, downregulation of genes associated with cellular responses to external stimuli, stress, heat stress, and regulation of HSF-1-mediated heat shock response in high-RFI beef steers suggests that low-RFI steers have better adaptive mechanisms to cope with environmental stressors, thereby, reducing energy expenditure and increasing energy availability for improved growth performance and better feed efficiency.

In this study, we observed enrichment of gene sets (*HBB, HBA1,* and *HBA*) associated with erythrocytes take up/release carbon dioxide, release/take up oxygen, scavenging of heme from plasma, and binding and uptake of ligands by scavenger receptors in high-RFI, relative to low-RFI beef

TABLE 1 | Altered pathways identified by Gene Set Enrichment Analysis in high-RFI compared to low-RFI beef steers.

Pathway	FDR	NES	Gene set size (# of leading edge genes)	Leading edge genes
Binding and uptake of ligands by scavenger receptors	0.01	1.82	4 (3)	*HBB, HBA1, HBA*
Scavenging of heme from plasma	0.01	1.82	4 (3)	*HBB, HBA1, HBA*
Erythrocytes take up carbon dioxide and release oxygen	0.01	1.68	3 (3)	*HBB, HBA1, HBA*
Erythrocytes take up oxygen and release carbon dioxide	0.01	1.68	3 (3)	*HBB, HBA1, HBA*
O_2/CO_2 exchange in erythrocytes	0.01	1.68	3 (3)	*HBB, HBA1, HBA*
Metabolism of proteins	0.01	−1.70	248 (85)	*LOC101907518, RPL39, LOC101902490, UBE2D1, FUCA2, B4GALT6, FBXL3, SOCS3, COMMD8, RPLP2, RPL34*
Cellular responses to external stimuli	0.01	−1.99	69 (19)	*HSPA1A, HSPH1, BAG2, DNAJA1, JUN, HSPA4, UBE2D1, DNAJB1, H3C13, H2BC7, H4C2, ELOC, ELOB, H2AC8, SIRT1, FLCN, ATP6V1G1, HSPA14, H2BU1*
Cellular responses to stress	0.01	−1.99	69 (19)	*HSPA1A, HSPH1, BAG2, DNAJA1, JUN, HSPA4, UBE2D1, DNAJB1, H3C13, H2BC7, H4C2, ELOC, ELOB, H2AC8, SIRT1, FLCN, ATP6V1G1, HSPA14, H2BU1*
Cellular response to heat stress	0.01	−2.05	16 (5)	*HSPA1A, HSPH1, BAG2, HSPA4, DNAJB1*
Regulation of HSF1-mediated heat shock response	0.01	−2.05	16 (5)	*HSPA1A, HSPH1, BAG2, HSPA4, DNAJB1*

High-RFI, feed inefficient beef steers; low-RFI, feed-efficient beef steers; False discovery rate (FDR) ≤ 0.01; NES, normalized enrichment score (high-RFI vs. low-RFI). Leading edge genes are those that are enriched within the gene set. See ***Supplementary Table 3*** *for the full list of leading edge genes associated with metabolism of proteins. #Means number.*

cattle. Erythrocytes contain hemoglobins which carry oxygen to the body and are continuously exposed to high oxygen content which pre-disposes them to oxidative stress damage (30, 31). Heme scavenger proteins, such as hemopexin and alpha-1-microglobulin, scavenge extracellular heme, a physiological ligand (32), synthesized from hemoglobin degradation via the activity of heme-oxygenase, an enzyme that is inducible by stressors such as oxygen free radicals (33, 34). Previous investigations have shown that cellular expression of alpha-1-microglobulin is enriched during increased oxidative stress and heme exposure (30, 34). In ruminants, oxidative stress has been implicated in many pathophysiological conditions that are relevant for growth performance, reproduction, and health (35). In fact, several studies have shown that oxidative damage of cell organelles and biomolecules is a source of energy drain and negatively affects several cellular processes including lipid and protein metabolism (36, 37). The major source of intracellular reactive oxygen species production is the mitochondria (38) and previous studies have reported higher mitochondrial ROS production in less feed-efficient compared to high feed efficient animals (36, 39, 40). In addition, Casal et al. (41) reported increased hepatic abundance of protein carbonyls and thiobarbituric acid reactive species, which are products of protein and lipid oxidative damage, and reduced protein expression of antioxidant enzymes, including mitochondrial manganese superoxide dismutase, in high-RFI when compared with low-RFI beef steers. Similarly, Tizioto et al. (42) observed upregulation of oxidative stress-induced transcription factors in muscle of high-RFI beef steers. Therefore, it is reasonable to speculate that enrichment of genes associated with erythrocytes take up/release carbon dioxide, scavenging of heme from plasma, and binding and uptake of ligands by scavenger receptors in high-RFI compared to low-RFI beef steers suggests that they may be more prone to oxidative stress, thereby resulting in reduced efficiency of energy use for metabolic processes such as growth.

It is important to note that though whole blood transcriptome data might encompass gene activities of several body tissues and organs including liver, kidney, muscles, and rumen, the contribution of each tissue to the whole blood transcriptome is not known and should be determined in future studies. In addition, biological validation of the RNA-Seq data on selected genes by RT-qPCR is also needed to confirm the results of this study.

CONCLUSION

Results of GSEA of whole blood transcriptome data in beef steers divergently selected for low or high RFI revealed differential expression of genes related to protein metabolism, erythrocytes take up/release carbon dioxide and release/take up oxygen, and stress responsiveness. These results are similar to those of several studies that utilized other tissues including liver, muscle, and ruminal epithelium. Thus, this study demonstrates the

suitability of whole blood transcriptome data for understanding the biological mechanisms regulating RFI in animals. Due to the small number of animals used in this study and the effect of different diets and breeds on RFI ranking, further validation using a larger cohort of beef cattle fed different diets is needed to confirm these findings.

DATA AVAILABILITY STATEMENT

All raw and processed sequencing data were submitted to the Gene Expression Omnibus (GEO) at the National Center for Biotechnology Information (NCBI) and can be accessed via accession number GSE198068.

ETHICS STATEMENT

The animal study was reviewed and approved by the Institutional Animal Care and Use Committees of West Virginia University (protocol number 1608003693).

AUTHOR CONTRIBUTIONS

IO and APC designed the experiment. GT and MI conducted the experiment. JD analyzed the RNA-Seq data. IO, GT, and APC drafted the manuscript. All authors reviewed and approved the final manuscript.

FUNDING

This work was funded by West Virginia University Experimental Station (scientific article number 3430) in support of U.S. Department of Agriculture hatch multi-state regional project W-3010.

SUPPLEMENTARY MATERIAL

The Supplementary Material for this article can be found online at: https://www.frontiersin.org/articles/10.3389/fvets.2022.848027/full#supplementary-material

REFERENCES

1. Koch RM, Swiger LA, Chambers D, Gregory KE. Efficiency of food use in beef cattle. *J Anim Sci.* (1963) 22:486–94. doi: 10.2527/jas1963.222486x
2. Alexandre PA, Kogelman LJ, Santana MH, Passarelli D, Pulz LH, Fantinato-Neto P, et al. Liver transcriptomic networks reveal main biological processes associated with feed efficiency in beef cattle. *BMC Genomics*. (2015) 16:s12864–015. doi: 10.1186/s12864-015-2292-8
3. Kong RS, Liang G, Chen Y, Stothard P, Guan I. Transcriptome profiling of the rumen epithelium of beef cattle differing in residual feed intake. *BMC Genomics*. (2016) 17:592. doi: 10.1186/s12864-016-2935-4
4. Mukiibi R, Vinsky M, Keogh KA, Fitzsimmons C, Stothard P, Waters SM, et al. Transcriptome analyses reveal reduced hepatic lipid synthesis and accumulation in more feed efficient beef cattle. *Sci Rep*. (2018) 8:7303. doi: 10.1038/s41598-018-25605-3
5. MacNeil MD, Berry DP, Clark SA, Crowley JJ, Scholtz MM. Evaluation of partial body weight for predicting body weight and average daily gain in growing beef cattle. *Transl Anim Sci.* (2021) 5:1–12. doi: 10.1093/tas/txab126
6. Wells RS, Interrante SM, Sakkuma SS, Walker RS, Butler TJ. Accuracy of the VYTELLE SENSE in-pen weighing positions. *Applied Anim Sci.* (2021) 37:626–34. doi: 10.15232/aas.2021-02183
7. Benfield D, Garossino K, Sainz RD, Kerley MS, Huisma C. Conversion of high-frequency partial body weights to total body weight in feedlot cattle. *J Anim Sci*. (2017) 95:241–2. doi: 10.2527/asasann.2017.495
8. Durunna ON, Mujibi FDN, Goonewardene L, Okine EK, Wang Z, Moore SS. Feed efficiency differences and re-ranking in beef steers fed grower and finisher diets. *J Anim Sci.* (2011) 89:158–67. doi: 10.2527/jas.2009-2514
9. Bolger AM, Lohse M, Usadel B. Trimmomatic: a flexible trimmer for Illumina sequence data. *Bioinformatics*. (2014) 30:2114–20. doi: 10.1093/bioinformatics/btu170
10. Rosen BD, Bickhart DM, Schnabel RD, Koren S, Elsik CG, Tseng E, et al. De novo assembly of the cattle reference genome with single-molecule sequencing. *Gigascience*. (2020) 9:giaa021. doi: 10.1093/gigascience/giaa021
11. Kim D, Langmead B, Salzberg SL. HISAT: a fast-spliced aligner with low memory requirements. *Nat Methods*. (2015) 12:357–60. doi: 10.1038/nmeth.3317
12. Li H, Handsaker B, Wysoker A, Fennell T, Ruan J, Homer N, et al. The Sequence alignment/map format and SAMtools. *Bioinformatics*. (2009) 25:2078–89. doi: 10.1093/bioinformatics/btp352
13. Lawrence M, Huber W, Pages H, Aboyoun P, Carlson M, Gentleman R, et al. Software for computing and annotating genomic ranges. *PLoS Comput Biol*. (2013) 9:e1003118. doi: 10.1371/journal.pcbi.1003118
14. Love MI, Huber W, Anders S. Moderated estimation of fold change and dispersion for RNA-seq data with DESeq2. *Genome Biol*. (2014) 15:550–8. doi: 10.1186/s13059-014-0550-8
15. Jassal B, Matthews L, Viteri G, Gong C, Lorente P, Fabregat A, et al. The reactome pathway knowledgebase. *Nucleic Acids Res*. (2020) 48:498–503. doi: 10.1093/nar/gkz1031
16. Reimand J, Isserlin R, Voisin V, Kucera M, Tannus-Lopes C, Rostamianfar A, et al. Pathway enrichment analysis and visualization of omics data using g: Profiler, GSEA, Cytoscape and EnrichmentMap. *Nat Protoc*. (2019) 14:482–517. doi: 10.1038/s41596-018-0103-9
17. Luo W, Friedman MS, Shedden K, Hankenson K, Woolf PJ. GAGE: Generally applicable gene set enrichment for pathway analysis. *BMC Bioinform*. (2009) 10:161. doi: 10.1186/1471-2105-10-161
18. Wu G. Amino acids: metabolism, functions, and nutrition. *Amino Acids*. (2009) 37:1–17. doi: 10.1007/s00726-009-0269-0
19. Richardson E, Herd R. Biological basis for variation in residual feed intake in beef cattle. 2 Synthesis of results following divergent selection. *Anim Prod Sci*. (2004) 44:431–40. doi: 10.1071/EA02221
20. Taiwo G, Idowu M, Collins S, Sidney T, Wilson M, Pech-Cervantes A, et al. Chemical group-based metabolome analysis identifies candidate plasma biomarkers associated with residual feed intake in beef steers. *Front Anim Sci*. (2022) 2:783314. doi: 10.3389/fanim.2021.783314
21. Elolimy AA, Abdel-Hamied E, Hu L, McCann JC, Shike DW, Loor JJ. Residual feed intake in beef cattle is associated with differences in protein turnover and nutrient transporters in ruminal epithelium. *J Anim Sci.* (2019) 97:2181–7. doi: 10.1093/jas/skz080
22. Jorge-Smeding E, Renand G, Centeno D, Pétéra M, Durand S, Polakof S, et al. Metabolomics reveals changes in urea cycle associated to residual feed intake in growing heifers. In: *Energy and Protein Metabolism and Nutrition*. Wageningen: Wageningen Academic (2019). p. 231–2. doi: 10.3920/978-90-8686-891-9_50
23. Goldansaz SA, Markus S, Berjanskii M, Rout M, Guo AC, Wang Z, et al. Candidate serum metabolite biomarkers of residual feed intake and carcass merit in sheep. *J Anim Sci*. (2020) 98:10. doi: 10.1093/jas/skaa298
24. Coleman DN, Lopreiato V, Alharthi A, Loor JJ. Amino acids and the regulation of oxidative stress and immune function in dairy cattle. *J Anim Sci*. (2020) 98:S175–93. doi: 10.1093/jas/skaa138
25. Lyles JL, Calvo-Lorenzo MS, Bill E. Kunkle Interdisciplinary Beef Symposium: Practical developments in managing animal welfare in beef cattle: What does the future hold? *J. Anim Sci.* (2014) 92:5334–44. doi: 10.2527/jas.2014-8149

26. Knott S, Cummins L, Dunshea F, Leury B. Rams with poor feed efficiency are highly responsive to an exogenous adrenocorticotropin hormone (ACTH) challenge. *Domest Anim Endocrinol.* (2008) 34:261–8. doi: 10.1016/j.domaniend.2007.07.002
27. Ralph C, Tilbrook A. The hypothalamo-pituitary-adrenal (HPA) axis in sheep is attenuated during lactation in response to psychosocial and predator stress. *Domest Anim Endocrinol.* (2016) 55:66–73. doi: 10.1016/j.domaniend.2015.11.003
28. Kelly AK, Lawrence P, Earley B, Kenny DA, McGee M. Stress and immunological response of heifers divergently ranked for residual feed intake following an adrenocorticotropic hormone challenge. *J Anim Sci Biotechnol.* (2017) 8:65. doi: 10.1186/s40104-017-0197-x
29. Gomes RC, Sainz RD, Leme PR. Protein metabolism, feed energy partitioning, behavior patterns and plasma cortisol in Nellore steers with high and low residual feed intake. *Revista Brasileira de Zootecnia.* (2013) 42:44–50. doi: 10.1590/S1516-35982013000100007
30. Olsson MG, Allhorn M, Olofsson T, Akerstrom B. Up-regulation of alpha1-microglobulin by hemoglobin and reactive oxygen species in hepatoma and blood cell lines. *Free Radic Biol Med.* (2007) 42:842–51. doi: 10.1016/j.freeradbiomed.2006.12.017
31. Maurya PK, Kumar P, Chandra P. Biomarkers of oxidative stress in erythrocytes as a function of human age. *World J Methodol.* (2015) 5:216–22. doi: 10.5662/wjm.v5.i4.216
32. Raghuram S, Stayrook KR, Huang P, Rogers PM, Nosie AK, McClure DB, et al. Identification of heme as the ligand for the orphan nuclear receptors REV-ERBalpha and REV-ERBbeta. *Nat Struct Mol Biol.* (2007) 14:1207–13. doi: 10.1038/nsmb1344
33. Nielsen MJ, Moller HJ, Moestrup SK. Hemoglobin and heme scavenger receptors. *Antioxid Redox Signal.* (2010) 12:261–73. doi: 10.1089/ars.2009.2792
34. Kalapotharakos G, Murtoniemi K, Åkerström B, Hämäläinen E, Kajantie E, Räikkönen K, et al. Plasma heme scavengers alpha-1-microglobulin and hemopexin as biomarkers in high-risk pregnancies. *Front Physiol.* (2019) 10:300. doi: 10.3389/fphys.2019.00300
35. Miller JK, Brzezinska-Slebodzinska E, Madsen FC. Oxidative stress, antioxidants, and animal function. *J Dairy Sci.* (1993) 76:2812–23. doi: 10.3168/jds.S0022-0302(93)77620-1
36. Bottje WG, Carstens G. Association of mitochondrial function and feed efficiency in poultry and livestock species. *J Anim Sci.* (2009) 87:48–63. doi: 10.2527/jas.2008-1379
37. Radi R. Oxygen radicals, nitric oxide, and peroxynitrite: redox pathways in molecular medicine. *Proc Natl Acad Sci USA*. (2018). 115:5839–48. doi: 10.1073/pnas.1804932115
38. Boveris A, Chance B. The mitochondrial generation of hydrogen peroxide. general properties and effect of hyperbaric oxygen. *Biochem J.* (1973) 134:707–16. doi: 10.1042/bj1340707
39. Iqbal M, Pumford N, Lassiter K, Tang ZX, Wing T, Cooper M, et al. Compromised liver mitochondrial function and complex activity in low feed efficient broilers within a single genetic line associated with higher oxidative stress and differential protein expression. *Poult Sci.* (2005) 84:933–41. doi: 10.1093/ps/84.6.933
40. Grubbs JK, Fritchen AN, Huff-Lonergan E, Dekkers JC, Gabler NK, Lonergan SM. Divergent genetic selection for residual feed intake impacts mitochondria reactive oxygen species production in pigs. *J Anim Sci.* (2013) 91:2133–40. doi: 10.2527/jas.2012-5894
41. Casal A, Garcia-Roche M, Navajas EA, Cassina A, Carriquiry M. Differential hepatic oxidative status in steers with divergent residual feed intake phenotype. *Animal.* (2020) 14:78–85. doi: 10.1017/S1751731119001332
42. Tizioto PC, Coutinho LL, Oliveira PS, Cesar AS, Diniz WJ, Lima AO, et al. Gene expression differences in longissimus muscle of Nelore steers genetically divergent *for* residual feed intake. *Sci Rep*. (2016) 6:39493. doi: 10.1038/srep39493

Conflict of Interest: The authors declare that the research was conducted in the absence of any commercial or financial relationships that could be construed as a potential conflict of interest.

Publisher's Note: All claims expressed in this article are solely those of the authors and do not necessarily represent those of their affiliated organizations, or those of the publisher, the editors and the reviewers. Any product that may be evaluated in this article, or claim that may be made by its manufacturer, is not guaranteed or endorsed by the publisher.

frontiers | Frontiers in Veterinary Science

ORIGINAL RESEARCH
published: 15 June 2022
doi: 10.3389/fvets.2022.890978

11S Glycinin Up-Regulated NLRP-3-Induced Pyroptosis by Triggering Reactive Oxygen Species in Porcine Intestinal Epithelial Cells

*Lei Wang[1], Zhifeng Sun[1], Weina Xie[1], Chenglu Peng[2], Hongyan Ding[1], Yu Li[1], Shibin Feng[1], Xichun Wang[1], Chang Zhao[1] and Jinjie Wu[1]**

[1] College of Animal Science and Technology, Anhui Agricultural University, Hefei, China, [2] Department of Food Science and Engineering, School of Agriculture and Biology, Shanghai Jiao Tong University, Shanghai, China

11S glycinin is a major soybean antigenic protein, which induces human and animal allergies. It has been reported to induce intestinal porcine epithelial (IPEC-J2) cell apoptosis, but the role of pyroptosis in 11S glycinin allergies remains unknown. In this study, IPEC-J2 cells were used as an *in vitro* physiological model to explore the mechanism of 11S glycinin-induced pyroptosis. The cells were incubated with 0, 1, 5, and 10 mg·ml^{-1} 11S glycinin for 24 h. Our results revealed that 11S glycinin significantly inhibited cell proliferation, induced DNA damage, generated active oxygen, decreased mitochondrial membrane potential, and increased the NOD-like receptor protein 3 (NLRP-3) expression of IPEC-J2 cells in a dose-dependent manner. Further, IPEC-J2 cells were transfected with designed sh-NLRP-3 lentivirus to silence *NLRP-3*. The results showed that 11S glycinin up-regulated the silenced *NLRP-3* gene and increased the expression levels of apoptosis-related spot-like protein (ASC), caspase-1, the cleaved gasdermin D, and interleukin-1β. The IPEC-J2 cells showed pyrolysis morphology. Moreover, we revealed that N-acetyl-L-cysteine can significantly inhibit the production of reactive oxygen species and reduce the expression levels of NLRP-3 and the cleaved gasdermin D. Taken together, 11S glycinin up-regulated NLRP-3-induced pyroptosis by triggering reactive oxygen species in IPEC-J2 cells.

Keywords: 11S glycinin, allergy, ROS, NLRP-3, lentiviral transfection, IPEC-J2 cell, pyroptosis

OPEN ACCESS

Edited by:
Rita Payan Carreira, University of Evora, Portugal

Reviewed by:
Dario Loureiro Santos, Universidade de Trás-os-Montes e Alto Douro, Portugal
Hui Zhang, South China Agricultural University, China

***Correspondence:**
Jinjie Wu
wjj@ahau.edu.cn

Specialty section:
This article was submitted to Animal Nutrition and Metabolism, a section of the journal Frontiers in Veterinary Science

Received: *07 March 2022*
Accepted: *02 May 2022*
Published: *15 June 2022*

Citation:
Wang L, Sun Z, Xie W, Peng C, Ding H, Li Y, Feng S, Wang X, Zhao C and Wu J (2022) 11S Glycinin Up-Regulated NLRP-3-Induced Pyroptosis by Triggering Reactive Oxygen Species in Porcine Intestinal Epithelial Cells. Front. Vet. Sci. 9:890978. doi: 10.3389/fvets.2022.890978

INTRODUCTION

Soybean is an important economic crop and is the main source of plant protein in food, feed, and other industries (1). Soybean is one of the eight allergic foods that can affect the respiratory system (2), digestive system (3, 4), and seriously affect animal growth and health (5). 11S glycinin is the main antigenic component of soybean protein. It is a hexamer protein consisting of different subunits, each of which consists of an acidic peptide chain and a basic peptide chain. The structure is very stable and is not easily damaged in its natural state. After eating 11S soybean protein, an intestinal immune response is triggered in young animals, damaging the intestinal mucosal barrier, resulting in growth retardation, dyspepsia, and allergic diarrhea (6, 7).

The intestinal epithelial cell (IEC) layer is exposed to the intestinal lumen contents, participates in the selective absorption of nutrients, and acts as a barrier to the passive paracellular permeability of the intestinal lumen contents through the expression of a tight-junction between adjacent IECs. Soybean allergy usually induces intestinal inflammatory diseases, characterized by the atrophy and proliferation of crypt villi, which accelerate the apoptosis and migration of intestinal cells (8, 9). Our previous studies have determined that 11S glycinin decreases intestinal porcine epithelial (IPEC-J2) cell membrane potential (10), damages the cell cytoskeleton and cell tight junctions, and induces IPEC-J2 cell apoptosis *via* the p38/JNK/NF–κB signaling pathway (11). Abnormal activation of the MAPK and NF–κB signaling pathways promotes an inflammatory response, leading to inflammatory damage of the small intestine tissue of piglets (12). However, the inflammatory response is a complex process and is the result of the interaction and mutual regulation of multiple pathways. In the recent years, a large number of studies have revealed that epithelial pyroptosis plays a key role in allergic diseases (13, 14). Pyroptosis is a pro-inflammatory form of programmed cell death (PCD), which is characterized by the continuous expansion of cells until the rupture of the cell membrane, resulting in the release of cellular contents and then activating a strong inflammatory response (15, 16). NOD-like receptor protein 3 (NLRP-3) is a protein complex in cells. Its main function is to activate caspase-1, activated caspase-1 cleaves gasdermin D (GSDMD), induces pyroptosis and promotes the secretion of interleukin-1β (IL-1β), causing an inflammatory response (17, 18).

In our previous studies, it was often found that some IPEC-J2 cells were swollen, the cell membrane was ruptured, there were holes in the cell membrane, the cytoplasm flowed out, and the cell morphology was highly redolent of pyrolysis. However, whether cell pyroptosis exists in 11S glycinin-induced IPEC-J2 cell injury and the molecular mechanism thereof, has not been reported. Therefore, in this study, we aim to explore the underlying molecular mechanisms of 11S glycinin in inducing IPEC-J2 cells pyroptosis.

MATERIALS AND METHODS

Chemicals and Reagents

11S glycinin was provided by Professor Shuntang Guo of China Agricultural University (patent number 200 410 029 589.4, China). The fetal bovine serum (FBS) was provided by Clark Bioscience (Richmond, VA, USA). The RPMI 1,640 medium was obtained from Thermo Fisher Scientific, Waltham, MA, USA. The cell Counting Kit-8 (CCK-8) was provided by Achieve Perfection Explore Biotechnology (Houston, USA). The LIVE/DEAD Cell Imaging Kit and Terminal Deoxynucleotidyl Transferase-mediated dUTP-biotin Nick end Labeling (TUNEL) Assay Kit were bought from Beyotime Biotechnology (Shanghai, China). 4,6-Benzamidine-2-phenylindole (DAPI) was obtained from Abcam (Cambridge, UK).

Cell Culture

The IPEC-J2 cell lines were purchased from the China Center for Type Culture Collection (Wuhan, China) and cultured with RPMI 1,640 containing 10% FBS, 1% penicillin, and 1% streptomycin at 37 °C with 5% CO_2 in a humidified atmosphere.

Cell Viability Assay

IPEC-J2 cells were seeded into sterile 96-well plates at a density of 5×10^3 cells per well. After a 24 h stabilization period, the cells were treated with different concentrations (0, 1, 5, and 10 mg·ml^{-1}) of 11S glycinin for 24 h. After stimulation, CCK-8 regent was added followed by incubation at 37 °C in a 5% CO_2 humidified atmosphere for 1 h. The absorbance was determined at 450 nm using a Multiskan MS plate reader (Thermo Fisher Scientific, Waltham, MA, USA). The ratio of viability of control cells was taken as 100%.

Visual Fluorescence Effect of Live and Dead Cells

IPEC-J2 cells were seeded into sterile-glass-bottomed dishes at a density of 1.6×10^4 cells/dish and cultured for 24 h. The cells were treated with different concentrations (0, 1, 5, and 10 mg·ml^{-1}) of 11S glycinin. After 24 h stimulation, the cells were stained by the LIVE/DEAD Cell Imaging Kit, as per the manufacturer's instructions. The living and dead cells were observed and photographed using a JEM-1230 transmission electron microscope (JEOL, Akishima, Tokyo, Japan).

Cellular ROS Detection

IPEC-J2 cells were seeded into sterile-6-well-culture plates at a density of 1.2×10^5 cells/hole and cultured for 24 h. The cells were treated with different concentrations (0, 1, 5, and 10 mg·ml^{-1}) of 11S glycinin. After 24 h stimulation, all the cells were treated with 10 μM of DCFH-DA (Elabscience Biotechnology, Wuhan, China) for 30 min, and the cells were observed and photographed using a fluorescent microscope (Olympus, Japan). The signal of cellular ROS was evaluated by flow cytometry (BD Biosciences, Franklin Lakes, NJ, USA), and the data were statistically analyzed by FlowJo software (Ashland, OR, USA).

Flow Cytometric Analysis of JC-1 Staining

IPEC-J2 cells were seeded into sterile-6-well-culture plates at a density of 1.2×10^5 cells/hole and cultured for 24 h. The cells were treated with different concentrations (0, 1, 5, and 10 mg·ml^{-1}) of 11S glycinin. After 24 h stimulation, 500 μL $^{-1}$ × JC-1 staining solution and 500 μL DMEM solution were used to stain the cells for 30 min. The signal of cellular JC-1 was detected by flow cytometry (BD Biosciences, Franklin Lakes, NJ, USA).

Terminal Deoxynucleotidyl Transferase-Mediated DUTP-Biotin Nick End Labeling Assay (TUNEL)

IPEC-J2 cells were seeded into sterile 24-well plates at a density of 8×10^4 cells per hole for 24 h. The cells were incubated in different concentrations (0, 1, 5, and 10 mg·ml^{-1}) of 11S glycinin for 24 h. The mode of cell death was determined according to the instructions of the deoxynucleotide terminal

transferase-mediated nick TUNEL assay kit. The TUNEL-positive cells were marked with red fluorescence, and the nuclei were stained with 4′,6-diamidino-2-phenylindole (DAPI, Abcam, Cambridge, UK). The images were observed and collected under a fluorescence microscope.

Immunofluorescence Assay

The IPEC-J2 cells were seeded at a density of 8×10^4 cells per well into sterile 24-well plates covered with 14 mm cell slides and incubated with 1, 5, and 10 mg·ml^{-1} 11S glycinin for 24 h. The supernatant was discarded and the cells were washed three times in phosphate-buffered saline (PBS, 5 min/time). Polyoxymethylene (4%) was used to fix cells for 30 min and PBS was used to wash cells (3 times, 5 min/time). Triton X-100 (0.5%) was used to permeate the cell membrane for 15 min. The reaction was blocked with BCA (0.5%, 1 h). The IPEC-J2 cells were cultured overnight at 4°C with primary antibodies NLRP-3, after washing three times with PBS for 5 min each time. The FITC-bound secondary antibody (dilution of 1:100, E-AB-1016) was added and the cells were incubated for 1 h, and then washed with PBS (3 times, 5 min/time). After 10 min of nuclei staining with DAPI, cells were washed three times for 5 min each time with PBS. The sections were sealed with anhydrous glycerol and imaged under a confocal microscope (Olympus, Tokyo, Japan).

Western Blotting

IPEC-J2 cells in logarithmic growth phase were seeded in sterile 6-well plates at a density of 1.6×10^5 cells/ml for 24 h, and then treated with 0, 1, 5, and 10 mg·ml^{-1} 11S for 24 h, respectively. Samples were collected and IPEC-J2 cells were lysed with radioimmunoprecipitation assay (RIPA), lysis buffer (Beyotime Biotechnology, Shanghai, China), centrifuged (12,000 × g for 15 min at 4 °C), and the supernatant was collected. The Bicinchoninic acid (BCA) protein assay kit (Beyotime Biotechnology, Shanghai, China) was used to determine the protein concentration. The protein content of samples was adjusted to 40 μg and then diluted with 5 × loading buffer. The protein of samples was separated by 5% stacking gel and 10–15% separating gel and transferred to polyvinylidene fluoride (PVDF) membranes. The membranes were blocked with bovine serum albumin (BSA) for 4 h, washed 4 times with TBST, and then incubated with the indicated primary antibodies overnight at 4 °C. After washing with TBST, they were incubated with goat anti-rabbit immunoglobulin G (IgG) secondary antibody (1:5,000, Zen Bioscience, Chengdu, China) at room temperature for 1 h. After washing with TBST again, the pictures were collected by gel imager. The gray value of protein bands was analyzed using the ImageJ software.

Lentiviral Transfection of IPEC-J2 Cells

Lentivirus (LV) recombinant expression *NLRP-3* and short hairpin RNA (shRNA) were synthesized using the GeneChem (Guangzhou, China). IPEC-J2 cells were transfected with designed sh-NLRP-3 lentivirus to silence *NLRP-3* (multiplicity of infection, MOI = 100). Transfection efficiency was observed using quantitative real-time polymerase chain reaction (qRT-PCR) and the western blot analysis. According to the results of the transfection efficiency, the cells were randomly divided into four groups. Control group (untreated), negative control (NC) group (transfected with empty vector lentivirus), sh-NLRP-3 group (transfected with designed sh-NLRP-3 lentivirus), sh-NLRP-3+10 mg·ml^{-1} 11S group (transfected with designed shNLRP3 lentivirus, then added 10 mg·ml^{-1} 11S glycinin and cultured for 24 h).

TABLE 1 | Primer sequences for qRT-PCR amplification.

Gene	Forward primer (5′ → 3′)	Reverse primer (5′ → 3′)	product (bp)
NLPR3	GACCTCAGCCAAGATGCAAG	TGCCCAGTCCAACATGATCT	163
ASC	ATCGACCTCACTGACAAGCT	TCAGGGGAAGGGCTTTGATT	169
IL-1β	TCTCTCACCCCTTCTCCTCA	CAGACACTGCTGCTTCTTGG	182
Caspase-1	CAGCCCCTCAGACAGTACAA	GCAGATTATGAGGGCAAGGC	173
GSDMD	TTCATGGTTCTGGAGACCCC	TCATGGAAGTAGAAGGGGCC	114
GAPDH	TGACCCCTTCATTGACCTCC	CCATTTGATGTTGGCGGGAT	160

qRT-PCR Assay

The mRNA expressions were detected using the qRT-PCR assay. Briefly, after IPEC-J2 cells were transfected by LV and incubated with 11S, samples were collected. Total RNA of samples were isolated and reverse transcribed into cDNA. The primer sequences used in qRT-PCR were shown in **Table 1**. The qRT-PCR detection method steps were performed as described previously (10).

Transmission Electron Microscopy

After the samples were transfected and treated according to the method in Lentiviral transfection of IPEC-J2 cells, the supernatant was discarded after centrifugation at 1,000 rpm for 5 min. Then, 1 ml of 4% paraformaldehyde was added to each tube and fixed at 4°C for 12 h. The PBS was washed three times (4°C, 5,000 × *g*, 15 min) and then fixed with 2% osmotic acid for 4 h. After rinsing with PBS, gradient dehydration with 30–100% alcohol, osmotic embedding, cutting, and staining of ultra-thin sections were carried out. Photographs were clicked with a transmission electron microscope (JEM-1230, JEOL, Akishima, Tokyo, Japan).

Enzyme-Linked Immunosorbent Assay

IPEC-J2 cells were seeded into sterile 6-well plates at a density of 1.6×10^5 cells per well and transfected and treated according to the method described in Lentiviral transfection of IPEC-J2 cells. Subsequently, 500 μL of 0.1 mol/L Tris-HCl was added to each sample (pH 7.4, Beyotime Biotechnology, Shanghai, China), and the samples were sonicated. The samples were centrifuged for 10–15 min (1,000 rpm, 4°C) and the supernatant was collected. The cell lysates were collected, centrifuged at 1,000 rpm for 10 min,

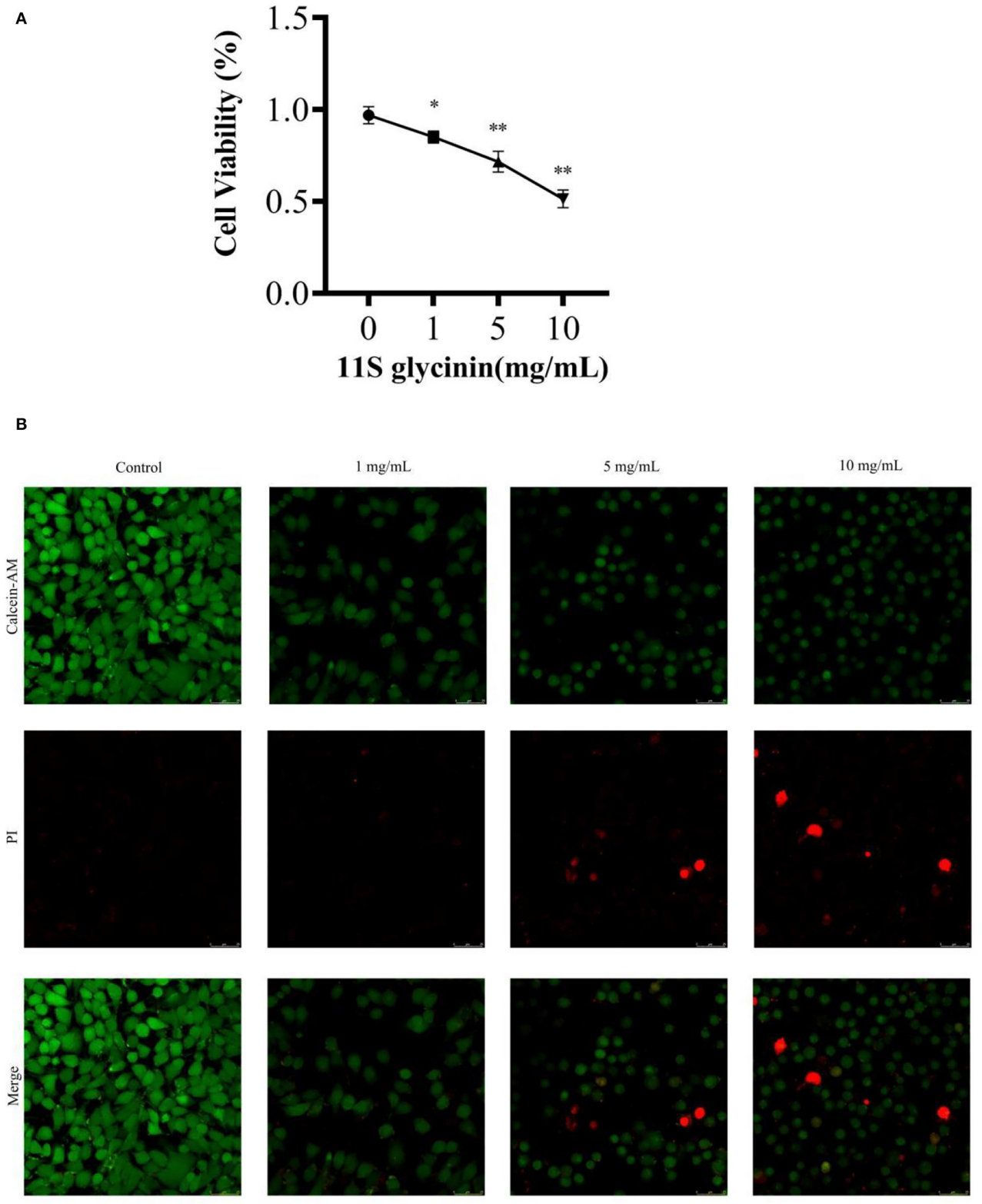

FIGURE 1 | 11S glycinin suppressed IPEC-J2 cells. **(A)** IPEC-J2 cells were stimulated with different concentrations (0, 1, 5, and 10 mg·ml^{-1}) of 11S glycinin for 24 h, and cell viability was determined using the CCK-8 assay, $n = 4$. **(B)** Fluorescence photographs of IPEC-J2 cells stained by using the LIVE/DEAD^{TM} kit. Data are shown as mean ± SD.*$P < 0.05$, ** $P < 0.01$, compared with the control.

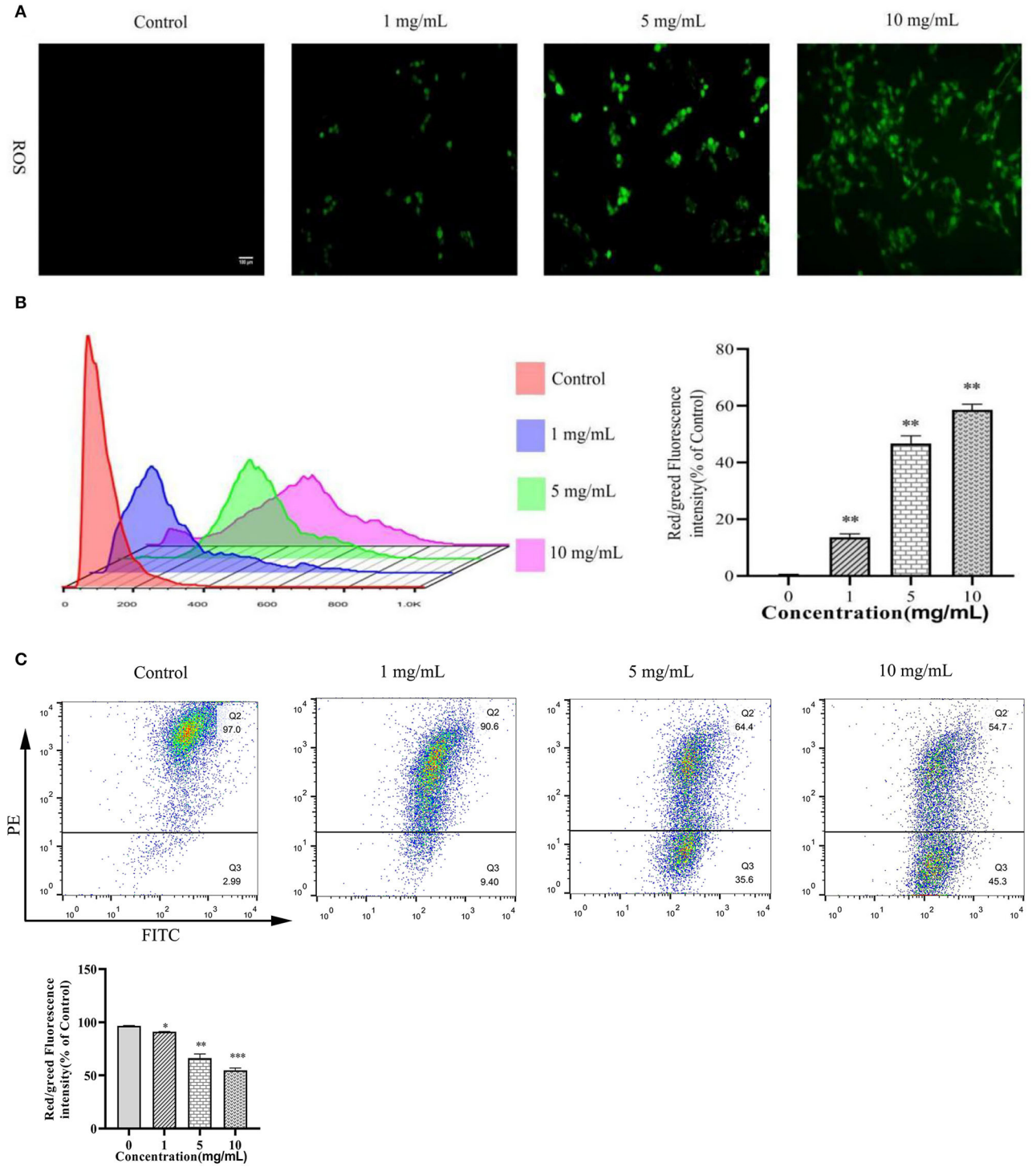

FIGURE 2 | 11S glycinin induced ROS generation and reduced MMP in IPEC-J2 cells. **(A)** IPEC-J2 cells were stimulated with 0, 1, 5, and 10 mg·ml^{-1} 11S glycinin for 24 h, and ROS were detected using DCFH–DA staining. **(B)** The red/green fluorescence intensity was measured using flow cytometry. **(C)** The mitochondrial membrane potential in IPEC-J2 cells were measured using the flow cytometry. Data are shown as mean ± SD. *$P < 0.05$, **$P < 0.01$, ***$P < 0.001$, compared with the control.

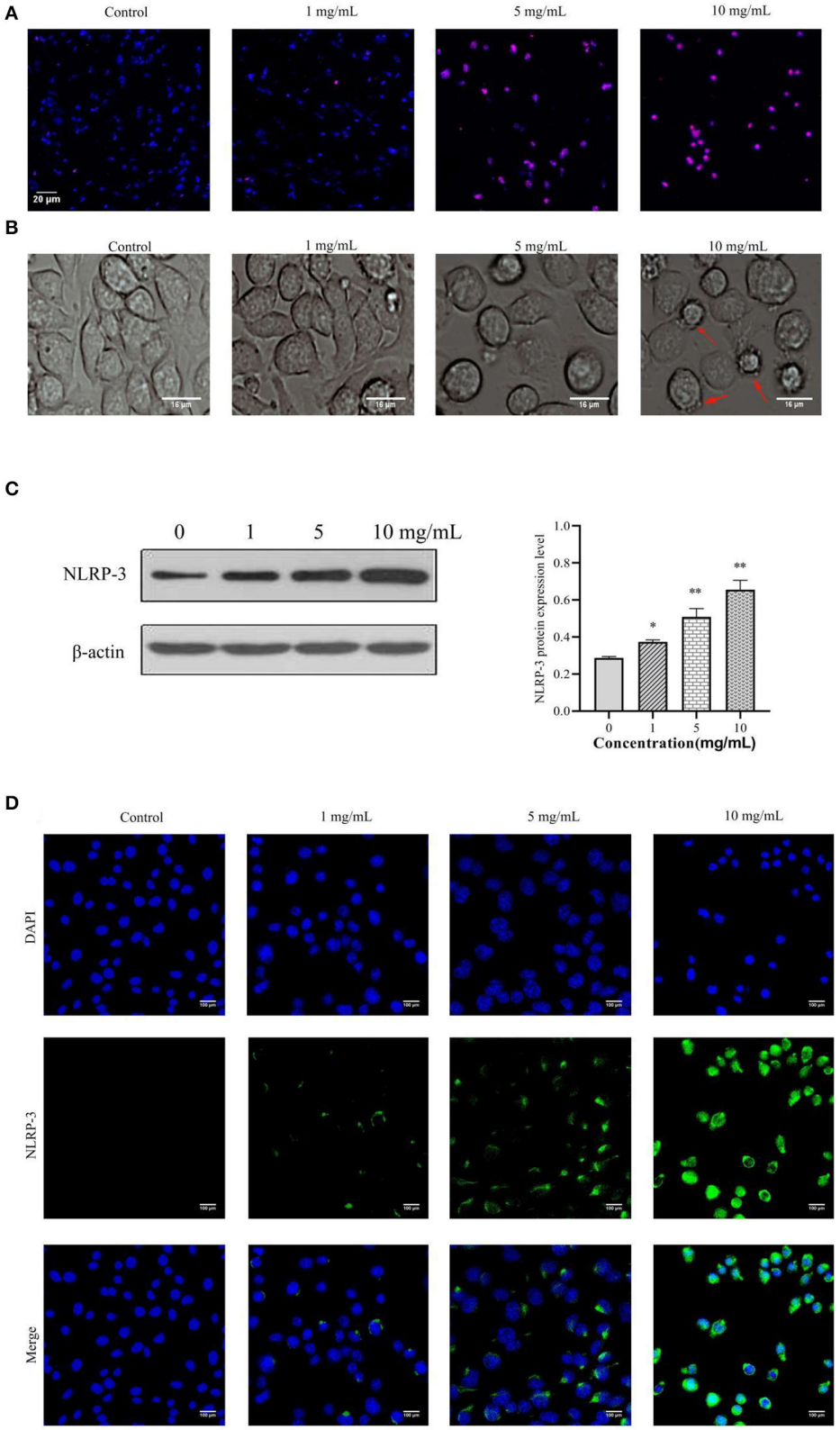

FIGURE 3 | 11S glycinin induced DNA damage and increased the NLRP-3 expression in IPEC-J2 cells. IPEC-J2 cells were treated with different concentration of 11S glycinin (0, 1, 5, or 10 mg·ml^{-1}) for 24 h, respectively. **(A)** TUNEL shown the DNA damage of IPEC-J2 cells. **(B)** The morphology of IPEC-J2 cells after 11S glycinin treatment. **(C)** Western blotting presented the protein expression level of NLRP-3 in IPEC-J2 cells. **(D)** Immunofluorescence imaging of the NLRP-3 antibody in IPEC-J2 cells. Data are shown as mean ± SD. *$P < 0.05$, **$P < 0.01$, compared with the control group.

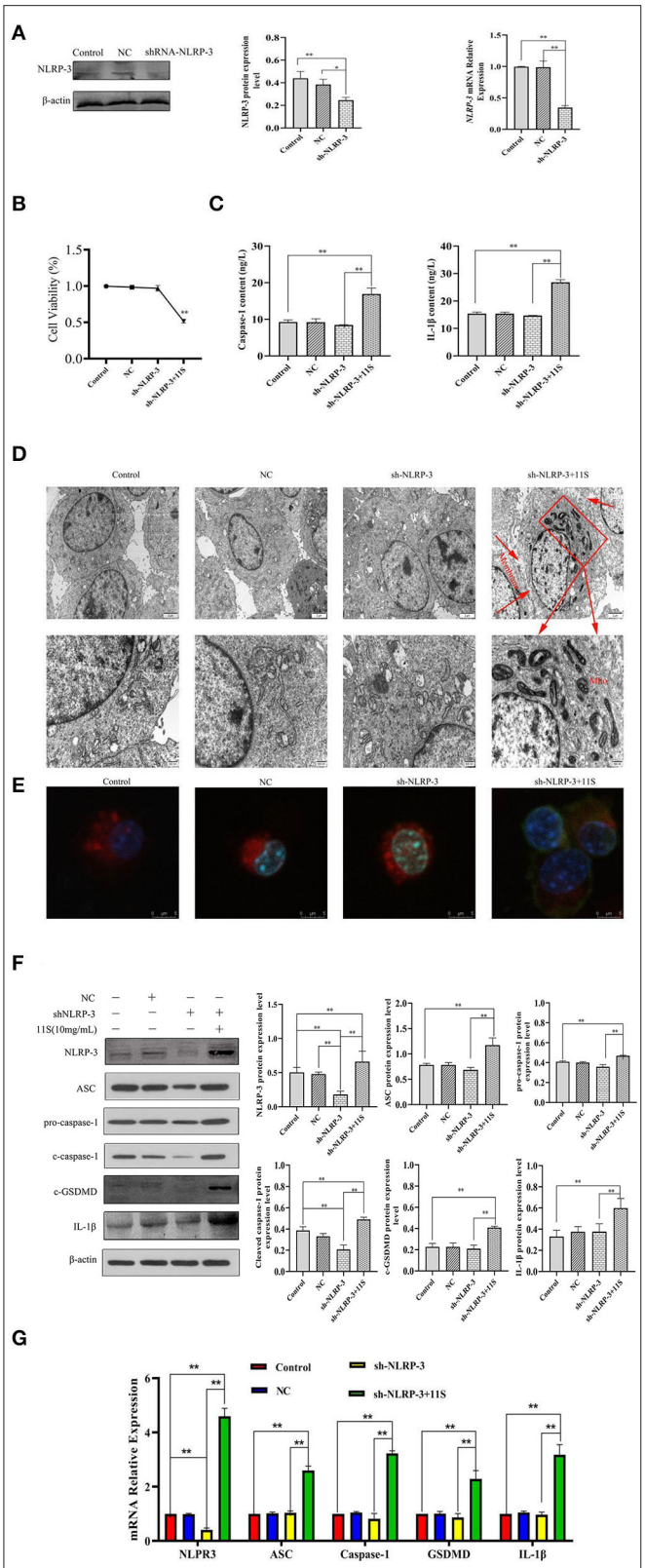

FIGURE 4 | 11S glycinin induced pyroptosis by up-regulating the silenced *NLRP-3* gene in IPEC-J2 cells. IPEC-J2 cells were transfected with designed *(Continued)*

FIGURE 4 | sh-NLRP-3 lentivirus, then treated with 11S glycinin (10 mg·ml^{-1}) for 24 h. **(A)** Western blotting and qRT-PCR verified the silencing effect of the target gene, *NLRP-3*. **(B)** The cell viability of IPEC-J2 cells was assessed using the CCK-8 assay, $n = 4$. **(C)** The content of caspase-1 and IL-1β determined using ELISA. **(D)** The ultrastructure of IPEC-J2 cells was observed *via* transmission of electron microscopy. **(E)** The fluorescent photographs of MMP in IPEC-J2 cells. **(F)** Western blotting indicated the expression level of NLRP-3, ASC, pro-caspase-1, cleave-caspase-1, c-GSDMD, and IL-1β in IPEC-J2 cells. **(G)** qRT–PCR results showed the mRNA expression of *NLRP-3*, *ASC*, *caspase-1*, *GSDMD*, and *IL-1β* in IPEC-J2 cells. Data are shown as mean ± SD. $^{*}P < 0.05$, $^{**}P < 0.01$, compared with the control group. Control (untreated); NC (negative control, transfected IPEC-J2 cells with empty vector lentivirus); sh-NLRP-3 (transfected IPEC-J2 cells with designed sh-NLRP-3 lentivirus); sh-NLRP-3+11S (transfected IPEC-J2 cells with designed sh-NLRP-3 lentivirus, then added 10 mg·ml^{-1} 11S glycinin and cultured for 24 h).

and the supernatant was aspirated. Caspase-1 and IL-1β content was assayed according to the ELISA kit instructions.

Fluorescence Detection of Mitochondrial Membrane Potential

Mitochondrial membrane potential (MMP) was assayed using the Mitochondrial Membrane Potential and Apoptosis Detection Kit with MitoTracker Red CMXRos and Annexin V-FITC (Beyotime Biotechnology, Shanghai, China). IPEC-J2 cells were seeded into sterile 6-well plates at a density of 1.6×10^5 cells per well and transfected and treated according to the method discussed in Lentiviral transfection of IPEC-J2 cells, following the instructions of the kit and observing under a fluorescence microscope (Olympus, Tokyo, Japan).

Data Analysis and Processing

The experimental data are expressed as mean ± SD. ANOVA of SPSS 17.0 software was used for variance analysis, and the LSD method was used for significant comparison, with $P < 0.05$ indicating significant difference and $P < 0.01$ indicating extremely significant difference. Graph Pad Prism 7.0 software was used to draw the histogram.

RESULTS

11S Glycinin Suppressed IPEC-J2 Cells

We evaluated the effect of 11S glycinin on the viability of IPEC-J2 cells using the CCK8 assay. 11S glycinin exhibited a strong inhibitory effect on the proliferation of IPEC-J2 cells in a dose-dependent manner ($P < 0.05$ or $P < 0.01$, **Figure 1A**). To further detect the inhibition of 11S glycinin on the proliferation of IPEC-J2 cells, LIVE/DEAD™ staining was used. The quantity of dead cells increased with the raise of 11S glycine concentration, which was consistent with the results of CCK8 analysis (**Figure 1B**). All of the aforementioned results demonstrated that 11S glycine could suppress IPEC-J2 cells.

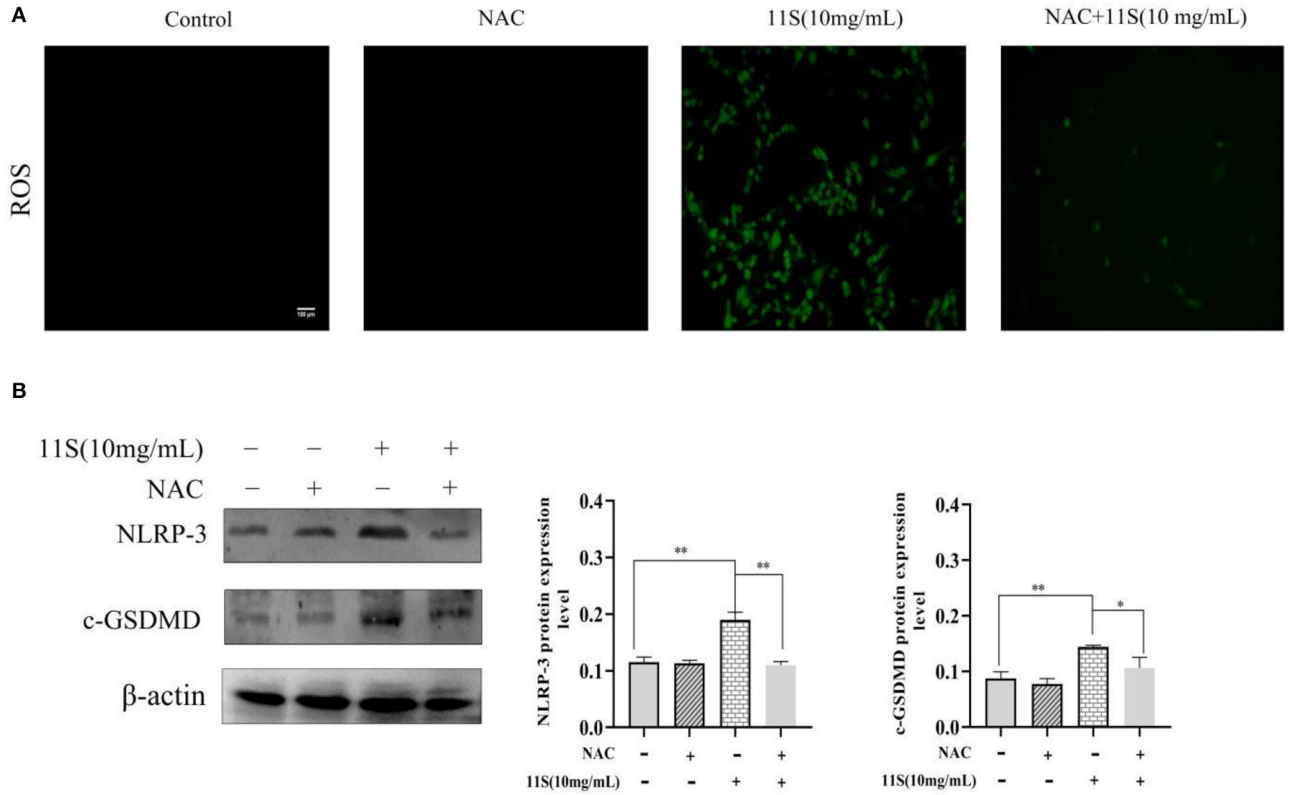

FIGURE 5 | 11S glycinin up-regulates NLRP-3-induced pyroptosis by triggering ROS in IPEC-J2 cells. **(A)** IPEC-J2 cells were treated with or without NAC (6 mM) for 1 h before a 24 h treatment of 11S glycinin (10 mg·ml^{-1}). **(A)** ROS were detected using DCFH–DA staining. **(B)** Western blotting indicates the protein expression of NLRP-3 and c-GSDMD in IPEC-J2 cells. Data are shown as mean ± SD. *$P < 0.05$, **$P < 0.01$, compared with the control group.

11S Glycinin Induced ROS Generation and Decreased MMP in IPEC-J2 Cells

As shown in **Figures 2A,B**, ROS generation was significantly increased after 11S glycinin treatment ($P < 0.01$). As shown in **Figure 2C**, the mitochondrial membrane potential of IPEC-J2 cells which was treated with 11S glycinin was significantly reduced, compared with the control group ($P < 0.05$, $P < 0.01$ or $P < 0.001$).

11S Glycinin Induced DNA Damage and Increased the NLRP-3 Expression in IPEC-J2 Cells

We evaluated whether 11S glycinin induced DNA damage in IPEC-J2 cells by TUNEL staining. As presented in **Figure 3A**, after treating the cells with 11S glycinin, the immunofluorescence intensity significantly increased, indicating that the number of positive cells increased significantly. According to the principle of TUNEL assay, the increase of positive cells evidenced that their DNA was fragmented. As revealed in **Figure 3B**, the morphology of IPEC-J2 cells in the low concentration (1 mg·ml^{-1}) group was slightly damaged. In the middle concentration (5 mg·ml^{-1}) group, the morphology of IPEC-J2 cells had reduced. While in the high concentration (10 mg·ml^{-1}) group, we observed significant morphological changes, including cell swelling and the generation of large bubbles, which was highly redolent of pyrolysis. The NLRP-3 protein was assessed by the western blotting and immunofluorescence. As shown in **Figures 3C,D**, after 11S glycinin stimulation, the NLRP-3 protein expression ($P < 0.05$ or $P < 0.01$) and immunofluorescence signal were increased significantly.

11S Glycinin Induced Pyroptosis by Up-Regulating NLRP-3 in IPEC-J2 Cells

We transfected IPEC-J2 cells with the designed sh-NLRP-3 lentivirus and successfully silenced the *NLRP-3* (**Figures 4A,B**). As **Figure 4C** shows, transfection of the designed sh-NLRP-3 lentivirus did not affect the cell activity of IPEC-J2,but the cell activity of IPEC-J2 transfected with the designed sh-NLRP-3 lentivirus decreased significantly after stimulation with 10 mg·ml^{-1} 11S glycinin ($P<0.01$). As **Figure 4D** shows, we observed the typical pyroptosis morphology in sh-NLRP-3+11S group, including cell membrane rupture, cell swelling, and mitochondrial degeneration. The green fluorescent significant enhancement in sh-NLRP-3+11S group cells suggests that mitochondrial membrane potential was decreased (**Figure 4E**). As shown in **Figures 4C,G**, the cells of sh-NLRP-3+11S group showed a significant increase in protein level and mRNA expression of NLRP-3, apoptosis-related spot-like protein (ASC), cysteine-containing aspartate-specific

proteases-1 (caspase-1), c-GSDMD, and IL-1β ($P < 0.05$ or $P < 0.01$). The contents of proinflammatory factor caspase-1 and IL-1β were assessed by ELISA. As shown in **Figure 4F**, the contents of caspase-1 and IL-1β in sh-NLRP-3+11S group were significantly increased than control group and NC group ($P < 0.01$).

11S Glycinin Up-Regulated NLRP-3 by Triggering ROS in IPEC-J2 Cells

As shown in **Figure 5A**, the ROS immunofluorescence signal of IPEC-J2 cells in 11S glycinin treatment group was significantly enhanced. **Figure 5B** showed a significant increase in the protein expression of NLRP-3 and GSDMD after incubation with 10 $mg{\cdot}ml^{-1}$ 11S glycinin at 24 h ($P < 0.01$). Treatment with the inhibitor (NAC) significantly weakened the ROS immunofluorescence signal, inhibited the up-regulated expression of NLRP-3 and GSDMD ($P < 0.05$ or $P < 0.01$).

DISCUSSION

Previous studies demonstrated that soybean antigen protein allergic can induce IPEC-J2 cell apoptosis (11), and can lead to inflammatory injury of the piglet small intestine (12). However, in the pathogenesis of acute and chronic enteritis, cell death has many forms, including apoptosis, cell scorching, iron death, necrosis, and autophagy. Although a recent study reported that common allergens can cause pyroptosis and lead to allergic diseases (19), the role of pyroptosis in allergy with 11S glycinin remains to be understood. Pyroptosis was a kind of death that was characterized by cell membrane rupture, which shares certain features with apoptosis, such as a decrease in mitochondrial membrane potential and DNA fragmentation (20). Our results demonstrated that 11S glycinin induced mitochondrial membrane potential decrease. We also demonstrated that 11S glycinin induced DNA damage in IPEC-J2 cells using the TUNEL assay; this contributes to pyrolysis. With the increase in the concentration of 11S glycinin, we observed distinct changes in morphology, including cellular swelling and the production of bubbles on IPEC-J2 cell membrane, which resemble the pyroptosis induced by the gasdermin D (GSDMD) (17, 21).

Recently, it has been shown that *NLRP-3* was an inflammatory compound widely existing in epithelial cells and played an important role in the occurrence and development of allergic diseases (22). We found that the expressions of *NLRP-3*, caspase-1, and IL-1β were significantly elevated in IPEC-J2 cells with increasing concentrations of 11S glycinin. The accumulation of NLRP3 inflammasome is considered to be an important activator of pyroptosis. Mature NLRP3 induces adapter ASC polymerization and ASC spot assembly (23, 24). ASC spots recruit and activate caspase-1, which then triggers the cleavage of GSDMD family proteins and promotes the release of interleukin-1β (IL-1β), as well as pyroptosis (25, 26). Therefore, we speculated that 11S glycinin may induce pyroptosis of IPEC-J2 cells by activating *NLRP-3*.

Few studies have shown the role of pyroptosis in 11S glycinin allergy. In order to fully prove our conjecture, we used the designed sh-NLRP-3 lentivirus to transfect IPEC-J2 cells and successfully silenced the target gene, *NLRP-3*. The *NLRP-3* gene silenced IPEC-J2 cells that were incubated with 11S glycinin for 24 h. Our results demonstrated that 11S glycinin significantly up-regulated mRNA and protein levels in IPEC-J2 cells of the NLRP-3 and other signaling molecules downstream, such as ASC, caspase-1, and IL-1β. More importantly, the mRNA of GSDMD and the protein levels of c-GSDMD were significantly increased as well. The secretion of IL-1β increased, which is common in pyroptosis. A recent study showed that GSDMD was an executor of pyroptosis and was required for the secretion of IL-1β (27). Furthermore, 11S could reduce the mitochondrial membrane potential in IPEC-J2 cells when the *NLPR-3* gene was silenced. Under the transmission electron microscope, the IPEC-J2 mitochondria were degenerated, the mitochondrial cristae disappeared, and the cell membrane was damaged, which were the main morphological features of pyroptosis. Our results suggested that 11S glycinin up-regulated *NLRP-3* expression, activated caspase-1, cleaved GSDMD, induced pyroptosis, and released inflammatory factors, which may be responsible for amplifying the inflammatory response. These results have not been reported earlier.

It is widely accepted that inflammation and oxidative stress usually occur simultaneously. ROS is an important cellular signal product responsible for oxidative stress (28), and is related to intestinal tissue injury and intestinal cell death (29, 30). ROS could promote the cleavage of GSDMD by activating NLRP-3, thereby inducing inflammatory processes (31). In this study, we verified that ROS production increased in a dose-dependent manner after 11S soybean globulin treated IPEC-J2 cells. The addition of NAC, a specific inhibitor of ROS, significantly weakened the fluorescence expression of ROS. More importantly, we also found that NAC significantly reduced the expression of NLRP-3 and c-GSDMD. Therefore, we believed that 11S glycinin induced IPEC-J2 cell pyroptosis, which was related to ROS and NLRP-3 in IPEC-J2 cells.

CONCLUSION

In conclusion, our results demonstrated that 11S glycinin induced cell membrane rupture, DNA damage, mitochondrial membrane potential decrease, and ROS generation in IPEC-J2 cells. Furthermore, 11S glycinin up-regulated the expression of NLRP-3, activated caspase-1, cleaved GSDMD, and promoted the secretion of inflammatory cytokine IL-1β. Reducing ROS production could inhibit the expression of NLRP-3 and cleaved GSDMD. Taken together, our findings demonstrated that 11S glycinin up-regulated NLRP-3-mediated pyroptosis by triggering ROS in IPEC-J2 cells. This study provided new ideas for the prevention and treatment of the allergic diseases, which was induced by 11S glycinin. Allergic reaction in the organism is a very complex process involving multiple molecular pathways. However, our results were based on *in vitro* experiments, only revealing one of the possible mechanisms. Therefore, in the

subsequent studies, weaned piglets will be used to construct animal models, and many prospective clinical trials will be conducted to reveal the mechanism of soybean antigenic protein-induced allergy.

DATA AVAILABILITY STATEMENT

The original contributions presented in the study are included in the article/supplementary material, further inquiries can be directed to the corresponding author.

AUTHOR CONTRIBUTIONS

JW and CP conceived and designed this experiment. JW coordinated financial and technical support. LW and ZS performed experiments and wrote the manuscript. WX and HD collect the experimental samples. JW, YL, SF, XW, and CZ reviewed the manuscript. All authors read and approved the final manuscript.

FUNDING

This research was supported by the National Natural Science Foundation of China (No. 31972750).

ACKNOWLEDGMENTS

We gratefully acknowledge the professors of the College of Animal Science and Technology of Anhui Agricultural University.

REFERENCES

1. Friedman M, Brandon DL. Nutritional and health benefits of soy proteins. *J Agric Food Chem.* (2001) 49:1069–86. doi: 10.1021/jf0009246
2. Green B, Cummings K, Rittenour W, Hettick J, Bledsoe T, Blachere F, et al. Occupational sensitization to soy allergens in workers at a processing facility. *Clin Exp Allergy NLM.* (2011) 41:1022–30. doi: 10.1111/j.1365-2222.2011.03756.x
3. Gagnon C, Poysa V, Cober ER, Gleddie S. Soybean allergens affecting North American patients identified by 2D gels and mass spectrometry. *Food Anal Methods.* (2010) 3:363–74. doi: 10.1007/s12161-009-9090-3
4. Murakami H, Ogawa T, Takafuta A, Yano E, Zaima N, Moriyama T. Identification of the 7S and 11S globulins as percutaneously sensitizing soybean allergens as demonstrated through epidermal application of crude soybean extract. *Biosci Biotechnol Biochem.* (2018) 82:1408–16. doi: 10.1080/09168451.2018.1460573
5. Zheng S, Qin G, Chen J, Zhang F. Acidic polypeptides A 1a, A 3, and A 4 of Gly m 6 (glycinin) are allergenic for piglets. *Vet Immunol Immunopathol.* (2018) 202:147–52. doi: 10.1016/j.vetimm.2018.06.003
6. Taliercio E, Kim SW. Epitopes from two soybean glycinin subunits are antigenic in pigs. *J Sci Food Agric.* (2013) 93:2927–32. doi: 10.1002/jsfa.6113
7. Sun H, Liu X, Wang Y, Liu J, Feng J. Soybean glycinin- and β-conglycinin-induced intestinal immune responses in a murine model of allergy. *Food Agr Immunol.* (2013) 24:357–69. doi: 10.1080/09540105.2012.704507
8. Qiao S, Li D, Jiang J, Zhou H, Thacker PA. Effects of moist extruded full-fat soybeans on gut morphology and mucosal cell turnover time of weanling pigs. *Asian Austral J Anim.* (2003) 16:1. doi: 10.5713/ajas.2003.63
9. Zhao Y, Qin G, Sun Z, Zhang B, Wang T. Effects of glycinin and β-conglycinin on enterocyte apoptosis, proliferation and migration of piglets. *Food Agr Immunol.* (2010) 21:209–18. doi: 10.1080/09540101003596644
10. Peng C, Sun Z, Wang L, Shu Y, Wu J. Soybean antigen protein induces caspase-3/mitochondrion-regulated apoptosis in IPEC-J2 cells. *Food Agr Immunol.* (2020) 31:100–19. doi: 10.1080/09540105.2019.1702926
11. Peng C, Ding X, Zhu L, He M, Shu Y, Zhang Y. β-conglycinin-induced intestinal porcine epithelial cell damage via the nuclear factor κB/mitogen-activated protein kinase signaling pathway. *J Agric Food Chem.* (2019) 67:9009–21. doi: 10.1021/acs.jafc.9b02784
12. Peng C, Cao C, He M, Shu Y, Tang X, Wang Y. Soybean glycinin and β-conglycinin-induced intestinal damage in piglets via the p38/JNK/NF-κB signaling pathway. *J Agric Food Chem.* (2018) 66:9534–41. doi: 10.1021/acs.jafc.8b03641
13. Yu X, Wang M, Zhao H, Cao Z. Targeting a novel hsa_circ_0000520/miR-556-5p/NLRP3 pathway-mediated cell pyroptosis and inflammation attenuates ovalbumin (OVA)-induced allergic rhinitis (AR) in mice models. *Inflamm Res.* (2021) 70:9809. doi: 10.1007/s00011-021-01472-z
14. Zasłona Z, Flis E, Wilk M, Carroll G, O'Neill L. Caspase-11 promotes allergic airway inflammation. *Nat Commun.* (2020) 11:1. doi: 10.1038/s41467-020-14945-2
15. Cookson BT, Brennan MA. Pro-inflammatory programmed cell death. *Trends Microbiol.* (2001) 9:113–4. doi: 10.1016/S0966-842X(00)01936-3
16. Man S, Karki R, Kanneganti TD. Molecular mechanisms and functions of pyroptosis, inflammatory caspases and inflammasomes in infectious diseases. *Immunol Rev.* (2017) 277:61–75. doi: 10.1111/imr.12534
17. Shi J, Zhao Y, Wang K, Shi X, Wang Y, Huang H, et al. Cleavage of GSDMD by inflammatory caspases determines pyroptotic cell death. *Nature.* (2015) 526:660–5. doi: 10.1038/nature15514
18. Yang R, Yu H, Chen J, Zhu J, Zhang Q. Limonin attenuates LPS-induced hepatotoxicity by inhibiting pyroptosis via NLRP3/gasdermin D signaling pathway. *J Agric Food Chem.* (2021) 69:982–91. doi: 10.1021/acs.jafc.0c06775
19. Tsai Y, Chiang K, Hung J, Chang W, Lin H, Shieh JM. Der f1 induces pyroptosis in human bronchial epithelia via the NLRP3 inflammasome. *Int J Mol Med.* (2017) 41:757–64. doi: 10.3892/ijmm.2017.3310
20. Lammert CR, Frost EL, Bellinger CE, Bolte AC, Lukens JR. AIM2 inflammasome surveillance of DNA damage shapes neurodevelopment. *Nature.* 580:647–52. doi: 10.1038/s41586-020-2174-3
21. Xiao J, Wang C, Yao J, Alippe Y, Xu C, Kress D. Gasdermin D mediates the pathogenesis of neonatal-onset multisystem inflammatory disease in mice. *PLoS Biol.* (2018) 16:e3000047. doi: 10.1371/journal.pbio.3000047
22. Allen IC, Jania CM, Wilson JE, Tekeppe EM, Hua X, Brickey WJ. Analysis of NLRP3 in the development of allergic airway disease in mice. *J Immunol.* (2012) 188:2884–93. doi: 10.4049/jimmunol.1102488
23. Jin C, Flavell RA. Molecular mechanism of NLRP3 inflammasome activation. *J Clin Immunol.* (2010) 30:628–31. doi: 10.1007/s10875-010-9440-3
24. Schroder K, Tschopp J. The inflammasomes. *Cell.* (2010) 140:821–32. doi: 10.1016/j.cell.2010.01.040
25. Bergsbaken T, Fink S, Cookson BT. Pyroptosis: host cell death and inflammation. *Nat Rev Microbiol.* (2009) 7:99–109. doi: 10.1038/nrmicro2070
26. Keller M, Rüegg A, Werner S, Beer HD Active caspase-1 is a regulator of unconventional protein secretion. *Cell.* (2008) 132:818–31. doi: 10.1016/j.cell.2007.12.040
27. He W, Wan H, Hu L, Chen P, Wang X, Huang Z. Gasdermin D is an executor of pyroptosis and required for interleukin-1β secretion. *Cell Res.* (2015) 25:1285–98. doi: 10.1038/cr.2015.139
28. Yang S, Han Y, He J, Yang M, Zhang W, Zhan M. Mitochondria targeted peptide SS-31 prevent on cisplatin-induced acute kidney injury via regulating mitochondrial ROS-NLRP3 pathway. *Biomed Pharmacother.* (2020) 130:110521. doi: 10.1016/j.biopha.2020.110521
29. Abbasi-Oshaghi E, Mirzaei F, Pourjafar M. NLRP3 inflammasome, oxidative stress, and apoptosis induced in the intestine and liver of rats treated with

titanium dioxide nanoparticles: *in vivo* and *in vitro* study. *Int J Nanomedicine*. (2019) 14:1919–36. doi: 10.2147/IJN.S192382
30. Li L, Tan H, Zou Z, Gong J, Zhou J, Peng N. North American hyperthermia group preventing necroptosis by scavenging ROS production alleviates heat stress-induced intestinal injury. *Int J Hyperthermia.* (2020) 37:517–30. doi: 10.1080/02656736.2020.1763483
31. Zhang R, Chen J, Mao L, Guo Y, Hao Y, Deng Y. Nobiletin triggers reactive oxygen species-mediated pyroptosis through regulating autophagy in ovarian cancer cells. *J Agric Food Chem.* (2020) 68:1326–36. doi: 10.1021/acs.jafc.9b07908

Conflict of Interest: The authors declare that the research was conducted in the absence of any commercial or financial relationships that could be construed as a potential conflict of interest.

Publisher's Note: All claims expressed in this article are solely those of the authors and do not necessarily represent those of their affiliated organizations, or those of the publisher, the editors and the reviewers. Any product that may be evaluated in this article, or claim that may be made by its manufacturer, is not guaranteed or endorsed by the publisher.

frontiers | Frontiers in Veterinary Science

ORIGINAL RESEARCH
published: 29 June 2022
doi: 10.3389/fvets.2022.922817

The Response of Ruminal Microbiota and Metabolites to Different Dietary Protein Levels in Tibetan Sheep on the Qinghai-Tibetan Plateau

Xungang Wang[1], *Tianwei Xu*[1], *Xiaoling Zhang*[1,2], *Na Zhao*[1], *Linyong Hu*[1], *Hongjin Liu*[1], *Qian Zhang*[1,2], *Yuanyue Geng*[1,2], *Shengping Kang*[3] *and Shixiao Xu*[1]*

[1] *Northwest Institute of Plateau Biology, Chinese Academy of Sciences, Xining, China,* [2] *University of Chinese Academy of Sciences, Beijing, China,* [3] *State Key Laboratory of Plateau Ecology and Agriculture, Qinghai University, Xining, China*

OPEN ACCESS

Edited by:
Rita Payan Carreira, University of Evora, Portugal

Reviewed by:
Manuela Oliveira, Universidade de Lisboa, Portugal
Neeta Agarwal, Indian Veterinary Research Institute (IVRI), India

***Correspondence:**
Shixiao Xu
sxxu@nwipb.cas.cn

Specialty section:
This article was submitted to Animal Nutrition and Metabolism, a section of the journal Frontiers in Veterinary Science

Received: *18 April 2022*
Accepted: *31 May 2022*
Published: *29 June 2022*

Citation:
Wang X, Xu T, Zhang X, Zhao N, Hu L, Liu H, Zhang Q, Geng Y, Kang S and Xu S (2022) The Response of Ruminal Microbiota and Metabolites to Different Dietary Protein Levels in Tibetan Sheep on the Qinghai-Tibetan Plateau. Front. Vet. Sci. 9:922817. doi: 10.3389/fvets.2022.922817

Ruminal microbiota and metabolites play crucial roles in animal health and productivity. Exploring the dynamic changes and interactions between microbial community composition and metabolites is important for understanding ruminal nutrition and metabolism. Tibetan sheep (*Ovis aries*) are an important livestock resource on the Qinghai-Tibetan Plateau (QTP), and the effects of various dietary protein levels on ruminal microbiota and metabolites are still unknown. The aim of this study was to investigate the response of ruminal microbiota and metabolites to different levels of dietary protein in Tibetan sheep. Three diets with different protein levels (low protein 10.1%, medium protein 12.1%, and high protein 14.1%) were fed to Tibetan sheep. 16S rRNA gene sequencing and gas chromatography coupled with time-of-flight mass spectrometry (GC-TOF-MS) were used to study the profile changes in each group of ruminal microbes and metabolites, as well as the potential interaction between them. The rumen microbiota in all groups was dominated by the phyla Bacteroidetes and Firmicutes regardless of the dietary protein level. At the genus level, *Prevotella_1*, *Rikenellaceae_RC9_gut_group* and *Prevotellaceae_UCG-001* were dominant. Under the same forage-to-concentrate ratio condition, the difference in the dietary protein levels had no significant impact on the bacterial alpha diversity index and relative abundance of the major phyla and genera in Tibetan sheep. Rumen metabolomics analysis revealed that dietary protein levels altered the concentrations of ruminal amino acids, carbohydrates and organic acids, and significantly affected tryptophan metabolism ($p < 0.05$). Correlation analysis of the microbiota and metabolites revealed positive and negative regulatory mechanisms. Overall, this study provides detailed information on rumen microorganisms and ruminal metabolites under different levels of dietary protein, which could be helpful in subsequent research for regulating animal nutrition and metabolism through nutritional interventions.

Keywords: Tibetan sheep, rumen, microbiota, metabolomics, dietary protein

INTRODUCTION

Tibetan sheep are the most economically important domestic animals on the Qinghai-Tibetan Plateau (QTP), providing native Tibetan herders with meat, wool and milk (1). On the QTP, Tibetan sheep adapt well to plateau environments and poor feeding conditions, and they mainly search for forage in the alpine meadow (2, 3). Nonetheless, the QTP environment is extremely harsh, with heavy snowfalls during the long cool-season from November to May, with average temperatures ranging from −5 to −15°C. Climate conditions and fluctuations directly affect forage yield and quality (particularly crude protein content), and herbage biomass and nutritional status are insufficient to meet the daily nutritional requirements of grazing animals (4–6). A previous study showed that Tibetan sheep suffered serious live-weight loss (−20.54%) under traditional pastoral herding, resulting in severe economic loss during the cold season (7). In addition to growth performance and economic benefits, cold season grazing also reduces growth hormone levels and damages the immune defense system of Tibetan sheep (8). Therefore, scientific management and rearing are particularly important in Tibetan sheep production.

The rumen is the primary organ system for nutrient digestion and absorption in ruminants, and it contains abundant microbiota and metabolites. Rumen microorganisms play an important role in the fermentation of plant fibers and polysaccharides (9, 10). Previous studies have shown that rumen microbial community structure and function are influenced by different factors, such as host breed, sex, diet and external environment (11–13). As one of the most important factors, dietary nutrition can change the relative abundance of dominant bacterial groups (e.g., Bacteroidetes, Firmicutes, Proteobacteria) and metabolic functions (e.g., carbohydrate, amino acid, and energy metabolism) (14–16). Metabolomics is a newly emerging field, following the application of genomics and transcriptomics based on detection techniques and includes nuclear magnetic resonance (NMR), gas chromatography-mass spectrometry (GC-MS), and liquid chromatography-mass spectrometry (LC-MS) (17). Metabolite profiles include a huge array of organic endogenous metabolites that play a vital role in nutrient regulation in animals. Previous studies have reported that ruminal lipids, amino acids and carbohydrates change significantly by changing the dietary forage-to-concentrate ratio (18, 19).

Dietary protein level is considered an essential factor that affects the growth, development and health conditions of animals (20, 21). Proteins fed to ruminants are degraded by microbes into peptide-bound amino acids and free amino acids for microbial protein synthesis (22). However, the effect of dietary protein levels on the ruminal microbiota and metabolites of Tibetan sheep and the interaction between ruminal microbiota and metabolites remain unclear. Recent rapid developments and applications in multi-omics technology have been devoted to gaining a better understanding of the ruminal ecosystem, especially the relationships among the microbiota, metabolites and host (23, 24).

In the current study, we hypothesize that dietary protein levels would influence rumen microorganisms and ruminal metabolites in Tibetan sheep. 16S rRNA sequencing and GC-TOF-MS were used to determine the effects of three different dietary protein levels on the profiles of the ruminal microbiota and metabolites in Tibetan sheep. Furthermore, the potential relationships between the ruminal microbiota and metabolites were explored.

MATERIALS AND METHODS

Ethics Statement

The animal experiments in this study were approved by the Experimental Animal Use Ethics Committee of the Northwest Institute of Plateau Biology, Chinese Academy of Sciences (Approval No. NWIPB20160302).

Experimental Design and Sample Collection

A detailed description of the experimental design has been previously provided (25). The experiment was conducted at the Haibei Demonstration Zone of Plateau Modern Ecological Husbandry Science and Technology in Qinghai Province (China) (36°55′N, 100°57′E, altitude at 3,100 m). A total of eighteen 1-yr-old healthy castrated Tibetan sheep with similar initial body weight (BW: 31.71 ± 0.72 kg) were randomly assigned to three different dietary treatment groups, with each group containing 6 sheep. All those sheep were bred in the same demonstration zone and under the same feeding management practices before the experiment. The protein levels of the three different diets were low protein 10.1% (LP), medium protein 12.1% (MP) and high protein 14.1% (HP). Diets were designed according to the National Research Council guidelines (26) (**Table 1**). The sheep were fed with the mixed diet twice daily at 08:00 and 17:00. The experiment was lasted 105 days after 15 days of adaptation to the experimental diets and all sheep were provided with water ad libitum. At the end of the experiment, rumen fluid samples were collected before the morning feeding using an oral stomach tube and placed in frozen tubes to avoid contamination. The samples were immediately frozen in liquid nitrogen, and stored at −80°C for microbiome and metabolome analysis.

Microbiome Composition Analysis

Total genomic DNA was extracted from the rumen fluid samples using the bacterial genomic DNA extraction kit from TIANamp (TIANGEN, Beijing, China). The 16S rRNA gene targeting the V3-V4 region was amplified from the total genomic DNA and sequenced using the Illumina NovaSeq 6000 platform. After sequencing, the raw sequences were analyzed using USEARCH 10.0 and scripts written by Liu et al. (27). The quality of the paired-end Illumina reads was checked using FastQC v.0.11.5 (28) and processed using USEARCH. Unique reads were denoised into ASVs using unoise3 in USEARCH (29). A feature table was generated using VSEARCH (30). The SILVA v123 (31) database was used to classify the taxonomy of the representative sequences, and the plastids and non-bacteria were removed. Alpha diversity indices, including richness and the Shannon index, were calculated. For beta diversity, variations in microbial

TABLE 1 | Ingredients and nutrient levels of the experimental diets with three different protein levels (on a dry matter basis).

Item	Diet		
	LP	MP	HP
Ingredients, g/kg			
Oat hay	500	500	500
Corn grain	210	165	120
Wheat grain	135	120	105
Wheat bran	70	75	80
Soybean meal	35	55	75
Rapeseed meal	25	60	95
NaCl	5	5	5
$CaHPO_4 \cdot 2H_2O$	3	3	3
Bentonite	5	5	5
$CaCo_3$	4.5	4.5	4.5
NaHCO3	2.5	2.5	2.5
Premix [a]	5	5	5
Nutrient levels [b]			
CP (%)	10.1	12.1	14.1
ME (MJ/kg)	10.1	10.1	10.1
EE (%)	2.7	2.8	2.9
NDF (%)	37.5	38.5	39.5
ADF (%)	19.1	20.1	21.1
Ca (%)	0.6	0.7	0.7
P (%)	0.4	0.5	0.5

[a] *Premix provided per kg of feed: Vitamin A, 50,000 IU; Vitamin D3, 12,500 IU; Vitamin E, 1,000 IU; Cu, 250 mg; Fe, 12,000 mg; Zn, 1,000 mg; Mn, 1,000 mg and Se, 7.5 mg.*
[b] *ME, metabolizable energy = total digestible nutrients×0.04409×0.82, according to the National Research Council; CP, crude protein; EE, ether extract; NDF, neutral detergent fiber; ADF, acid detergent fiber.*

composition among the three different groups were investigated using constrained PCoA (CPCoA).

Metabolomics Data Analysis

Rumen fluid samples were centrifuged at 4 °C for 5 min at 10,000 rpm and transferred into a 1.5 ml tube, and pre-cold methanol with 10 μl internal standard 2-Chloro-L-phenylalanine was added. After centrifugation, 200 μl of supernatant was transferred to a fresh tube. Fifty microliters of each sample were removed and combined to prepare a quality control sample. After evaporation in a vacuum concentrator, 30 μl of methoxyamination hydrochloride was added and derivatized with 40 μl of BSTFA reagent at 70 °C for 1.5 h. All samples were then analyzed by GC-TOF-MS. The GC-TOF-MS analysis was performed using an Agilent 7890 GC-TOF-MS. The system used a DB-5MS capillary column (30 m×250 μm×0.25 μm). Chroma TOF (V 4.3x, LECO) and the LECO-Fiehn Rtx5 database were used for the raw data analysis, including peak extraction, baseline adjustment, deconvolution, alignment and integration. Finally, peaks detected in less than half of the quality control samples or RSD > 30% in the quality control samples were removed.

The resulting data were imported into software SIMCA 14.1 software (Umetrics, Umea, Sweden) for orthogonal projections to latent structures-discriminant analysis (OPLS-DA). Differential metabolites were identified by combining the VIP values obtained from the OPLS-DA analysis and t-test (VIP > 1.5 and $p < 0.05$). Differential metabolites were identified and validated using the Human Metabolome Database (HMDB; https://hmdb.ca/) and Kyoto Encyclopedia of Genes and Genomes (KEGG; https://www.kegg.jp/). The data analysis tool MetaboAnalyst 5.0 (https://www.metaboanalyst.ca/) was used to view the metabolic pathway distribution and enrichment of the differential metabolites.

Correlations Between Microbial Communities and Rumen Metabolites

Rumen metabolites with VIP > 1.5, $p < 0.05$, and the top 10 microbial genera were used for interactive analysis. Spearman's rank correlations and *p*-value were calculated using the GenesCloud tool, a website for microbial analysis (http://www.genescloud.cn).

RESULTS

Sequencing and Diversity Estimates of Rumen Microbiomes

Totally 2,144,910 raw reads were obtained for the bacterial 16S rRNA genes from 18 rumen fluid samples using the sequencing procedure. After quality control, 2,046,323 high-quality reads were obtained (average of 85,263 reads per sample). A total of 3,921 ASVs were produced based on the results. The statistics of the bacterial alpha diversity indices (richness and Shannon index) for each sample were calculated, and the results are shown in **Figures 1A,B**. Richness and Shannon values were not significant among the three groups ($p > 0.05$). The result of beta diversity based on the CPCoA showed that the rumen microbiota of Tibetan sheep clustered three distinct parts, and these three groups were largely separated from each other with 15.1% of the variance ($p = 0.0001$) (**Figure 1C**).

Bacterial Community Compositions

At the taxonomic level, 16 bacterial phyla, 26 classes, 37 orders, 56 families, and 163 genera were detected in the rumen microbiota of Tibetan sheep. At the phylum level (**Figure 2A**), Bacteroidetes (54.37–59.58%), Firmicutes (21.68–26.10%), Proteobacteria (8.81–18.46%), Actinobacteria (0.27–4.78%), Tenericutes (0.23–0.36%), Spirochaete (0.07–0.15%), Saccharibacteria (0.06–0.10%) and Candidate_division_SR1 (0.02–0.35%) were the dominant bacteria. Among these phyla, Bacteroidetes and Firmicutes had the highest relative abundances in all three groups. However, no significant between-group differences in relative abundance were detected at the phylum level. At the genus level (**Figure 2B**), *Prevotella_1* (21.10–32.38%), *Rikenellaceae_RC9_gut_group* (4.94–7.52%), *Prevotellaceae_UCG-001* (2.18–2.47%), *Prevotellaceae_UCG-003* (1.28–2.61%) and *Christensenellaceae_R-7_group* (1.45–2.45%) were the dominant bacteria. In addition, the relative abundance of these dominant bacterial genera was also not significantly affected by dietary protein levels ($p > 0.05$).

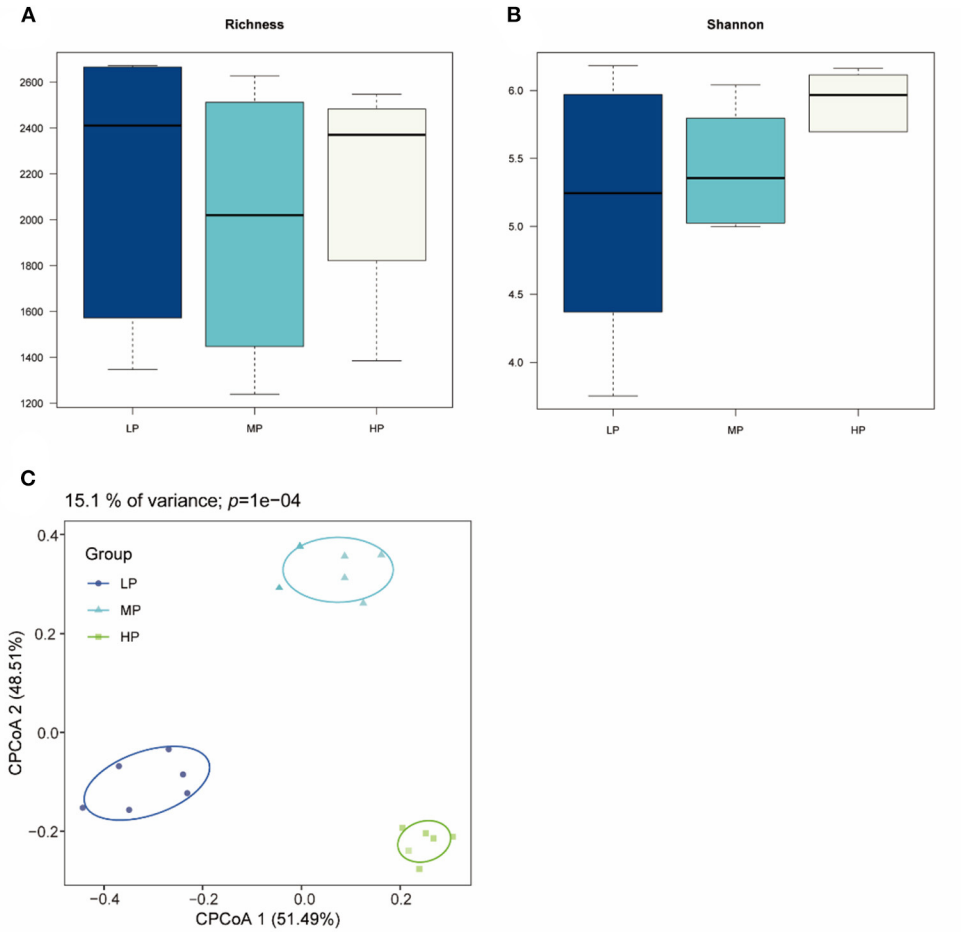

FIGURE 1 | Bacterial diversity of rumen fluid samples among three different groups. **(A)** Richness index; **(B)** Shannon index; **(C)** CPCoA plot based on ASVs.

Identification and Quantification of GC-TOF-MS Metabolites in the Rumen

In total, 411 valid peaks were identified in 18 rumen fluid samples. After rigorous quality control and identification, 189 metabolites, including organic acids and derivatives, organoheterocyclic compounds, organic oxygen compounds, benzenoids, organic oxygen compounds, lipids, lipid-like molecules and benzenoids, were obtained from the metabolomics library of the three groups, which shared the same metabolite categories.

For further analysis, OPLS-DA was conducted to characterize the differences in rumen metabolic profiles between the different groups. The parameters for the assessment of the OPLS-DA model in differentiating the three groups is represented by validation plots (**Figure 3**). The corresponding R^2Y values of the OPLS-DA model for LP vs. HP, MP vs. HP and LP vs. MP were 0.954, 0.98 and 0.835, respectively. This indicates that this model can be used to identify differences between the groups. OPLS-DA results also showed that these groups had distinctly different metabolite compositions.

Rumen Metabolomic Profiles

Based on the statistical analysis results and the VIP values obtained from OPLS-DA, 17 metabolites ($p < 0.05$, and VIP > 1.5) were found to be significantly different in the comparisons of HP vs. LP, MP vs. LP, and HP vs. MP. Among these, three metabolites were classified into benzenoids (super class level; the same as below); four were classified into lipids and lipid-like molecules; three were classified into organic acids and derivatives; three were classified into organic oxygen compounds; three were classified into oganioheterocyclic compounds; and one was classified into homogeneous non-metal compounds.

With an increase in dietary protein level, 17 metabolites showed an increase (**Figure 4**; **Supplementary Table 1**). Compared with the LP group, three metabolites (beta-Alanine, Hydroxypropanedioic acid and 5-Hydroxyindoleacetic acid) in the HP group increased significantly (VIP > 1.5, $p < 0.05$). Compared with the MP group, six metabolites (D-Mannose, Allose, Phenylethylamine, Indan-1-ol, D-Maltose and Maltulose) in the HP group increased significantly (VIP > 1.5, $p < 0.05$). Compared with the LP group, eight

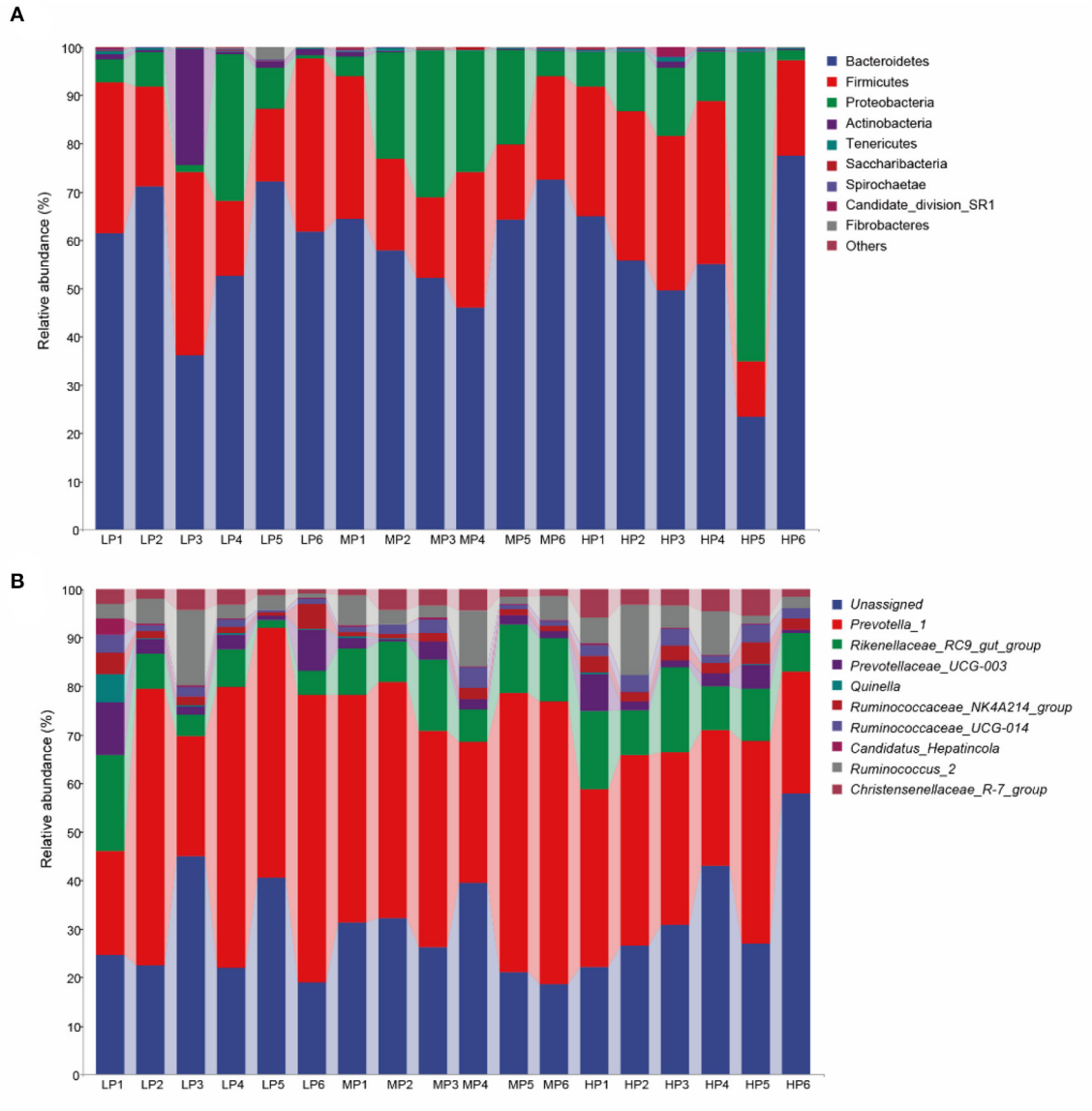

FIGURE 2 | Microbial composition of rumen fluid samples at the **(A)** phylum and **(B)** genus level.

metabolites (Pyrrole-2-carboxylic acid, Indoleacetic acid, 3-Hydroxypalmitic acid, 2,2-Dimethylsuccinic acid, Maleamate, 3-Hydroxynorvaline, Hydroxylamine and 4-Methylcatechol) in the MP group increased significantly (VIP > 1.5, $p < 0.05$).

Metabolic Pathways of Differential Metabolites

Differential metabolites in rumen fluid samples from the three groups were analyzed using MetaboAnalyst 5.0 software to reveal their association with metabolic pathways (**Figure 5**). According to KEGG pathway identification, seven pathways (tryptophan metabolism, phenylalanine metabolism, starch and sucrose metabolism, pantothenate and CoA biosynthesis, beta-alanine metabolism, propanoate metabolism and pyrimidine metabolism) were identified. Tryptophan metabolism was the most altered metabolic pathway among the three groups ($p < 0.05$).

Relationship Between the Ruminal Microbiome and Metabolome

Based on the results of Spearman correlation coefficients and p values, and clear positive and negative correlations were detected between the main ruminal microbiota and differential metabolites (**Figure 6**). For example, *Rikenellaceae_RC9_gut_group* was positively associated with 5-Hydroxyindoleacetic acid, D-Mannose, Pyrrole-2-carboxylic acid, Maleamate, 3-Hydroxynorvaline and Hydroxylamine ($p < 0.05$). *Ruminococcus_2* was positively

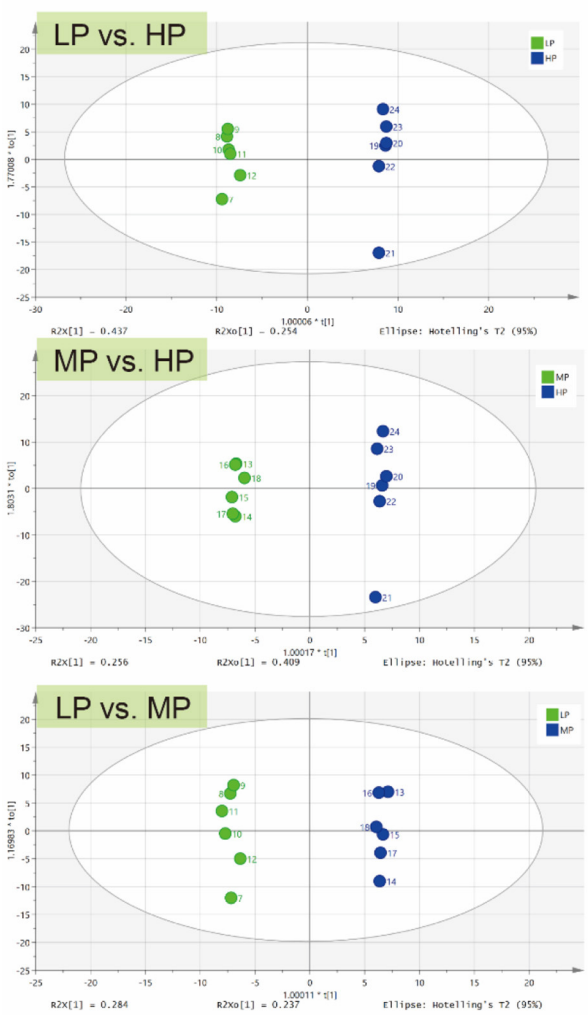

FIGURE 3 | OPLS-DA of ruminal metabolites between different groups.

correlated with Allose and Maltulose levels ($p < 0.05$). *Christensenellaceae_R-7_group* was positively correlated with beta-Alanine, Hydroxypropanedioic acid and Indoleacetic acid ($p < 0.05$). *Ruminococcaceae_UCG-014* was positively correlated with beta-Alanine and Hydroxypropanedioic acid levels ($p < 0.05$). *Ruminococcaceae_NK4A214_group* was positively correlated with Hydroxypropanedioic acid, D-Mannose and Phenylethylamine ($p < 0.05$) while *Quinella* was negatively associated with beta-Alanine levels ($p < 0.05$).

DISCUSSION

Rumen bacterial communities and metabolites play important roles in the growth, development and organismal health of ruminants (32, 33). The objective of this study was to investigate the effects of different dietary protein levels with the same metabolizable energy level on ruminal microbiota and metabolites in Tibetan sheep using 16S rRNA sequencing and GC-TOF-MS and to detect the potential relationships between ruminal bacteria and metabolites.

In this study, the dietary protein levels did not have a significant influence on alpha diversity (based on the richness and Shannon index) or the relative abundance of the main bacterial phyla and genera. A previous study showed that under the same forage-to-concentrate ratio, the alteration of dietary energy level had no significant influence on the alpha diversity and bacterial community structure in Holstein heifers (34). This finding is consistent with research that shows that changing one nutrient content of the diet (e.g., protein or energy) under the same food ingredients was not sufficient to cause a strong fluctuation in the ruminal microbiota. Several studies (18, 35–37) showed that the dietary forage-to-concentrate ratio under the same food ingredients was the most critical environmental factors shaping rumen microbial structures and composition. In our study, Bacteroidetes, Firmicutes, and Proteobacteria were the predominant bacterial phyla in the rumen of Tibetan sheep, and their relative abundances did not show significant impact among the three groups. Bacteroidetes and Firmicutes play a critical role in microbial ecology and are involved in the decomposition of fibrous and non-fibrous diets (38, 39). The phylum Proteobacteria is the largest phylum of bacteria, including many pathogenic bacteria, such as *Escherichia coli*, *Salmonella*, *Vibrio cholerae* and *Helicobacter pylori*. Although the relative abundance of Proteobacteria is much lower compared to the Bacteroidetes and Firmicutes, it still plays an important role in rumen metabolism, such as biofilm formation and digestion of soluble carbohydrates (40). Besides, Bacteroidetes and Proteobacteria are the two major N-metabolizing microbial communities (41). Liu et al. (42) demonstrated that Tibetan sheep fed high-concentrate (45–60%) diets significantly increased the relative abundance of Bacteroidetes and reduced the Proteobacteria to adapt to a diet containing more non-fibrous carbohydrates and polysaccharides. At the genus level, the dominant genera (e.g., *Prevotella_1*, *Rikenellaceae_RC9_gut_group*, *Prevotellaceae_UCG-001*, *Prevotellaceae_UCG-003* and *Christensenellaceae_R-7_group*) were also not influenced by dietary protein levels. *Prevotella* has been found predominant in the rumen of sheep and can enhance the capacity to utilize starch and non-cellulosic polysaccharides and promote the production of total volatile fatty acids (VFA) (43, 44). Moreover, *Prevotella* can ferment proteins and attain a N balance status in the gut (45). *Rikenellaceae_RC9_gut_group*, which is the main gene of Rikenellaceae, plays an important role in the fermentation of carbohydrates and crude protein (46, 47). Fan et al. (8) also revealed that Tibetan sheep could enhance forage degradation and fermentation by increasing the relative abundance of Bacteroidetes, *Prevotella_1*, and *Prevotellaceae_UCG-003* during the summer season compared with the winter season. Christensenellaceae are belonged to Firmicutes, which widespread in the intestines and mucous membranes of humans and animals and are important for host health due to several enzymes (48). Overall, Bacteroidetes, Firmicutes and *Prevotella* were the most dominant bacterial taxa in the rumen of Tibetan sheep, corroborating the results of previous studies on goats (49), cows (50), beef cattle (51) and yaks

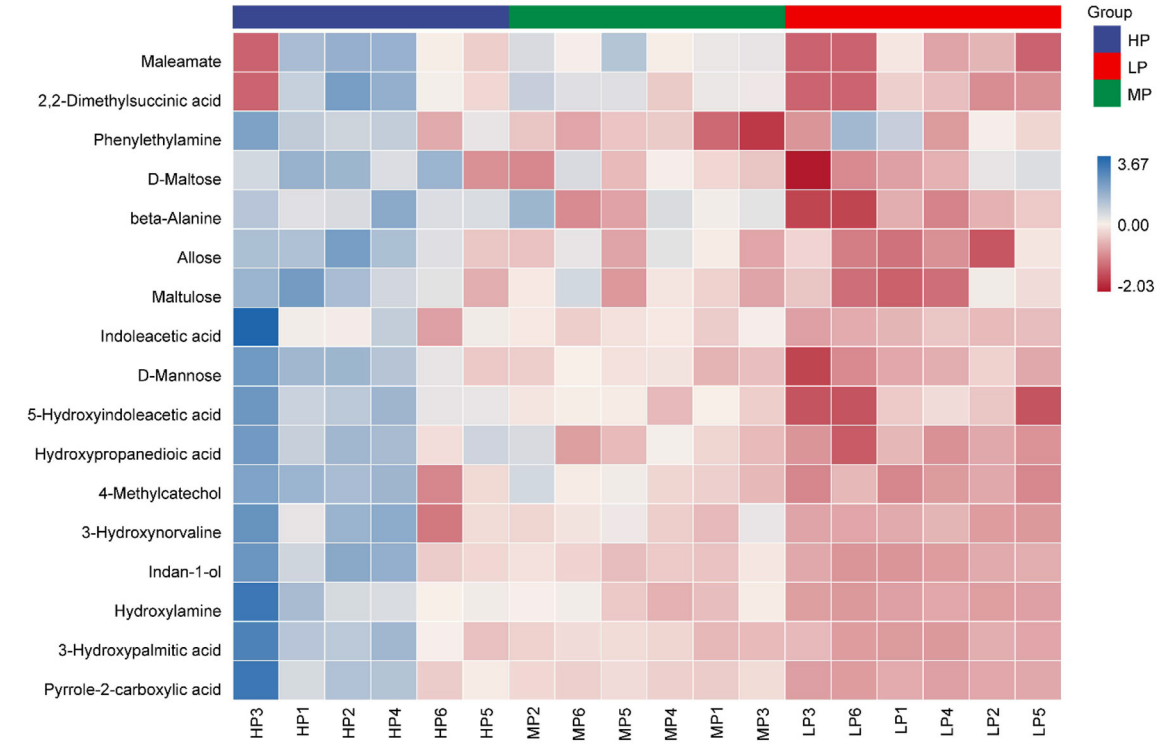

FIGURE 4 | Heatmap of differential metabolites in rumen fluid samples between different groups.

(52), indicating that these bacteria play a major role in immunity, health, and the ecological function of the gastrointestinal tract in ruminants. In the present study, Tibetan sheep had a strong capacity to digest protein in the feed and optimize dietary amino acid utilization with the assistance of ruminal microorganisms.

Our study showed that the ruminal metabolite composition was significantly different among the three treatment groups based on OPLS-DA analysis, suggesting that the dietary nutrient content is likely to alter the rumen metabolomic profiles of Tibetan sheep. These results were comparable with previous study of Liu et al. (53), who found that feed type could significantly change the metabolites and functional pathway of yaks. In the present study, 17 metabolic biomarkers showed significant differences between the different groups, including benzenoids, lipids and lipid-like molecules, organic acids and derivatives, organic oxygen compounds, organoheterocyclic compounds and homogeneous non-metal compounds. Notably, all 17 metabolites showed a clear increasing trend with increasing dietary protein levels. Among these metabolites, beta-Alanine and Phenylethylamine are important amino acids for animals and enriched in sheep with the higher dietary protein. Beta-Alanine is a non-essential amino acid that is synthesized in the liver tissue and is presumed to be an intermediate required for the synthesis of acrylamide and acetonitrile (54, 55). Previous studies have confirmed that beta-Alanine can improve the digestibility of soluble starch and readily fermentable carbohydrates and induce the transition from VFAs to carbohydrates (53, 56). Phenylethylamine is an essential amino acid for animals and

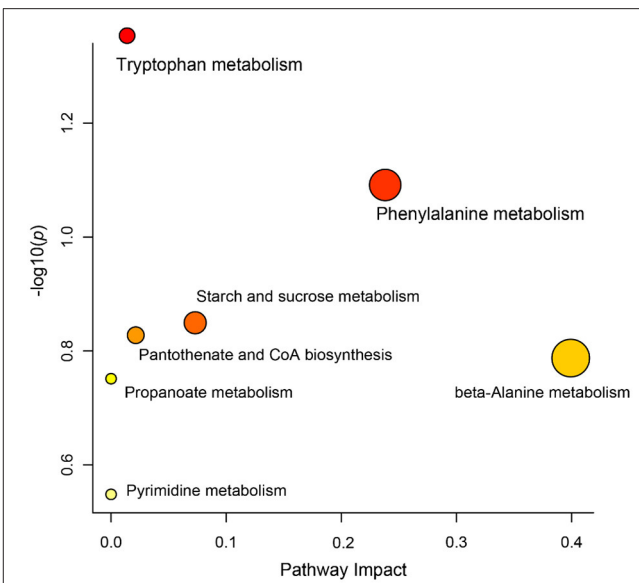

FIGURE 5 | KEGG pathways based on the differential metabolites identified in different groups.

can synthesize neurotransmitters and hormones, and participates in glucose metabolism and fat metabolism (57). In addition to these amino acids, several carbohydrates, such as D-Mannose, Allose and D-Maltose, were also enriched in the higher dietary

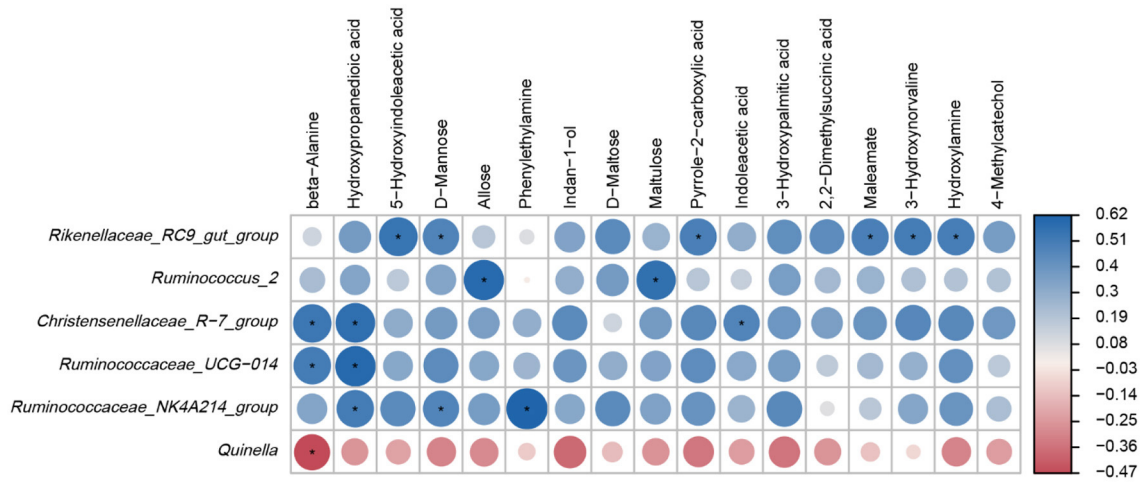

FIGURE 6 | Heatmap of Spearman correlations between main genera and differential metabolites. *$p < 0.05$.

protein groups. The main function of these carbohydrates is to provide energy for animal growth and development (58). For example, D-Mannose is an important monosaccharide for protein glycosylation in mammals and thought to promote immunity and boost energy metabolism in organisms (59, 60). KEGG analysis revealed that tryptophan metabolism was the most altered metabolic pathway among the three groups. Tryptophan metabolism is a multi-pathway and complex process that occurs in the host and its intestinal symbiotic microbiota. Several metabolites generated by the tryptophan pathway have various effects on immune function, including tryptophan metabolism in animals (61). It was found that intestinal microorganisms such as bacteria, fungi and protozoa could contribute to the formation of key tryptophan metabolites, such as anabolic D-Tryptophan in the microbial community, small peptides synthesized by fungi, indoles and their derivatives (62). The same tryptophan metabolites produced by animal intestinal bacteria are indole derivatives, such as indoleacetic acid (IAA), indole sulfuric acid (ISA), indole-3-acetaldehyde (IAAId) and tryptamine (63). In addition, tryptophan metabolites of intestinal microbes could affect host physiological health by stimulating target gene expression, modulating the mucosal immune system, and targeting specific receptors. In our study, the content of indoleacetic acid showed higher concentration in the rumen of Tibetan sheep fed the higher dietary protein level. Based on the above results, we speculate that higher dietary protein may regulate nutrient absorption and growth performance through the composition and function of ruminal metabolites.

Metabolomics is used to study the small-molecule metabolites changes in animals produced by the external disturbance and can reflect the state of physical function more accurately. Compared to microorganisms, the metabolome can reflect the most intuitive physiological state of the animal. Therefore, the rumen metabolomic profiles were more sensitive to different dietary protein levels than bacterial community compositions in the present study. Additionally, an association was found between the structure of the rumen microbiota and metabolic profiles. These results were consistent with those in donkeys (64), yaks (65), Holstein heifers (18), mice (66) and humans (67), revealing a close relationship between microbiota, metabolites and organismal health. Our study also found significant positive correlations between the dominant bacterial groups and differential metabolites using Spearman correlation analysis. Our previous study demonstrated that higher dietary protein levels could improve growth performance, carcass performance and meat quality (25). Based on these findings, it is speculated that rumen bacterial groups may promote nutrient absorption capability by positively regulating the concentration of amino acids (e.g., beta-Alanine, Phenylethylamine), carbohydrates (e.g., D-Mannose, Allose, D-Maltose, Maltulose) and organic acids (e.g., Hydroxypropanedioic acid, Indoleacetic acid, and Maleamate), and promote the nutrient absorption and growth performance of Tibetan sheep.

CONCLUSIONS

In summary, we applied multi-omics analysis combined with microbiome and metabolomics analyses to investigate the effects of dietary protein levels on ruminal microbial communities and metabolites in Tibetan sheep. Under the same forage-to-concentrate ratio condition, the difference in dietary protein levels had no significant impact on rumen bacterial groups. Meanwhile, with increasing dietary protein levels, the concentrations of metabolites related to nutrient absorption significantly increased. In addition, the dominant microbiota was associated with different metabolites, indicating a close link between microbes and metabolites. Taking the above points into consideration, the higher protein levels (12.1 and 14.1%) were recommended as the appropriate dietary protein level in Tibetan sheep during the cold season. This study allowed us to gain a better understanding of ruminal microbial and metabolic functions and can lead to improvements in the

protein level requirements within Tibetan sheep diets and nutritional regulation.

DATA AVAILABILITY STATEMENT

The datasets presented in this study can be found in online repositories. The names of the repository/repositories and accession number(s) can be found below: https://www.ncbi.nlm.nih.gov/, PRJNA801776.

ETHICS STATEMENT

The animal study was reviewed and approved by Experimental Animal Use Ethics Committee of the Northwest Institute of Plateau Biology, Chinese Academy of Sciences.

AUTHOR CONTRIBUTIONS

XW, SX, and TX: conception and experiment design. XW, TX, XZ, NZ, and YG: experiment conduction. XW, HL, and XZ: statistical analysis. SK, LH, and QZ: resources. XW: writing original draft preparation. All authors have read and agreed to the published version of the manuscript.

FUNDING

This work was funded by the Strategic Leading Science and Technology Program of the Chinese Academy of Sciences (XDA2005010406 and XDA23060603), Platform of Adaptive Management on Alpine Grassland-livestock System (2020-ZJ-T07), and Joint Research Project of Sanjiangyuan National Park (LHZX-2020-7).

SUPPLEMENTARY MATERIAL

The Supplementary Material for this article can be found online at: https://www.frontiersin.org/articles/10.3389/fvets.2022.922817/full#supplementary-material

REFERENCES

1. Zhou JW, Guo XS, Degen AA, Zhang Y, Liu H, Mi JD, et al. Urea kinetics and nitrogen balance and requirements for maintenance in Tibetan sheep when fed oat hay. *Small Ruminant Res.* (2015) 129:60–8. doi: 10.1016/j.smallrumres.2015.05.009
2. Langda S, Zhang C, Zhang K, Gui B, Ji D, Deji C, et al. Diversity and composition of rumen bacteria, fungi, and protozoa in goats and sheep living in the same high-altitude pasture. *Animals.* (2020) 10:186. doi: 10.3390/ani10020186
3. Yang C, Gao P, Hou F, Yan T, Chang S, Chen X, et al. Relationship between chemical composition of native forage and nutrient digestibility by Tibetan sheep on the Qinghai-Tibetan Plateau. *J Anim Sci.* (2018) 96:1140–9. doi: 10.1093/jas/sky002
4. Long RJ, Apori SO, Castro FB, Ørskov ER. Feed value of native forages of the Tibetan Plateau of China. *Anim Feed Sci Technol.* (1999) 80:101–13. doi: 10.1016/S0377-8401(99)00057-7
5. Zhao X, Zhou X. Ecological basis of alpine meadow ecosystem management in Tibet: Haibei alpine meadow ecosystem research station. *Ambio.* (1999) 28:642–7.
6. Xue B, Zhao XQ, Zhang YS. Seasonal changes in weight and body composition of yak grazing on alpine-meadow grassland in the Qinghai-Tibetan Plateau of China. *J Anim Sci.* (2005) 83:1908–13. doi: 10.2527/2005.8381908x
7. Xu T, Xu S, Hu L, Zhao N, Liu Z, Ma L, et al. Effect of dietary types on feed intakes, growth performance and economic benefit in Tibetan sheep and yaks on the Qinghai-Tibet Plateau during cold season. *PLoS ONE.* (2017) 12:e0169187. doi: 10.1371/journal.pone.0169187
8. Fan Q, Cui X, Wang Z, Chang S, Wanapat M, Yan T, et al. Rumen microbiota of Tibetan sheep (*Ovis aries*) adaptation to extremely cold season on the Qinghai-Tibetan Plateau. *Front Vet Sci.* (2021) 8:554. doi: 10.3389/fvets.2021.673822
9. Vahidi MF, Gharechahi J, Behmanesh M, Ding X-Z, Han J-L, Salekdeh GH. Diversity of microbes colonizing forages of varying lignocellulose properties in the sheep rumen. *PeerJ.* (2021) 9:e10463. doi: 10.7717/peerj.10463
10. Yang C, Tsedan G, Liu Y, Hou F. Shrub coverage alters the rumen bacterial community of yaks (*Bos grunniens*) grazing in alpine meadows. *J Anim Sci Technol.* (2020) 62:504. doi: 10.5187/jast.2020.62.4.504
11. Ma L, Xu S, Liu H, Xu T, Hu L, Zhao N, et al. Yak rumen microbial diversity at different forage growth stages of an alpine meadow on the Qinghai-Tibet Plateau. *PeerJ.* (2019) 7:e7645. doi: 10.7717/peerj.7645
12. Zhang T, Mu Y, Zhang D, Lin X, Wang Z, Hou Q, et al. Determination of microbiological characteristics in the digestive tract of different ruminant species. *Microbiologyopen.* (2019) 8:e00769. doi: 10.1002/mbo3.769
13. Zhao S, Min L, Zheng N, Wang J. Effect of heat stress on bacterial composition and metabolism in the rumen of lactating dairy cows. *Animals.* (2019) 9:925. doi: 10.3390/ani9110925
14. Park T, Ma L, Ma Y, Zhou X, Bu D, Yu Z. Dietary energy sources and levels shift the multi-kingdom microbiota and functions in the rumen of lactating dairy cows. *J Anim Sci Biotechnol.* (2020) 11:1–16. doi: 10.1186/s40104-020-00461-2
15. Wang Q, Zeng Y, Zeng X, Wang X, Wang Y, Dai C, et al. Effects of dietary energy levels on rumen fermentation, gastrointestinal tract histology and bacterial community diversity in fattening male Hu lambs. *Front Microbiol.* (2021) 12:695445. doi: 10.3389/fmicb.2021.695445
16. Zhao ZW, Ma ZY, Wang HC, Zhang CF. Effects of rumen-protected methionine and lysine supplementation on milk yields and components, rumen fermentation, and the rumen microbiome in lactating yaks (*Bos grunniens*). *Anim Feed Sci Technol.* (2021) 277:114972. doi: 10.1016/j.anifeedsci.2021.114972
17. Foroutan A, Fitzsimmons C, Mandal R, Piri-Moghadam H, Zheng J, Guo A, et al. The bovine metabolome. *Metabolites.* (2020) 10:233. doi: 10.3390/metabo10060233
18. Zhang J, Shi H, Wang Y, Li S, Cao Z, Ji S, et al. Effect of dietary forage to concentrate ratios on dynamic profile changes and interactions of ruminal microbiota and metabolites in Holstein heifers. *Front Microbiol.* (2017) 8:2206. doi: 10.3389/fmicb.2017.02206
19. Zhang R, Zhu W, Jiang L, Mao S. Comparative metabolome analysis of ruminal changes in Holstein dairy cows fed low-or high-concentrate diets. *Metabolomics.* (2017) 13:1–15. doi: 10.1007/s11306-017-1204-0
20. Tamminga S. Nutrition management of dairy cows as a contribution to pollution control. *J Dairy Sci.* (1992) 75:345–57. doi: 10.3168/jds.S0022-0302(92)77770-4
21. Schroeder GF, Titgemeyer EC, Awawdeh MS, Smith JS, Gnad DP. Effects of energy level on methionine utilization by growing steers. *J Anim Sci.* (2006) 84:1497–504. doi: 10.2527/2006.8461497x
22. Xie Y, Xu Q, Wu Y, Huang X, Liu J. Duodenum has the greatest potential to absorb soluble non-ammonia nitrogen in the nonmesenteric gastrointestinal tissues of dairy cows. *J Zhejiang Univ Sci B.* (2015) 16:503–10. doi: 10.1631/jzus.B1400299
23. Gharechahi J, Salekdeh GH, A. metagenomic analysis of the camel rumen's microbiome identifies the major microbes responsible for

lignocellulose degradation and fermentation. *Biotechnol Biofuels.* (2018) 11:1–19. doi: 10.1186/s13068-018-1214-9
24. Xue M-Y, Sun H-Z, Wu X-H, Liu J-X, Guan LL. Multi-omics reveals that the rumen microbiome and its metabolome together with the host metabolome contribute to individualized dairy cow performance. *Microbiome.* (2020) 8:1–19. doi: 10.1186/s40168-020-00819-8
25. Wang X, Xu T, Zhang X, Geng Y, Kang S, Xu S. Effects of dietary protein levels on growth performance, carcass traits, serum metabolites, and meat composition of Tibetan sheep during the cold season on the Qinghai-Tibetan Plateau. *Animals.* (2020) 10:801. doi: 10.3390/ani10050801
26. Council NR. *Nutrient Requirements of Small Ruminants: Sheep, Goats, Cervids, and New World Camelids.* Washingto, DC: The National Academies Press (2007).
27. Liu Y, Qin Y, Chen T, Lu M, Qian X, Guo X, et al. A practical guide to amplicon and metagenomic analysis of microbiome data. *Protein Cell.* (2021) 12:315. doi: 10.1007/s13238-020-00724-8
28. Andrews S. *FastQC: A Quality Control tool for High Throughput Sequence Data*. Babraham: Babraham Bioinformatics (2013).
29. Edgar RC, Flyvbjerg H. Error filtering, pair assembly and error correction for next-generation sequencing reads. *Bioinformatics.* (2015) 31:3476–82. doi: 10.1093/bioinformatics/btv401
30. Rognes T, Flouri T, Nichols B, Quince C, Mahé F, VSEARCH. a versatile open source tool for metagenomics. *PeerJ.* (2016) 4:e2584. doi: 10.7717/peerj.2584
31. Quast C, Pruesse E, Yilmaz P, Gerken J, Schweer T, Yarza P, et al. The SILVA ribosomal RNA gene database project: improved data processing and web-based tools. *Nucleic Acids Res.* (2012) 41:D590–D6. doi: 10.1093/nar/gks1219
32. Xue BC, Zhang JX, Wang ZS, Wang LZ, Peng QH Da LC, et al. Metabolism response of grazing yak to dietary concentrate supplementation in warm season. *Animal.* (2021) 15:100175. doi: 10.1016/j.animal.2021.100175
33. Goad DW, Goad CL, Nagaraja TG. Ruminal microbial and fermentative changes associated with experimentally induced subacute acidosis in steers. *J Anim Sci.* (1998) 76:234–41. doi: 10.2527/1998.761234x
34. Bi Y, Zeng S, Zhang R, Diao Q, Tu Y. Effects of dietary energy levels on rumen bacterial community composition in Holstein heifers under the same forage to concentrate ratio condition. *BMC Microbiol.* (2018) 18:1–11. doi: 10.1186/s12866-018-1213-9
35. Wang H, Pan X, Wang C, Wang M, Yu L. Effects of different dietary concentrate to forage ratio and thiamine supplementation on the rumen fermentation and ruminal bacterial community in dairy cows. *Anim Prod Sci.* (2014) 55:189–93. doi: 10.1071/AN14523
36. Han X, Li B, Wang X, Chen Y, Yang Y. Effect of dietary concentrate to forage ratios on ruminal bacterial and anaerobic fungal populations of cashmere goats. *Anaerobe.* (2019) 59:118–25. doi: 10.1016/j.anaerobe.2019.06.010
37. Chen H, Wang C, Huasai S, Chen A. Effects of dietary forage to concentrate ratio on nutrient digestibility, ruminal fermentation and rumen bacterial composition in Angus cows. *Sci Rep.* (2021) 11:1–11. doi: 10.1038/s41598-021-96580-5
38. Shanks OC, Kelty CA, Archibeque S, Jenkins M, Newton RJ, McLellan SL, et al. Community structures of fecal bacteria in cattle from different animal feeding operations. *Appl Environ Microbiol.* (2011) 77:2992–3001. doi: 10.1128/AEM.02988-10
39. Zhang X-L, Xu T-W, Wang X-G, Geng Y-Y, Liu H-J, Hu L-Y, et al. The effect of transitioning between feeding methods on the gut microbiota dynamics of yaks on the Qinghai-Tibet Plateau. *Animals.* (2020) 10:1641. doi: 10.3390/ani10091641
40. Shin N-R, Whon TW, Bae J-W. Proteobacteria: microbial signature of dysbiosis in gut microbiota. *Trends Biotechnol.* (2015) 33:496–503. doi: 10.1016/j.tibtech.2015.06.011
41. Xie B, Lv Z, Hu C, Yang X, Li X. Nitrogen removal through different pathways in an aged refuse bioreactor treating mature landfill leachate. *Appl Microbiol Biotechnol.* (2013) 97:9225–34. doi: 10.1007/s00253-012-4623-x
42. Liu H, Xu T, Xu S, Ma L, Han X, Wang X, et al. Effect of dietary concentrate to forage ratio on growth performance, rumen fermentation and bacterial diversity of Tibetan sheep under barn feeding on the Qinghai-Tibetan plateau. *PeerJ.* (2019) 7:e7462. doi: 10.7717/peerj.7462
43. Bekele AZ, Koike S, Kobayashi Y. Genetic diversity and diet specificity of ruminal Prevotella revealed by 16S rRNA gene-based analysis. *FEMS Microbiol Lett.* (2010) 305:49–57. doi: 10.1111/j.1574-6968.2010.01911.x
44. Lv X, Chai J, Diao Q, Huang W, Zhuang Y, Zhang N. The signature microbiota drive rumen function shifts in goat kids introduced to solid diet regimes. *Microorganisms.* (2019) 7:516. doi: 10.3390/microorganisms7110516
45. Gibson SA, McFarlan C, Hay S, MacFarlane GT. Significance of microflora in proteolysis in the colon. *Appl Environ Microbiol.* (1989) 55:679–83. doi: 10.1128/aem.55.3.679-683.1989
46. Tian Y, Zhang H, Zheng L, Li S, Hao H, Yin M, et al. Process analysis of anaerobic fermentation exposure to metal mixtures. *Int J Environ Res Public Health.* (2019) 16:2458. doi: 10.3390/ijerph16142458
47. Liu T, Ahn H, Sun W, McGuinness LR, Kerkhof LJ, H4ggblom MM. Identification of a Ruminococcaceae species as the methyl tert-butyl ether (MTBE) degrading bacterium in a methanogenic consortium. *Environ Sci Technol.* (2016) 50:1455–64. doi: 10.1021/acs.est.5b04731
48. Waters JL, Ley RE. The human gut bacteria Christensenellaceae are widespread, heritable, and associated with health. *BMC Biol.* (2019) 17:1–11. doi: 10.1186/s12915-019-0699-4
49. Lei Y, Zhang K, Guo M, Li G, Li C, Li B, et al. Exploring the spatial-temporal microbiota of compound stomachs in a pre-weaned goat model. *Front Microbiol.* (2018) 9:1846. doi: 10.3389/fmicb.2018.01846
50. Shabat SKB, Sasson G, Doron-Faigenboim A, Durman T, Yaacoby S, Berg Miller ME, et al. Specific microbiome-dependent mechanisms underlie the energy harvest efficiency of ruminants. *ISME J.* (2016) 10:2958–72. doi: 10.1038/ismej.2016.62
51. Chen F, Cheng G, Xu Y, Wang Y, Xia Q, Hu S. Rumen microbiota distribution analyzed by high-throughput sequencing after oral doxycycline administration in beef cattle. *Front Vet Sci.* (2020) 7:251. doi: 10.3389/fvets.2020.00251
52. Xue D, Chen H, Luo X, Guan J, He Y, Zhao X. Microbial diversity in the rumen, reticulum, omasum, and abomasum of yak on a rapid fattening regime in an agro-pastoral transition zone. *J Microbiol.* (2018) 56:734–43. doi: 10.1007/s12275-018-8133-0
53. Liu C, Wu H, Liu S, Chai S, Meng Q, Zhou Z. Dynamic alterations in yak rumen bacteria community and metabolome characteristics in response to feed type. *Front Microbiol.* (2019) 10:1116. doi: 10.3389/fmicb.2019.01116
54. Hoffman JR, Emerson NS, Stout JR. β-alanine supplementation. *Curr Sports Med Rep.* (2012) 11:189–95. doi: 10.1249/JSR.0b013e3182604983
55. Matthews MM, Traut TW. Regulation of N-carbamoyl-beta-alanine amidohydrolase, the terminal enzyme in pyrimidine catabolism, by ligand-induced change in polymerization. *J Biol Chem.* (1987) 262:7232–7. doi: 10.1016/S0021-9258(18)48228-2
56. Saleem F, Ametaj BN, Bouatra S, Mandal R, Zebeli Q, Dunn SM, et al. A metabolomics approach to uncover the effects of grain diets on rumen health in dairy cows. *J Dairy Sci.* (2012) 95:6606–23. doi: 10.3168/jds.2012-5403
57. Li H, Yu Q, Li T, Shao L, Su M, Zhou H, et al. Rumen microbiome and metabolome of Tibetan Sheep (*Ovis aries*) reflect animal age and nutritional requirement. *Front Vet Sci.* (2020) 7:609. doi: 10.3389/fvets.2020.00609
58. Jones SA, Jorgensen M, Chowdhury FZ, Rodgers R, Hartline J, Leatham MP, et al. Glycogen and maltose utilization by *Escherichia coli* O157: H7 in the mouse intestine. *Infect Immun.* (2008) 76:2531–40. doi: 10.1128/IAI.00096-08
59. Zhang L, Wang Y, Liu D, Luo L, Wang Y, Ye C. Identification and characterization of ALS genes involved in D-Allose metabolism in lineage II strain of Listeria monocytogenes. *Front Microbiol.* (2018) 9:621. doi: 10.3389/fmicb.2018.00621
60. Wen X, Hu Y, Zhang X, Wei X, Wang T, Yin S. Integrated application of multi-omics provides insights into cold stress responses in pufferfish Takifugu fasciatus. *BMC Genomics.* (2019) 20:1–15. doi: 10.1186/s12864-019-5915-7
61. Alcazar O, Hernandez LF, Tschiggfrie A, Muehlbauer MJ, Bain JR, Buchwald P, et al. Feasibility of localized metabolomics in the study of pancreatic islets and diabetes. *Metabolites.* (2019) 9:207. doi: 10.3390/metabo9100207
62. Kepert I, Fonseca J, Müller C, Milger K, Hochwind K, Kostric M, et al. D-tryptophan from probiotic bacteria influences the gut microbiome and allergic airway disease. *Journal of Allergy and Clinical Immunology.* (2017) 139:1525–35. doi: 10.1016/j.jaci.2016.09.003
63. Zhang J, Zhu S, Ma N, Johnston LJ, Wu C, Ma X. Metabolites of microbiota response to tryptophan and intestinal mucosal immunity: A therapeutic target to control intestinal inflammation. *Med Res Rev.* (2021) 41:1061–88. doi: 10.1002/med.21752

64. Zhang C, Zhang C, Wang Y, Du M, Zhang G, Lee Y. Dietary energy level impacts the performance of donkeys by manipulating the gut microbiome and metabolome. *Front Vet Sci.* (2021) 8:694357. doi: 10.3389/fvets.2021.694357
65. Zhang X, Xu T, Wang X, Geng Y, Zhao N, Hu L, et al. Effect of dietary protein levels on dynamic changes and interactions of ruminal microbiota and metabolites in yaks on the Qinghai-Tibetan Plateau. *Front Microbiol.* (2021) 12:684340. doi: 10.3389/fmicb.2021.684340
66. Lu K, Abo RP, Schlieper KA, Graffam ME, Levine S, Wishnok JS, et al. Arsenic exposure perturbs the gut microbiome and its metabolic profile in mice: an integrated metagenomics and metabolomics analysis. *Environ Health Perspect.* (2014) 122:284–91. doi: 10.1289/ehp.1307429
67. De Filippis F, Pellegrini N, Vannini L, Jeffery IB, La Storia A, Laghi L, et al. High-level adherence to a Mediterranean diet beneficially impacts the gut microbiota and associated metabolome. *Gut.* (2016) 65:1812–21. doi: 10.1136/gutjnl-2015-309957

Conflict of Interest: The authors declare that the research was conducted in the absence of any commercial or financial relationships that could be construed as a potential conflict of interest.

Publisher's Note: All claims expressed in this article are solely those of the authors and do not necessarily represent those of their affiliated organizations, or those of the publisher, the editors and the reviewers. Any product that may be evaluated in this article, or claim that may be made by its manufacturer, is not guaranteed or endorsed by the publisher.

frontiers | Frontiers in Veterinary Science

ORIGINAL RESEARCH
published: 12 July 2022
doi: 10.3389/fvets.2022.931264

Peroxisome Proliferator-Activated Receptor Activation in Precision-Cut Bovine Liver Slices Reveals Novel Putative PPAR Targets in Periparturient Dairy Cows

Sebastiano Busato[1], *Hunter R. Ford*[1], *Alzahraa M. Abdelatty*[2], *Charles T. Estill*[1,3] *and Massimo Bionaz*[1]*

[1] *Department of Animal and Rangeland Sciences, Oregon State University, Corvallis, OR, United States,* [2] *Department of Nutrition and Clinical Nutrition, Faculty of Veterinary Medicine, Cairo University, Giza, Egypt,* [3] *College of Veterinary Medicine, Oregon State University, Corvallis, OR, United States*

Metabolic challenges experienced by dairy cows during the transition between pregnancy and lactation (also known as peripartum), are of considerable interest from a nutrigenomic perspective. The mobilization of large amounts of non-esterified fatty acids (**NEFA**) leads to an increase in NEFA uptake in the liver, the excess of which can cause hepatic accumulation of lipids and ultimately fatty liver. Interestingly, peripartum NEFA activate the Peroxisome Proliferator-activated Receptor (**PPAR**), a transcriptional regulator with known nutrigenomic properties. The study of PPAR activation in the liver of periparturient dairy cows is thus crucial; however, current *in vitro* models of the bovine liver are inadequate, and the isolation of primary hepatocytes is time consuming, resource intensive, and prone to errors, with the resulting cells losing characteristic phenotypical traits within hours. The objective of the current study was to evaluate the use of precision-cut liver slices (**PCLS**) from liver biopsies as a model for PPAR activation in periparturient dairy cows. Three primiparous Jersey cows were enrolled in the experiment, and PCLS from each were prepared prepartum (−8.0 ± 3.6 DIM) and postpartum (+7.7± 1.2 DIM) and treated independently with a variety of PPAR agonists and antagonists: the PPARα agonist WY-14643 and antagonist GW-6471; the PPARδ agonist GW-50156 and antagonist GSK-3787; and the PPARγ agonist rosiglitazone and antagonist GW-9662. Gene expression was assayed through RT-qPCR and RNAseq, and intracellular triacylglycerol (TAG) concentration was measured. PCLS obtained from postpartum cows and treated with a PPARγ agonist displayed upregulation of *ACADVL* and *LIPC* while those treated with PPARδ agonist had increased expression of *LIPC*, *PPARD*, and *PDK4*. In PCLS from prepartum cows, transcription of *LIPC* was increased by all PPAR agonists and NEFA. TAG concentration tended to be larger in tissue slices treated with PPARδ agonist compared to CTR. Use of PPAR isotype-specific antagonists in PCLS cultivated in autologous blood serum failed to decrease expression of PPAR targets, except for *PDK4*, which was confirmed to be a PPARδ target. Transcriptome sequencing revealed considerable differences in response to PPAR agonists at a false discovery rate-adjusted *p*-value of 0.2, with the most notable effects exerted by the PPARδ and

OPEN ACCESS

Edited by:
Rita Payan Carreira,
University of Evora, Portugal

Reviewed by:
Juan J. Loor,
University of Illinois at Urbana-Champaign, United States
Saif ur Rehman,
Guangxi University, China

***Correspondence:**
Massimo Bionaz
massimo.bionaz@oregonstate.edu

Specialty section:
This article was submitted to Animal Nutrition and Metabolism, a section of the journal Frontiers in Veterinary Science

Received: *28 April 2022*
Accepted: *06 June 2022*
Published: *12 July 2022*

Citation:
Busato S, Ford HR, Abdelatty AM, Estill CT and Bionaz M (2022) Peroxisome Proliferator-Activated Receptor Activation in Precision-Cut Bovine Liver Slices Reveals Novel Putative PPAR Targets in Periparturient Dairy Cows. Front. Vet. Sci. 9:931264. doi: 10.3389/fvets.2022.931264

PPARγ agonists. Differentially expressed genes were mainly related to pathways involved with lipid metabolism and the immune response. Among differentially expressed genes, a subset of 91 genes were identified as novel putative PPAR targets in the bovine liver, by cross-referencing our results with a publicly available dataset of predicted PPAR target genes, and supplementing our findings with prior literature. Our results provide important insights on the use of PCLS as a model for assaying PPAR activation in the periparturient dairy cow.

Keywords: PPAR, nutrigenomics, PCLS, dairy cows, liver, peripartum

INTRODUCTION

Dairy cows experience drastic metabolic challenges during the peripartum, the period encompassing 3 weeks before to 3 weeks after calving. A decrease in feed intake, combined with a sharp increase in energy demands dictated by the rapidly changing metabolic landscape, result in a state of energetic deficiency. This status is counterbalanced by the mobilization of non-esterified fatty acids (**NEFA**) that are used as energy (1, 2). At the crux of these metabolic changes is the liver, as the central organ for gluconeogenesis and lipid metabolism, contributing to the maintenance of energy homeostasis (3). In particular, during the early postpartum hepatic uptake and metabolism of NEFA sharply increase (4). In the liver, absorbed NEFA are either oxidized or esterified into triacylglycerols (**TAG**) that are stored in the tissue or secreted back into circulation through very low density lipoproteins (**VLDL**) (4). Ruminants, and particularly cattle, are biologically predisposed to secrete TAG in VLDL at a lower rate than other species (5); consequently, increases in circulating NEFA can result in steatosis in the liver, significantly limiting hepatic function at a time when it is the most crucial (6). Further, partial oxidation of NEFA leads to the production of ketones, including β-hydroxybutyrate, supraphysiological levels of which (>3.0 mmol/L) lead to clinical ketosis, with detrimental effects on the animal (7). Thus, it is not surprising that studies on the biology of the periparturient dairy cow focus particularly on liver activity, metabolites, and liver-specific pathways.

Perhaps counterintuitively, evidence shows that energy restriction in prepartum improves the ability of the liver to cope with postpartum stressors, leading to lower postpartum NEFA, total hepatic lipids and TAG, when compared to overfed cows (8), or cows fed *ad libitum* (9). From a molecular standpoint, prepartum feed restriction in dairy cows leads to greater hepatic NEFA uptake and intracellular transport postpartum (10), increases gluconeogenic capacity (11, 12), as well as the expression of genes involved in lipid metabolism (11). Early regulation of pathways related to energy homeostasis and lipid metabolism in the liver may "prime" the organ, and lead to a quicker metabolic response in the early postpartum, contributing to the underrepresentation of pathophysiological conditions; in this context, the role of the Peroxisome Proliferator-activated Receptors (PPAR) could be crucial (13).

PPAR are a group of transcriptional regulators that belong to the nuclear receptor superfamily, of which three isotypes are known and characterized: PPARα, PPARδ, and PPARγ (14). In bovine, expression of PPARα is detected primarily in the liver, while PPARγ is highly abundant in the adipose tissue, and PPARδ is rather ubiquitously expressed (13, 15). PPAR activity, dependent on intracellular concentration of suitable ligands, is known to be modulated by fatty acids and their metabolites (14). Broadly speaking, genes that were identified as PPAR targets code for proteins involved in fatty acid metabolism in the liver, lipid catabolism and insulin sensitivity in the adipose tissue, and in regulation of inflammation and the immune response (13). Crucially, some of the genes upregulated by energy restriction and/or the transition from pregnancy to lactation are targets of PPAR (16), which suggest a strong involvement of PPAR in the hepatic response to metabolic changes in the peripartum. Recently our group showed that, in immortalized mammary, liver, and endothelial bovine cells, PPAR activity is strongly induced by NEFA present in blood serum of early lactation Jersey cows (17). Our results support the hypothesis that a moderate increase in circulating NEFA prepartum, brought forth by energy restriction, improves hepatic fitness postpartum through activation of PPAR.

The study of hepatic metabolism and gene expression *in vitro* can aid in the quantification of parameters of interest with remarkable precision. Currently, the gold standard for cell-based hepatic studies is the isolation and purification of parenchymal cells (hepatocytes) using a two-step perfusion method on either whole liver or the caudate lobe alone (18). While feasible in smaller species, whole-liver or single-lobe isolation of hepatocytes in livestock remains incredibly impractical, with relatively low viability and rapid phenotype loss in culture (19, 20). An alternative can be the use of hepatic cells isolated from newborn calves (21–24); however, extrapolation of results to hepatic metabolism of periparturient dairy cows is problematic, as from a biological standpoint liver of newborn calves is radically different than the liver of an adult cow (25).

A valuable alternative could be the use of precision-cut liver slices (PCLS), obtained through precise dissection of cylindrical liver samples under conditions that facilitate cell survival and allow maintenance of tissue morphology. As demonstrated in other species, PCLS can be a valuable tool to estimate hepatic lipid metabolism (26) and transcriptomic changes (27) *ex vivo*. However, the adoption of PCLS as a research tool for ruminants remains low. To the best of our knowledge, no published manuscript utilizes PCLS culture to study whole-transcriptome changes in the bovine liver.

The objective of the present study was to evaluate the feasibility of using PCLS obtained from periparturient dairy cows to assess activation of PPAR *via* transcriptomics-based approaches and identify PPAR target genes in bovine. We hypothesize that culture and treatment of PCLS with known PPAR agonists and antagonists would result in measurable changes in gene expression, the identification of which could shed light on the consequences of greater PPAR activation in the peripartum.

MATERIALS AND METHODS

Animals and Collection of Blood and Liver Tissue

Experimental procedures used in this study were approved by the Institutional Animal Care and Use Committee (IACUC) of Oregon State University (protocol# 4894). Liver biopsies were performed on four primiparous Jersey cows; however, one cow had to be removed from the study (see RT-qPCR). The biopsy was performed both during prepartum (−8.0 ± 3.6 DIM, henceforth referred to as "−10 DIM") and postpartum (+7.7 ± 1.2 DIM, henceforth referred to as "+10 DIM"). The area selected for puncture was clipped, and decontaminated using povidone iodine medical scrub (055478, Covetrus, OH, USA) followed by a solution of 75% ethanol, applied with a surgical gauze (100-1444, Henry Schein, NY, USA). A small incision was made using a #10 surgical blade (327-1504, Integra Miltex, PA, USA), and a 6 mm i.d. trocar was used to collect liver tissue up to 3 times until sufficient tissue was obtained (∼500–800 mg). The tissue was immediately transferred to a sterile tissue culture dish (351029, Corning Falcon, NY, USA), rinsed immediately in sterile phosphate buffered saline (25-508P, Genclone, CA, USA), and transferred to a 50 mL conical tube containing ice-cold Krebs-Henseleit buffer [KHB, prepared as previously described (28)] until further processing. Liver samples were transported from the collection site to the laboratory within 1 h. Pre-prandial blood samples were collected from each animal immediately before the liver biopsy, using Vacutainer blood collection tubes without anti-coagulants (366430, Becton, Dickinson and Company, NJ, USA). Samples were allowed to coagulate at room temperature for no <30 min. The serum was separated by centrifugation (15 min, 1,500 × g, 25°C), and kept at room temperature until all the liver slices were prepared (<1 h).

PCLS Preparation and Culture

PCLS were prepared following the protocol developed by De Graaf and collaborators (28), with few modifications. Briefly, liver tissue samples were transported to the laboratory in ice-cold KHB; upon arrival, they were immediately embedded in low temperature gelling ultrapure agarose (16500-100, Invitrogen, CA, USA) inside an 8 mm mold-plunger assembly (MD2200, tissue embedding unit, Alabama Research & Development, AL, USA). The plunger with the embedded tissue was then transferred to a Krumdieck Tissue Slicer (MD1000-A1, Alabama Research & Development, AL, USA), pre-filled with ice-cold KHB; slice thickness was set at 280–300 μm, with a cycle speed of ∼35 and using the "intermittent blade mode". Slices were then collected and placed on a new tissue culture dish, prefilled with a minimum amount of cold KHB to prevent dehydration. A total of 36 PCLS were selected for each animal at each timepoint, evaluating visually to identify those with the a clear circular shape, and without holes or patent morphological irregularities. The 36 PCLS were thus transferred to three 12-well culture plates (665180, Greiner Bio One, NC, USA) and the treatments were applied in duplicates. In Plates 1 and 2, PCLS were cultured in William's Medium E (WME, A1217601, Gibco, Thermo Fisher Scientific, MA, USA), supplemented with GlutaMAX (35050-061, Gibco, NY, USA), 14 mM of D-glucose monohydrate (0643-1KG, VWR, OH, USA), and 50 μg/mL of gentamycin (15750060, Life Technologies, OR, USA). Within the plate, PCLS were treated with 100 μM of the PPARα agonist WY-14643 (70730, Cayman Chemicals, MI, USA), 50 μM of the PPARδ agonist GW-501516 (ALX-420-032-M005, Enzo, NY, USA), or 100 μM of the PPARγ agonist rosiglitazone (R0106, TCI, OR, USA); 200 μM of palmitic acid (100905, MP Biomedicals, CA, USA) or 100 μM of serum NEFA, isolated *via* solid phase extraction as previously described (17). Palmitate was supplied unbound from albumin to mimic a local concentrated release (17). WY-14643 concentration was selected based on prior reports (29); additionally, according to our findings in an immortalized model of bovine liver (17), the dose-dependent response to PPARα and PPARγ was similar (hence the 100 μM concentration of both WY and rosiglitazone), while PPARδ modulation was about twice as sensitive (hence the 50 μM dose for GW-501516). Additionally, peak PPAR activation for palmitic acid was achieved at 200 μM. The concentration of NEFA was chosen to mimic the physiological concentration of NEFA in the lactating dairy cow. In Plate 3, PCLS from each cow were cultured in blood serum isolated from the same cow on the day of the liver biopsy; PPAR antagonists were added at 50 μM in duplicates to the wells: for PPARα, GW-6471 (9453, CAS# 880635-03-0, BioVision incorporated, CA, USA); for PPARδ, GSK-3787 (3961/10, CAS# 188591-46-0, Tocris, Bio-Techne Corporation, MN, USA); for PPARγ, GW-9662 (70785, CAS# 22978-25-2, Cayman Chemicals, MI, USA). Additionally, palmitic acid and serum NEFA were also supplemented with doses as in Plates 1 and 2. All treatments were adjusted for the vehicle (DMSO, D2438, Millipore Sigma, MO, USA) at a volume of 0.8%. Plates were placed in a modular incubator chamber (MIC-101, Billups-Rothenberg, CA, USA), clamped shut, and flushed with carbogen (95% O2, 5% CO2) for 10 min. The modular chamber was placed inside a cell culture incubator, and atop a benchtop orbital shaker located inside of the incubator. The slices were incubated for 18 h at 37°C, ∼100 rpm.

TAG Quantification

PCLS from Plate 1 were collected, and the two replicates for each treatment were pooled. Slices were homogenized using a handheld tissue homogenizer (850101019999, Scilogex, CT, USA), and whole-homogenate TAG were measured according to the manufacturer's instructions (10010303, Cayman Chemicals, MI, USA). A small amount of tissue homogenate from the first dilution was retained separately, and protein concentration was assessed using a Pierce BCA Protein Assay Kit (23225, Thermo Scientific, MA, USA), following the manufacturer's

instructions. Assayed TAG concentration was normalized to the protein concentration.

RNA Sequencing and RT-qPCR

RNA Isolation

PCLS from Plates 2 and 3 were collected after incubation, and transferred to separate screw-cap vials (490003-520, VWR, PA, USA), pre-filled with 600 μL of ice-cold TRIzol reagent (15596026, Thermo Scientific, MA, USA) and two 3.2 mm beads, homogenized using a Geno/Grinder Automated Tissue Homogenizer (2010-115, SPEX SamplePrep, NJ, USA; courtesy of the Department of Crop and Soil Sciences, Oregon State University, OR, USA). The tissue was disrupted in short burst (45 s) at 1,500 rpm, followed by incubation on ice for 3 min; the disruption-incubation cycle was repeated up to three times, or until no tissue pieces were visible within the tubes. Immediately after disruption, 120 μL of pre-chilled chloroform was added to the tube, and the samples were mixed by inverting the tube, and incubated on ice for 5 min. After incubation, the samples were transferred to a new 1.7 mL microcentrifuge tube, and centrifuged at 4°C for 15 min, 15,000×g. The upper-phase supernatant (∼200 μL) was collected and RNA was purified using a Mag-MAX-96 Total RNA Isolation Kit (AM1830, Invitrogen, MA, USA) following the manufacturer's instructions, with minor modifications: briefly, 100 μL of each sample was transferred to the first row (A) of a 96-Well DeepWell Storage Plate (260251, Thermo Scientific, MA, USA). Rows B-F contained reagents supplied with the kit: 20 μL of the magnetic beads mix (row B), 150 μL of wash solution 1 (row C), 150 μL of wash solution 2 (row D), and 50 μL of DNAse-RNAse free water (VWRL0201-0500, VWR, PA, USA) in rows E and F. A suitable protocol was then generated to mimic the manufacturer's protocol with a KingFisher Duo Purification System (5400110, Thermo Scientific, MA, USA). Eluted RNA was measured using a SpectraDrop Micro-Volume Microplate in a SpectraMax plus 384 spectrophotometer (89212-396, Molecular Devices, CA, USA). Average 260/230 and 260/280 ratios were 2.06 ± 0.24 and 1.69 ± 0.27, respectively. RNA integrity was assessed by the Center for Genome Research and Bioinformatics at Oregon State University using an Agilent Bioanalyzer 2100 (G2939BA, Agilent, CA, USA). For one animal, the RIN for the +10 DIM PCLS was below 3. Further, principal component analysis of RNAseq data revealed that animal to be a clear outlier and was removed from the study. Upon removal of that animal, resulting RNA integrity numbers were 7.26 ± 0.64 (mean ± SD).

RT-qPCR

Complementary DNA (cDNA) synthesis, PCR, and data analysis using LinRegPCR were performed as previously described (25). Primers used in this study are listed in **Supplementary Table S1**; all primers not sourced from a prior study were assessed by amplifying a mixture of bovine cDNA, and the resulting amplicon was sequenced by the Center for Genome Research and Bioinformatics (currently Center for Quantitative Life Sciences) at Oregon State University using an ABI 3730 capillary sequencer machine. Amplicons were aligned against the bovine genome using NCBI Basic Local Alignment Search Tool (BLAST) (30) to ensure specificity. Selection of internal control genes was accomplished using GeNorm (31). Potential reference genes *GAPDH, MRPL39* and *UXT* were tested *via* GeNorm. Results from GeNorm indicated that the geometrical mean of those 3 reference genes provided a robust normalization (V2/3 < 0.18).

Library Preparation and Sequencing

RNA isolated from PCLS from postpartum animals cultivated in William's E Medium and treated with the three isotype-specific PPAR agonists, as well as the control group, were sent to the Center for Genome Research and Bioinformatics at Oregon State University for high-throughput sequencing. Library construction was obtained using a QuantSeq 3' mRNA-Seq Library Prep Kit FWD for Illumina (015.96, Lexogen, NH, USA). Sequencing was performed on an Illumina HiSeq3000 platform, at 60 samples/lane. The raw reads have been deposited (GEO accession number GSE183063).

Quality Control and Differential Gene Expression Analysis

Quality control was assayed using MultiQC v1.8 (32) (https://multiqc.info/). Reads were then trimmed based on PHRED score and adapter presence using TRIMMOMATIC v0.39 (33) (https://github.com/usadellab/Trimmomatic) with arguments LEADING:5 TRAILING:5 SLIDINGWINDOW:4:5 MINLEN:3. A genome index was generated using the ARS-UCD1.2 *Bos Taurus* genome (http://ftp.ensembl.org/pub/release-104/fasta/bos_taurus/dna/) and the ARS-UCD1.2.104 annotation (http://ftp.ensembl.org/pub/release-104/gtf/bos_taurus/), using the genomeGenerate function of STAR v2.7.1 (34) (https://github.com/alexdobin/STAR). Trimmed reads were aligned against the reference genomic index using STAR, and the average overall alignment rate was 85.46%. Aligned.sam files were sorted and converted to.bam using samtools v1.0 (35) (https://github.com/samtools/samtools), and gene count matrices were generated using stringtie v 2.0 (https://ccb.jhu.edu/software/stringtie/).

Differential expression was determined using the DESeq2 package, v1.30.1 (36) (https://bioconductor.org/packages/release/bioc/html/DESeq2.html) in R v3.9, after filtering for low counts (any transcript with raw count ≤ 4). Three contrasts were generated (PPARA agonist vs. CTR, PPARD agonist vs. CTR, and PPARG agonist vs. CTR) and DEG were considered significant with an FDR-adjusted *p*-values below 0.2.

Bioinformatics Analyses: Ontology and Function

Functional analysis was performed using the Dynamic Impact Approach (37), as well as DAVID (38) (https://david.ncifcrf.gov/). Figures regarding functional analysis results were generated using the ggplot2 R package v3.3.3 (https://ggplot2.tidyverse.org/reference/ggplot.html), and treemaps using REVIGO (39) (http://revigo.irb.hr/).

To discriminate between actual gene targets of PPAR and genes that are differentially expressed in response to the treatment but not regulated by PPAR, we cross-referenced our results with the publicly available PPARgene database (http://www.ppargene.org/). This resource provides a comprehensive list

of 2,683 predicted targets, based on a logistic regression model that utilizes both experimental high-throughput sequencing data and the degree of conservation of the PPAR binding site within the human and mouse genome (40). A prediction score from 0 to 1 is assigned to each gene, with the authors defining a value below 0.6 as "low confidence", between 0.6 and 0.8 as "medium confidence", and between 0.8 and 1 as "high confidence". We extracted only medium and high confidence genes from the dataset to reduce potential confounding factors.

Statistical Analysis

Normalized RT-qPCR data were $\log_2$ transformed prior statistical analysis. Data were checked for outliers using PROC REG of SAS and datapoints with a studentized-t >2.8 were removed. Statistical analysis was performed as four separated datasets: PCLS from prepartum cows cultivated in artificial media; PCLS from prepartum cows cultivated in blood serum; PCLS from postpartum cows cultivated in artificial media; and PCLS from postpartum cows cultivated in blood serum. Final datasets were analyzed using PROC GLIMMIX of SAS (v9.4, SAS, NC, USA) using treatment as explanatory variable and cow as random variable using the default covariate model. Postpartum TAG data were analyzed through PROC GLM of SAS (v9.4, SAS, NC, USA), using treatment as the only explanatory variable. In all cases, a *p*-value of 0.1 was considered as the threshold for tendencies and a *p*-value of 0.05 was set as the threshold for significance between the pairwise comparisons.

RESULTS

RT-qPCR and TAG Quantification

In the first experiment we assessed the transcription of PPAR target genes upon treatment with various PPAR isotypes synthetic agonists in PCLS obtained from pre- and post-partum cows cultivated in synthetic media. In the same experiment we also treated PCLS with C16:0 and NEFA, both previously observed to be agonist of PPAR in bovine cells (17). The PCLS from each cow was treated with NEFA isolated from the same cow. Analysis of relative gene expression through RT-qPCR revealed minimal differences across treatments in the late prepartum (−10 DIM, **Figure 1A**), as well as the early postpartum (+10 DIM, **Figure 1B**). In the prepartum, transcription of *LIPC* was increased by all treatments except C16:0, with the highest effect observed for slices treated with a PPARδ agonist (GW-501516; 3.4-fold increase vs. untreated control). In the postpartum, treating liver slices with a PPARγ agonist (rosiglitazone) resulted in 2-fold increased transcription of *ACADVL* vs. untreated control. Treatment with GW-501516 increased expression of *PDK4*, *LIPC*, and *PPARD*. Only a tendency for higher TAG content in cells was observed in response to PPARδ agonist (**Figure 2**).

In a second experiment we assessed which PPAR isotype is activated by blood serum by using various PPAR isotype-specific antagonists with PCLS. Our assumption was that blood serum containing NEFA would activate PPAR. The dose of the antagonists was based on our prior work in immortalized bovine liver cells (17). We also treated cells with C16:0, to mimic

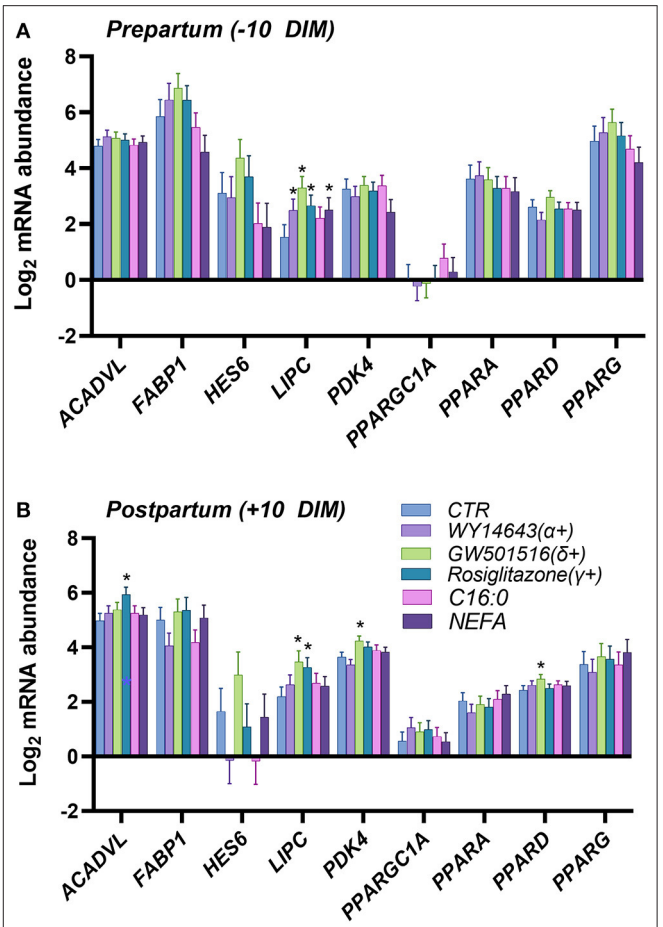

FIGURE 1 | Relative normalized expression of *ACADVL, FABP1, HES6, LIPC, PDK4, PGC1A, PPARA, PPARD* and *PPARG* in response to synthetic PPAR agonists (100 μM WY-14643, a PPARα agonist; 50 μM GW-501516, a PPARδ agonist; and 100 μM Rosiglitazone, a PPARγ agonist), 200 μM palmitic acid, or 100 μM NEFA isolated from each respective animal, in PCLS obtained from prepartum [**(A)**, −10 DIM] and postpartum [**(B)**, +10 DIM] cows, and cultured for 18 h in William's Medium E. *indicates significant differences ($P < 0.05$) when compared to WME control.

supplementation of this fatty acid in live animals. As for the first experiment, we detected a minimal effect on transcription of genes, especially in the PCLS obtained from pre-partum cows. We did not observe any overlap between the two experiments. In the prepartum (**Figure 3A**), transcription of *ACADVL* was increased in response to C16:0. The addition of the PPARγ antagonist increased the expression of *HES6* and *PPARG,* while the use of the PPARδ antagonist reduced the transcription of *PDK4*. In the postpartum (**Figure 3B**), treating liver slices with palmitic acid increased expression of *FABP1*, while the PPARδ antagonist significantly downregulated *PDK4* and the PPARγ antagonist decreased transcription of *LIPC* and *PPARGC1A*.

RNA Sequencing and Functional Analysis

Differentially Expressed Genes

Gene expression profiling was performed through RNA sequencing for PCLS from postpartum animals (+10 DIM),

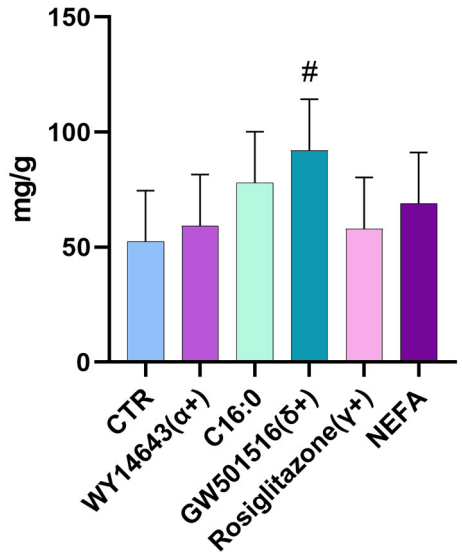

FIGURE 2 | Amount of triacylglycerol in PCLS from postpartum cows (+10 DIM) treated with PPAR isotype-specific agonists (100 μM WY-14643, a PPARα agonist; 50 μM GW-501516, a PPARδ agonist; and 100 μM Rosiglitazone, a PPARγ agonist), 200 μM palmitic acid, or 100 μM NEFA isolated from each respective animal. Results are presented as fold change vs. each animal's control group (PCLS cultured in William's Medium E only). #indicates tendencies ($P < 0.1$) when compared to control. Incubation time was 18 h.

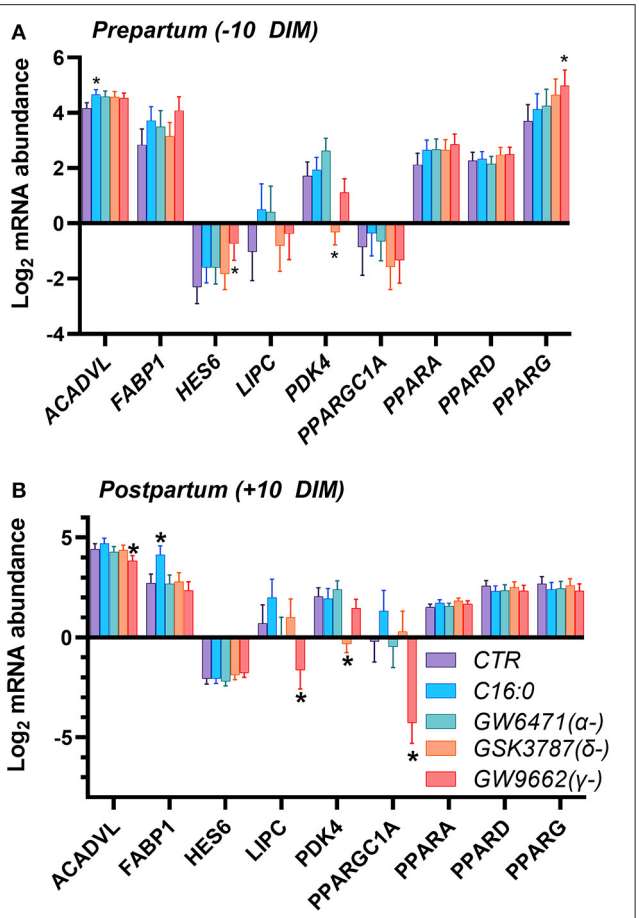

FIGURE 3 | Relative normalized expression of *ACADVL, FABP1, HES6, LIPC, PDK4, PGC1A, PPARA, PPARD* and *PPARG* in response to synthetic PPAR antagonists (50 μM GW-6471, a PPARα antagonist; 50 μM GSK-3787, a PPARδ antagonist; and 50 μM GW-9662, a PPARγ antagonist) or 200 μM palmitic acid, in PCLS obtained from prepartum (**A**, −10 DIM) and postpartum (**B**, +10 DIM) cows, and cultured in blood serum. *Indicates significant differences ($P < 0.05$) when compared to serum control; Incubation time was 18 h.

which were treated with isotype-specific agonists for PPARα (WY-14643), PPARδ (GW-501516) and PPARγ (rosiglitazone). Complete dataset is available in **Supplementary File 1**.

Principal component analysis revealed considerable separation with minimal overlap between the treatment groups, suggesting moderate differences in the gene expression landscape (**Supplementary Figure S1**). Analysis through DESeq2 (**Table 1**) revealed a total of 140, 173, and 222 DEG with a cut-off of FDR-adjusted p-values = 0.1 by the PPARα, PPARδ, and PPARγ agonist, respectively. A more liberal cutoff of FDR-adjusted p-values = 0.2 indicated 308, 501, and 379 DEG by the PPARα, PPARδ, and PPARγ agonist, respectively. The latter statistical results were used for downstream analyses.

Dynamic Impact Approach

The Dynamic Impact Approach (**DIA**) analysis (**Figure 4**) revealed a large impact of both the PPARα and PPARδ agonists on KEGG categories related to metabolism, chiefly carbohydrate and lipid metabolism, all of which had a pattern toward activation of the pathways. Of note, though the impact of the PPARγ agonist on metabolism was lower than the other two PPAR agonists, a strong effect on lipid metabolism was maintained, also with a positive trend. Additionally, samples treated with the PPARγ agonist displayed a strong inhibitory effect on KEGG subcategories related to "Signaling Molecules and Interaction" and under the "Immune System" subcategory of pathways, while the other two PPAR agonists did not.

TABLE 1 | List of differentially expressed genes in PCLS for the three comparisons of interest.

vs. CTR	FDR-Adj	DEG up	DEG down	DEG total
PPARα agonist	0.1	59	81	140
PPARδ agonist	0.1	47	126	173
PPARγ agonist	0.1	127	95	222
PPARα agonist	0.2	191	117	308
PPARδ agonist	0.2	334	167	501
PPARγ agonist	0.2	174	205	379

In terms of individual pathways within the KEGG subcategories (**Figure 5**), for the "Carbohydrate Metabolism" subcategory, all three groups had a modest positive impact on "Pentose and glucuronate interconversions", as well as "Glyoxylate and dicarboxylate metabolism", and "Ascorbate and aldarate metabolism". In the "Lipid Metabolism" subcategory,

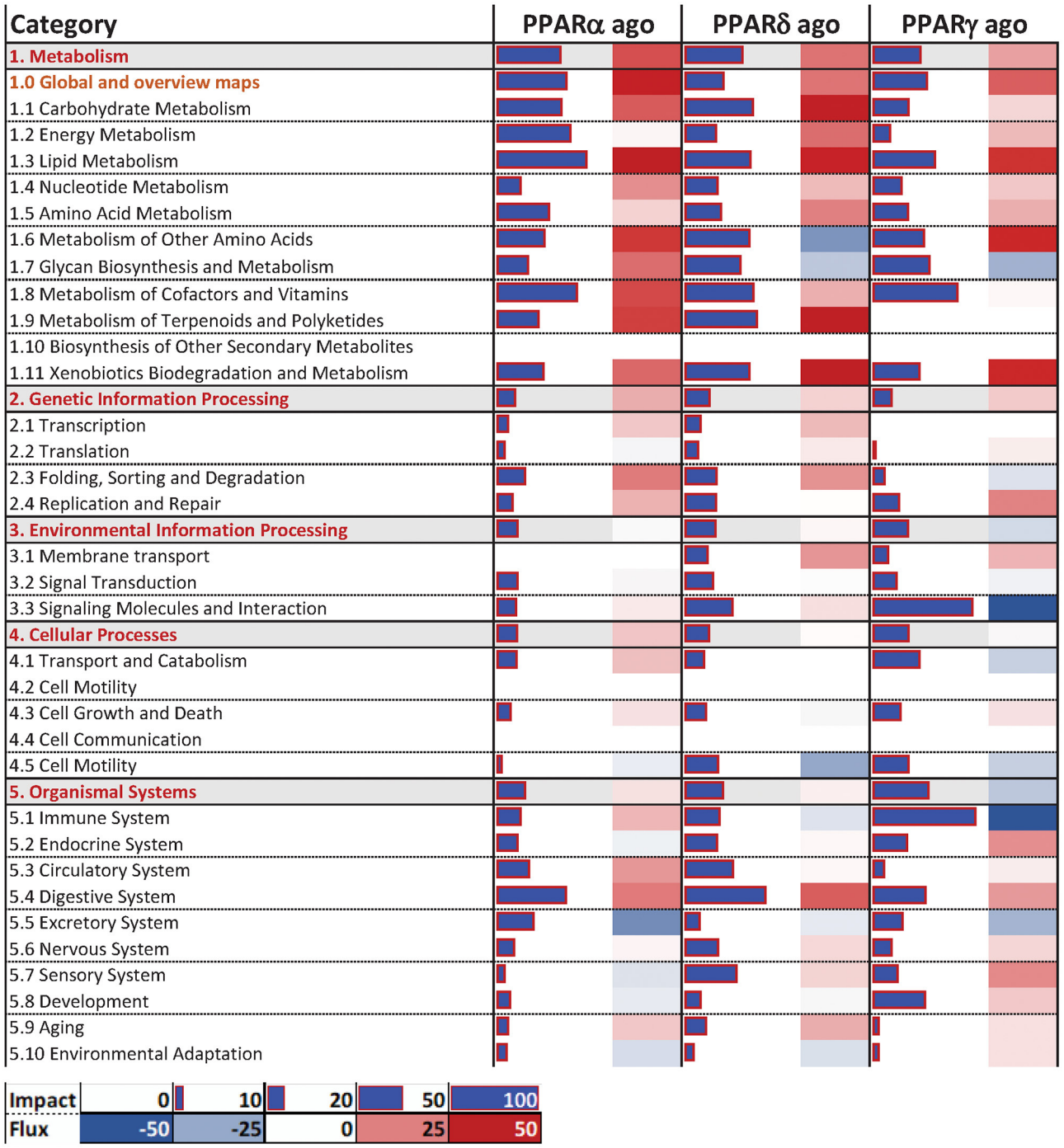

FIGURE 4 | Main categories and subcategories of KEGG pathways induced *via* the use of isotype-specific PPAR agonists in PCLS, as summarized by the Dynamic Impact Approach. Blue bars refer to the impact in terms of overrepresented genes in the pathways, while the shaded cell denotes the flux, i.e., the overall effect on the pathway, with red denoting activation and green denoting inhibition.

PPAR agonists had comparable positive impacts on "Metabolism of linoleic acid", as well as "Fatty acid degradation" and the "Metabolism of ether lipids" (although to a lesser degree). Additionally, only the PPARα and PPARδ agonists induced the pathway "Synthesis and degradation of ketone bodies". In the "Signaling Molecules and Interaction" and "Immune System" subcategories of KEGG pathways, the most consistent and noticeable effect was brought forth by the PPARγ agonist,

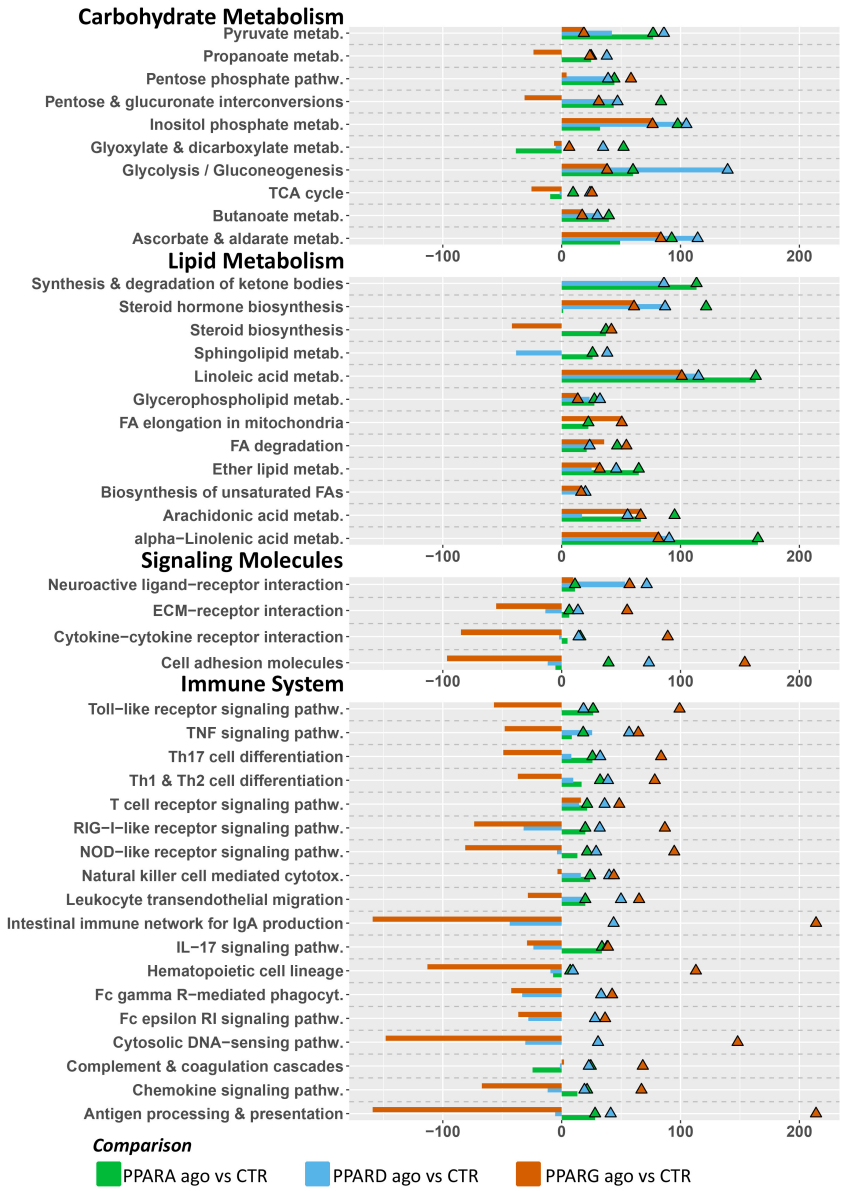

FIGURE 5 | Main KEGG pathways highlighted by DIA, divided by subcategory. Triangles (color-coded) represent the impact in terms of overrepresented genes in the pathways, whereas bars (also color-coded) refer to the overall flux of the pathway, with negative numbers indicating inhibition of the pathway, and positive numbers indicating induction of the pathway.

moderately or strongly inhibiting signaling-related pathways such as "Cytokine-cytokine receptor interaction" and "Cell adhesion molecules". Additionally, signaling of several immune-related receptors like the toll-like receptor (TLR), tumor necrosis factor (TNF), and RIG-I-like receptor and NOD-like receptor was inhibited. Further, the PPARγ agonist inhibited the "Antigen processing and presentation" and "Chemokine signaling" pathways.

DAVID

The analysis of enriched Gene Ontology (GO) terms by DAVID confirmed results from the DIA (**Figure 6**; **Supplementary Figures S2–S7**), where samples treated with a PPARγ agonist present an enrichment of the terms "T cell activation," "response to cytokine," "chemokine activity," "immune response", "inflammatory response," and "immune system process" within the cohort of downregulated genes. Further, upregulated genes in response to the PPARδ agonist were overrepresented in the "TAG homeostasis" GO term.

Predicted PPAR Targets

Combining the database in PPARgene with our DEGs, and sub-setting the database to include only values with prediction score > 0.6, reveals a total of 91 predicted targets that were

FIGURE 6 | Overrepresented gene ontology (GO) terms with a p-value < 0.01, according to DAVID, by the three PPAR agonists. Pathways associated with positive numbers are overrepresented in the subset of genes significantly upregulated by the treatment, whereas pathways represented by a negative number are overrepresented in the genes significantly downregulated by the treatment. Absolute numbers correspond to fold enrichment of the pathway.

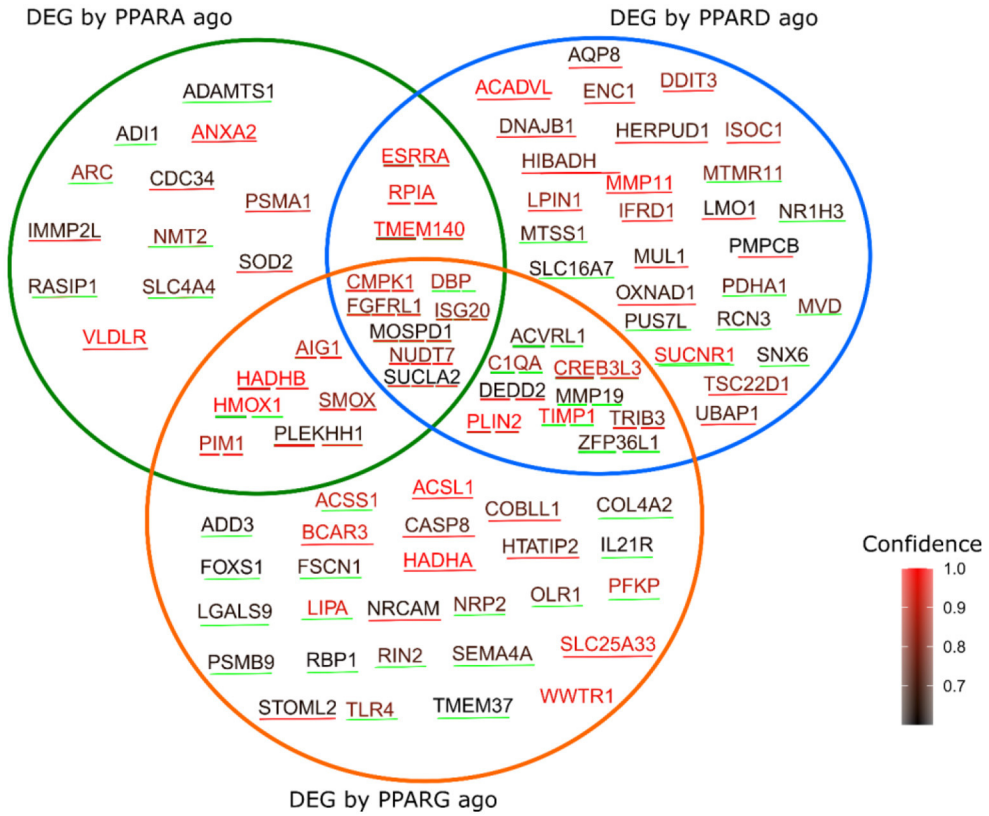

FIGURE 7 | Genes predicted as PPAR target by the PPARgene algorithm, which were also differentially expressed by the three treatments in the current study. The color of the words corresponds to the degree of confidence of the prediction, while the color of the underlining line indicates the direction of the differential expression, with red indicating upregulation in response to the treatment, and green indicating downregulation.

differentially expressed in the three contrasts in our experiment (**Figure 7**); namely, 12 predicted targets were differentially expressed by the PPARα agonist alone (five were up-regulated), 27 by the PPARδ agonist alone (17 up-regulated), and 27 by the PPARγ agonist alone (eight were up-regulated). Further, three genes were differentially expressed by both the PPARα and PPARδ agonists (all up-regulated), six by both the PPARα and PPARγ agonists (five up-regulated), nine by both the PPARδ and PPARγ agonists (four up-regulated), and seven by all three agonists (six up-regulated).

DISCUSSION

Synthetic PPAR Agonists and Antagonists Modulate Very Few Putative PPAR Targets and in the Postpartum Only

A reliable indicator of PPAR activation is the expression of canonical PPAR target genes in response to a putative ligand. Our results indicate a minor modulation of putative PPAR targets in response to PPAR agonists and antagonists in bovine liver PCLS both when cultivated in culture medium or in homologous blood serum. Although we observed minor effects, any effect on the transcription of putative PPAR targets was mostly detectable in post-partum PCLS samples. Prior studies in bovine, which highlight that modulation of PPAR target through supplementation of saturated fatty acids elicits a response primarily in the postpartum, are in line with our results: cows supplemented with saturated fatty acids, proven to be a PPAR ligand in bovine cells (17), displayed an increase in hepatic expression of putative PPAR targets (e.g., *PLIN2*, *FABP1*, *ACOX1*) between −14 and +7 days relative to parturition (16). The same design revealed similar outcomes in the adipose tissue, where canonical PPARγ targets were found to be upregulated slightly in the prepartum, but the greatest impact was found in the postpartum in response to either saturated fat or fish oil (rich in unsaturated fatty acids) (41).

Our present data appear to contrast with our prior study, where data indicated a stronger PPAR activation in cultured bovine cells when treated with pre-partum rather than post-partum blood serum (17). Among all genes measured, the *PDK4*, a well-established PPARδ target (42) was consistently affected by the use of synthetic PPARδ agonist or antagonist in the present study confirming results from our prior study using bovine immortalized cells (17, 43). Those data indicated a key role of PPARδ in bovine liver but also

confirm that PDK4 is a reliable marker of PPARδ activation in bovine.

The minor effect on the transcription of the RT-qPCR measured putative PPAR target genes in the PCLS treated with the various PPAR agonists may indicate poor response of the liver to PPAR agonist. This is a possibility, considering the poor response observed in prior studies using *in vivo* supplementation of C16:0 on liver transcriptome (16, 44, 45) or the lack of response on P450 enzyme activity to the PPARα agonist Wy-14643 in goats (46). This possibility would be a major obstacle for any nutrigenomic interventions to improve liver performance in dairy cows *via* activation of PPAR, as previously advocated (13).

The genes selected for the RT-qPCR are only putative PPAR targets in bovine, since studies to identify true PPAR isotype specific target genes are still lacking [although the problem has been pointed out for almost a decade (13)]. Thus, it is possible that the relatively minor effect observed through RT-qPCR may be due to an inaccurate choice of target genes on our part. For this reason, we analyzed gene expression at a whole-transcriptome level to assess if there was any response of PCLS to PPAR agonists and, if so, determine PPAR targets in bovine liver.

Activation of PPAR Does Not Affect TAG in Bovine PCLS

The relatively minor changes in terms of canonical PPAR targets were apparently in line with the minor effect on the amount of TAG in the PCLS. The level of TAG in liver of cows are the combined result of re-esterification of circulating NEFA in TAG that are accumulated as lipid droplets and then released with the VLDL. The synthetic media used in our experiment was supplemented with 10% FBS, containing an overall low amount of free fatty acids (**FA**); thus, the addition of NEFA and C16:0 should have increased accumulation of TAG, if no increase in oxidation was present. On the other hand, the activation of PPARα and PPARδ should have increased oxidation of fatty acids and, perhaps, even increase VLDL secretion (13); thus, we were expecting a decrease in TAG with those treatments.

The role of PPAR in the regulation of hepatic TAG is unclear as prior studies on the topic have revealed. In mice fed a diet deficient in methionine and choline (simulating conditions experienced during non-alcoholic steatohepatitis), administration of the PPARδ agonist GW501516 and the pan-agonist bezafibrate markedly reduced hepatic TAG and lipid droplet size in hepatocytes (47); on the other hand, the same PPARδ agonist failed to reduce liver TAG in mice consuming a "Western type" high-fat diet, though circulating plasma TAG were significantly lower (48). Finally, in mice chronically exposed to carbon tetrachloride (causing fibrosis in the liver), treatment with GW501516 caused a net increase in liver TAG, which was not observed in the PPARδ-knockout population, indicating that activation of PPARδ is required for TAG accumulation under those conditions (49). It is unclear why we observed a tendency for higher TAG accumulation in PCLS treated with PPARδ in our experiment, but we cannot exclude that activation of PPARδ could increase TAG accumulation *in vivo*.

For the PPARα (WY-14643) and PPARγ (rosiglitazone) agonists, the situation is remarkably similar: though most studies report a reduction of plasma TAG (postprandial) when administering PPARα and PPARγ agonist (50–52), conflicting reports exist on the impact on hepatic TAG. In mice fed a high-fat diet, both rosiglitazone and WY-14643, as well as ragaglitazar (dual PPARα/PPARγ agonist) significantly decreased both TAG accumulation and TAG production rates in the liver, with the dual agonist achieving TAG concentrations equal to the control group fed a normal diet (53). In addition, mice exposed to a methionine- and choline-deficient diet (similar to the scenario discussed for the PPARδ agonist above), had a sharp reduction in hepatic TAG after treatment with WY-14643 (54). On the other hand, WY-14643 effected a sharp increase in TAG in primary mouse hepatocytes (55), and induced expression of *HILPDA* in mouse PCLS, the overexpression of which caused a marked decrease in hepatic TAG secretion, and a consequent increase in TAG content within the liver (56). In the present experiment with bovine PCLS, the same transcript was not affected by WY-14643 (**Supplementary File 1**). Similarly, treatment of genetically diabetic mice with rosiglitazone increased hepatic TAG (57, 58). Other studies have noted that liver-specific expression levels of PPARγ determine the outcome of administering the agonist, as mice with low hepatic *Pparg* expression saw a reduction in TAG accumulation, while mice with high hepatic *Pparg* expression displayed a consistent increase in hepatic TAG (59).

The available evidence seems to suggest that in certain pathophysiological conditions and drastic metabolic alterations, the activation of PPAR (regardless of isotype) can contribute to the clearance of TAG, whereas in metabolically stable animals the outcome is the opposite. It is worth considering that in the studies cited above the agonists were administered for at least 12 days (in the shortest trial) and up to 9 weeks (in the longest); though PCLS are technically viable up to 96 h (28), we noticed significant RNA degradation (RIN < 6) after 24 h of incubation (data not shown). As such, a combination of different metabolic conditions between the animals in our study and those in the cited studies, combined with a markedly shorter incubation time with the agonists, might explain the lack of significant differences in our results.

Activation of All PPAR Isotypes Induce Pathways Related to Lipid Metabolism

Based on the findings revealed by the DIA analysis, activation of any of the three PPAR isotypes leads to a strong activation of lipid metabolism. The apparent activation of lipid metabolism aligns with the findings of previous investigations. Treatment of liver slices of dairy calves with the PPARα agonist clofibrate led to a significant increase in expression of genes associated with lipid metabolism (60), while an *in vitro* investigation in goat mammary epithelial cells found that activation of PPARδ with the synthetic agonist GW0742 resulted in increased expression of genes associated with fatty acid activation and lipid transport (61). Interestingly, both these studies found significant upregulation of *ACSL1*, the long-chain member of the acyl-coenzyme A synthetase family. Although *PPARG* is typically more abundant in the adipose tissue than in the liver of dairy cattle, we did

find a significant upregulation of genes associated with lipid metabolism when the PPARγ agonist rosiglitazone was used as well. Prior work examining PPARγ activity in the liver of ruminants is limited, but activation of PPARγ in the liver of non-ruminants seems to produce a similar upregulation of genes associated with lipid accumulation as is seen in the adipose tissue (62).

Activation of PPARγ Modulates Pathways Associated With the Immune Response in Liver

Activation of PPARγ resulted in a general inhibition of pathways associated with the immune system. PPARγ has a well-investigated role in modulating the immune response and inflammation (63), with activation of PPARγ limiting the expression of pro-inflammatory cytokines like TNFα (64). Activation of PPARγ in the liver could also impact biliary duct maintenance by regulating intracellular TLR signaling (65).

The inhibition of the immune system revealed by the DIA and DAVID when the liver slices were treated with the PPARγ agonist seems to be driven by several pathways, with the stronger effect observed in the IgA production and antigen processing and presentation. The inhibition of those pathways is mainly driven by the downregulation in transcription coding for major histocompatibility complex-associated proteins involved in the antigen processing and presentation. This effect is likely from the immune cells present in the liver, including Kupfer dendritic cells, Kupffer cells and monocyte-derived myeloid cells that are the most important when considering the antigen processing and presentation in the liver (66). Our tissue culture model likely included all those cells, as indicated by the relatively high RNSA abundance of Kupffer cells markers (**Supplementary File 1**).

Our results indicate a potential role of activation of PPARγ in reducing inflammation and immune activation in the liver. This can have important practical implications for transition dairy cows, due to the known negative effect of the liver's response to inflammation on performance and liver function in dairy cows (67).

In silico Analysis and Gene Expression Patterns Identifies Novel Putative PPAR Targets in Dairy Cattle

Confirmed PPAR Targets

Most of Confirmed PPAR Targets Are Involved in Lipid Metabolism

The comparison between PPAR targets predicted by PPARgene and DEG in response to PPAR agonists in this study revealed significant overlap. Some of the identified targets across treatment groups are well-documented PPAR targets: *ACADVL*, involved in the oxidation of very long chain FA, is a known target of PPARδ in monogastrics (68) as well as in cattle (13, 69), and its expression was found to be responsive to NEFA and modulated by metabolic changes in the peripartum (10, 70). In our RNAseq data, *ACADVL* was upregulated in response to the PPARδ agonist. This was not confirmed by the RTqPCR data (see the limitation session). Similarly, perilipin 2 (*PLIN2*), upregulated by both the PPARδ and PPARγ agonists, is a known PPAR target in monogastrics (71), though it is of note that while in monogastrics *PLIN2* is identified as a target of PPARα, studies in goats found its expression to be responsive to rosiglitazone, the same PPARγ agonist used in this study (72). *VLDLR*, the gene encoding the VLDL receptor, was upregulated by the PPARα agonist, and substantial evidence exists indicating it as a target gene of PPARδ (73) and PPARα (74), through which it contributes to lowering serum TAG in mice. Transcription of *LPIN1* was upregulated by the PPARδ agonist in PCLS in our study, the same transcript was previously identified as a PPAR target in bovine cells (13) and several monogastric species (75).

Most of the genes identified as putative targets have a role in the metabolism of lipids and fatty acids, inflammation, the immune response, and the antioxidant system. Of the ones related to lipid and fatty acid metabolism, *ACSS1* and *ACSL1*, encoding acyl-CoA synthetase 2 and acyl-CoA synthetase long-chain, respectively, were differentially expressed in response to the PPARγ agonist rosiglitazone in our study, and are known PPAR targets in monogastrics (76, 77). *ACSL1* in particular was shown to regulate plasma TAG amount through the PPARγ pathway in humans (77); however, these results do not seem to be replicated in prior bovine studies, at least as it pertains to mammary epithelial cells, as the expression of *ACSL1* was not altered by rosiglitazone or several fatty acids (78). Whether modulation of *ACSL1* can be possible and relevant beyond the liver in bovine remains to be determined. Within the same category, *HTATIP2* was upregulated, and *LIPA* and *OLR1* were downregulated in PCLS treated with a PPARγ agonist. *HTATIP2*, which encodes an oxidoreductase, was previously shown to form a complex with acyl-CoA synthase 4 (79), and its overexpression in mouse hepatocytes altered fatty acid metabolism by reducing oxidation rates, and increased esterification as either TAG or cholesteryl esters (80). Additionally, *HTATIP2* expression increased in the liver of ciprofibrate-treated *Cynomolgus* monkeys (81); though ciprofibrate (and fibrates in general) are regarded as PPARα agonists, which would suggest that *HTATIP2* is a PPARα target in monogastric, some evidence exists for the role of ciprofibrate in activating PPARγ at larger doses (82).

LIPA, encoding a lysosomal lipase, was previously found to be downregulated in PPARγ-knockout mouse prostate epithelial cells (83), and by overexpression of PPARγΔ5, a recently-discovered isoform of PPARγ, in HEK293 cells (84). Interestingly, mutations in the *LIPA* gene can lead to defects in the storage of cholesteryl esters, which would suggest a plausible link between *LIPA* and *HTATIP2*. Finally, *OLR1*, a receptor for oxidized LDL, was found to be upregulated by rosiglitazone and downregulated in response to the PPARγ antagonist PD068235 in 3T3-L1 mouse adipocytes (85), and its expression was highly correlated with that of PPARγ in porcine adipose tissue (86). An upregulation of the oxidized LDL receptor can lead to increased uptake of oxidized LDL, as well as the accumulation of TAG (86). Downregulation of *OLR1* and *LIPA* suggest that, in the bovine liver, PPARγ agonists may lead to decreased accumulation of TAG; this is further substantiated by the upregulation of *COBLL1*

in response to the PPARγ agonist, and of *CREB3L3* by both the PPARγ and PPARδ agonist. In human SGBS preadipocytes, knockout of *COBLL1* increased TAG accumulation by ∼30% (87), while *CREB3L3* ablation in mice led to a dramatic increase (∼4-fold) in circulating TAG and a consequent increase in hepatic TAG, along with increased ketogenesis (88), though existing evidence in monogastrics highlights a major interaction with PPARα (89), not PPARδ or PPARγ. Our results seem in partial disagreement with these findings, as the amount of TAG in post-partum slices was not significantly different between treatment groups. As mentioned earlier in the discussion, a plausible explanation could be the limited incubation time (∼18 h) of the PCLS, suggesting that a longer timeframe may be needed to witness biologically relevant effects.

Among the putative targets, evidence emerges for a role of PPAR agonists in the regulation of FA oxidation through novel mechanisms. *HADHA* and *HADHB*, encoding the subunits of the mitochondrial trifunctional protein MTP, were upregulated by the PPARγ agonist (*HADHA*) and by the PPARα and PPARγ agonist (*HADHB*). MTP is an enzyme associated with the inner mitochondrial membrane, and it catalyzes the final steps of the beta oxidation of long-chain FA in the mitochondria (90). Bezafibrate, a PPARα agonist, upregulated both *HADHA* and *HADHB* in human skin fibroblasts (90), while the PPARα/PPARγ dual agonist LY465608 increased expression of *HADHB* in both rat and dog hepatocytes, simultaneously increasing FA oxidation as measured by acyl-CoA and carnitine palmitoyl transferase I activity (91). Additionally, *NUDT7*, upregulated by all of three PPAR agonists in our study, is known to regulate peroxisomal FA oxidation by modulating coenzyme A degradation (92), and its expression is responsive to PPARα agonist WY-14643 in mouse liver (93). Limited evidence exists for the role of *HADHA/B* and *NUD7* in bovines, most of which is in regards to unrelated production parameters such as meat color (94).

Few PPAR Targets Are Coding for Proteins Involved in Antioxidant Response

Two of the putative targets suggest a possible role of PPAR isotypes in regulating the antioxidant response: *SOD2*, encoding mitochondrial manganese superoxide dismutase, is directly regulated by PPARα, and downregulated in PPARα-/– mice (95), and accordingly our results found it upregulated in response to the PPARα agonist. On the other hand, *HMOX1* (hemoxygenase-1) was downregulated by both the PPARα and PPARγ agonists. Studies in rat liver identified a response of *HMOX1* to pioglitazone (PPARγ agonist) (96); this may be a product of indirect regulation, as PPARγ agonist rosiglitazone is known to activate the AMP kinase pathway, of which *HMOX1* is a target (97). To our knowledge, a link between PPAR isotypes and *HMOX1*/*SOD2* has not been elucidated in bovines.

PPAR Targets and Insulin Signaling-Related Functions

DBP, downregulated by all three PPAR agonists, and *TRIB3*, upregulated by both the PPARδ and PPARγ agonists, are involved in regulating insulin sensitivity. Acetylation of histone 3 lysine 9 at the promoter region of *DBP*, and its consequent upregulation, plays a role in regulation of glucose homeostasis and is related to PPARγ in mice (98) and humans with type 2 diabetes (99), while *TRIB3* affects response to insulin by inhibiting Akt phosphorylation (100), and its activity is directly related to that of PPARγ (101). The differential expression of *TRIB3* observed in response to the PPARδ agonist may be a feature unique to the bovine liver: though a possible link between *TRIB3* expression and PPARα has been established (102), no evidence of an interaction with PPARδ has been elucidated.

Confirmed Targets Repressed by PPARγ Are Involved in Inflammation and Immune Regulation

Five genes among the identified putative targets are involved in the regulation of the immune response: *IL21R, LGALS9, SEMA4A, NRP2,* and *TLR4* were all downregulated in the PPARγ agonist group. *IL21R*, encoding an interleukin receptor, is known to play a role in ensuring proper function of T cells in mice (103), and was previously found upregulated by the pan-PPAR agonist elafibranor (104). *LGALS9* (galectin 9) is involved in T cell exhaustion (105), and activates AMPK (106), and was found to be strongly downregulated in response to rosiglitazone (the same PPARγ agonist as in our study) in 3T3-L1 preadipocytes (107). *SEMA4A* encodes semaphorin-4a and its activity is directly dependent on its receptors, neuropilins (of which *NRP2* is one); *SEMA4A* is involved in the proliferation of CD4+ T cells in mice and human (108), and in the function and survival of regulatory T cells in mice (109). Though no direct evidence exists of a link between PPAR and *SEMA4A*, other studies have shown that PPAR agonists can regulate other semaphorins, such as *SEMA6B* [downregulated by all PPAR isotypes in human genomic fragments *in vitro* (110)] and *SEMA3G* [upregulated by PPARγ ligands in human endothelial cells (111)]. Finally, Toll-like receptor 4 (*TLR-4*), also downregulated by the PPARγ in our study, regulates the adaptive immune response by triggering production of pro-inflammatory cytokines. In accordance with our results, rosiglitazone-treated rats displayed lower expression of *TLR4* (112), and human HMEC-1 mammary epithelial cells treated with hypaphorine, which decreased PPARγ expression, had a drastic upregulation of *TLR4* (113).

Novel PPAR Targets Are Likely Involved in Regulation of Inflammation

A considerable number of genes related to metalloproteinases (MMP) was observed among the novel putative targets, mostly modulated by the PPARδ and PPARγ agonists. *MMP19* was downregulated in both groups, as well as *TIMP1*, a protein involved in the intracellular regulation of MMP, the abundance of which was markedly lower in rat chondrocytes treated with GW-501516 and rosiglitazone, the same PPARδ and PPARγ agonists used in this study (114). On the other hand, *MMP11* was upregulated in response to the PPARδ agonist in our study. Finally, *ADAMTS1*, a zinc-binding metalloproteinase, was downregulated in response to the PPARα agonist. MMPs have a known role in regulating inflammation, and some evidence of a link with PPAR activity is present in the literature for monogastrics (115, 116). This is certainly the case for *MMP19*, involved in the development of T cells in mice (117); *MMP11*, related to several cytokines in breast cancer cells (118); and

ADAMTS1, a known regulator of the inflammatory response (119). The concerted modulation of several MMPs in our study suggests an intricated landscape of the inflammatory response as regulated by PPAR.

LIMITATIONS

1) Slice thickness and compound absorption: though the Krumdieck tissue slicer provides relatively consistent precision throughout the slices, prior studies have shown that the thickness of bovine PCLS is remarkably less consistent between slices than that of human, pig, rat and mouse (120). The absorption of small molecules (such as the PPAR agonists used in this manuscript, or C16:0) relies heavily on slice thickness, as the rate of diffusion is limited by the rapid extraction of the compound by the cells in the outer layer (121). A reduction of the slice thickness to 100 μm could ensure that all cells are metabolizing the compound (121); however, the likelihood of obtaining brittle tissue (especially in the inconsistency-prone bovine PCLS) increases greatly, rendering the endeavor practically impossible. Future studies may benefit from the use of more accurate machines in the preparation of PCLS, such as the Leica VT1200 S (120).
2) Cellular composition of PCLS: utilizing liver slices ensures that the histology and morphology of the tissue is maintained; however, obtaining liver samples through liver biopsy does not guarantee homogenous composition of each sample, as the operator cannot visually identify the lobes of the liver prior to puncture. Though these differences are bound to be minor, two slices proceeding from different areas of the liver are likely to display different patterns of gene expression. In future studies, the use of ultrasonographic examination to determine liver morphology prior to sampling may allow to obtain more consistent results.
3) Statistical power: the study had a relatively low sample size (originally four animals but in the final analysis only three animals, especially for the RNAseq dataset). This led to large variability between biological replicates, especially in the prepartum, where the range of DIM of the four samples was rather large (prepartum samples were collected based on expected calving dates, which can be an imprecise estimate for some animals). The reason for such limitation is 2-fold: one was financial, the utilization of different treatments resulted in a relatively large number of samples to be sequenced reaching the maximum financial allowance for such analysis; the other reason was the attempt to minimize the use of animals. To partially addressed those issues and minimize technical variation, samples from each animal were run in duplicate *in vitro* and post-treatment duplicates were pooled, as indicated above. Future studies will benefit from a more limited range of treatments and larger replication for each group, which will undoubtedly be more feasible considering the rapidly declining costs of NGS technologies.
4) Breed and parity: our study included only primiparous Jersey cows. Other breeds and multiparous cows may have a different response to our experimental setup. For example: Holstein cows have a greater loss of body condition in the peripartum, as well as higher NEFA and BHBA postpartum, and overall higher negative energy balance (122–124). All of these would like impact the response of PCLS to PPAR activation. The present study is meant to be a starting point for further exploration of PPAR activation in bovines using PCLS; future studies will undoubtedly benefit from including other breeds and test multiparous cows.
5) To optimize the use of the limited funding available to achieve the stated objective, many samples (60) were sequenced in each lane. Though the library prep kit used is apt at maximizing sequencing depth when compared with other commercial solutions, we noticed that many transcripts with (typically) a relatively low expression were either not detected or detected at very low level, with zero-counts in most samples. Despite being able to detect >14,000 transcripts with a count>4 in at the least one sample, which is somewhat similar to what previously reported in RNAseq analysis of bovine liver (125–127), many transcripts with a relatively medium-low expression were either not detected or detected at very low level, with lack of detection in most samples. Most of the genes used for the RT-qPCR were in this category, such as all PPAR transcripts and *LIPC*. Other were undetectable in RNAseq, such as *PPARGC1A* and *HES6*. Among the transcripts detected in all the samples (i.e., *PDK4*, *ACADVL*, and *FABP1*), a positive correlation was observed between results of RTqPCR and RNAseq when both were normalized using reference genes (**Supplementary File 2**). The low depth likely limited the discovery of other PPAR target genes.

CONCLUSIONS

Bovine PCLS are responsive to treatment with PPAR agonists and reveal a complex and heterogeneous transcriptomic response. Though minimal changes in TAG accumulation were detected, suggesting no effective changes in oxidation and esterification rates, several genes involved in lipid metabolism were altered in response to the PPAR agonists in the postpartum, suggesting that the lack of enzymatic effect may be due to the relatively short incubation time. An important suggestion from our study is a relationship between PPARγ activation and potential decreased inflammation in the liver, that can tremendously benefit post-partum cows. Of the differentially expressed genes identified in the study, a considerable number of them corresponds to putative PPAR target genes, predicted *in silico*; further, many of these find support in the literature, as prior studies highlight their link with PPAR activation. In summary, PCLS represent a valuable model of the bovine liver of periparturient dairy cows

DATA AVAILABILITY STATEMENT

Raw sequencing reads have been deposited to NCBI Gene Expression Omnibus (GEO accession number GSE183063). All relevant processed data is provided in the **Supplementary Materials**. Any additional documents will be provided by the authors upon request.

ETHICS STATEMENT

The animal study was reviewed and approved by Institutional Animal Care and Use Committee (IACUC) of Oregon State University (protocol# 4894).

AUTHOR CONTRIBUTIONS

SB helped performing liver biopsy, collected blood, optimized the PCLS, performed all the experiments, analyzed the data, interpreted the data, and wrote the manuscript. HF helped interpreting the data and revised the manuscript. AA performed RT-qPCR analysis and revised the manuscript. CE performed liver biopsies and revised the manuscript. MB received the funding, helped in interpreting the data, helped writing the manuscript, and revised the final manuscript. All authors contributed to the article and approved the submitted version.

FUNDING

This project was funded by the Oregon Beef Council.

ACKNOWLEDGMENTS

The authors acknowledge the help of Larissa Lewis, manager of the Oregon State University Dairy Center in getting and preparing the cows for the experiment. We thank Dr. William E. David, University Distinguished Professor, Department of Environmental and Molecular Toxicology at Oregon State University for lending us the Krumdieck Tissue Slicer for this experiment.

SUPPLEMENTARY MATERIAL

The Supplementary Material for this article can be found online at: https://www.frontiersin.org/articles/10.3389/fvets.2022.931264/full#supplementary-material

Supplementary File 1 | Complete dataset with annotation and statistical results.

Supplementary File 2 | Comparison between RTqPCR and RNAseq for selected transcripts.

Supplementary Figure S1 | Principal component analysis of the RNAseq.

Supplementary Figure S2 | Enriched GO terms within the cohort of genes significantly upregulated (FDR-adjusted *p*-value <0.2) by treatment with the PPARα agonist.

Supplementary Figure S3 | Enriched GO terms within the cohort of genes significantly downregulated (FDR-adjusted *p*-value <0.2) by treatment with the PPARα agonist.

Supplementary Figure S4 | Enriched GO terms within the cohort of genes significantly upregulated (FDR-adjusted *p*-value <0.2) by treatment with the PPARδ agonist.

Supplementary Figure S5 | Enriched GO terms within the cohort of genes significantly downregulated (FDR-adjusted *p*-value <0.2) by treatment with the PPARδ agonist.

Supplementary Figure S6 | Enriched GO terms within the cohort of genes significantly upregulated (FDR-adjusted *p*-value <0.2) by treatment with the PPARγ agonist.

Supplementary Figure S7 | Enriched GO terms within the cohort of genes significantly downregulated (FDR-adjusted *p*-value <0.2) by treatment with the PPARγ agonist.

Supplementary Table S1 | Accession number, gene symbol, sequence, and amplicon size of quantified genes, and internal control genes. If reference is lacking, primers were designed for this manuscript.

REFERENCES

1. Pascottini OB, Leroy JLMR, Opsomer G. Metabolic stress in the transition period of dairy cows: focusing on the prepartum period. *Animals.* (2020) 10:1419. doi: 10.3390/ani10081419
2. Drackley JK. Biology of dairy cows during the transition period: the final frontier? *J Dairy Sci.* (1999) 82:2259–73. doi: 10.3168/jds.S0022-0302(99)75474-3
3. Aschenbach JR, Kristensen NB, Donkin SS, Hammon HM, Penner GB. Gluconeogenesis in dairy cows: the secret of making sweet milk from sour dough. *IUBMB Life.* (2010) 62:869–77. doi: 10.1002/iub.400
4. Hocquette JF, Bauchart D. Intestinal absorption, blood transport and hepatic and muscle metabolism of fatty acids in preruminant and ruminant animals. *Reprod Nutr Dev.* (1999) 39:27–48. doi: 10.1051/rnd:19990102
5. Pullen DL, Liesman JS, Emery RS. A species comparison of liver slice synthesis and secretion of triacylglycerol from nonesterified fatty acids in media2. *J Anim Sci.* (1990) 68:1395–9. doi: 10.2527/1990.6851395x
6. Grummer RR. Nutritional and management strategies for the prevention of fatty liver in dairy cattle. *Vet J.* (2008) 176:10–20. doi: 10.1016/j.tvjl.2007.12.033
7. Adewuyi AA, Gruys E, van Eerdenburg FJCM. Non esterified fatty acids (NEFA) in dairy cattle: a review. *Vet Q.* (2005) 27:117–26. doi: 10.1080/01652176.2005.9695192
8. Janovick NA, Boisclair YR, Drackley JK. Prepartum dietary energy intake affects metabolism and health during the periparturient period in primiparous and multiparous Holstein cows1. *J Dairy Sci.* (2011) 94:1385–400. doi: 10.3168/jds.2010-3303
9. Van den Top AM, Geelen MJ, Wensing T, Wentink GH. Van 't Klooster AT, Beynen AC. Higher postpartum hepatic triacylglycerol concentrations in dairy cows with free rather than restricted access to feed during the dry period are associated with lower activities of hepatic glycerolphosphate acyltransferase. *J Nutr.* (1996) 126:76–85. doi: 10.1093/jn/126.1.76
10. Gross JJ, Schwarz FJ, Eder K, van Dorland HA, Bruckmaier RM. Liver fat content and lipid metabolism in dairy cows during early lactation and during a mid-lactation feed restriction. *J Dairy Sci.* (2013) 96:5008–17. doi: 10.3168/jds.2012-6245
11. Akbar H, Bionaz M, Carlson DB, Rodriguez-Zas SL, Everts RE, Lewin HA, et al. Feed restriction, but not l-carnitine infusion, alters the liver transcriptome by inhibiting sterol synthesis and mitochondrial oxidative phosphorylation and increasing gluconeogenesis in mid-lactation dairy cows. *J Dairy Sci.* (2013) 96:2201–13. doi: 10.3168/jds.2012-6036
12. Velez JC, Donkin SS. Feed restriction induces pyruvate carboxylase but not phosphoenolpyruvate carboxykinase in dairy cows*. *J Dairy Sci.* (2005) 88:2938–48. doi: 10.3168/jds.S0022-0302(05)72974-X
13. Bionaz M, Chen S, Khan MJ, Loor JJ. Functional role of PPARs in ruminants: potential targets for fine-tuning metabolism during growth and lactation. *PPAR Res.* (2013) 2013:e684159. doi: 10.1155/2013/684159
14. Michalik L, Auwerx J, Berger JP, Chatterjee VK, Glass CK, Gonzalez FJ, et al. International union of pharmacology. LXI peroxisome proliferator-activated receptors. *Pharmacol Rev.* (2006) 58:726–41. doi: 10.1124/pr.58.4.5
15. Bionaz M, Vargas-Bello-Pérez E, Busato S. Advances in fatty acids nutrition in dairy cows: from gut to cells and effects on performance. *J Anim Sci Biotechnol.* (2020) 11:110. doi: 10.1186/s40104-020-00512-8
16. Akbar H, Schmitt E, Ballou MA, Corrêa MN, DePeters EJ, Loor JJ. Dietary lipid during late-pregnancy and early-lactation to manipulate

metabolic and inflammatory gene network expression in dairy cattle liver with a focus on PPARs. *Gene Regul Syst Biol.* (2013) 7:GRSB.S12005. doi: 10.4137/GRSB.S12005
17. Busato S, Bionaz M. The interplay between non-esterified fatty acids and bovine peroxisome proliferator-activated receptors: results of an in vitro hybrid approach. *J Anim Sci Biotechnol.* (2020) 11:91. doi: 10.1186/s40104-020-00481-y
18. Godoy P, Hewitt NJ, Albrecht U, Andersen ME, Ansari N, Bhattacharya S, et al. Recent advances in 2D and 3D in vitro systems using primary hepatocytes, alternative hepatocyte sources and non-parenchymal liver cells and their use in investigating mechanisms of hepatotoxicity, cell signaling and ADME. *Arch Toxicol.* (2013) 87:1315–530. doi: 10.1007/s00204-013-1078-5
19. Giantin M, Gallina G, Pegolo S, Lopparelli RM, Sandron C, Zancanella V, et al. Primary hepatocytes as an useful bioassay to characterize metabolism and bioactivity of illicit steroids in cattle. *Toxicol In Vitro.* (2012) 26:1224–32. doi: 10.1016/j.tiv.2012.06.003
20. Elgendy R, Giantin M, Dacasto M. Transcriptomic characterization of bovine primary cultured hepatocytes; a cross-comparison with a bovine liver and the Madin-Darby bovine kidney cells. *Res Vet Sci.* (2017) 113:40–9. doi: 10.1016/j.rvsc.2017.08.006
21. Zhang Z-G, Li X-B, Gao L, Liu G-W, Kong T, Li Y-F, Wang H-B, Zhang C, Wang Z, Zhang R-H. An updated method for the isolation and culture of primary calf hepatocytes. *Vet J Lond Engl 1997.* (2012) 191:323–6. doi: 10.1016/j.tvjl.2011.01.008
22. Zhu Y, Guan Y, Loor JJ, Sha X, Coleman DN, Zhang C, et al. Fatty acid-induced endoplasmic reticulum stress promoted lipid accumulation in calf hepatocytes, and endoplasmic reticulum stress existed in the liver of severe fatty liver cows. *J Dairy Sci.* (2019) 102:7359–70. doi: 10.3168/jds.2018-16015
23. Zhao B, Luo C, Zhang M, Xing F, Luo S, Fu S, et al. Knockdown of phosphatase and tensin homolog (PTEN) inhibits fatty acid oxidation and reduces very low density lipoprotein assembly and secretion in calf hepatocytes. *J Dairy Sci.* (2020) 103:10728–41. doi: 10.3168/jds.2019-17920
24. Zhang B, Yang W, Wang S, Liu R, Loor JJ, Dong Z, et al. Lipid accumulation and injury in primary calf hepatocytes challenged with different long-chain fatty acids. *Front Vet Sci.* (2020) 7:547047. doi: 10.3389/fvets.2020.547047
25. Rosa F, Busato S, Avaroma FC, Linville K, Trevisi E, Osorio JS, et al. Transcriptional changes detected in fecal RNA of neonatal dairy calves undergoing a mild diarrhea are associated with inflammatory biomarkers. *PLoS ONE.* (2018) 13:e0191599. doi: 10.1371/journal.pone.0191599
26. Harvey TN, Sandve SR, Jin Y, Vik JO, Torgersen JS. Liver slice culture as a model for lipid metabolism in fish. *PeerJ.* (2019) 7:e7732. doi: 10.7717/peerj.7732
27. Yadetie F, Zhang X, Hanna EM, Aranguren-Abadía L, Eide M, Blaser N, et al. RNA-Seq analysis of transcriptome responses in Atlantic cod (*Gadus morhua*) precision-cut liver slices exposed to benzo[a]pyrene and 17α-ethynylestradiol. *Aquat Toxicol.* (2018) 201:174–86. doi: 10.1016/j.aquatox.2018.06.003
28. de Graaf IAM, Olinga P, de Jager MH, Merema MT, de Kanter R, van de Kerkhof EG, et al. Preparation and incubation of precision-cut liver and intestinal slices for application in drug metabolism and toxicity studies. *Nat Protoc.* (2010) 5:1540–51. doi: 10.1038/nprot.2010.111
29. Janssen AWF, Betzel B, Stoopen G, Berends FJ, Janssen IM, Peijnenburg AA, et al. The impact of PPARα activation on whole genome gene expression in human precision cut liver slices. *BMC Genomics.* (2015) 16:760. doi: 10.1186/s12864-015-1969-3
30. NCBI Resource Coordinators. Database resources of the National Center for Biotechnology Information. *Nucleic Acids Res.* (2016) 44:D7–19. doi: 10.1093/nar/gkv1290
31. Vandesompele J, De Preter K, Pattyn F, Poppe B, Van Roy N, De Paepe A, Speleman F. Accurate normalization of real-time quantitative RT-PCR data by geometric averaging of multiple internal control genes. *Genome Biol.* (2002) 3:RESEARCH0034. doi: 10.1186/gb-2002-3-7-research0034
32. Ewels P, Magnusson M, Lundin S, Käller M. MultiQC: summarize analysis results for multiple tools and samples in a single report. *Bioinformatics.* (2016) 32:3047–8. doi: 10.1093/bioinformatics/btw354
33. Bolger AM, Lohse M, Usadel B. Trimmomatic: a flexible trimmer for Illumina sequence data. *Bioinformatics.* (2014) 30:2114–20. doi: 10.1093/bioinformatics/btu170
34. Dobin A, Davis CA, Schlesinger F, Drenkow J, Zaleski C, Jha S, et al. ultrafast universal RNA-seq aligner. *Bioinformatics.* (2013) 29:15–21. doi: 10.1093/bioinformatics/bts635
35. Li H, Handsaker B, Wysoker A, Fennell T, Ruan J, Homer N, et al. 1000 genome project data processing subgroup. The sequence alignment/map format and SAMtools. *Bioinformatics.* (2009) 25:2078–9. doi: 10.1093/bioinformatics/btp352
36. Love MI, Huber W, Anders S. Moderated estimation of fold change and dispersion for RNA-seq data with DESeq2. *Genome Biol.* (2014) 15:550. doi: 10.1186/s13059-014-0550-8
37. Bionaz M, Periasamy K, Rodriguez-Zas SL, Hurley WL, Loor JJ. A Novel dynamic impact approach (DIA) for functional analysis of time-course omics studies: validation using the bovine mammary transcriptome. *PLoS ONE.* (2012) 7:e32455. doi: 10.1371/journal.pone.0032455
38. Huang DW, Sherman BT, Lempicki RA. Systematic and integrative analysis of large gene lists using DAVID bioinformatics resources. *Nat Protoc.* (2009) 4:44–57. doi: 10.1038/nprot.2008.211
39. Supek F, Bošnjak M, Škunca N, Šmuc T, REVIGO summarizes and visualizes long lists of gene ontology terms. *PLoS ONE.* (2011) 6:e21800. doi: 10.1371/journal.pone.0021800
40. Fang L, Zhang M, Li Y, Liu Y, Cui Q, Wang N. PPARgene: a database of experimentally verified and computationally predicted PPAR target genes. *PPAR Res.* (2016) 2016:e6042162. doi: 10.1155/2016/6042162
41. Schmitt E, Ballou MA, Correa MN, DePeters EJ, Drackley JK, Loor JJ. Dietary lipid during the transition period to manipulate subcutaneous adipose tissue peroxisome proliferator-activated receptor-γ co-regulator and target gene expression. *J Dairy Sci.* (2011) 94:5913–25. doi: 10.3168/jds.2011-4230
42. Kleiner S, Nguyen-Tran V, Baré O, Huang X, Spiegelman B, Wu Z. PPARδ agonism activates fatty acid oxidation via PGC-1α but does not increase mitochondrial gene expression and function. *J Biol Chem.* (2009) 284:18624–33. doi: 10.1074/jbc.M109.008797
43. Lohakare J, Osorio JS, Bionaz M. Peroxisome proliferator-activated receptor β/δ does not regulate glucose uptake and lactose synthesis in bovine mammary epithelial cells cultivated in vitro. *J Dairy Res.* (2018) 85:295–302. doi: 10.1017/S0022029918000365
44. Weld KA, Erb SJ, White HM. Short communication: Effect of manipulating fatty acid profile on gluconeogenic gene expression in bovine primary hepatocytes. *J Dairy Sci.* (2019) 102:7576–82. doi: 10.3168/jds.2018-16150
45. Rico DE, Parales JE, Corl BA, Lengi A, Chouinard PY, Gervais R. Abomasally infused SFA with varying chain length differently affect milk production and composition and alter hepatic and mammary gene expression in lactating cows. *Br J Nutr.* (2020) 124:386–95. doi: 10.1017/S0007114520000379
46. Cappon GD, Liu RCM, Frame SR, Hurtt ME. Effects of the rat hepatic peroxisome proliferator, Wyeth 14,643, on the lactating goat. *Drug Chem Toxicol.* (2002) 25:255–66. doi: 10.1081/DCT-120005888
47. Nagasawa T, Inada Y, Nakano S, Tamura T, Takahashi T, Maruyama K, et al. Effects of bezafibrate, PPAR pan-agonist, and GW501516, PPARδ agonist, on development of steatohepatitis in mice fed a methionine- and choline-deficient diet. *Eur J Pharmacol.* (2006) 536:182–91. doi: 10.1016/j.ejphar.2006.02.028
48. Barroso E, Rodríguez-Calvo R, Serrano-Marco L, Astudillo AM, Balsinde J, Palomer X, et al. The PPARβ/δ activator GW501516 prevents the down-regulation of AMPK caused by a high-fat diet in liver and amplifies the PGC-1α-Lipin 1-PPARα pathway leading to increased fatty acid oxidation. *Endocrinology.* (2011) 152:1848–59. doi: 10.1210/en.2010-1468
49. Kostadinova R, Montagner A, Gouranton E, Fleury S, Guillou H, Dombrowicz D, et al. GW501516-activated PPARβ/δ promotes liver fibrosis via p38-JNK MAPK-induced hepatic stellate cell proliferation. *Cell Biosci.* (2012) 2:34. doi: 10.1186/2045-3701-2-34
50. Tan GD, Fielding BA, Currie JM, Humphreys SM, Désage M, Frayn KN, et al. The effects of rosiglitazone on fatty acid and triglyceride metabolism in type 2 diabetes. *Diabetologia.* (2005) 48:83–95. doi: 10.1007/s00125-004-1619-9
51. Chaput E, Saladin R, Silvestre M, Edgar AD. Fenofibrate and rosiglitazone lower serum triglycerides with opposing effects on body weight. *Biochem Biophys Res Commun.* (2000) 271:445–50. doi: 10.1006/bbrc.2000.2647

52. van Wijk JPH, de Koning EJP, Cabezas MC, Rabelink TJ. Rosiglitazone improves postprandial triglyceride and free fatty acid metabolism in type 2 diabetes. *Diabetes Care.* (2005) 28:844–9. doi: 10.2337/diacare.28.4.844
53. Ye J-M, Iglesias MA, Watson DG, Ellis B, Wood L, Jensen PB, et al. PPARα/γ ragaglitazar eliminates fatty liver and enhances insulin action in fat-fed rats in the absence of hepatomegaly. *Am J Physiol-Endocrinol Metab.* (2003) 284:E531–40. doi: 10.1152/ajpendo.00299.2002
54. Ip E, Farrell G, Hall P, Robertson G, Leclercq I. Administration of the potent PPARα agonist, Wy-14,643, reverses nutritional fibrosis and steatohepatitis in mice. *Hepatology.* (2004) 39:1286–96. doi: 10.1002/hep.20170
55. Edvardsson U, Ljungberg A, Lindén D, William-Olsson L, Peilot-Sjögren H, Ahnmark A, et al. PPARα activation increases triglyceride mass and adipose differentiation-related protein in hepatocytes. *J Lipid Res.* (2006) 47:329–40. doi: 10.1194/jlr.M500203-JLR200
56. Mattijssen F, Georgiadi A, Andasarie T, Szalowska E, Zota A, Krones-Herzig A, et al. Hypoxia-inducible lipid droplet-associated (HILPDA) is a novel peroxisome proliferator-activated receptor (PPAR) target involved in hepatic triglyceride secretion. *J Biol Chem.* (2014) 289:19279–93. doi: 10.1074/jbc.M114.570044
57. Hemmeryckx B, Gaekens M, Gallacher DJ, Lu HR, Lijnen HR. Effect of rosiglitazone on liver structure and function in genetically diabetic akita mice. *Basic Clin Pharmacol Toxicol.* (2013) 113:353–60. doi: 10.1111/bcpt.12104
58. Watkins SM, Reifsnyder PR, Pan H, German JB, Leiter EH. Lipid metabolome-wide effects of the PPARγ agonist rosiglitazones. *J Lipid Res.* (2002) 43:1809–17. doi: 10.1194/jlr.M200169-JLR200
59. Gao M, Ma Y, Alsaggar M, Liu D. Dual outcomes of rosiglitazone treatment on fatty liver. *AAPS J.* (2016) 18:1023–31. doi: 10.1208/s12248-016-9919-9
60. Litherland NB, Bionaz M, Wallace RL, Loor JJ, Drackley JK. Effects of the peroxisome proliferator-activated receptor-α agonists clofibrate and fish oil on hepatic fatty acid metabolism in weaned dairy calves1. *J Dairy Sci.* (2010) 93:2404–18. doi: 10.3168/jds.2009-2716
61. Shi HB, Zhang CH, Zhao W, Luo J, Loor JJ. Peroxisome proliferator-activated receptor delta facilitates lipid secretion and catabolism of fatty acids in dairy goat mammary epithelial cells. *J Dairy Sci.* (2017) 100:797–806. doi: 10.3168/jds.2016-11647
62. Lee YK, Park JE, Lee M, Hardwick JP. Hepatic lipid homeostasis by peroxisome proliferator-activated receptor gamma 2. *Liver Res.* (2018) 2:209–15. doi: 10.1016/j.livres.2018.12.001
63. Croasdell A, Duffney PF, Kim N, Lacy SH, Sime PJ, Phipps RP. PPARγ and the innate immune system mediate the resolution of inflammation. *PPAR Res.* (2015) 2015:549691. doi: 10.1155/2015/549691
64. Nakajima A, Wada K, Miki H, Kubota N, Nakajima N, Terauchi Y, et al. Endogenous PPAR gamma mediates anti-inflammatory activity in murine ischemia-reperfusion injury. *Gastroenterology.* (2001) 120:460–9. doi: 10.1053/gast.2001.21191
65. Harada K, Nakanuma Y. Biliary innate immunity: function and modulation. *Mediators Inflamm.* (2010) 2010:373878. doi: 10.1155/2010/373878
66. Mehrfeld C, Zenner S, Kornek M, Lukacs-Kornek V. The contribution of non-professional antigen-presenting cells to immunity and tolerance in the liver. *Front Immunol.* (2018) 9:635. doi: 10.3389/fimmu.2018.00635
67. Veas F. *Acute Phase Proteins as Early Non-Specific Biomarkers of Human and Veterinary Diseases.* London: BoD – Books on Demand (2011). 424 p.
68. Roberts LD, Murray AJ, Menassa D, Ashmore T, Nicholls AW, Griffin JL. The contrasting roles of PPARδ and PPARγ in regulating the metabolic switch between oxidation and storage of fats in white adipose tissue. *Genome Biol.* (2011) 12:R75. doi: 10.1186/gb-2011-12-8-r75
69. Thering BJ, Bionaz M, Loor JJ. Long-chain fatty acid effects on peroxisome proliferator-activated receptor-α-regulated genes in Madin-Darby bovine kidney cells: optimization of culture conditions using palmitate. *J Dairy Sci.* (2009) 92:2027–37. doi: 10.3168/jds.2008-1749
70. van Dorland HA, Richter S, Morel I, Doherr MG, Castro N, Bruckmaier RM. Variation in hepatic regulation of metabolism during the dry period and in early lactation in dairy cows. *J Dairy Sci.* (2009) 92:1924–40. doi: 10.3168/jds.2008-1454
71. Fornes D, Gomez Ribot D, Heinecke F, Roberti SL, Capobianco E, Jawerbaum A. Maternal diets enriched in olive oil regulate lipid metabolism and levels of PPARs and their coactivators in the fetal liver in a rat model of gestational diabetes mellitus. *J Nutr Biochem.* (2020) 78:108334. doi: 10.1016/j.jnutbio.2019.108334
72. Shi H, Luo J, Zhu J, Li J, Sun Y, Lin X, et al. PPARγ regulates genes involved in triacylglycerol synthesis and secretion in mammary gland epithelial cells of dairy goats. *PPAR Res.* (2013) 2013:e310948. doi: 10.1155/2013/310948
73. Zarei M, Barroso E, Palomer X, Escolà-Gil JC, Cedó L, Wahli W, et al. Pharmacological PPARβ/δ activation upregulates VLDLR in hepatocytes. *Clín Investig Arterioscler Engl Ed.* (2019) 31:111–8. doi: 10.1016/j.arteri.2019.01.004
74. Gao Y, Shen W, Lu B, Zhang Q, Hu Y, Chen Y. Upregulation of hepatic VLDLR via PPARα is required for the triglyceride-lowering effect of fenofibrate. *J Lipid Res.* (2014) 55:1622–33. doi: 10.1194/jlr.M041988
75. Sugden MC, Caton PW, Holness MJ, PPAR. control: it's SIRTainly as easy as PGC. *J Endocrinol.* (2010) 204:93–104. doi: 10.1677/JOE-09-0359
76. Basu-Modak S, Braissant O, Escher P, Desvergne B, Honegger P, Wahli W. Peroxisome proliferator-activated receptor β regulates acyl-CoA synthetase 2 in reaggregated rat brain cell cultures*. *J Biol Chem.* (1999) 274:35881–8. doi: 10.1074/jbc.274.50.35881
77. Li T, Li X, Meng H, Chen L, Meng F. ACSL1 affects triglyceride levels through the PPARγ pathway. *Int J Med Sci.* (2020) 17:720–7. doi: 10.7150/ijms.42248
78. Kadegowda AKG, Bionaz M, Piperova LS, Erdman RA, Loor JJ. Peroxisome proliferator-activated receptor-γ activation and long-chain fatty acids alter lipogenic gene networks in bovine mammary epithelial cells to various extents. *J Dairy Sci.* (2009) 92:4276–89. doi: 10.3168/jds.2008-1932
79. Zhang C, Li A, Zhang X, Xiao H, A. Novel TIP30 protein complex regulates EGF receptor signaling and endocytic degradation *. *J Biol Chem.* (2011) 286:9373–81. doi: 10.1074/jbc.M110.207720
80. Liao BM, Raddatz K, Zhong L, Parker BL, Raftery MJ, Schmitz-Peiffer C. Proteomic analysis of livers from fat-fed mice deficient in either PKCδ or PKCε identifies Htatip2 as a regulator of lipid metabolism. *Proteomics.* (2014) 14:2578–87. doi: 10.1002/pmic.201400202
81. Cariello NF, Romach EH, Colton HM Ni H, Yoon L, Falls JG, Casey W, et al. Gene expression profiling of the PPAR-alpha agonist ciprofibrate in the cynomolgus monkey liver. *Toxicol Sci.* (2005) 88:250–64. doi: 10.1093/toxsci/kfi273
82. Guerre-Millo M, Gervois P, Raspé E, Madsen L, Poulain P, Derudas B, et al. Peroxisome proliferator-activated receptor α activators improve insulin sensitivity and reduce adiposity *. *J Biol Chem.* (2000) 275:16638–42. doi: 10.1074/jbc.275.22.16638
83. Strand DW, Jiang M, Murphy TA Yi Y, Konvinse KC, Franco OE, Wang Y, et al. γ isoforms differentially regulate metabolic networks to mediate mouse prostatic epithelial differentiation. *Cell Death Dis.* (2012) 3:e361. doi: 10.1038/cddis.2012.99
84. Aprile M, Cataldi S, Ambrosio MR, D'Esposito V, Lim K, Dietrich A, et al. PPARγΔ5, a naturally occurring dominant-negative splice isoform, impairs PPARγ function and adipocyte differentiation. *Cell Rep.* (2018) 25:1577–92.e6. doi: 10.1016/j.celrep.2018.10.035
85. Chui PC, Guan H-P, Lehrke M, Lazar MA. PPARγ regulates adipocyte cholesterol metabolism via oxidized LDL receptor 1. *J Clin Invest.* (2005) 115:2244–56. doi: 10.1172/JCI24130
86. Sun C, Liu C, Zhang Z. Cloning of OLR1 gene in pig adipose tissue and preliminary study on its lipid-accumulating effect. *Asian-Australas J Anim Sci.* (2009) 22:1420–8. doi: 10.5713/ajas.2009.90121
87. Chen Z, Yu H, Shi X, Warren CR, Lotta LA, Friesen M, et al. Functional screening of candidate causal genes for insulin resistance in human preadipocytes and adipocytes. *Circ Res.* (2020) 126:330–46. doi: 10.1161/CIRCRESAHA.119.315246
88. Ruppert PMM, Park J-G, Xu X, Hur KY, Lee A-H, Kersten S. Transcriptional profiling of PPARα-/– and CREB3L3–/– livers reveals disparate regulation of hepatoproliferative and metabolic functions of PPARα. *BMC Genomics.* (2019) 20:199. doi: 10.1186/s12864-019-5563-y
89. Nakagawa Y, Satoh A, Tezuka H, Han S, Takei K, Iwasaki H, et al. CREB3L3 controls fatty acid oxidation and ketogenesis in synergy with PPARα. *Sci Rep.* (2016) 6:39182. doi: 10.1038/srep39182
90. Djouadi F, Habarou F, Bachelier CL, Ferdinandusse S, Schlemmer D, Benoist JF, et al. Mitochondrial trifunctional protein deficiency in human cultured fibroblasts: effects of bezafibrate. *J Inherit Metab Dis.* (2016) 39:47–58. doi: 10.1007/s10545-015-9871-3

91. Guo Y, Jolly RA, Halstead BW, Baker TK, Stutz JP, Huffman M, et al. Underlying mechanisms of pharmacology and toxicity of a novel PPAR agonist revealed using rodent and canine hepatocytes. *Toxicol Sci.* (2007) 96:294–309. doi: 10.1093/toxsci/kfm009
92. Shumar SA, Kerr EW, Fagone P, Infante AM, Leonardi R. Overexpression of Nudt7 decreases bile acid levels and peroxisomal fatty acid oxidation in the liver. *J Lipid Res.* (2019) 60:1005–19. doi: 10.1194/jlr.M092676
93. Reilly S-J, Tillander V, Ofman R, Alexson SEH, Hunt MC. The nudix hydrolase 7 is an Acyl-CoA diphosphatase involved in regulating peroxisomal coenzyme A homeostasis. *J Biochem.* (2008) 144:655–63. doi: 10.1093/jb/mvn114
94. Marín-Garzón NA, Magalhães AFB, Mota LFM, Fonseca LFS, Chardulo LAL, Albuquerque LG. Genome-wide association study identified genomic regions and putative candidate genes affecting meat color traits in Nellore cattle. *Meat Sci.* (2021) 171:108288. doi: 10.1016/j.meatsci.2020.108288
95. Kim T, Yang Q. Peroxisome-proliferator-activated receptors regulate redox signaling in the cardiovascular system. *World J Cardiol.* (2013) 5:164–74. doi: 10.4330/wjc.v5.i6.164
96. Elshazly S, Soliman E, PPAR. gamma agonist, pioglitazone, rescues liver damage induced by renal ischemia/reperfusion injury. *Toxicol Appl Pharmacol.* (2019) 362:86–94. doi: 10.1016/j.taap.2018.10.022
97. Fischhuber K, Matzinger M, Heiss EH. AMPK enhances transcription of selected Nrf2 target genes via negative regulation of Bach1. *Front Cell Dev Biol.* (2020) 8:628. doi: 10.3389/fcell.2020.00628
98. Suzuki C, Ushijima K, Ando H, Kitamura H, Horiguchi M, Akita T, et al. Induction of Dbp by a histone deacetylase inhibitor is involved in amelioration of insulin sensitivity via adipocyte differentiation in ob/ob mice. *Chronobiol Int.* (2019) 36:955–68. doi: 10.1080/07420528.2019.1602841
99. Ushijima K, Suzuki C, Kitamura H, Shimada K, Kawata H, Tanaka A, et al. Expression of clock gene Dbp in omental and mesenteric adipose tissue in patients with type 2 diabetes. *BMJ Open Diabetes Res Care.* (2020) 8:e001465. doi: 10.1136/bmjdrc-2020-001465
100. Du K, Herzig S, Kulkarni RN, Montminy M. TRB3: a tribbles homolog that inhibits Akt/PKB activation by insulin in liver. *Science.* (2003) 300:1574–7. doi: 10.1126/science.1079817
101. Weismann D, Erion DM, Ignatova-Todorava I, Nagai Y, Stark R, Hsiao JJ, et al. Knockdown of the gene encoding Drosophila tribbles homologue 3 (Trib3) improves insulin sensitivity through peroxisome proliferator-activated receptor-γ (PPAR-γ) activation in a rat model of insulin resistance. *Diabetologia.* (2011) 54:935–44. doi: 10.1007/s00125-010-1984-5
102. Luo X, Zhong L, Yu L, Xiong L, Dan W, Li J, et al. TRIB3 destabilizes tumor suppressor PPARα expression through ubiquitin-mediated proteasome degradation in acute myeloid leukemia. *Life Sci.* (2020) 257:118021. doi: 10.1016/j.lfs.2020.118021
103. Fröhlich A, Kisielow J, Schmitz I, Freigang S, Shamshiev AT, Weber J, et al. IL-21R on T cells is critical for sustained functionality and control of chronic viral infection. *Science.* (2009) 324:1576–80. doi: 10.1126/science.1172815
104. Ratziu V, Harrison SA, Francque S, Bedossa P, Lehert P, Serfaty L, et al. Elafibranor, an agonist of the peroxisome proliferator-activated receptor-α and -δ, induces resolution of nonalcoholic steatohepatitis without fibrosis worsening. *Gastroenterology.* (2016) 150:1147–59.e5. doi: 10.1053/j.gastro.2016.01.038
105. Anderson AC. Tim-3, a negative regulator of anti-tumor immunity. *Curr Opin Immunol.* (2012) 24:213–6. doi: 10.1016/j.coi.2011.12.005
106. Jia J, Abudu YP, Claude-Taupin A, Gu Y, Kumar S, Choi SW, et al. Galectins control MTOR and AMPK in response to lysosomal damage to induce autophagy. *Autophagy.* (2019) 15:169–71. doi: 10.1080/15548627.2018.1505155
107. Milton FA, Lacerda MG, Sinoti SBP, Mesquita PG, Prakasan D, Coelho MS, et al. Dibutyltin compounds effects on PPARγ/RXRα activity, adipogenesis, and inflammation in mammalians cells. *Front Pharmacol.* (2017) 8:507. doi: 10.3389/fphar.2017.00507
108. Lu N, Li Y, Zhang Z, Xing J, Sun Y, Yao S, et al. Human Semaphorin-4A drives Th2 responses by binding to receptor ILT-4. *Nat Commun.* (2018) 9:742. doi: 10.1038/s41467-018-03128-9
109. Delgoffe GM, Woo S-R, Turnis ME, Gravano DM, Guy C, Overacre AE, et al. Stability and function of regulatory T cells is maintained by a neuropilin-1–semaphorin-4a axis. *Nature.* (2013) 501:252–6. doi: 10.1038/nature12428
110. Collet P, Domenjoud L, Devignes MD, Murad H, Schohn H, Dauça M. The human semaphorin 6B gene is down regulated by PPARs. *Genomics.* (2004) 83:1141–50. doi: 10.1016/j.ygeno.2004.01.002
111. Liu W, Li J, Liu M, Zhang H, Wang N. PPAR-γ promotes endothelial cell migration by inducing the expression of Sema3g. *J Cell Biochem.* (2015) 116:514–23. doi: 10.1002/jcb.24994
112. Ji Y, Liu J, Wang Z, Liu N, Gou W, PPAR. γ agonist, rosiglitazone, regulates angiotensin II-induced vascular inflammation through the TLR4-dependent signaling pathway. *Lab Invest.* (2009) 89:887–902. doi: 10.1038/labinvest.2009.45
113. Sun H, Zhu X, Cai W, Qiu L. Hypaphorine attenuates lipopolysaccharide-induced endothelial inflammation via regulation of TLR4 and PPAR-γ dependent on PI3K/Akt/mTOR signal pathway. *Int J Mol Sci.* (2017) 18:844. doi: 10.3390/ijms18040844
114. Poleni P-E, Etienne S, Velot E, Netter P, Bianchi A. Activation of PPARs α, β/δ, and γ impairs TGF-β1-induced collagens' production and modulates the TIMP-1/MMPs balance in three-dimensional cultured chondrocytes. *PPAR Res.* (2010) 2010:635912.
115. Alwayn IPJ, Andersson C, Lee S, Arsenault DA, Bistrian BR, Gura KM, et al. Inhibition of matrix metalloproteinases increases PPAR-α and IL-6 and prevents dietary-induced hepatic steatosis and injury in a murine model. *Am J Physiol Gastrointest Liver Physiol.* (2006) 291:G1011–9. doi: 10.1152/ajpgi.00047.2006
116. Cheng G, Zhang X, Gao D, Jiang X, Dong W. Resveratrol inhibits MMP-9 expression by up-regulating PPAR α expression in an oxygen glucose deprivation-exposed neuron model. *Neurosci Lett.* (2009) 451:105–8. doi: 10.1016/j.neulet.2008.12.045
117. Beck IM, Rückert R, Brandt K, Mueller MS, Sadowski T, Brauer R, et al. MMP19 is essential for T cell development and T cell-mediated cutaneous immune responses. *PLoS ONE.* (2008) 3:e2343. doi: 10.1371/journal.pone.0002343
118. Eiró N, Fernandez-Garcia B, González LO, Vizoso FJ. Cytokines related to MMP-11 expression by inflammatory cells and breast cancer metastasis. *Oncoimmunology.* (2013) 2:e24010. doi: 10.4161/onci.24010
119. Rodríguez-Baena FJ, Redondo-García S, Peris-Torres C, Martino-Echarri E, Fernández-Rodríguez R, del Plaza-Calonge M, et al. ADAMTS1 protease is required for a balanced immune cell repertoire and tumour inflammatory response. *Sci Rep.* (2018) 8:13103. doi: 10.1038/s41598-018-31288-7
120. Zimmermann M, Lampe J, Lange S, Smirnow I, Königsrainer A, Hann-von-Weyhern C, et al. Improved reproducibility in preparing precision-cut liver tissue slices. *Cytotechnology.* (2009) 61:145–52. doi: 10.1007/s10616-009-9246-4
121. Graaf IA de, Groothuis GM, Olinga P. Precision-cut tissue slices as a tool to predict metabolism of novel drugs. *Expert Opin Drug Metab Toxicol.* (2007) 3:879–98. doi: 10.1517/17425255.3.6.879
122. French PD. Dry matter intake and blood parameters of nonlactating holstein and jersey cows in late gestation. *J Dairy Sci.* (2006) 89:1057–61. doi: 10.3168/jds.S0022-0302(06)72173-7
123. Grummer RR, Mashek DG, Hayirli A. Dry matter intake and energy balance in the transition period. *Vet Clin Food Anim Pract.* (2004) 20:447–70. doi: 10.1016/j.cvfa.2004.06.013
124. Guretzky NAJ, Carlson DB, Garrett JE, Drackley JK. Lipid metabolite profiles and milk production for holstein and jersey cows fed rumen-protected choline during the periparturient period1. *J Dairy Sci.* (2006) 89:188–200. doi: 10.3168/jds.S0022-0302(06)72083-5
125. Pareek CS, Sachajko M, Jaskowski JM, Herudzinska M, Skowronski M, Domagalski K, et al. Comparative analysis of the liver transcriptome among cattle breeds using RNA-seq. *Vet Sci.* (2019) 6:36. doi: 10.3390/vetsci6020036
126. Gao ST, Girma DD, Bionaz M, Ma L, Bu DP. Hepatic transcriptomic adaptation from prepartum to postpartum in dairy cows. *J Dairy Sci.* (2021) 104:1053–72. doi: 10.3168/jds.2020-19101
127. McCabe M, Waters S, Morris D, Kenny D, Lynn D, Creevey C. RNA-seq analysis of differential gene expression in liver from lactating dairy

cows divergent in negative energy balance. *BMC Genomics.* (2012) 13:193. doi: 10.1186/1471-2164-13-193

Conflict of Interest: The authors declare that the research was conducted in the absence of any commercial or financial relationships that could be construed as a potential conflict of interest.

Publisher's Note: All claims expressed in this article are solely those of the authors and do not necessarily represent those of their affiliated organizations, or those of the publisher, the editors and the reviewers. Any product that may be evaluated in this article, or claim that may be made by its manufacturer, is not guaranteed or endorsed by the publisher.

frontiers | Frontiers in Veterinary Science

TYPE Original Research
PUBLISHED 31 October 2022
DOI 10.3389/fvets.2022.926721

OPEN ACCESS

EDITED BY
Rajib Deb,
National Research Center on Pig (ICAR), India

REVIEWED BY
Yang Li,
Northeast Agricultural University, China
Anusorn Cherdthong,
Khon Kaen University, Thailand

*CORRESPONDENCE
Ao Changjin
changjinao@aliyun.com

†These authors have contributed equally to this work

SPECIALTY SECTION
This article was submitted to Animal Nutrition and Metabolism, a section of the journal Frontiers in Veterinary Science

RECEIVED 23 April 2022
ACCEPTED 03 October 2022
PUBLISHED 31 October 2022

CITATION
Yaxing Z, Erdene K, Zhibi B, Changjin A and Chen B (2022) Effects of *Allium mongolicum* regel essential oil supplementation on growth performance, nutrient digestibility, rumen fermentation, and bacterial communities in sheep. *Front. Vet. Sci.* 9:926721. doi: 10.3389/fvets.2022.926721

Effects of *Allium mongolicum* regel essential oil supplementation on growth performance, nutrient digestibility, rumen fermentation, and bacterial communities in sheep

Zhao Yaxing[1†], Khas Erdene[1†], Bao Zhibi[2†], Ao Changjin[1*] and Bai Chen[1]

[1]Inner Mongolia Key Laboratory of Animal Nutrition and Feed Science, College of Animal Science, Inner Mongolia Agricultural University, Hohhot, China, [2]Animal Husbandry Service Center for Bayannaoer, Bayannaoer, China

The objectives of this research were to investigate the effects of *Allium mongolicum* Regel essential oil on growth performance, nutrient digestibility, rumen fermentation, and bacterial communities in sheep Twenty sheep were randomly divided into two dietary groups with 10 replicates each: (1) a basal diet without AMO as the control group ($n = 10$) and (2) a basal diet supplemented with 40 mg/kg AMO as the AMO group ($n = 10$). The average daily gain (ADG) was increased ($P < 0.05$), and the feed conversion ratio (FCR) was reduced ($P < 0.05$) in the AMO group compared with the control. The ruminal acetate, propionate, total volatile fatty acids (TVFA), and microbial protein (MCP) were higher ($P < 0.05$) in the AMO group than in the control. Moreover, ruminal pH and ammonia nitrogen (NH_3-N) were lower ($P < 0.05$) in the AMO group than in the control. The relative abundances of the phylum levels of *Firmicutes*, *Actinobacteriota,* and *Verrucomicrobiota* were higher ($P < 0.05$) in the AMO group than in the control, and the relative abundances of *Bacteroidetes* and *Spirochaetota* were lower ($P < 0.05$) in the AMO group than in the control. The relative abundance of *Prevotella* and *Prevotellaceae_UCG-003* at the genus level was increased ($P < 0.05$) in the AMO group compared with the control; however, the relative abundance of *Succiniclasticum*, *Norank_f__F082*, *Christensenellaceae_R-7_group,* and *Norank_f__Muribaculaceae* was decreased ($P < 0.05$) in the AMO group compared with the control. The activities of cellulase, α-amylase, and proteinase were higher ($P < 0.05$) in the AMO group than in the control. The apparent digestibility of dry matter (DM) and crude protein (CP) was increased

($P < 0.05$) in the AMO group compared with the control. In conclusion, AMO supplementation has the potential to improve growth performance. Moreover, supplementation with AMO improved nutrient digestibility, rumen fermentation, and bacterial communities in the rumen of sheep.

KEYWORDS

allium mongolicum regel, essential oil, growth performance, rumen fermentation, bacterial communities

Introduction

Ionophores (monensin) have been extensively used in ruminant production to reduce energy and protein losses in the rumen (1). The appearance of residues in products and the spread of antibiotic-resistant microbes have led to restrictions in the European Union and a ban in China on their use (2, 3). Consequently, the feed industry has investigated safe and effective alternatives that can functionally replace antibiotics, such as plant extracts (phytobiotics) and essential oils (EOs), which provide similar results as antibiotics in terms of feed efficiency and rumen fermentation (4).

EOs are natural bioactive compounds extracted from plants *via* distillation methods, or they can be obtained by chemical extraction (1). EOs as alternatives to antibiotics have the potential to be used in livestock feed. EOs were found to improve nutrient digestibility and increase growth performance in animals (5, 6). Laura et al. noted that a blend of EO dietary supplementation decreased the concentration of acetate and ammonia nitrogen (NH_3-N) in the rumen of finishing beef cattle (7). Moreover, oregano EO was shown to increase the relative abundance of *Prevotella* and *Dialister* in ruminal fluids *in vitro* (8). This capacity has become a promising research field for investigating the potential of EOs to alter rumen fermentation, resulting in improved feed efficiency in ruminants, but studies have mostly been conducted *in vitro* (9). In small ruminants, only a few *in vivo* studies have been performed to appraise the effects of EOs on animal growth performance, nutrient digestibility, rumen fermentation, and bacterial communities.

The *Allium* genus consists of many species, including shallot (*Allium ascalonicum*), leek (*Allium ampeloprasum*), garlic (*Allium sativum*), onion (*Allium cepa*), and chive (*Allium* schoenoprasum) (10). *Allium mongolicum Regel* (AM) is an *Allium* plant that grows widely in northern China (11). AM is a precious source of forage as it offers extensive nutrients and the contents of protein, ether extract (EE), flavonoids, minerals, amino acids, essential trace elements, and other components (12). A recent study noted that the use of AM water extract could increase the average daily gain (ADG) and decrease the feed conversion ratio (FCR) in sheep (13). In addition, Zhao et al. found that AM ethanol extract at doses of 2.8 g with diets lowered ruminal NH_3-N values after feeding in sheep (14). AM could increase the dry matter digestibility (DMD) and acid detergent fiber digestibility (ADFD) of Simmental calves (15). According to our previous literature, the use of polysaccharides from AM could decrease the abundances of *f-Prevotellaceae* and *g-Prevotellaceae_UCG-001* in the Bacteroidetes of sheep (16).

To date, no study has assessed the possible impact of *Allium mongolicum* Regel essential oil (AMO) on growth performance, nutrient digestibility, rumen fermentation, and bacterial communities in sheep. The purpose of this study, therefore, was to fill the gap in knowledge in this field and explore the potential of AMO as an antibiotic substitute for sheep.

Materials and methods

Ethics approval and consent to participate

All the animal procedures were carried out according to the protocols approved by the College of Animal Science, Inner Mongolia Agricultural University, China. We confirm that the authors complied with the Animal Research Reporting of *in vivo* Experiments (ARRIVE) guidelines.

Extraction process of AMO

Dried powder derived from AM leaves was purchased from Hao Hai Biological Co., Ltd. (Alashan League, Inner Mongolia, China). AMO was processed from the AM by hydrodistillation (1 kg in 5 L of distilled water) using a Clevenger-type apparatus for 3 h in line with the procedure noted in the European Pharmacopeia (17). The oil acquired above the aqueous distillate was dried with anhydrous sodium sulfate (1 mg/2 mL). The AMO was kept in a stainless sealed container at 4°C until use. AMO was analyzed for its chemical compounds using a GC/MS apparatus at the Atomic and Molecular Physics Unit. The major components of AMO

are anethole (37.63%), aromatic hydrocarbon (30.52%), and gingerol (12.60%).

Animals, diets, and experimental design

Twenty healthy male Dorper sheep with a mean BW (± SD) of 34.5 kg (± 2.5 kg) and an average age of 6 months were used. The sheep were randomly divided into two dietary groups with 10 replicates each: (1) a basal diet without AMO as the control group ($n = 10$) and (2) a basal diet supplemented with 40 mg/kg AMO as the AMO group ($n = 10$). The doses of the AMO were determined based on rumen fermentation using *in vitro* 24-h batch incubation (18). The basal diet was formulated to meet the standard nutrient requirements of sheep according to NRC recommendations (19). The dietary ingredients and nutrient levels of the diet are presented in Table 1. The AMO was completely mixed with the concentrate portion of the TMR before being mixed with the forage component. The diets were provided *ad libitum* twice per day at 07:00 and 18:00. Fresh water was available for the sheep during the whole feeding trial. The experiment lasted 75 days and comprised 15 days for the adaptation period and 60 days for the data and sample collection period.

Data and sample collection

During the trial, sheep were measured for health status, and their body weight was measured at 15-day intervals. Feed was suspended before initial and final weighing. The ADG and dry matter intake (DMI) of sheep were recorded, and the FCR was computed. FCR was determined as average daily DMI/ADG.

The rumen fluid was sampled at 2 h after the morning feeding *via* a stomach tube linked to an Erlenmeyer flask and a vacuum pump on the 60th day of the experimental period. The first 100 mL rumen fluid collected was discarded to prevent saliva contamination, and 100 mL rumen fluid was acquired. pH was immediately determined using an electric handheld pH meter (PHS-3C, Beijing Huoze Experimental Instrument Co., Ltd., Beijing, China). After that, the rumen fluid was then strained immediately through four layers of cheesecloth. One tube of the filtrate with 250 g/L (w/v) metaphosphoric acid (8: 2, v/v) was stored (−20°C) to detect the volatile fatty acids (VFA), and another tube of 10 mL filtrate was preserved by adding 2 mL of 20 g/L (w/v) H_2SO_4 for NH_3-N determination in another tube. The third tube of the filtrate was kept at −20°C to determine the microbial protein (MCP), cellulase, β-glucanase, α-amylase, lipase, and proteinase contents. The fourth tube of the filtrate was stored at – 80°C for analysis of the bacterial composition.

Approximately 100 g of fecal samples was collected from the rectum at 08:00, 11:00, 14:00, and 17:00 on the 58th, 59th, and 60th days of the experimental period to estimate the DMD, organic matter digestibility (OMD), crude protein digestibility (CPD), EE digestibility (EED), neutral detergent fiber digestibility (NDFD), and ADFD. Fecal yield was determined using acid-insoluble ash as an internal indicator (20).

TABLE 1 Composition and nutrient levels of basal diets of the sheep (DM basis).

Ingredients	Content%
Alfalfa	27.78
Corn	19.25
Whole corn silage	15.52
Gourd seed skin	12.15
DDGS [1]	4.33
Flax seed meal	4.62
Sunflower seed meal	6.09
Wheat bran	4.29
Red dates	1.68
Limestone	1.48
$CaHPO_4$	0.69
NaCl	0.72
Premix [2]	1.40
Total	100.00
Nutrient levels [3]	
DE[4] (MJ/kg)	16.83
DM%	91.20
CP%	15.32
ADF%	29.69
NDF%	50.98
EE%	3.09
Ca%	1.02
P%	0.55

[1]Distillers Dried Grains with Soluble.
[2]The premix provided the following per kilogram of diets: 25 mg iron (as $FeSO_4$), 29 mg zinc (as $ZnSO_4$), 8 mg copper (as $CuSO_4$), 30 mg manganese (as $MnSO_4$), 0.04 mg iodine (as KI), 0.1 mg cobalt (as $CoSO_4$), 3200 IU vitamin A, 1200 IU vitamin D, and 20 IU vitamin E.
[3]Digestible energy was a calculated value, whereas the others were measured values.
[4]DE, digestible energy; CP, crude protein; ADF, acid detergent fiber; NDF, neutral detergent fiber; EE, ether extract; Ca, calcium; P, phosphorus.

Sample analysis

Ruminal NH_3-N, MCP, and VFA

The VFA contents were measured using gas chromatography (Trace 1100; Thermo Fisher Scientific Co., Ltd., Beijing, China) as described by Zhou et al. (21). The NH_3-N contents were determined using the method described by the Kjeldahl assay (22). The concentration of MCP yield was determined by urinary purine derivative excretion according to the method described

by Hu et al. (23). The cellulase, β-glucanase, α-amylase, lipase, and proteinase activities were analyzed using kits (Nanjing Jiancheng Biological Technology Co. Ltd., Nanjing, China) according to the method of Laura et al. (7).

DNA extraction and PCR amplification

Microbial community genomic DNA was extracted from ruminal samples using the E.Z.N.A.® soil DNA Kit (Omega Bio-Tek, Norcross, GA, U.S.) according to the manufacturer's instructions. The DNA was extracted according to Jiang (24). The hypervariable region V3-V4 of the bacterial 16S rRNA gene was amplified with the primer pairs 338F (5'-ACTCCTACGGGAGGCAGCAG-3') and 806R (5'-GGACTACHVGGGTWTCTAAT-3') by an ABI GeneAmp® 9700 PCR thermocycler (ABI, CA, USA) (8). The PCR amplification of the 16S rRNA gene was performed according to Liu (25). The PCR mixtures refer to Wang (26). The PCR product was extracted from a 2% agarose gel, purified using the AxyPrep DNA Gel Extraction Kit (Axygen Biosciences, Union City, CA, USA) according to the manufacturer's instructions, and quantified using a Quantus™ Fluorometer (Promega, USA) (26).

Illumina MiSeq sequencing

Purified amplicons were pooled in equimolar amounts and paired-end sequenced on an Illumina MiSeq PE300 platform/NovaSeq PE250 platform (Illumina, San Diego, USA) according to the standard protocols by Majorbio Bio-Pharm Technology Co. Ltd. (Shanghai, China).

Processing of sequencing data

The raw 16S rRNA gene sequencing reads were demultiplexed, quality-filtered by fastp version 0.20.0 (27), and merged by FLASH version 1.2.7 (28).

Feed and fecal chemical analyses

The fecal samples and diets were dried in a forced-air oven at 55°C for 72 h and ground using a 1 mm screen. All feeds were analyzed in duplicate for DM, calcium (Ca), phosphorus (P), EE, CP, and ADF (29). The NDF content was analyzed with sodium sulfite and α-amylase (30). The total fecal output for each sheep was measured based on the content of indigestible neutral detergent fiber (iNDF) and used as an endogenous indicator. The iNDF content was calculated to determine *in vivo* digestibility using the following equation from Menezes et al. (31).

$$\text{iNDF (\% DM)} = \text{iNDF (g)/DM (\%)} \times 100$$

TABLE 2 Effects of AMO supplementation in sheep diet on growth performance.

Items[2]	Treatments[1]		SEM[3]	*P*-value
	CON	AMO		
Initial body weight	34.23	35.19	0.734	0.376
Final body weight	46.55	48.62	3.103	0.535
ADG / (kg/d)	0.167	0.178	0.004	0.043
DMI / (g/d)	1380.66	1406.67	25.353	0.363
FCR	8.27	7.89	0.077	0.005

[1]Treatments: CON, basal diet; AMO, *Allium mongolicum* Regel essential oil.
[2]DMI, dry matter intake; ADG, average daily gain; FCR, feed conversion ratio.
[3]Standard error of mean.

Statistical analysis

The data were analyzed using SAS software (version 9.0, SAS Inst. Inc., Cary, NC). Before analysis, all data were examined for normality using the UNIVARIATE procedure. Data on growth performance, rumen fermentation parameters, rumen enzyme activities, bacterial relative abundance, and nutrient digestibility were analyzed separately using a one-way analysis of variance (ANOVA) with dietary treatments used as the main factor.

Statistically significant differences among treatments were evaluated using Tukey's multiple range test. Probability values of $P \leq 0.05$ were declared significant, and probability values were declared statistical trends when $0.05 < P \leq 0.10$.

Results

Effects of AMO on growth performance and feed efficiency

The effects of AMO on the growth performance and feed efficiency of sheep are shown in Table 2. Dietary supplementation with AMO increased ($P < 0.05$) ADG compared with the control. Dietary supplementation with AMO decreased ($P < 0.05$) FCR compared with the control. There was no effect of AMO inclusion in the diet on DMI ($P > 0.05$).

Effects of AMO on rumen fermentation parameters

The effects of AMO on the rumen fermentation parameters of sheep are shown in Table 3. Dietary supplementation with

TABLE 3 Effect of AMO on ruminal fermentation in sheep.

Items[2]	Treatments[1]		SEM[3]	*P*-value
	CON	AMO		
pH	6.61	6.49	0.026	0.010
NH_3-N mg/dL	18.83	16.80	0.272	0.005
TVFA mmol/L	97.13	100.76	1.054	0.034
MCP mg/dL	163.66	175.65	3.986	0.040
Acetate mmol/L	59.37	63.66	0.909	0.016
Propionate mmol/L	23.07	25.33	0.625	0.037
Butyrate mmol/L	10.94	9.10	2.285	0.387
Isobutyrate mmol/L	1.37	1.46	0.082	0.109
Valerate mmol/L	1.27	1.22	2.049	0.570
Isovalerate mmol/L	1.13	1.20	3.029	0.061
A/P	2.57	2.51	0.070	0.459

[1]Treatments: CON, basal diet; AMO, *Allium mongolicum* Regel essential oil.
[2]NH_3-N, ammonia nitrogen; TVFA, total VFA; MCP, microbial protein; A/P, Acetate/Propionate.
[3]Standard error of mean.

TABLE 4 Effect of AMO on rumen bacterial diversity.

Items	Treatments[1]		SEM[2]	*P*-value
	CON	AMO		
OTU[3]	1417	1452	18.70	0.179
Shannon	4.88	5.14	0.169	0.268
Simpson	0.03	0.02	0.01	0.770
Ace	1057.66	1155.32	38.32	0.060
Chao1	1079.29	1169.51	60.31	0.273
Coverage	0.95	0.96	0.01	0.770

[1]Treatments: CON, basal diet; AMO, *Allium mongolicum* Regel essential oil.
[2]Standard error of mean.
[3]OTU, Operational Taxonomic Unit.

AMO increased ($P < 0.05$) the concentrations of MCP, TVFA, acetate, and propionate compared with the control. Moreover, a lower rumen pH ($P < 0.05$) and a lower NH_3-N ($P < 0.05$) concentration were noted in the AMO group. There were no effects of AMO inclusion in the diet on the acetate-to-propionate ratio or the concentrations of butyrate, isobutyrate, valerate, and isovalerate ($P > 0.05$).

Effects of AMO on the rumen bacterial community

Table 4 shows that the OTU (Operational Taxonomic Unit), Shannon, Simpson, Ace, Chao1, and coverage indices were not affected ($P > 0.05$) by AMO. Table 5 shows that the relative abundance of the phylum level *Bacteroidetes* and *Spirochaetota* in the AMO group was lower than that in the control. Conversely, the relative abundances of *Firmicutes*, *Actinobacteriota*, and *Verrucomicrobiota* of sheep fed the AMO diet were higher ($P < 0.05$) than those fed the control diet. Furthermore, no differences were noted for the relative abundances of other rumen bacterial phyla between treatments.

TABLE 5 Effect of AMO on rumen bacterial composition at phylum level (%).

Items	Treatments[1]		SEM[2]	*P*-value
	CON	AMO		
Bacteroidetes	50.50	58.45	0.859	0.001
Firmicutes	45.12	37.65	0.722	0.001
Actinobacteriota	1.52	0.71	0.084	0.001
Desulfobacterota	0.65	0.66	0.056	0.827
Spirochaetota	0.27	0.85	0.049	0.000
Verrucomicrobiota	0.43	0.23	0.018	0.001
Synergistota	0.33	0.31	0.054	0.690
Patescibacteria	0.35	0.37	0.047	0.743
Unclassified_k_norank_d_bacteria	0.34	0.33	0.029	0.754
Chloroflex	0.08	0.08	0.010	0.770

[1]Treatments: CON, basal diet; AMO, *Allium mongolicum* Regel essential oil.
[2]Standard error of mean.

Table 6 shows that the relative abundances of the genera *Prevotella* ($P < 0.05$) and *Prevotellaceae_UCG-003* ($P < 0.05$) were increased in the AMO group compared with those in the control. In contrast, sheep fed the AMO diet decreased the relative abundance of *Succiniclasticum*, *norank_f__F082*, *Christensenellaceae_R-7_group*, and *norank_f__Muribaculaceae* ($P < 0.05$). Moreover, no differences were noted for the relative abundances of other rumen bacterial genera between treatments.

Effects of AMO on rumen enzyme activities

The effects of AMO on the rumen enzyme activities of sheep are shown in Table 7. Dietary supplementation with AMO increased ($P < 0.05$) the activities of cellulase, α-amylase, and proteinase. In addition, no difference was found for the activities of rumen lipase and β-glucanase ($P > 0.05$).

Effects of AMO on nutrient digestibility

The effects of AMO on the apparent digestibility of sheep are shown in Table 8. Dietary supplementation with AMO increased ($P < 0.05$) the apparent digestibility of DM and CP. No difference was found for the apparent digestibility of OM, EE, ADF, and NDF ($P > 0.05$).

Discussion

Effects of AMO on growth performance and feed efficiency

As one of the main components of AM, AM flavonoids have been used as feed additives to increase the growth hormone (GH) level in the serum and ADG of sheep (32). Du et al. reported an improvement in the growth performance of sheep with dietary inclusion of AM extract (3.4 g/sheep/day) (16). However, scarce literature is available with regard to the effects of dietary supplementation with AMO on the DMI and ADG of sheep. The present research investigated whether sheep-fed AMO had a change in DMI compared with the control group. However, in contrast to this finding, an enhancement in ADG was found for sheep fed the diet supplemented with AMO. In the current study, the addition of AMO to the diet of sheep clearly decreased FCR, resulting from the increased ADG and similar DMI. These results are consistent with Zhao et al., who stated that diets supplemented with AM water extract in sheep resulted in changes in ADG and FCR (14). Such favorable effects on ADG and FCR were likely due to an increase in the relative abundance of bacteria involved in carbohydrate metabolism in the rumen, thereby enhancing the digestibility of DM and CP. Furthermore, the increases in growth performance may be partly related to the immunoenhancement and antioxidative effects of AMO (33).

Effects of AMO on rumen fermentation parameters

The decrease in ruminal Ph following AMO supplementation was in accordance with the increase in TVFA content (34). A lower ruminal pH was reported in sheep receiving AMO addition and was 6.49, which was suitable for rumen microbial growth and nutrient degradation. The major products of carbohydrate fermentation in the rumen are VFAs, which are the primary energy sources of ruminants (24). The total and molar proportions of VFA generated in the rumen depend on the substrate composition, nutrient availability, ruminal microbial community, and rumen pH reached (35). These alterations in TVFA proportions could be due to the stimulating action of AMO on propionate- and acetate-producing bacteria, indicating that AMO increased the fermentation of carbohydrates. It was also noted that AM water extract and AM ethanol extract could increase the quantity of amylolytic bacteria and cellulolytic bacteria in the rumen (14). This could be used for carbohydrate fermentation, generating high VFA. These current results differ in part from those of Ding et al., who did not observe a difference in the ruminal concentrations of TVFA or acetic and propionic acids in the rumen fluid of sheep-fed AM diets (36). Zhao et al. also found that feeding sheep with AM water extract increased the content of butyric acid and isobutyric acid (14). The difference between studies could be related to the source of AMO and AM water extract, the amount consumed, and the basic diet.

TABLE 6 Effect of AMO on rumen bacterial composition (%) at genus level.

Items	Treatments[1]		SEM[2]	*P*-value
	CON	AMO		
Prevotella	15.82	26.20	1.24	0.004
Rikenellaceae_RC9_gut_group	17.67	16.59	0.736	0.218
Succiniclasticum	7.51	3.85	0.40	0.007
Norank_f__F082	6.68	4.70	0.172	0.006
Christensenellaceae_R-7_group	4.71	4.42	0.049	0.015
Norank_f__Muribaculaceae	3.63	2.40	0.317	0.033
NK4A214_group	2.74	2.62	0.144	0.432
Norank_f__UCG-011	2.85	2.75	0.098	0.355
Prevotellaceae_UCG-003	1.99	2.66	0.074	0.004
Quinella	2.79	2.72	0.355	0.846
Norank_f__Bacteroidales_UCG-001	2.02	2.10	0.104	0.519

[1]Treatments: CON = basal diet; AMO = *Allium mongolicum* Regel essential oil.
[2]Standard error of mean.

TABLE 7 Effect of AMO on enzyme activities in sheep.

Items	Treatments[1]		SEM[2]	*P*-value
	CON	AMO		
Cellulase (U/L)	419.82	477.68	6.140	0.000
β-glucanase (U/mL)	6.30	6.36	0.217	0.484
α-amylase (U/dL)	47.92	59.83	0.897	0.000
Lipase (U/L)	87.59	91.80	2.664	0.145
Proteinase (U/dL)	80.34	83.10	0.913	0.024

[1]Treatments: CON, basal diet; AMO, *Allium mongolicum* Regel essential oil.
[2]Standard error of mean.

TABLE 8 Effect of AMO on nutrient digestibility in sheep (%).

Items[2]	Treatments[1]		SEM[3]	*P*-value
	CON	AMO		
DMD	66.51	69.66	0.907	0.026
OMD	67.46	69.39	0.843	0.084
CPD	61.58	63.43	0.459	0.016
EED	80.53	79.23	0.625	0.105
NDFD	45.8	45.92	0.799	0.891
ADFD	27.04	25.95	0.701	0.195

[1]Treatments: CON, basal diet; AMO, *Allium mongolicum* Regel essential oil.
[2]DMD, dry matter digestibility; OMD, organic matter digestibility; CPD, crude protein digestibility; EED, ether extract digestibility; NDFD, neutral detergent fiber digestibility; ADFD, acid detergent fiber digestibility.
[3]Standard error of mean.

Our previous research found that the use of AMO decreases the content of NH_3-N in *in vitro* rumen fermentation (18). Consistent with the above study, the addition of AMO decreased the NH_3-N content in the rumen of sheep. Wallace et al. affirmed that a rumen NH_3-N content between 15 and 30 mg/dL was more reasonable (37). Consequently, we reported that using AMO as a dietary additive could accelerate nitrogen metabolism in the rumen within a legitimate range (16.80 mg/dL) in the present study. MCP is synthesized by rumen microorganisms using NH_3-N, peptide, and amino acids in the rumen, and energy is necessary during the whole process of MCP synthesis (24). The contents of MCP and NH_3-N maintain a balance in the rumen, and excessive NH_3-N will increase the loss of nitrogen in the nitrogen cycle, while less NH_3-N will influence the production of MCP (24). The present research found that the output of MCP in the rumen was increased by feeding a diet with AMO to sheep, which indicates that AMO addition supplies an adequate nitrogen source, carbon skeleton, and energy for MCP synthesis. A similar consequence was acquired with dietary supplementation with different levels of AMO in the diet, which enhanced the rumen MCP yield *in vitro* (18).

Effects of AMO on the rumen bacterial community

The rumen is colonized by some microorganism communities (38), which play significant roles in fermenting and digesting nutrients to supply protein and energy resources (39), improving resistance to external stress, and enhancing growth and performance (40). The most significant microorganisms in the rumen were bacteria, as were also mentioned in previous literature (41). These bacterial communities live in dynamic conditions that could be influenced by several factors, such as diet, animal age, and feed additives (42). In the current study, there was no significant difference in OTU, Ace, Chao1, Simpson, Shannon, and coverage, which suggested that the addition of AMO had no negative effect on the alpha diversity of rumen microbes.

In the present research, *Bacteroidetes* and *Firmicutes* were the superior phyla in the ruminal microbial community, which is in accordance with previous literature in sheep (43, 44). In the current study, AMO addition in diets increased the relative abundance of the phylum *Firmicutes* and decreased the relative abundance of the phylum *Bacteroidetes*, consequently increasing the *Firmicutes* to *Bacteroidetes* (F:B) ratio, which could be beneficial for energy utilization and growth performance (45). The increased F:B ratio might be due to the acceleration of growth of *Firmicutes* by the antimicrobial function of the active ingredient in AMO.

In ruminants, *Prevotella* is the genus of the phylum *Bacteroidetes* with the highest relative abundance (26). *Prevotella* plays an important role in secreting the enzyme xylanase, which contributes to polysaccharide degradation (46). Some species of *Prevotella* are involved in the degradation and utilization processes of fiber, hemicellulose, pectin, and protein (47). In agreement with these results, our study found that the relative abundance of *Prevotella* seemed to be the most abundant in all rumen fluid samples at the genus level. Furthermore, the current work also found that the use of AMO in the sheep diet could promote the relative abundance of *Prevotellaceae_UCG-003*. The connection between the substrate and growth of *Prevotella* is not apparent. Previous studies have confirmed that *Prevotellaceae UCG-003* participates in glucose metabolism, generating acetic acids as the primary fermentation final products (25). This explains why acetic acid was present at a higher level in the AMO group.

Effects of AMO on enzyme activity

Meanwhile, the rumen cellulase, α-amylase, and proteinase activity apparently increased in the AMO group compared with the control. This could be sensed by a higher rumen *Prevotella* and *Prevotellaceae_UCG-003* in the AMO group, which contribute to the production of cellulase, α-amylase, and proteinase. Similar to the results observed in this study by Zhao et al., AM extracts could enhance the activities of cellulase, α-amylase, and proteinase in the rumen (14).

Effects of AMO on nutrient digestibility

Because AMO has been observed to decrease NH_3-N accumulation and change microbial community structure, we supposed that AMO would enhance nutrient digestibility in sheep by improving rumen microbial synthesis efficiency. Qiao et al. suggested that dietary AMO addition promoted the apparent total tract digestibility of CP in sheep (48). In addition, Yaxing et al. (33) noted increased DM digestibility in *in vitro* batch cultures with rumen fluid of sheep supplemented with increasing levels of AMO. Data from our research found that the digestibility of DM and CP in sheep with AMO supplementation was increased, which was similar to what we hypothesized. Similarly, several studies have reported that nutrient digestibility is enhanced by cinnamon oil in chickens (49), by oregano essential oil in lambs (8), and by essential oil in beef cattle (50). There are three reasons for the results of the present study. First, the decreased ruminal NH_3-N with sheep AMO inclusion suggested that the synthesis of MCP had accelerated and led to the increased CP digestibility. Second, Dowd et al. observed that *Prevotella* was very significant for the degradation and absorption of proteins as well as for the fermentation of peptides in the rumen (51). Based on the above findings, our present research detected that the relative abundance of

Prevotella was most abundant in the rumen fluid of sheep in the two treatments at the genus level. Moreover, the current research also demonstrated that supplementation with AMO in the diet could increase the relative abundance of *Prevotella* and *Prevotellaceae_UCG-003*. These results revealed that dietary addition of AMO had a favorable effect on enhancing the degradation of CP in the rumen, thereby boosting rumen fermentation. Third, we surmised that the improved digestibility of DM and CP was partially due to the elevated ruminal proteinase enzyme activity.

Conclusion

In general, supplementation with AMO in sheep diets increased growth performance by increasing ADG and decreasing FCR, promoted rumen fermentation, diversified the bacterial community composition in the rumen, enhanced the apparent digestibility of DM and CP, and improved rumen enzyme activities.

Data availability statement

The datasets presented in this study can be found in online repositories. The names of the repository/repositories and accession number(s) can be found below: NCBI; PRJNA833585.

Ethics statement

The animal study was reviewed and approved by College of Animal Science, Inner Mongolia Agricultural University, China. Written informed consent was obtained from the owners for the participation of their animals in this study.

Author contributions

ZY wrote the main manuscript. KE and BZ prepared Tables 1–4, and BC prepared Tables 5–8. AC edited the manuscript. All authors have read and agreed to the published version of the manuscript.

Funding

This study was funded by the landmark achievement of Inner Mongolia Agricultural University (BZCG202102).

Conflict of interest

The authors declare that the research was conducted in the absence of any commercial or financial relationships that could be construed as a potential conflict of interest.

Publisher's note

All claims expressed in this article are solely those of the authors and do not necessarily represent those of their affiliated organizations, or those of the publisher, the editors and the reviewers. Any product that may be evaluated in this article, or claim that may be made by its manufacturer, is not guaranteed or endorsed by the publisher.

Supplementary material

The Supplementary Material for this article can be found online at: https://www.frontiersin.org/articles/10.3389/fvets.2022.926721/full#supplementary-material

References

1. EI-essawy AM, Anele UY, Abdel-Wahed AM, Abdou AR, Khattab IM. Effects of anise, clove and thyme essential oils supplementation on rumen fermentation, blood metabolites, milk yield and milk composition in lactating goats. *Animal Feed Sci Technol.* (2020) 10:114760. doi: 10.1016/j.anifeedsci.2020.114760

2. Magnusson U. Prudent and effective antimicrobial use in adiverse livestock and consumer's world. *J. Anim. Sci.* (2020) 98:S4–S8. doi: 10.1093/jas/skaa148

3. Guo S, Lei J, Liu L, Qu X, Li P, Liu X, et al. Effects of Macleaya cordata extract on laying performance, egg quality and serum indices in Xuefeng Black-Bone Chicken. *Poult Sci.* (2021)100[4]:101031. doi: 10.1016/j.psj.2021.101031

4. Aziz MS. Karboune S. Natural antimicrobial/antioxidant agents in meat and poultry products as well as fruits and vegetables: a review. *Crit Rev Food Sci Nutr.* (2018) 58:486–511. doi: 10.1080/10408398.2016.1194256

5. Ruan D, Fan Q, Fouad AM, Sun Y, Huang S, Wu A, et al. Effects of dietary oregano essential oil supplementation on growth performance, intestinal antioxidative capacity, immunity and intestinal microbiota in yellow-feathered chickens. *J Animal Sci.* (2021) 99:1–11. doi: 10.1093/jas/skab033

6. Parvar R, Ghoorchi T, Kashfi H, Parvar K. Effect of Ferulago angulata (Chavil) essential oil supplementation on lamb growth performance and meat quality characteristics. *Small Ruminant Res.* (2018) 7:26. doi: 10.1016/j.smallrumres.2018.07.026

7. Toseti LB, Goulart RS, Gouvêa VN, Acedo TS, Vasconcellos GS, Pires AV, et al. Effects of a blend of essential oils and exogenous α- amylase in diets containing different roughage sources for finishing beef cattle. *Animal Feed Sci Technol.* (2020) 269:114643. doi: 10.1016/j.anifeedsci.2020.114643

8. Zhou R, Wu J, Lang X, Liu L, Casper DP, Wang C, et al. Effects of oregano essential oil on *in vitro* ruminal fermentation, methane production, and ruminal microbial community. *J Dairy Sci.* (2020) 103:2303–14. doi: 10.3168/jds.2019-16611

9. Joch M, Kudrna V, Hakl J, Božik M, Homolka P, Illek J, et al. *In vitro* and *in vivo* potential of a blend of essential oil compounds to improve rumen fermentation and performance of dairy cows. *Animal Feed Sci Technol.* (2019) 3:009. doi: 10.1016/j.anifeedsci.2019.03.009

10. Zeng Y, Li Y, Yang J, Pu X, Du J, Yang X, et al. Therapeutic role of functional components in alliums for preventive chronic disease in human being. *Evid. Based Complem. Altern. Med*. (2017) 94:02849. doi: 10.1155/2017/9402849

11. Schmitt B, Schulz H, Storsberg, J, Keusgen M. Chemical characterization of Allium ursinum L. depending on harvesting time. *J Agric Food Chem*. (2005) 53:e94. doi: 10.1021/jf0504768

12. Huang QC, Chu YL. Zhao YH, Zhao HT, Liu JM, Zhou RY. Status and prospect of plant fiber industry in Guangxi province. *Plan Fib Sci*. (2011) 33:202–5. doi: 10.3969/j.issn.1671-3532.2011.04.010

13. Yaxing Z, Erdene K, Changjin A, Zhibi B, Hongxi D, Zejun F, et al. Effects of Allium mongolicum Regel and its extracts supplementation on the growth performance, carcass parameters and meat quality of sheep. *Italian J Animal Sci*. (2021) 20:1899–1908. doi: 10.1080/1828051X.2021.1971572

14. Zhao Y, Ao C, Bao Z, Fan Z, Liu W, Ding H, et al. Effects of Allium monogolium Regel and its extracts on rumen fermentation and microflora of sheep. *Anim Nutr*. (2019) 31:2313–22. doi: 10.3969/j.issn.1006-267x.2019.05.038

15. Xie K, Wang Z, Wang Y, Wang C, Chang S, Zhang C, et al. Effects of Allium mongolicum Regel supplementation on the digestibility, methane production, and antioxidant capacity of Simmental calves in northwest China. *Animal Sci J*. (2020) 91:e13392. doi: 10.1111/asj.13392

16. Du H, Khas E, Chen S, Qi S, Bao Z, Zhao Y. Correlation of the rumen fluid microbiome and the average daily gain with a dietary supplementation of allium mongolicum regel extracts in sheep. *J Anim Sci*. (2019) 97:2865–77. doi: 10.1093/jas/skz139

17. Egyptian Pharmacopoeia (EP), General Organization for Governmental Printing Affairs, Cairo, Egypt (2005).

18. Mu CT, Ding N, Hao XY, Zhao YB, Wang PJ, Zhao JX, et al. Effects of Allium mongolicum Regel essential oil on *in vitro* rumen fermentation and substrate degradability of sheep. *Anim Nutr*. (2021) 33:4740–47. doi: 10.3969/j.issn.1006-267x.2021.08.052

19. NRC. *Nutrient requirements of sheep. 11th rev. edn*. Washington, DC: National Academic Press (2012).

20. Van Keulen J, Young BA. Evaluation of acid-insoluble ash as a natural marker in ruminant digestibility studies. *J. Anim. Sci*. (1977) 44:282–289. doi: 10.2527/jas1977.442282x

21. Zhou JW, Mi JD, Degen AA, Guo XS, Wang HC, Ding LM, et al. Apparent digestibility, rumen fermentation and nitrogen balance in Tibetan and fine-wool sheep offered forage-concentrate diets differing in nitrogen concentration. *J. Agric. Sci*. (2015) 153:1135–45. doi: 10.1017/S0021859615000465

22. Broderick GA, Kang JH. Automated simultaneous determination of ammonia and total amino acids in ruminal fluid and *in vitro* media. *J. Dairy Sci*. (1980) 63:64–75. doi: 10.3168/jds.S0022-0302(80)82888-8

23. Hu WL, Liu JX, Ye JA, Wu YM, Guo YQ. Effect of tea saponin on rumen fermentation *in vitro*. *Anim Feed Sci Technol*. (2005) 120:333–9. doi: 10.1016/j.anifeedsci.2005.02.029

24. Jiang X, Liu X, Liu S, Li Y, Zhao HB, Zhang YG. Growth, rumen fermentation and plasma metabolites of Holstein male calves fed fermented corn gluten meal during the postweaning stage. *Animal Feed Sci Technol*. (2019) 249:1–9. doi: 10.1016/j.anifeedsci.2019.01.012

25. Liu YZ, Chen X, Zhao W, Lang M, Zhang XF, Wang T, et al. Effects of yeast culture supplementation and the ratio of non-structural carbohydrate to fat on rumen fermentation parameters and bacterial-community composition in sheep. *Animal Feed Sci Technol*. (2019) 2:3. doi: 10.1016/j.anifeedsci.2019.02.003

26. Wang T, Jiao J, Wang H, Degen AA, Gou N, Li S, et al. The effects of supplementing sweet sorghum with grapeseeds on dry matter intake, average daily gain, feed digestibility and rumen parameters and microbiota in lambs. *Animal Feed Sci Technol*. (2020) 14:114750. doi: 10.1016/j.anifeedsci.2020.114750

27. Chen S, Zhou Y, Chen Y, Gu J. Fastp: an ultra-fast all-in-one FASTQ. Preprocessor. *Bioinformatics*. (2018) 34:i884–90. doi: 10.1093/bioinformatics/bty560

28. Magoč T, Salzberg SL. FLASH: fast length adjustment of short reads to improve genome assemblies. *Bioinformatics*. (2011) 27:2957–63. doi: 10.1093/bioinformatics/btr507

29. Association of Official Analytical Chemists (AOAC). Changes in official methods of analysis of the Association of Official Analytical Chemists. *Arlington*. (1990) 110:123–35.

30. Van Soest PJ, Robertson JB. Lewis BA. Methods for dietary fiber, neutral detergent fiber, and nonstarch polysaccharides in relation to animal nutrition. *J Dairy Sci*. (1991) 74:3583–97. doi: 10.3168/jds.S0022-0302(91)78551-2

31. Menezes AC, Valadares Filho SC, e Silva LC, Pacheco MV, Pereira JM, Rotta PP, et al. Does a reduction in dietary crude protein content affect performance, nutrient requirements, nitrogen losses, and methane emissions in finishing Nellore bulls? *Agric Ecosyst Environ*. (2016) 3:015. doi: 10.1016/j.agee.2016.03.015

32. Ren WC, Cui FW. Chang JA. Effects of flavonoids from Allium mongolicum Regel on growth performance and growth-related hormones in meat sheep. *Anim Nutr*. (2017) 3:33–8. doi: 10.1016/j.aninu.2017.01.003

33. Yaxing Z, Erdene K, Changjin A, Zhibi B, Hongxi D, Zejun F, et al. Effects of essential oil from Allium mongolicum Regel on slaughter performance, physicochemical property of meat and Antioxidant activity in mutton sheep. *Feed Ind*. (2021) 42:60–64. doi: 10.13302/j.cnki.fi.2021.17.011

34. Dijkstra J, Ellis JL, Kebreab, E, Strathe AB, L'opez S, France J, Bannink A. Ruminal pH regulation and nutritional consequences of low pH. *Anim. Feed. Sci. Tech*. (2012) 172:22–33. doi: 10.1016/j.anifeedsci.2011.12.005

35. Ceconi I, Ruiz-Moreno MJ, DiLorenzo N, DiCostanzo A, Crawford GI. Effect of urea inclusion in diets containing corn dried distillers grains on feedlot cattle performance, carcass characteristics, ruminal fermentation, total tract digestibility, and purine derivatives-to-creatinine index. *J. Anim. Sci*. (2015) 93:357–369. doi: 10.2527/jas.2014-8214

36. Ding H, Liu W, Ao C, Li S, Li Y, Zhang Z. Effects of dietary allium mongolicum regel powder or probiotic complex preparation on ruminal fermentation parameters and rumen fluid bacterial diversity of dorper×thin-tailed han crossbred sheep. *Anim Nutr*. (2018) 31:324–33. doi: 10.3969/j.issn.1006-267x.2019.01.039

37. Wallace RJ, Rooke JA, McKain N, Duthie CA, Hyslop JJ, Ross DW, et al. Effect of ruminal NH [[sb]]3[[/s]] -N levels on ruminal fermentation, purine derivatives, digestibility and rice straw intake in swamp buffaloes. Asian-Australas. *J. Anim. Sci*. (1999) 12:904–907. doi: 10.5713/ajas.1999.904

38. Zhang RY, Jin W, Feng PF, Liu JH, Mao SY. High-grain diet feeding altered the composition and functions of the rumen bacterial community and caused the damage to the laminar tissues of goats. *Animal*. (2018) 12:1–10. doi: 10.1017/S175173111800040X

39. Vymazal J, Kröpfelová L. Ruminal microbiota developing in different *in vitro* simulation systems inoculated with goats' rumen liquor. *Anim. Feed Sci. Technol*. (2013) 185:9–18. doi: 10.1016/j.anifeedsci.2013.06.003

40. Cani P D, Delzenne NM. The role of the gut microbiota in energy metabolism and metabolic disease. *Curr. Pharm. Design*. (2009) 15:1546–58. doi: 10.2174/138161209788168164

41. Wang YY, Cao PH, Wang L, Zhao ZY, Chen YL, Yang YX. Bacterial community diversity associated with different levels of dietary nutrition in the rumen of sheep. *Appl. Microbiol. Biot*. (2017) 101:3717–28. doi: 10.1007/s00253-017-8144-5

42. O'Hara E, Kenny DA, McGovern E, Byrne CJ, McCabe MS, Guan LL, et al. Investigating temporal microbial dynamics in the rumen of beef calves raised on two farms during early life. *FEMS Microbiol. Ecol*. (2020) 96:114802. doi: 10.1093/femsec/fiz203

43. Trabi EB, Seddik H, Xie F, Wang X, Liu J, Mao S. Effect of pelleted high-grain total mixed ration on rumen morphology, epithelium-associated microbiota and gene expression of proinflammatory cytokines and tight junction proteins in Hu sheep. *Anim. Feed Sci. Technol*. (2020) 263:114453. doi: 10.1016/j.anifeedsci.2020.114453

44. Xia G, Sun J, Fan J, Zhao F, Ahmed G, Jin Y, Zhang Y, Wang H. β-sitosterol attenuates high grain diet-induced inflammatory stress and modifies rumen fermentation and microbiota in Sheep. *Animals*. (2020) 10:171. doi: 10.3390/ani10010171

45. Thomas M, Webb M, Ghimire S, Blair A, Olson K, Fenske GJ, et al. Metagenomic characterization of the effect of feed additives on the gut microbiome and antibiotic resistome of feedlot cattle. *Sci. Rep*. (2017) 7:12257. doi: 10.1038/s41598-017-12481-6

46. Kim M, Morrison M, Yu ZT. Status of the phylogenetic diversity census of ruminal microbiomes. *FEMS Microbiol. Ecol*. (2011) 76:49–63. doi: 10.1111/j.1574-6941.2010.01029.x

47. Wei Y, Zhao CX, Li XW, Cong LX, Zhang H, Liu GW. Effect of different crude fiber source diets on rumen microflora of sika deer. *Chin. J. Vet. Sci*. (2018) 38:217–21. doi: 10.16303/j.cnki.1005-4545.2018.01.35

48. Qiao Y J. Effects of adding allium mongolicum regel essential oil in diets on production performance, apparent digestibility of nutrients and small intestine morphology and structure of mutton sheep. *Master's Thesis*. (2021) 43:24–29. doi: 10.13302/j.cnki.fi.2021.11.001

49. Chowdhury, Subrata, Mandal, Guru P, Patra, Amlan K. Different essential oils in diets of chickens: 1.Growth performance, nutrient utilization, nitrogen excretion, carcass traits and chemical composition of meat. *Animal Feed Sci Technol*. (2017) 12:2. doi: 10.1016/j.anifeedsci.2017.12.002

50. Torres RN, Paschoaloto JR, Ezequiel JM, da Silva DA, Almeida MT, et al. Meta-analysis of the effects of essential oil as an alternative to monensin in diets for beef cattle. *The Veterinary Journal*. (2021)272:105659. doi: 10.1016/j.tvjl.2021.105659

51. Dowd SE, Callaway TR, Wolcott RD, Sun Y, McKeehan T, Hagevoort RG, et al. Evaluation of the bacterial diversity in the feces of cattle using 16S rDNA bacterial tag-encoded FLX amplicon pyrosequencing (bTEFAP). *BMC Microbiol*. (2008) 8:125. doi: 10.1186/1471-2180-8-125

Advantages of publishing in Frontiers

OPEN ACCESS
Articles are free to read for greatest visibility and readership

FAST PUBLICATION
Around 90 days from submission to decision

HIGH QUALITY PEER-REVIEW
Rigorous, collaborative, and constructive peer-review

TRANSPARENT PEER-REVIEW
Editors and reviewers acknowledged by name on published articles

Frontiers
Avenue du Tribunal-Fédéral 34
1005 Lausanne | Switzerland

Visit us: www.frontiersin.org
Contact us: frontiersin.org/about/contact

REPRODUCIBILITY OF RESEARCH
Support open data and methods to enhance research reproducibility

DIGITAL PUBLISHING
Articles designed for optimal readership across devices

FOLLOW US
@frontiersin

IMPACT METRICS
Advanced article metrics track visibility across digital media

EXTENSIVE PROMOTION
Marketing and promotion of impactful research

LOOP RESEARCH NETWORK
Our network increases your article's readership